MOONLIGHTING tRNA SYNTHETASES AS EXTRACELLULAR TARGETS OF MATRIX METALLOPROTEINASES

by

PARKER JOBIN

B.Sc., The University of British Columbia, 2013

A DISSERTATION SUBMITTED IN PARTIAL FULFILMENT OF THE REQUIREMENTS FOR THE DEGREE OF

DOCTOR OF PHILOSOPHY

in

THE FACULTY OF GRADUATE AND POSTDOCTORAL STUDIES

(Biochemistry and Molecular Biology)

THE UNIVERSITY OF BRITISH COLUMBIA

(Vancouver)

June 2019

The following individuals certify that they have read, and recommend to the Faculty of Graduate and Postdoctoral Studies for acceptance, the dissertation entitled:

Moonlighting tRNA synthetases as extracellular targets of matrix metalloproteinases

submitted by Parker Jobin in partial fulfillment of the requirements for

the degree of Doctor of Philosophy

in Biochemistry and Molecular Biology

Examining Committee:

Christopher M. Overall
Supervisor

Stuart Turvey
Supervisory Committee Member

Eric Jan
Supervisory Committee Member

Mary MacDougall
University Examiner

Calvin Roskelley
University Examiner

Additional Supervisory Committee Members:

Dieter Brömme
Supervisory Committee Member

Abstract

Protease activity is of particular interest because of its irreversible nature and hence commitment by living systems to post-translationally truncate or remove by degradation its substrates. Degradomics, a combination of approaches used to study proteases, their inhibitors, and their substrates, allows powerful analyses of proteolytic networks. Degradomics has allowed the identification of a vast number of novel protease substrates, leading to speculation of molecular partnerships previously unknown to biology.

For the matrix metalloproteinase (MMP) family of extracellular proteases, degradomic screens have led us to realize that many proteins with intracellular roles are secreted by non-canonical means to perform novel extracellular functions that may be modulated by MMPs. Where it was once thought MMPs only degraded extracellular matrix (ECM), they are now known to process diverse signaling substrates.

Interesting multifunctional targets of MMP processing are “moonlighting” proteins that have more than one unique activity and can shuttle between intracellular and extracellular compartments to exhibit different functions in each. Recently, intracellular tRNA synthetases have been identified as extracellular moonlighting proteins. Despite the lack of signal peptides, six tRNA synthetases have been found to be secreted and perform different functions in the extracellular environment, notably activation of the immune response.

I hypothesized that MMP processing of tryptophanyl-tRNA synthetase (WRS), a cytokine, and tyrosyl-tRNA synthetase (YRS), fragments of which are proinflammatory, would modify the inflammatory activities of these tRNA synthetases. First, WRS and YRS secretion from human cells was confirmed. I then expressed and purified full-length WRS and YRS to evaluate MMP processing of these proteins. MMP cleavage sites within WRS and YRS were determined, revealing that MMPs cut the N-terminus from WRS but cleave within the YRS C-terminus, generating stable proteoforms. Cell culture assays revealed that both WRS and YRS have proinflammatory functions, each activating Toll-like receptors (TLRs). While removal of the N-terminus of WRS by MMP processing attenuated these activities, conversely, MMP cleavage of YRS increased proinflammatory functions, suggesting that MMPs play differing roles depending on the substrate being processed. This research exposes the exciting biology that awaits in tapping a previously unknown well of moonlighting MMP substrates with diverse bioactive roles.

Lay Summary

Proteases, like matrix metalloproteinases (MMPs), are proteins that cut other proteins to change their activity and thereby control both normal and disease processes in the body. Recently, new roles of MMPs have been revealed, cutting signaling proteins that are important in inflammation and cell communication. New technologies, designed to identify proteins cut by extracellular proteases, have found cut proteins involved in cell to cell signaling that are typically found only within cells and not outside including tRNA synthetases. These proteins with new functions outside of the cell distinct from the jobs they do inside are called “moonlighting” proteins and may represent new therapeutic targets. tRNA synthetase cutting by MMPs and the effect of this cutting was evaluated, revealing cutting one tRNA synthetase inactivated its activities while cutting another enhanced its activities. Learning how protein activities in the body are affected by protease cutting will help us better understand disease processes.

Preface

The research presented herein was conducted in the research laboratory of Professor Christopher Overall at the University of British Columbia, Point Grey Campus. The projects and described methods were approved by the University of British Columbia Clinical Research Ethics Board (certificate #H06-00047).

Both Chapter 2 and Chapter 3 have been prepared in the publishable format acceptable according to the University of British Columbia and the Department Biochemistry and Molecular Biology. Introducing these two chapters is the focus of Chapter 1, however portions of Chapter 1 have been augmented with material from a review that has been previously published (Jobin, P.G., Butler, G.S., and Overall C.M. (2017) New intracellular activities of matrix metalloproteinases shine in the moonlight. *Biochim. Biophys. acta. Mol. cell Res.* **1864**, 2043-2055). I was the lead author of this article used in Chapter 1, responsible for conception, planning, and writing of the manuscript. Georgina Butler and Professor Christopher Overall wrote and edited the review. This article and its materials are used in Chapter 1 with permission from the copyright holder, Elsevier.

A version of Chapter 2 has been submitted as a manuscript to an academic journal. I was the first author, responsible for planning, and performing of experiments, collection and analysis of the data, and writing the manuscript. Nestor Solis and Yoan Machado performed the ATOMS and LC-MS/MS experiments, respectively, and with Peter Bell analysed the data and wrote the paper under my direction. Georgina Butler and Professor Christopher Overall conceived the project, the experiments, wrote and edited the paper, analysed data, interpreted the results, supervised, and provided support for the project. Nam Hoon Kwan and Sunghoon Kim provided recombinant human WRS and Δ1-47 WRS plasmids for the project.

A version of Chapter 3 has been submitted as a manuscript to an academic journal. I was the first author, responsible for planning, and performing of experiments, collection and analysis of the data, and writing the manuscript. Nestor Solis and Yoan Machado performed the ATOMS and LC-MS/MS experiments, respectively, and with Peter Bell analysed the data and wrote the paper under my direction. Georgina Butler and Professor Christopher Overall conceived the project, the experiments, wrote and edited the paper, analysed data, interpreted the results, supervised, and provided support for the project. Nam Hoon Kwan and Sunghoon Kim provided the recombinant human YRS plasmid for the project.

Table of Contents

List of Tables

List of Figures

List of Abbreviations

APMA	*p*-aminophenylmercuric acetate
ATOMS	Amino terminal oriented mass spectrometry of substrates
CCL	CC chemokine ligand
CCS	Cosmic calf serum
CD	Cluster of differentiation
CXCL	CXC chemokine ligand
DMEM	Dulbecco's modified Eagle's medium
ECM	Extracellular matrix
EMAPII	Endothelial-monocyte activating polypeptide II
HMGB1	High mobility group box 1
HSP	Heat shock protein
IFN	Interferon
IκB-α	Inhibitor of kappa B-alpha
IL	Interleukin
LC-MS/MS	Liquid chromatography tandem mass spectrometry
LPS	Lipopolysaccharide
MMP	Matrix metalloproteinase
MT-MMP	Membrane-type MMPs
NET	Neutrophil extracellular traps
NF-κB	Nuclear factor-kappa B
PBMC	Peripheral blood mononuclear cells
PI3K	Phosphatidyl-inositol 3 kinase
PMA	Phorbol 12-myristate 13-acetate
PMN	Polymorphonuclear leukocyte
RPMI	Roswell Park Memorial Institute
TAILS	Terminal amine isotopic labelling of substrates
TIMP	Tissue inhibitor of metalloproteinases
TLR	Toll-like receptor
TNF	Tumor necrosis factor
WRS	Tryptophanyl-tRNA synthetase
YRS	Tyrosyl-tRNA synthetase

Acknowledgements

First, I thank Professor Christopher Overall for having me as a student, supporting and supervising my work. His energy and curiosity were contagious, and this work would not have been possible without him. I also thank Georgina Butler, her support and mentorship helped me keep going and thanks to her steadiness and faith in success, I managed completed this project. My supervisory committee members also have my gratitude. The ideas and perspectives of Eric Jan, Dieter Brömme, and Stuart Turvey were enormously beneficial to me and this research. I also thank Stuart Turvey for providing the Toll-like receptor reporter cell lines used for this research.

It is important to acknowledge the current and past members of the Overall laboratory whose work in maintaining and facilitating research are important to everyone's work. Special thanks go to Reinhild Kappelhoff, whose tireless management ensures the place does not collapse into the Salish Sea. Notably, Nestor Solis, Yoan Machado, and Peter Bell with their mass spectrometry expertise make the Overall lab a place of cutting-edge research and without whom I would not have been able to incorporate proteomic techniques into the presented work. Nestor deserves extra praise, as his herculean efforts in maintaining the mass spectrometry equipment allowed me to attempt my research in the first place. Thanks to all of them for their assistance.

I thank the sources of financial support for this work. I was supported by a VCHRI-CIHR-UBC MD/PhD Studentship, CIHR Vanier Canada Graduate Scholarship, UBC 4-Year Doctoral Fellowship, and a Centre for Blood Research Graduate Award.

This work was funded by a Canadian Institutes of Health Research (CIHR) grant (MOP-111055 to Christopher Overall and Georgina Butler), a CIHR foundation grant (FDN-148408 to Christopher Overall), the Michael Smith Foundation for Health Research to establish the British Columbia Proteomics Network (IN-NPG-00105 to Christopher Overall), and the Canada Foundation for Innovation (31059 to Christopher Overall).

Dedication

I dedicate this work to my family. My parents, Brenda and Alain, who have always encouraged me throughout my education, I cannot thank them enough for their ceaseless support throughout my career. My fiancé Kristina, whose support and patience has kept me going for 4 years. She celebrates every success, no matter how small, and helps me survive the failures, it is her I thank the most.

Chapter 1: Introduction

Before completion of the Human Genome Project, the expectation was that the complexity of an organism would correlate to the number of protein-coding genes, with higher estimates reaching 120,000 for vertebrates (1, 2). However, the human genome is now estimated to contain 19,467 protein-coding genes (3, 4), indicating that there are multiple mechanisms to facilitate the vast number of cellular processes from this limited number of protein-coding genes. For multicellular organisms, multifunctional proteins have emerged as one solution to increase biological complexity (1, 5). Unlike alternative splicing of RNA transcripts, where multiple protein products are derived from a single gene (6, 7), multifunctional proteins consist of a single polypeptide that attains multiple activities through a variety of mechanisms including: changes in subcellular location; alterations in extracellular environment; complex formation with different partners; and post-translational modifications *e.g.* phosphorylation and proteolysis (5). Such proteins with dual roles, enjoying distinct functions in addition to their best characterized or predominant function, are termed “moonlighting” or “pleiotropic” proteins (5) and complicate drug targeting (8).

Moonlighting proteins are unique and differ from other multifunctional proteins as they perform 2 or more unique and unrelated functions (5, 9–15), *i.e.* these are not promiscuous enzyme activities, where the same active site catalyzes different reactions under different conditions. While the definition of moonlighting proteins does include proteins that perform unrelated roles within the same cellular compartment (5), much of the focus of the moonlighting research community has arguably been directed towards how localization between cellular compartments affords proteins new functions once shuttled into a new environment (16) *i.e.* intracellular proteins shuttling to the extracellular milieu. The number of moonlighting proteins now exceeds 300 (1, 17, 18), with the best studied examples, *e.g.* the glycolytic enzyme glyceraldehyde-3-phosphate dehydrogenase (19) and the transcription factor high mobility group box 1 (HMGB1) (20), reaching double-digits in number of independent functions. Both glyceraldehyde-3-phosphate dehydrogenase and HMGB1 are known to shuttle to the extracellular milieu to perform moonlighting functions.

Moonlighting challenges the typical expectation that enzymes function in either the intracellular or the extracellular environment of a cell and remain in that location. The cellular localization of a protein can be vital to determining its function (8), but traditional biochemistry has overlooked the possibility of proteins gaining functions by shuttling between locations partly due to constraints of dogma: Intracellular proteins found in extracellular locations are often regarded as artifacts of cell

death and extracellular proteins found within nuclear and cytosolic extracts are considered contaminants of secretion or rare artifacts.

Interest is growing in how moonlighting protein pleiotropic activities are regulated. Insider proteins moonlighting on the outside, lacking a traditional signal peptide for secretion, may represent a vast subset of proteins that cells have adapted in order to achieve the long list of extracellular functions a multi cellular organism needs to carry out. Thus, they require a sophisticated system of regulatory steps. One such regulatory step is post-translational modification by means of proteolysis. Proteolytic processing by a protease differs from simple degradation. Processing requires limited and specific cleavage of a protein substrate by a protease with only one or two cuts. Degradation is the indiscriminate cleavage of a substrate into peptides. Specific processing has become recognized as a common mechanism to regulate the activities of many proteins, including moonlighting proteins (8, 16, 21–25). This chapter will address how intracellular proteins exit the subcellular environment, their roles in maintaining homeostatic and diseased processes such as inflammation, and the discovery that these moonlighting proteins are regulated by proteolysis.

For the matrix metalloproteinase (MMP) family of extracellular proteases, as with all protease families, the development of innovative proteomic technologies has rapidly changed our understanding of the *in vivo* function of these enzymes (8). The first 50 years of research on MMPs classified these enzymes according to their extracellular matrix (ECM) substrates (26, 27). The collagenases (MMP1, MMP8, MMP13), gelatinases (MMP2 and MMP 9), stromelysins (MMP3, MMP10, and MMP 11), matrilysins (MMP7 and MMP 26), and membrane-anchored MMPs (MMP14, MMP15, MMP16, MMP17, MMP24, and MMP25) make up most of the family (27). The remaining MMPs include MMP12 (macrophage metalloelastase), MMP18, MMP19, MMP20 (enamelysin), MMP21, MMP22, MMP27,and MMP28 (epilysin) (22, 27). Recent research has shown that MMPs process a wide array of substrates including chemokines and other cytokines, leading to a shift in interest from ECM turnover to cell signaling roles in homeostasis and pathology (8, 28).

1.1 Matrix metalloproteinases

MMPs are a family of secreted zinc-dependent metalloproteases comprised of both soluble and membrane-bound endopeptidases. Numbering 23 in humans, this group is expressed across most tissues, with some members only being expressed by specific cell-types (29) such as

MMP12 by macrophage and lung epithelial cells (27, 30). From their discovery in tadpole tail metamorphosis (31), MMPs earned their title as matrix proteases that collectively degrade most if not all ECM proteins (26, 32), despite the fact that never have all ECM proteins been shown to be substrates, with corresponding roles in angiogenesis, embryogenesis, wound healing, and metastasis (26–28, 33, 34).

Most MMPs have four domains: A secretion signal peptide, prodomain, catalytic domain, and hemopexin-like domain (27, 35). The common catalytic domain has a Zn^{2+} ion in the catalytic pocket chelated by three conserved histidine residues (36). MMPs are secreted with an N-terminal pro-domain containing a conserved cysteine residue responsible for keeping the enzymes latent by coordinating the Zn^{2+} ion in the catalytic pocket (36). In most MMPs (except MMP7, MMP23, and MMP26), a hinge region connects the catalytic domain to a C-terminal hemopexin-like domain, an exosite that facilitates non-proteolytic roles (37, 38). MMP2 and MMP9 have fibronectin type-II repeats inserted in their catalytic domains that bind native and denatured collagen (39–41). Membrane-type MMPs (MT-MMPs) are anchored at the extracellular cell surface, by either a single pass transmembrane domain or a glycophosphatidylinositol linkage (42).

There are multiple levels of MMP regulation. Transcription is a major checkpoint, with trigger and suppressor signals tightly controlling MMP production (43). Certain MMPs have roles in maintaining homeostasis and their expression can be detected in normal tissues, while others are specifically expressed under unique conditions in certain cell-types (44). For example, MMP2, with ubiquitous and constitutive expression across most cell-types mostly unaffected by proinflammatory stimuli, contrasts MMP9, expressed constitutively in fewer cell-types and requires induction by inflammatory signals for expression in others (27). Secreted inactive proMMPs await activation by either proteolytic cleavage, *e.g.* other MMPs or serine proteases, or thiol oxidation by compounds including reactive oxygen species (45–47). Once activated, MMPs become vulnerable to inhibition by general protease inhibitors and their specific natural inhibitors, the tissue inhibitors of metalloproteinases (TIMPs) (48).

1.2 Insider proteins moonlighting on the outside

Just more than 30 years ago, the first reports of secretion of what was then believed to be intracellular-only proteins that lack signal peptides necessary for classical secretion began to appear (49–51). Years before, the molecular chaperone heat shock protein (HSP)10, called a

different name at the time, was first discovered as an immunosuppressant factor in anti-fetal immunity (52, 53). After its correct identification as intracellular HSP10 more than a decade later (54), it became one of the earliest moonlighting proteins to be targeted by therapeutics (55–58). Even early than HSP10, the glycolytic enzyme glucose-6-phosphate isomerase was detected in the blood of cancer patients with malignant tumours (59). In the span of 60 years since that discovery, glucose-6-phosphate isomerase has been attributed multiple extracellular functions and has been called neuroleukin acting as a neurotrophic factor (60) and autocrine motility factor acting as a factor promoting epithelial-mesenchymal transformation (61). Unaware that one single protein could have such versatility and shuttle between intracellular and extracellular spaces, many researchers have been guilty of such mislabeling leading up to Jeffrey codifying the term moonlighting protein in 1999 (5).

Now, more and more of these insiders on the outside are being adapted into clinical applications. HMGB1 has been seized upon as a clinical biomarker (62–65) and a therapy target (66) in sepsis. Currently in clinical trials, binding immunoglobulin protein, originally thought to have been only a molecular chaperone, is being tested as an antiarthritic (67) due to the discovery of binding immunoglobulin protein inducing interleukin (IL)10 production in T cells (68–70). The interest in moonlighting proteins for therapy highlights how this nascent field will continue to grow.

1.2.1 Mechanisms of extracellular localization of intracellular proteins

It is important to explore how intracellular proteins reach the extracellular milieu without a hydrophobic secretory signal peptide so that they can be targeted by MMPs. Analogous to the first 50 years of MMP research being restricted to their extracellular roles in ECM turnover, the first half century of research into protein secretion has been dominated by a consensus (71) that clarifies secreted proteins carry a signal peptide, directing their insertion into the endoplasmic reticulum before moving onto the Golgi apparatus before finally reaching the plasma membrane for exocytosis (recently reviewed in (72)). However, example after example of non-canonical strategies adapted by cells to secrete proteins without signal peptides (reviewed in (8, 16, 73)) has spurned a reassessment of secretion, most recently by Rabouille (71), into four broad yet unique types of non-canonical protein secretion. Type IV, the Golgi-bypass pathway, will not be explored in depth here as it exists as its own separate category of proteins that possess a signal peptide (71).

The study of the mobilization of insider proteins for extracellular functions is hampered by long held dogma that intracellular proteins found in secretomes (all proteins secreted into the extracellular space) or biological fluids must result from artefacts of sample preparation or due to cell lysis (8, 73). Many intracellular proteins, but not all, have been detected in conditioned media of cultured cells, suggesting cell lysis does not account for all intracellular proteins released into the extracellular space (16). Certain intracellular moonlighting proteins like HMGB1 are speculated to be both actively secreted by non-canonical means and released passively through cellular lysis in order to exert their extracellular activities (74). Therefore, it is necessary to delineate the current understanding of non-classical protein secretion from other forms of intracellular protein release.

1.2.1.1 Non-canonical secretion

The first type of non-canonical secretion involves the formation of non-lethal pores within the plasma membrane to afford intracellular proteins direct paths into the extracellular milieu (71). Just as bacteria utilize pores for secretion (75), animal cells also generate pores in their membranes to release subcellular content. With some pores being constitutive (71) while others inducible by stimuli such as cellular stress (76), intracellular proteins lacking a signal peptide can be provided with a route of direct plasma membrane translocation.

These pores can be lipid-based, as is the case for fetal growth factor 2 (77) and HIV Transactivator of Transcription (78), where the secreted proteins interact with phospholipids to cross the membrane. Other proteins depend on cooperation with a secretory apparatus of heterologous protein complexes, including transglutaminase 2 and thioredoxin (79). It is notoriously difficult to elucidate the mechanisms of pores, evidenced by the secretion of fetal growth factor 1 which recruits numerous proteins to form a complex comprised of annexin a2 (80) and small calcium protein S100A13 (81) yet lacks evidence of pore activity. The pursuit of finding cell-specific pores and their mechanisms of action may fill in the uncertain gaps in the secretion posed by proteins like fetal growth factor 1.

ATP binding cassette transporters are membrane transporters ubiquitous across all living organisms reviewed recently in (82). In humans, mammalian multidrug resistance proteins mediate drug efflux and promote drug resistance among certain cancer cells (83). Classically composed of dimers of an ATP-binding domain and a transmembrane domain, these efflux pumps have little evidence supporting the export of proteins across the cellular membrane (8). As

research into these protein transporters as protein exporters is limited (71), no more time will be spent exploring them.

Intracellular vesicle-based trafficking, diverted to exocytosis to become extracellular secretory vesicles, is a third mechanism by which intracellular proteins lacking signal peptides are exported out of cells (84). The generation of exosomes or multivesicular bodies following endocytosis has been to known to not only incorporate typical endosomal proteins but engulf components of the cytosol (85–88). Its relation to non-canonical secretion of these randomly engulfed cytosolic components comes from the fate of these multivesicular bodies. Some proceed to fuse with lysosome for degradation of their components. Others are fated to re-fuse with the plasma membrane, effectively becoming exosomes carrying content into the extracellular space. Once external, these vesicles are reported to either remain at the site of discharge or travel to distal locations in biological fluids, eventually rupturing to release their payloads or fusing to other cells, providing means of intercellular communication (8, 73). Examples of this secretion strategy include moonlighting HSP70 (89), HSP90 (85), and glyceraldehyde-3-phosphate dehydrogenase (90).

Distinct from multivesicular body trafficking, ectosomes or microvesicles are not formed from any existing trafficking vesicle within the cell but rather form directly from the budding of the plasma membrane (84, 91, 92). As endosomes arise from intraluminal vesicles or endocytic cisternae, ectosomes form rapidly from membrane microdomains characterized by unique lipids and membrane associated proteins. Similar to endosomes, these vesicles act locally and can travel far from their source to mediate their effects (8, 73). The lipid and protein composition of ectosome membranes is unique to the cell-types that generate them, hinting at how this system is tightly controlled by the cells that use ectosomes to communicate (8). Much of the intracellular protein cargo detected in either exosomes or ectosomes has been detected in the other (73), suggesting much work remains in delineating between the two vesicles in order to contextualize their significance in non-canonical secretion.

Additional vesicles that can be adapted to export intracellular proteins are secretory lysosomes (8, 73). Rather than degrading intralumenal contents as is the normal function of the lysosome, secretory lysosomes depend on external stimuli to change their fate towards secretion. Secretory lysosomes are extracellular secretory vesicles, yet they remain distinct from exosomes due to the precursors of secretory lysosomes. What endosomes are to exosomes the endolysosome is to

secretory lysosomes (93). The packaging to intracellular proteins into endolysosomes remains unclear, as sources for these proteins are thought to come from endosomes directed to the endolysosome, proteins directed from the *trans*-Golgi network (94), and potentially from ATP binding cassette transporters pumping molecules into the organelle (73). Despite this uncertainty, cytoplasmic proteins like HMGB1 have been reported to be exported using secretory lysosomes (95), hinting at the importance of vesicle secretion in moonlighting.

1.2.1.2 Cell lysis

Apoptosis, programmed cell death, requires cells to undergo a stepwise process to prepare themselves for not only death, but for proper clearance to avoid unwanted inflammation (reviewed in (96, 97)). Professional phagocytic cells like macrophages require both “find-me” signals to migrate to the sites of apoptotic cells and “eat-me” signals to engulf apoptotic cells once the phagocytes arrive. Given that intracellular proteins lacking signal peptides, like calreticulin, localize to the surface of shedding apoptotic bodies from apoptotic cells to mediate phagocytic engulfment (98), intracellular proteins found in the extracellular space on account of apoptosis serve important functions and should not be discounted as artefacts.

Following similar logic, intracellular protein release by necrotic cell death should also be considered, under the correct circumstances, as a genuine source of intracellular proteins to the extracellular space. Cells succumbing to compromised cellular integrity caused by trauma or infection release all subcellular proteins to the site of injury, unleashing the moonlighting activities that these proteins carry out. Furthermore, necrotic cells are known to secrete a specific class of intracellular protein before membrane integrity is lost, the damage associated molecular patterns or alarmin proteins (reviewed in (99, 100)). These endogenous danger signals are vital in stimulating both innate and adaptive immune responses and count among their numbers moonlighting HMGB1 (101), HSP70, and HSP90 (102). Analogous to exogenous pathogen associated molecular pattern molecules of pathogens, endogenous damage associated molecular patterns are recognized by pattern recognition receptors on the surface of immune cells such as Toll-like receptors (TLRs) (103). While many detected intracellular proteins in extracellular spaces may be artefacts of sample preparation or indiscriminate cell lysis, cell lysis under specific circumstances should not be discounted as a genuine source of intracellular protein release as these proteins likely play important roles in both normal and disease processes.

The formation of neutrophil extracellular traps (NETs) by polymorphonuclear (PMN) leukocytes or neutrophils is another cell lytic event that results in intracellular protein release (104). Briefly, the nuclear membranes of neutrophils disintegrate upon exposure to inflammatory stimuli, leading to the cell filling with nuclear content and the mixing of subcellular compartments. Expulsion of this mixture of contents results in a fibrous, condensed chromatin structure apparatus that concentrates granular, cytosolic, and nuclear proteins, many which are antimicrobial or have other stimulatory activities in inflammation (reviewed in (105, 106)). While neutrophil death is associated with NET formation (termed NETosis), NET formation can exist distinct from cell death, that is viable neutrophils will generate NETs and are the lifespans of these cells will not be affected by NET formation (107). As intracellular protein expulsion is associated NET formation, NETs allow moonlighting intracellular proteins to hitch a ride into the extracellular space.

1.2.2 Moonlighting intracellular proteins, MMPs, and inflammation

Nearly all non-canonical secretory pathways occur during cellular stress (71, 108). Cellular stress, such as nutritional stress, endoplasmic reticulum stress, and oxidative stress, are linked to inflammation (109). Indeed, many intracellular proteins non-canonically secreted during cell stress possess distinct moonlighting extracellular activities important to inflammation, typically as signaling proteins (1). The activity of MMPs as extracellular proteases is also important to stress and inflammation as MMP proteolytic activity increases during these states (27, 110). Additionally, recent MMP research has exposed MMPs fine-tuned controllers of a diverse array of signaling proteins (reviewed in (8, 16, 28, 73, 111)). Thus, stress and inflammation, by releasing moonlighting intracellular proteins into the extracellular milieu, provide a previously unexplored pool of possible proteolytic substrates of MMPs. This includes both non-canonical secretion and the release of intracellular proteins due to cell lytic events common in inflammation.

The localization of a protein and the exposure of that protein to new interacting partners is not the only way for a moonlighting protein to alter its function. Post-translational modifications, specifically proteolytic processing, can allow proteins to switch between activities. Proteolysis not only enables clearance of extracellular proteins (degradation), but also specific targeted proteolysis (processing) can switch protein activity (112). This is true of both chemokines found normally in the extracellular milieu, such is the case of CC chemokine ligand (CCL) 7 converting from a receptor agonist to an antagonist upon MMP2 cleaving 4 residues from CCL7 (23), and intracellular proteins moonlighting in the extracellular space. An example of the latter would be annexin a1, cleaved by neutrophil-derived proteinase 3 in neutrophils to stimulate an inflammatory

response (113). If intracellular proteins with moonlighting extracellular functions leave subcellular compartments and are targeted as proteolytic substrates by MMPs, MMPs stand to expand their roles in processes like inflammation by cutting these moonlighting substrates and modulating their extracellular activities.

1.2.2.1 Inflammation

The host response to injury, either infectious or traumatic, is inflammation. Involving both a rapid response to stimuli within hours and resolution phase that can last days, acute inflammation is a process dependent on multiple cell-types and the products these cells generate. Blood flow increases to sites of injury carrying with it leukocytes which migrate and invade into the affected tissues (reviewed in (109, 114, 115)). Part of acute inflammation is the innate immune response, the first response of the immune system. It is dependent the temporal coordination of migratory immune cells or leukocytes: first neutrophils, then mononuclear phagocytes. These cells cause a rapid response in the affected site within hours and ensure this response is attenuated and eventually terminated days later to prevent additional cells from being recruited.

Neutrophils serve as first response of acute inflammation. These leukocytes are the most abundant of the white blood cells circulating in peripheral blood (116) and aggressively invade tissues during infection or injury (117). In addition to using NETs to kill foreign pathogens, neutrophils release secretory vesicles and granules filled with proteases (118), antimicrobial peptides (116, 119), and other compounds (120). The destruction of pathogens is furthered by the respiratory burst of reactive oxygen (121) and nitrogen species (122) produced by neutrophils.

Mononuclear phagocytes constitute the subset of leukocytes that includes dendritic cells, monocytes, and macrophages (123). These antigen presenting cells both serve as a vital link between the innate and adaptive immune response and mediate the later stages of inflammation. Blood monocytes differentiate into dendritic cells and macrophages under the influence of cytokines (124, 125), although the definition of these cell populations are constantly be revised as more is learned about them (see (123, 126) for recent reviews). While resident macrophages, tissue dendritic cells, and migratory dendritic cells are important in surveilling for infection, blood monocytes hold great significance to acute inflammation.

Circulating monocytes exist in two populations: inflammatory or classical monocytes (human cluster of differentiation (CD)$14^{+}CD16^{-}$) and patrolling or non-classical monocytes (human

$CD14^{low}CD16^{+}$) (127). Patrolling monocytes respond rapidly to infection (128) while also contributing to the resolution of inflammation by the production of wound healing factors (129). However, patrolling monocytes only constitute a fraction of the total number of circulating monocytes. The more numerous inflammatory monocytes begin to migrate to the site of injury after several hours and continue doing so over days (130), producing proinflammatory cytokines like tumour necrosis factor (TNF)α while demonstrating higher protease activity (129). These migrating monocytes eventually overtake neutrophils as the predominant cell-type over the course of days and direct inflammation into its resolution phase.

Recruited monocytes differentiate to macrophages during inflammation. Macrophages are vital in regulating inflammation and, like other members of the mononuclear phagocyte system, they are defined into separate polarized sub-populations constantly being updated as our understanding of these cells grows (see (131, 132) for recent reviews). Under the influence of specific stimuli, macrophages are activated to adopt a spectrum of polarized phenotypes loosely referred to as M1-type classically activated (133) and M2-type alternatively activated populations (134).

M1 macrophages, polarized under the influence of interferon (IFN)γ, lipopolysaccharide (LPS), and TNFα, are proinflammatory, producing respiratory bursts, proinflammatory cytokines such as IL6 and TNFα, and stimulate a Type 1 helper T cell response aimed to kill intracellular pathogens (131). Conversely, M2 macrophages are loosely considered anti-inflammatory and are associated to Type 2 helper T cells (131, 135, 136). Polarized under the influence of IL4 and IL13, M2 macrophages are important in the resolution stage of inflammation as M2 macrophages produce trophic polyamines, have higher matrix deposition and remodeling capability, and produce various anti-inflammatory cytokines such as IL10 and transforming growth factor-β (131). Additionally, M2 macrophages have increased scavenger receptor expression and are theorized to have enhanced phagocytic capabilities (137, 138), but differences in capacity for phagocytosis for this phenotype have been complicated by conflicting reports (134). However, it is generally accepted that M2 macrophages are the anti-inflammatory phenotype while M1 macrophages serve more proinflammatory roles.

1.2.2.2 MMPs and inflammation

The activity of proteases is vital to inflammation. Proteases participate in the antimicrobial response, process signaling proteins to control inflammatory signaling, and remodel the ECM to facilitate leukocyte invasion and wound-healing. MMPs are relevant maintaining proper

homeostasis in inflammation (reviewed in (21, 22, 110, 139)) evidenced by dysfunctional inflammation in murine MMP knockout models (organized in (22, 140)) and altered activity and expression of MMPs in human inflammatory diseases (24, 141–147). Moreover, naturally occurring human MMP variants are also linked to inflammatory diseases (148–152).

Briefly described in the beginning of this chapter, MMPs are carefully regulated by multiple checks on their activity including zymogen latency, gene expression, protease inhibitors, localization, and cell/tissue specificity. While both stromal cells and invading immune cells produce MMPs and several MMPs overlap in cellular source, certain MMPs are specific to cell-types (139). This cell-type specificity is important to inflammation — given that the response to injury requires specific cells to act in temporal sequence, first neutrophils and then mononuclear phagocytes, it follows MMPs specific to those cells aid in regulating inflammation in a temporal manner when MMPs are activated at the site of injury (22, 110). MMP7 and MMP9, both inducible to proinflammatory stimuli (22, 27), are expressed by both stromal and immune cells. Conversely, MMP8 and MMP12 are leukocyte-specific, the former in neutrophils (153) and the latter in macrophages (154).

MMP roles in inflammation are dependent on their substrates. While their name implies MMPs are responsible for ECM turnover to allow cell migration and neovascularization, ambitious attempts to target aforementioned functions of MMPs as a therapy strategy using broad-spectrum MMP inhibitors were unsuccessful and elicited unanticipated side effects (155–159). We know now MMP have a board substrate repertoire beyond the ECM, informative of the so-called “anti-target” functions of MMPs that should not be targeted by drugs (reviewed in (8, 16, 28, 73, 111, 112)). Many of these anti-target functions are derived from MMP substrates with beneficial roles in inflammation that should be spared from drugs.

Neoproteins (or cryptic proteins) are products of MMP cleavage that possess cryptic functions and were discovered early as a class of novel MMP substrates (160). Parent proteins plasminogen and type XVIII collagen release angiogenesis inhibiting fragments angiostatin (161) and endostatin (162) respectively upon MMP proteolysis. Fibronectin is cut by MMP2 to release fragments possessing anti-adhesive function (163). MMP cleavage regulates protein function in the extracellular milieu by cutting both structural and non-structural parent proteins into new fragments serving distinct functions.

The list of non-matrix substrates of MMPs has grown to include cytokines (24, 164), chemokines (23, 25, 165–168), insulin-like growth factor binding proteins (169), complement (170, 171), tissue

factor inhibitor (118), and serpins (172). MMP cleavage can increase or decrease the functions of bioactive molecules or generate completely new functions through proteolysis. Thus the diversity of MMP-substrate interactions suggests a sprawling protease web that can only be partially defined by classic matrix substrates (16, 173, 174). To avoid mistakes encountered in the first MMP inhibitor clinical trials, future research must turn to more robust and sensitive methods for identifying MMP substrates to better understand MMP functions.

1.2.3 Degradomics

To address the task of uncovering the regulatory web of MMPs, new techniques have emerged. Degradomics, all the approaches used to study proteases, their inhibitors, and their substrates, has progressed rapidly in the last two decades (112, 174–176). Distinct from proteomics, the study of the entire proteome of a biological system, degradomics specifically addresses proteases and their substrates, leading to speculation of partnerships previously unknown to biology. For MMPs, conventional hypothesis-driven approaches to identify and validate proteolytic targets using biochemical methods have been streamlined by degradomics (8).

This revolution in protease biology can be attributed to the substrate degradome. The substrate degradome is the substrate repertoire of a protease, the substrates a protease can process (177). Substrates define protease functions, thus screening technologies to find these substrates have modernized protease research. Degradomics encompasses genomic and proteomic analyses of protease (16). Innovations such as CLIP-CHIP (178) and quantitative real-time polymerase chain reaction (179) profile protease, substrate, and inhibitor expression while activity based-probes assess the activity of proteases (180). However, the substrate degradome is the most relevant area of degradomics to this thesis.

More dated degradomic techniques such as exosite scanning and inactive catalytic domain capture with yeast-2-hybrid analysis (23) have proved useful in identifying chemokines as MMP substrates, yet quantitative proteomic methods are now favored. Quantitative proteomic methods that capitalize on use of tandem mass spectrometry (MS/MS) are high throughput and discern differences in proteins (and thus substrates) between samples. These techniques use isotope labeling strategies including stable isotope labeling by amino acids in cell culture (also known as SILAC) (181), dimethylation (182), isotope-coded affinity tags (also known as ICAT) (183), and isobaric tags for relative and absolute quantification (also known as iTRAQ) (184). These screens reveal changes in substrate levels between proteomes treated with a protease of interest

compared to an untreated proteome. Adding a protease compared to a buffer to a proteome or secretome *in vitro* (185) would be an example. Cell culture systems have proved valuable in studying the substrate degradomes of proteases, as proteases can be transfected into cells and compared to control cell lines (39). Protease knock out cells have been used for comparison to wild-type controls (186). Further, culture experiments can be conducted in the presence or absence of protease inhibitors (187). Substrate degradomes have also been determined using tissues in the case of protease knockout animals versus wild-type controls (188, 189) but these experiments are even more complex than cell culture systems.

What makes quantitative comparisons effective is the relative peptide isotope ratio generated of protease:control for peptides of each protein identified using MS/MS. A ratio of greater than 1 indicates that peptide levels (and thus the protein) have been increased in the protease treated sample, whereas a ratio of less than 1 indicates the protein has been degraded by the protease. Isotope ratios enables substrates to be distinguished from the background proteolysis of the sample proteome in an unbiased manner.

N-terminomic techniques have also been developed to accomplish two aims of protease studies in a single experiment. First to find substrates for a protease and second to determine where in a substrate does a protease cut (the cleavage site). N-terminomic approaches depend on the chemistry of the N-termini of proteins to isolate proteolytically generated N-termini (also known as neo-N-termini) from mature N-termini to identify substrates and sites of cleavage. Techniques such as terminal amine isotopic labeling of substrates (TAILS) rely on reduction and alkylation of N-termini of proteomes before isotopic labeling (185, 190). What makes N-terminomic techniques unique is the negative selection strategy that discerns the neo-N-termini generated by the protease of interest. The negative selection strategy of TAILS depends on a reactive polymer. After mixing the isotopically labelled protease treated and untreated proteome samples, trypsin is used to digest the mixture. The reactive polymer removes any tryptic generated N-termini from the sample. Peptides that have had their N-termini “blocked” by reduction and alkylation before trypsinization do not react with the polymer, remaining in the mixture to be analyzed by liquid-chromatography (LC)-MS/MS. These labeled peptides provide the relative peptide isotope ratios necessary for determining the proteolytic fingerprint of a protease. Other N-terminomic techniques such as combined fractional diagonal chromatography (191, 192) have also been developed. Combined fractional diagonal chromatography also relies on a negative selection strategy that

uses strong cation exchange chromatography, but it will not be discussed further as most substrate degradome studies have relied on the TAILS method.

The power of degradomic techniques was demonstrated when experiments aimed at finding the MMP extracellular and membrane-bound substrate degradome in cell secretomes consistently identified intracellular substrates (39, 186, 187, 193–196). Quantitative screens have both identified intracellular proteins in secretomes and annotated MMP cleavage sites within them, suggesting MMPs directly or indirectly (through such processes that include the cleavage of another protease class inhibitor, activation of zymogen proteases, inactivation of other proteases, and domain shedding) process intracellular proteins. The only thing holding back the recognition of these intracellular proteins as MMP substrates has been dogma. Common assumptions such as protein mislocalization artefacts by cell lysis and sample contamination have hindered validation of candidate intracellular substrates. However, the non-canonical secretion mechanisms explored above and growing recognition of the phenomenon of moonlighting has stimulated interest in pursuing these intracellular proteins as *bona fide* MMP substrates (8, 16, 73).

1.2.4 Intracellular proteins as a new class of MMP substrates in inflammation

Despite the increasing reports of degradomic screens for MMP substrates, the reality is only a small fraction of the identified candidate substrates, especially intracellular proteins, have been validated using biochemical methods *in vitro* (16). Biochemical validation has clarified MMPs can directly cleave intracellular substrates, such as MMP14 processing of peptidyl prolyl cis-trans isomerase A and HSP90 (187). Given that numerous degradomic studies have identified moonlighting intracellular proteins as MMP substrates, there exists a need to validate these proteins as *bona fide* MMP substrates. How MMP processing affects moonlighting intracellular protein activity also needs to be answered.

The simplest context to begin studying intracellular proteins as MMP substrates is studying candidate substrates with known extracellular roles. Since most intracellular MMP candidate substrates have moonlighting functions as alarmins or damage associated molecular patterns, it follows MMPs may play roles in inflammation by processing these bimodal proteins to initiate clearance, remove functional domains, or generate new activities from these proteins. Some have proposed MMP cleavage of intracellular proteins would be necessary for clearance of these proteins (195), but that denies the possibility that MMP processing might activate functional

properties of otherwise inactive proteins. Many intracellular proteins have been annotated as existing in the extracellular space for which no extracellular functions are reported. By testing how MMP cleavage affects intracellular protein activity in functional assays, studies might uncover moonlighting functions that are completely novel, only unleashed by MMP cleavage. These studies will tease apart the additional layers of complexity of MMPs in cellular processes.

Regulation of intracellular alarmins by proteolysis has already been proposed (8, 16, 73). Nuclear HMGB1 has been reported cleaved by thrombin which attenuates HMGB1 proinflammatory moonlighting activity (197). As HMGB1, a sepsis mediator (198), is a candidate MMP substrate (187), MMPs might regulate sepsis by processing HMGB1. Interaction between HMGB1 and MMP may occur during sepsis, as MMP levels are higher in the blood of sepsis patients (199). Cytoskeletal vimentin moonlights as a chemokine and is secreted by macrophages following TNFα stimulation (200). MMP12 and MMP25 processing inactivates vimentin chemokine function in the human monocytic cell line THP1 but increases phagocytosis in macrophages (201). This suggest MMPs modulate intricate “find-me” and “eat-me” signals to precisely control inflammatory processes such as clearance of dying neutrophils by processing moonlighting intracellular substrates.

1.2.4.1 Aminoacyl-tRNA synthetases as MMP substrates

One class of moonlighting intracellular proteins that are also MMP candidate substrates are the aminoacyl-tRNA synthetases (39, 177, 185, 186, 189, 196). tRNA synthetases are a family of subcellular enzymes responsible for linking or charging tRNAs with their cognate amino acids for incorporation into growing polypeptide chains during translation (202). There are 37 human tRNA synthetases: 17 encoded in the nucleus, 17 encoded in the mitochondria, and 3 enzymes which can charge tRNAs in either the cytosol or the mitochondria as “bifunctional” (203). Despite having one common canonical function in translation, eukaryotic tRNA synthetases are diverse in molecular weight, primary sequence, and in quaternary structures (204). Not only are eukaryotic tRNA synthetase heterologous in their biophysical properties, they have appended domains and sequences not found in prokaryotic homologues which are unrelated to canonical function (204, 205). These novel structural and sequence additions, which can be modulated by alternative splicing (206) and proteolysis (206, 207), afford eukaryotic tRNA synthetases non-canonical activities both inside (208–210) and outside (211, 212) the cell, making tRNA synthetases a cytokine signaling family in their own right. Novel extracellular moonlighting activities have

implicated tRNA synthetases in regulating many biological processes including inflammation (207, 213–220).

Of the 37 human tRNA synthetases, 18 have been revealed to processed, either directly or indirectly, by MMPs in degradomic screens (Table 1.1). 6 tRNA synthetases have been reported both as MMP substrates and secreted by non-canonical means under the influence of vascular endothelial growth factor (214), TNFα (213, 214), Fas ligand (221), IFNγ (222), cellular stress (207, 216, 221, 223), and apoptosis (224). These 6 tRNA synthetases have been annotated cytokine or procytokine activities: histidyl-tRNA synthetase is targeted by autoantibodies in autoimmune diseases (223), lysyl-tRNA synthetase stimulates migration and TNFα release in macrophages (213), glycyl-tRNA synthetase stimulates proliferation and migration of multiple cell-types through cadherin-6 (216), threonyl-tRNA synthetase stimulates endothelial cell migration (214), fragments of tryptophanyl-tRNA synthetase (WRS) are anti-angiogenic (206), and fragments of tyrosyl-tRNA synthetase (YRS) act as chemokines (207).

Two non-canonically secreted tRNA synthetases, WRS (full length 1-471 residues) and YRS (full-length 1-528 residues), have been defined to function as a yin and yang to each other regarding extracellular moonlighting activity (225). Eukaryotic versions of both of these tRNA synthetases have appended domains not seen in their prokaryotic homologues that are unnecessary for aminoacylation activity. However, WRS and YRS differ on which termini these domains are appended to. The N-terminus of WRS possesses a vertebrate-specific extension (1-60) and a eukaryotic-specific extension (82-154). Conversely YRS possesses a C-terminal endothelial-monocyte activating polypeptide II-like (EMAPII) domain. Both WRS and YRS have been reported to have these domains removed either at the transcriptional level by alternative splicing (226, 227) or at the post-translational level by serine protease cleavage with neutrophil elastase (206, 228, 229) and plasmin (222, 229) (Fig. 1.1). The effect of this cleavage generates unique moonlighting activities for each of these tRNA synthetases. Functionally, the removal of the N-terminus of WRS uncovers its tryptophan binding pocket, allowing the truncated proteoforms to bind vascular-endothelin cadherin on the surface of endothelial cells resulting in anti-angiogenic activities (230–233). Cleavage or alternative splicing of YRS results in the splitting of the full-length enzyme into N- and C-terminal fragments, each possessing cytokine activities (207). The N-terminal fragment of YRS stimulates endothelial cell migration and proliferation as well as acts as a chemoattractant of leukocytes (207, 234, 235). The C-terminal fragment of YRS has also been reported to act as a potent cytokine, inducing TNFα secretion in mononuclear phagocytes and chemoattraction of

neutrophils (207, 228). Proteolytic processing converts both of these inert secreted tRNA synthetases into bioactive signaling molecules which can inhibit each other in angiogenesis, thus earning them yin and yang comparisons (236–239).

Recent interest has been turned to the roles WRS and YRS play in inflammation. WRS has recently been reported secreted from immune cells exposed to bacterial (215) or viral infections (217), while YRS has been reported as a general mediator of cellular stress including starvation, heat shock, and oxidative stresses (240, 241). WRS is found in the blood of sepsis patients with systemic infections (215) and in the blood of patients suffering from chronic kidney disease (218). YRS is reported to circulate in blood normally and can be found within platelets at a higher protein level compared to other tRNA synthetases (242). To study how appended domain removal and fragmentation affects WRS and YRS moonlighting activities, past research has depended on using recombinant protein fragments as cleavage analogues (206, 207, 215, 217, 219, 220, 228, 229, 233, 243, 244). Direct proteolytic processing of full-length WRS and YRS has never been studied even in the case of known WRS and YRS cleaving serine proteases, leaving the significance of proteolytic regulation for these proteins unclear. Only two serine proteases, neutrophil elastase (206, 207) and plasmin (222, 229), have been found to cut WRS and YRS, however even in this context most of the work has centered on how fragments of WRS and YRS regulate angiogenesis and has depended on recombinant cleavage analogues, never direct processing of full-length protein into new proteoforms (206, 245). As WRS and YRS are implicated as MMP substrates (39, 185, 186, 189, 196), studying the relationship between MMPs and these two tRNA synthetases may reveal previously unknown partnerships in inflammatory processes.

1.3 MMPs as moonlighters

While the focus of this thesis is moonlighting tRNA synthetases as extracellular targets of MMPs, MMPs also serve as an example of the moonlighting proteins, outsider proteins shuttling within the cell to perform unexpected roles. A new journey is taking MMP research even further into unexplored territory, as members of the family are being identified in unexpected locations within the cell, challenging their definition as extracellular matrix proteases. Here we review novel moonlighting roles of MMPs in intracellular locations to offer a comprehensive perspective on why MMPs deserve to shed their traditional “matrix” moniker.

Experimental rigor is required to definitively show that MMPs can function inside the cell and to interpret such claims. Indeed many initial reports of intracellular MMPs relied upon histology or

Western blots only, often with just one antibody, leaving the credibility of such claims open to doubt. For definitive proof of intracellular localization, multiple antibodies should be used that have been shown in *Mmp*$^{-/-}$ cells to have no background binding and staining and confirmed using orthogonal techniques such as Edman degradation of extracted intracellular proteins. Subcellular fractionation of nuclear and cytosolic compartments or subcellular organelles need to be performed for characterization with convincing, rigorous multiple positive and negative controls. Immunohistochemical and immunocytochemistry localization needs to be performed using high resolution imaging and complimented with confocal microscopy analysis which includes 3D slices throughout the cell where possible to avoid overlap artifacts being interpreted as evidence for cytosolic/nuclear MMP protein localization and activity. Extraordinary claims require extraordinary evidence. Alternative explanations also need to be considered and discounted. For example, extracellular activity of a MMP might lead to altered cell signaling and cell function to indirectly lead to the phenomena investigated rather than necessarily being due to direct interaction and intracellular cleavage. As more evidence of multicompartmental proteins with pleiotropic functions emerges from independent groups using multiple techniques, the holes in cellular networks that regulate homeostasis will be filled.

MMPs are classically viewed as extracellular, localized to the cell surface and matrix, but they have been found in other cellular compartments. Some studies are unconvincing as to whether the MMP is genuinely functioning intracellularly: For example, studies that rely solely upon immunolocalisation, cell fractionation, or *in vitro* cleavage of intracellular substrates that may themselves be located in multiple compartments. Criteria are needed to differentiate studies with reasonable evidence for intracellular moonlighting MMP functions from those that rely on insufficient methodology (246): First, demonstration that the MMP interacts specifically with an intracellular component of the cell, *e.g.* a shuttle protein or substrate; Second, demonstration that the interaction plays a physiological role in the cell; Finally, evidence that this role is carried out away from the extracellular environment. After applying these criteria, there remains compelling evidence that several, but not all, MMPs moonlight as intracellular proteases (Table 1.2) and have additional intracellular roles unrelated to proteolysis (Table 1.3). The alternative explanations and techniques to discount these described in the following section need to be presented. Thus, many studies are not considered conclusive and so are not further discussed here.

1.3.1 Mechanisms of subcellular localization

As MMPs are renowned extracellular proteases, it is important to consider how MMPs reach subcellular compartments. These mechanisms are far from understood and further study is paramount to understanding the intracellular roles of MMPs.

1.3.1.1 Faulty secretion

Secreted proteins depend on signal sequences to target them to the endoplasmic reticulum/Golgi pathway, yet a sizeable number of secreted proteins possess inefficient signal sequences that keep a fraction of that protein from crossing the endoplasmic reticulum membrane to be targeted for secretion (247). This has been suggested as a cytosolic-extracellular sorting mechanism for MMP1, MMP2, MMP8, MMP9, MMP13, and MMP14 (73). The secretion signal sequence of MMP3 has a helix breaking Pro as the fifth residue from the N-terminus that is proposed to "weaken" the signal peptide (248) similar to calreticulin (249) and allow a fraction of MMP3 to remain within the cell (248).

Alternative splicing can also target MMPs to subcellular locales. Under basal conditions, canonical MMP2 isoforms (72 kDa proMMP2, 68 kDa active MMP2) are "targeted" to the cytoplasm by their inefficient signal sequence (250–252). However, under oxidative stress conditions (250), a cytoplasmic 65 kDa alternatively spliced N-terminally truncated MMP2 (also known as $MMP2_{NTT-76}$) lacking the signal sequence and pro-domain beginning at ^{77}Met is induced in cardiomyocytes. Thus alternative splicing appears to afford a sophisticated level of control of MMP localization.

1.3.1.2 Cellular re-entry

Secreted MMPs re-enter cells by diverse endocytosis mechanisms: α2β1 integrins, tetraspanin CD151, heparin sulfate proteoglycan CD44 (253), cholesterol sulfate of lipid rafts (254), and low-density lipoprotein related protein 1 (255–257) have all been demonstrated to bind MMPs at the cell surface (31) and may facilitate internalization, but few examples have been shown unequivocally (258). Certain cases, such as MMP2 binding integrin αvβ3, have been debunked by follow up studies (259) yet evidence for other mechanisms continues to grow. Low-density lipoprotein-related protein 1-mediated endocytosis has been associated with MMP2 (255, 256), MMP3 (257), MMP9 (260, 261), and MMP13 (262). The caveolin scaffolding domains of caveolin-1 and -3 bind to MMP2 *in vitro* and associate with MMP2 in the endocytic membrane, suggesting that endocytic caveolae may bring MMP2 to the early endosome (263, 264). MMP7 has been

observed binding to the cell surface of multiple cell-types including epithelial, cancer (265), and neural cells (266) via receptors such as CD44 (253), lipid raft components (254), and other bilayer components (267). MMP9 may bind translocating proteins to move across membranes, as it associates with the nuclear protein Ku at the cell surface (268). Once inside the cell, vesicles containing intracellular MMP9 align with the cytoskeleton of neurons and astrocytes (269), possibly for retrograde trafficking back into subcellular locales. MMP14 is thought to be endocytosed via clathrin-dependent (270, 271) and caveolae-mediated endocytosis (272, 273) and has been observed inside fibrosarcoma cells (272), breast and colon carcinomas (274, 275), glioma cells (274–276), hepatocellular carcinoma cells (277), and normal endothelial cells (273).

Exogenous recombinant proMMP12 (30) and active MMP12 (258) have been observed rapidly entering HeLa cells. Also, MMP12 secreted from murine macrophages enters murine cardiomyocytes, human bronchial epithelial cells, or *Mmp12*$^{-/-}$ fibroblasts when these cells are co-cultured (30), suggesting a robust and rapid translocation ability for MMP12. Exogenous MMP12 rapidly binds to the plasma membrane and internal membranes, including the nuclear membrane, without the need for membrane protein partners (258). The interaction is facilitated by two complementary structural features on either side of the catalytic cleft that form a membrane-binding interface that makes favorable electrostatic and hydrophobic contacts with the head groups of phospholipids in lipid bilayers.

Cargo proteins released from their receptors in the mildly acidic lumen of the early endosome can be targeted for degradation, yet bacterial toxins and viruses are able to escape endosomes (73, 278). Although lipoprotein-related protein 1-mediated endocytosis is associated with down-regulation of excessive MMP activity by endocytosis (279), it is unknown if MMPs can escape the endosome to avoid degradation in the late endosome and lysosome. Inhibiting endosomal acidification in cultured rat neurons failed to prevent endocytosed MMP7 from cleaving an intracellular substrate (266, 280), thus the mechanism by which MMP7 escapes from endosomes appears to be unaffected by pH.

1.3.1.3 Intracellular organelle trafficking

At least 10 MMPs (MMP1, MMP2, MMP3, MMP9, MMP10, MMP12, MMP13, MMP14, MMP15, and MMP26) and 2 TIMPs (TIMP1 and TIMP4) have been reported in the nucleus (30, 73, 281), and at least 13 MMPs have putative internal nuclear localization sequences (MMP1, MMP2, MMP3, MMP8, MMP10, MMP13, MMP14, MMP16, MMP17, MMP19, MMP20, MMP23, and

MMP24) (1, 281, 282). However, many of these studies must be interpreted with caution as they have often relied upon one or two criteria only and other explanations are often possible. Mutation of the nuclear localization sequence of MMP3 drastically reduces nuclear localization (248) suggesting that this nuclear localization sequence is indeed responsible for nuclear targeting. ProMMP2, with nuclear localization sequence sites at its C-terminus, has been localized in the nucleus (283), but whilst active MMP3 enters the nucleus of chondrocytes, proMMP3 does not (248). It is likely that the nuclear localization sequence of MMP3, situated at the catalytic site, is masked by the pro-domain and thus nuclear translocation may be regulated by activation state (73). Exogenous MMP3 can enter chondrosarcoma cells and translocate to nuclei within 15 min, only to disappear after 60 min, suggesting a sophisticated MMP3 shuttle system balanced between the nuclear localization sequence and nuclear export signal in the hemopexin domain (248). Caveolae-associated MMP14, that has a putative nuclear localization sequence (282), translocates to the nucleus (277) yet MMPs without nuclear localization sequences associated with clathrin or caveolae-mediated endocytosis can translocate to the nucleus through undetermined mechanisms (284, 285), possibly by latching on to nuclear translocating proteins (268).

Co-immunoprecipitation studies of isolated mitochondria from retinas of diabetic mice or diabetic human donors and their nondiabetic counterparts suggests that MMP9 translocation into mitochondria relies on the cytosolic molecular chaperones, HSP60 and HSP70, and the organelle specific translocase of the outer membrane and translocase of the inner membrane receptors, also known as the TOM/TIM44 complex (286).

To date, we have limited knowledge of the mechanisms of localization of MMPs to other intracellular compartments. Perhaps the concept that MMPs can function inside the cell is more widely accepted, there will be more studies into this exciting aspect of MMP biology.

1.3.2 MMP2 within the myocyte and beyond

1.3.2.1 MMP2 in the cytosol

MMP2 is expressed by almost all cell-types and its classical substrates are denatured collagen (gelatin) and other ECM proteins. After its discovery within cardiomyocytes (287), analysis of multiple murine tissues revealed gelatinolytic activity co-localizing with MMP2 inside hepatocytes, kidney tubuli cells, adrenal cortical cells, and oral mucosal epithelial cells (288). However, exogenous recombinant MMP2 was not found to pass to the intracellular compartment in Hela

cells whereas MMP14 and MMP12 rapidly made ingress (30). Additional immunolocalisation, fractionation, and activity studies have described MMP2 at other intracellular sites, within the nucleus (283), mitochondria (289, 290), caveolae (263), cytoskeleton (291, 292), and the thick and thin myofilaments of cardiomyocytes (289, 293, 294). Cytoplasmic MMP2 can be activated by reactive oxygen species (*e.g.* peroxynitrite (292)) and inhibition may be mediated by intracellular TIMPs, *e.g.* TIMP4 that localizes to thin myofilaments (295), or by compartmental sequestration by caveolin-1 (263, 264). MMP2 activity also depends on post-translational modifications including phosphorylation, with at least five phosphorylation sites accessible on the surface of the enzyme (296, 297), and glutathiolation (298).

1.3.2.2 Cytosolic MMP2 and muscle function

In the cytosol, MMP2 has been defined as an intracellular protease based on extensive study of its roles in cardiovascular disease such as ischemia-reperfusion injury (also known as I/R injury) (250, 287). MMP2 is abundant and ubiquitously expressed in cardiomyocytes (298) and inhibiting MMP2 has yielded defects in heart organogenesis (299). In I/R injury, sudden heart reperfusion provides cardiomyocytes with the oxygen to produce peroxynitrite, activating MMP2 intracellularly by thiol oxidation to cleave cytoplasmic substrates (292, 296, 300).

Almost all reported cytoplasmic substrates of MMP2 are associated with the cytoskeleton and sarcomere, the functional unit of skeletal muscle responsible for muscle contraction (301) (Fig. 1. 1A). These targets include α-actinin (292), troponin I (289), myosin light-chain 1 (293), and titin (294). Activating MMP2 by infusing isolated rat hearts with peroxynitrite reduced α-actinin content in the myocardium, and α-actinin levels were restored by inhibiting MMP activity (292). An MMP2-α-actinin interaction is further supported by co-immunoprecipitation of these two proteins with MMP2 activity in normal heart tissue extracts (292). Similar analysis suggests MMP2 also processes myosin light-chain 1 in rat models of acute I/R injury (293), yet the authors, possessing data for both *in vivo* and *in vitro* MMP-generated myosin light-chain 1 fragments, did not compare the terminal cleavage site residues for identical sequence comparison between models. MMP2 activity towards troponin I is supported by co-localisation and co-immunoprecipitation of the proteins together in rat heart tissue, coupled with the loss of troponin I fragment generation in rat I/R injury models upon MMP inhibition (289). MMP2 co-localizes with the sarcomere protein titin at the Z-disk region of the sarcomere: Exogenous MMP2 added to cardiomyocytes in culture cleaves intracellular titin, MMP2 inhibition reduces titin cleavage fragments in I/R injured rat hearts, and MMP2-null mice show less titin degradation when subjected to I/R injury than wild-

type controls (294). In rat cardiomyoblast lysates, co-immunoprecipitation of MMP2 and glycogen synthase kinase-3β suggests an intracellular interaction (302). Broad MMP inhibition decreases glycogen synthase kinase-3β kinase activity in oxidative stress models using these cells (302), intimating intracellular MMP proteolysis of glycogen synthase kinase-3β potentially increases the pro-apoptotic capacity of glycogen synthase kinase-3β in oxidative stress (287). Thus, proteolytic cleavage of intracellular substrates by MMP2, activated by oxidation during reperfusion, may contribute to the loss of cardiac function following reperfusion of ischaemic heart tissue (250).

Immunohistochemistry, immunogold microscopy, and *in situ* zymography revealed MMP2 in the Z-lines of the sarcomere, mitochondria, and in the nuclear membrane of skeletal muscle cells (303). However, with a lack of validation against MMP2 null cells, no known or probed intracellular partners, and no mention of a possible re-entry mechanism leaves skeletal muscle intracellular MMP2 an uncertain quantity and reinforces the need for studies designed following the guidelines discussed in the previous section.

1.3.2.3 Cytosolic MMP2 in hemostasis

Human platelets are reported to contain MMP1, MMP2, and MMP9 (304–306), that each play a role in platelet activation. Platelets do not store MMPs in their granules, but MMP2 exists in the platelet "cytoplasm" (304). Typically, the final step of platelet activation requires the Ca^{2+}-dependent protease calpain to cleave cytoskeletal talin, activating the fibrinogen receptor glycoprotein IIb/IIIa (307). In an alternative pathway, MMP2 can rapidly hydrolyse talin to activate glycoprotein IIb/IIIa (308) (Fig. 1.2A). This finding, combined with long-lived MMP2 mRNA in platelets and a reduced platelet activation capability in MMP2-null mice, suggests that cytosolic platelet MMP2 participates in hemostasis.

1.3.2.4 Mitochondrial MMP2 in cardiac injury and diabetic retinopathy

Transgenic mice expressing a cardiac-specific mutant of constitutively active MMP2, have impaired myocardial mitochondrial structure and function, including respiration and lipid peroxidation, during post-ischemic reperfusion compared to wild-type controls (309). Thus, MMP2 may be a negative regulator of myocardial mitochondrial function under oxidative stress. The alternatively spliced MMP2 isoform, $MMP2_{NTT\text{-}76}$, localizes to the cytosol, mitochondria, and the mitochondrial-associated membrane (290), a specialized subdomain of the endoplasmic reticulum responsible for Ca^{2+} signal transmission between the endoplasmic reticulum and mitochondria (290). One substrate of mitochondrial oxidative stress-induced $MMP2_{NTT\text{-}76}$, inhibitor

of kappa B-alpha (IκB-α), reveals a mechanism by which the MMP2 isoform induces mitochondrial dysfunction (251). IκB-α cleavage leads the release of nuclear factor-kappa B (NF-κB) to the nucleus for transcription of pro-inflammatory cytokines and mitochondrial stress signals (251) (Fig. 1.3). However, it must be remembered that IκB-α is rapidly phosphorylated and then ubiquitinated in the classical activation of NF-κB and this rapid normal mechanism must be clearly discounted as participatory in this example and not in fact represent the real explanation.

MMP2 mediated mitochondrial dysfunction has also been demonstrated in diabetic retinopathy (310, 311) where oxidative stress in retinal microvascular cells (pericytes and endothelial cells) leads to mitochondrial abnormalities (310). Hyperglycemia increases MMP2 abundance and gelatinase activity in mitochondria of retinal endothelial cells, leading to decreased levels of the mitochondrial chaperone, HSP60, and the mitochondrial membrane gap junction protein, connexin 43 (310), both of which are necessary for mitochondrial integrity (Fig. 1.3). Connexin 43 also links the cytosols of adjacent cardiomyocytes through the plasma membrane to mediate myocardial electrical conduction patterns, perhaps suggesting an additional mechanism by which inappropriately activated intracellular MMP2 contributes to myocardial dysfunction via disrupting electrical conduction. In silico prediction of MMP cleavage sites within the connexin 43 structure suggested that in addition to MMP2, MMP9 might also process the protein (312) as does MMP7 (see MMP7). Mitochondrial MMP2 may destabilize the mitochondrial membrane, allowing apoptotic signals such as cytochrome c to leak out. MMP-mediated mitochondrial dysfunction (311) is described as both immediate, disrupting the mitochondrial membrane, and long-term, where MMP2 accumulates in mitochondria and damages mitochondrial DNA over months, overwhelming repair mechanisms. Thus, MMP2 may yet prove to be a major mediator of mitochondrial dysfunction in disease.

1.3.2.5 Nuclear MMP2 activity and apoptosis regulation

MMP2 gelatinolytic activity has been observed in nuclear extracts of rat liver (283), cigarette smoke-exposed pulmonary artery endothelial cells undergoing apoptosis (313), and hepatocellular carcinoma cells (277). However, zymograms are exquisitely sensitive and any contamination of samples by extracellular or membrane-bound MMP2 may in fact account for some of these reported activities. Nuclear gelatinase activity in neurons (314–316) has been observed in animal models of cerebral ischemia: Mice lacking superoxide dismutase, an antioxidant, demonstrated gelatinolytic activity in their cortex neuronal nuclei in focal cerebral ischemia reperfusion (314), and ischemic rat neurons subjected to transient middle cerebral artery

occlusion showed increased *in situ* gelatinolytic activity co-localizing with DAPI-counterstained neuronal nuclei as early as 15 min after reperfusion (315), but more antibodies need to be used to be definitive. Finally, many proteases have gelatinolytic activity in biochemical assay and unexpected or undescribed proteolytic activity of bona fide other intracellular proteases may also be present and thus needs to be discounted.

The increase and co-localisation of 8-hydroxy-2′-deoxyguanosine (a marker of oxidative DNA damage) with active nuclear MMPs in mouse models of cerebral ischemia (317, 318), was inhibited in the middle cerebral artery occlusion rat model by a general MMP inhibitor (319), prompting study into DNA repair proteins being nuclear MMP substrates. Nuclear gelatinase activity towards poly-(ADP-ribose) polymerase-1 and X-ray cross-complementary factor 1 (Fig. 1.3A), nuclear enzymes necessary for DNA base excision repair, has been characterized *in vitro* and *in vivo* in neuronal ischemic injury models (317, 319). MMP inhibitors prevented loss of these repair enzymes, leading to speculation that targeting MMPs early in cerebral ischemia may prevent neuronal apoptosis (320, 321). Decreases in nuclear abundance of both repair enzymes and poly-(ADP-ribose) polymerase-1 activity, induced by *in vitro* models of ischemia reperfusion in primary rat cortical neurons, was inhibited using a selective MMP2/MMP9 inhibitor, while extracellular abundance and activity of MMPs remained unchanged in the same models, indicating nuclear MMP activity towards DNA repair enzymes (317). Co-localization of gelatinase activity and both repair enzymes in the nuclei of ischemic rat brains, coupled with inhibition of poly-(ADP-ribose) polymerase-1 and X-ray cross-complementary factor 1 proteolytic fragment generation in nuclear extracts of these tissues using the MMP2/MMP9 inhibitor further support a nuclear role for MMP2 (319). However, studies that have identified nuclear MMP2 beyond neuronal tissues (and several others including MMP1, MMP10, MMP13, and MMP15) depend upon observational immunohistochemistry data (322), and the only biochemical evidence of a nuclear interaction comes from co-immunoprecipitation of poly-(ADP-ribose) polymerase-1 and MMP2 from the nuclei of cardiomyocytes (283). Future nuclear MMP2 research will need to clarify how MMP2 enters the nucleus and what its function/partners are within.

1.3.3 Moonlighting MMP3

1.3.3.1 Cytoplasmic MMP3 in neuronal dysfunction

Intracellular active MMP3 has been found in dopaminergic cells (323), dopaminergic neuroblastoma cells (324), hepatocytes (282), chondrosarcoma cells, and in normal and

osteoarthritic chondrocytes *in vivo* (248), but the cytosolic role of MMP3 has only been studied in neural cells (323–326) (Fig. 1.2B). MMP3 is supposedly activated intracellularly by an undetermined serine protease in murine dopaminergic cells (323). In these same cells, MMP3 expression and intracellular activity was increased during cellular stress and induced apoptosis upstream of caspase-3 and downstream of c-Jun N-terminal protein kinase: Pharmacological inhibition of MMP3, siRNA silencing, and MMP3 gene knockout prevented apoptosis and caspase-3 activation, yet extracellular MMP3 had no effect on cell death. A similar effect of MMP3 on apoptosis was observed downstream of caspase-12 in mouse neuronal cell and animal models, where MMP3 activity was increased following degradation of intracellular TIMP1 by caspase-12 (324). The cytosolic targets and intracellular partners of MMP3 that induce apoptosis have yet to be identified.

1.3.3.2 Nuclear MMP3 as a protease and a transcription factor

MMP3 was first observed in nuclei of hepatocellular carcinoma cells as well as adjacent hepatocytes and myofibroblasts (282). Transfected CHO-K1 cells, expressing an active MMP3 construct that localized to the nucleus, demonstrated faster apoptosis rates than cells transfected with a proMMP3 construct that remained in the cytosol (282). Pharmacologic inhibition or active site mutation of this activated MMP3 construct reduced apoptosis, which despite the lack of nuclear substrate identification, suggests that nuclear MMP3 proteolysis is a driver of apoptosis (282) (Fig. 1.3A).

Perhaps the most interesting moonlighting role of MMPs is the regulation of gene expression, a non-proteolytic role first described for nuclear MMP3 in chondrocytes (248) (Fig. 1.3B): Gel shift assays and chromatin immunoprecipitation discovered that the hemopexin domain and hinge of MMP3 bind transcription enhancer dominant in chondrocytes in the connective tissue growth factor promoter. MMP3 binding to this enhancer rapidly trans-activates transcription and expression of connective tissue growth factor, a growth factor that drives chondrocyte proliferation and ECM production. The same study identified nuclear MMP3-associated proteins including heterochromatin proteins, transcription coactivators/corepressors, RNA polymerase II, and nucleosome/chromatin assembly proteins. Thus it appears that MMP3 is a key regulator of ECM turnover, not only mediating degradation as an extracellular protease but also stimulating synthesis as a transcription factor in chondrocyte nuclei.

MMP3 also regulates gene expression in the context of viral immunity (327): MMP3 promoted a cellular anti-viral response against Dengue virus in cell culture models (Fig. 1.3B). In infected RAW264.7 macrophages, both MMP3 levels and the expression and secretion of anti-viral cytokines increased compared to control while intracellular viral loads decreased. This anti-viral response was lost and NF-κB activity was impaired following MMP3 siRNA silencing. A NF-κB luciferase reporter assay and co-immunoprecipitation in 293T cells showed that upon Dengue virus infection, MMP3 moves into the nucleus and directly binds and activates the NF-κB p65 subunit via the hinge and hemopexin domain. NF-κB also enhances MMP3 gene transcription, suggesting a positive feedback mechanism for MMP3 in viral immunity. MMP3 may be involved in other NF-κB-regulated immune responses since inhibiting MMP3 pharmacologically (328), using siRNA (327), or genetically with *Mmp3*-null mice (329) reduces NF-κB activity in response to LPS stimulation

1.3.4 MMP7 substrates in mucosal innate immunity and cell-cell communication

Murine small intestine Paneth cells secrete defensins (cryptins) from granules (73) that have antimicrobial activity once their N-terminal pro-region is proteolytically removed. MMP7 localizes to cryptin granules in Paneth cells and processes cryptins (330–332). Similarly, inactive pro-cryptin-related protein 4C-1 is converted to its bactericidal form by MMP7 processing *in vitro* (333). MMP7-null mice lack activated cryptins (330) and cryptin-related protein 4C-1 peptides (333) in their intestines and are unable to clear infections. Thus, intracellular MMP7 appears to be associated with mucosal immunity in mice (Fig. 1.2C). Nonetheless, extracellular activities of MMP7 that impact intracellular functions may account for this and a MMP7-defensin relationship has not been demonstrated in humans

Synaptosomal-associated protein of 25 kDa (266), a neuronal cytosolic soluble N-sensitive factor attachment protein receptor involved in synaptic vesicle exocytosis, was processed in cultured rat neurons between ^{128}Ala and ^{129}Ile to a 15 kDa fragment by exogenously added MMP7. This cleavage led to long lasting inhibition of vesicle recycling, reduced vesicular protein abundance, and increased synaptic atrophy (266). Exogenous MMP7 is proposed to enter the cytoplasm by clathrin-dependent endocytosis, inhibition of which prevents MMP7-mediated synaptosomal-associated protein of 25 kDa cleavage. Connexin 43, a mediator of electrical conduction in the myocardium, is also processed by MMP7: MMP7-null mice showed increased early survival and favorable heart conduction patterns upon myocardial infarction compared to wild-type mice, whereas infused MMP7 degraded connexin 43 generating arrhythmia and heart block (334).

1.3.5 Moonlighting MMP9

1.3.5.1 Cytosolic MMP9 in immunity

Intracellular MMP9 has been demonstrated in human and murine leukocytes (335), human neuroblastoma cells, rat primary macrophages (336), and murine astrocytes (269), but how MMP9 reaches intracellular compartments is unknown. The most convincing evidence for intracellular MMP9 activity has come from studies of human and murine immune cell responses. Heterotrimeric 5′ AMP activated protein kinase monitors the energy status of cells and suppresses protein synthesis when energy is low (335). The alpha subunit of this kinase is rapidly inactivated by proteolytic processing to 55 kDa and 35 kDa fragments upon TLR4 stimulation, *e.g.* by LPS, to allow production of innate immune response proteins. Intracellular MMP9 may be responsible for the alpha subunit inactivation: MMP9 coprecipitates with the alpha subunit and generates fragments resembling the expected alpha subunit cleavage products *in vitro*. The alpha subunit is not cleaved in MMP9-null murine leukocytes challenged with LPS *in vivo* (335). Intracellular MMP9 protein in leukocytes increases within 10 min of LPS stimulation and intracellular MMP9 can be activated by peroxynitrite produced in inflammation. Thus cytosolic MMP9 may function as a novel arm of TLR4 signaling in innate immunity (Fig. 1.2D). MMP9 also cleaves other intracellular substrates *in vitro* (195), *e.g.* myosin heavy chain (337), but it remains unclear whether this is degradation of proteins spilled from damaged cells or bona fide intracellular cleavage.

1.3.5.2 Mitochondrial and nuclear MMP9 in cellular damage

Mitochondrial MMP9 is proposed to mediate mitochondrial dysfunction (338) by similar mechanisms to MMP2 (Fig. 1.3) in cardiac mitochondria during cardiac injury (339) and retinal epithelial cell mitochondria in diabetic retinopathy (311): MMP9-null mice are protected from the diabetic retinopathy seen in wild-type mice—mitochondrial ultrastructure is preserved, their retinal capillary cells do not undergo apoptosis, and mitochondrial DNA damage is absent for 7 months after development of diabetes (286). In bovine retinal endothelial cells cultured in high glucose, intracellular MMP9 gelatinolytic activity, mRNA, and protein abundance all increase time-dependently, as does the MMP9 content and activity within the isolated mitochondria of these cells as well as within isolated mitochondria from the retinas of diabetic rats (311). It must be cautioned that MMPs in the normal secretary pathway can have activity in cell lysates of course, but this has to be distinguished from true cytosolic MMP presence and activity. Selective

pharmacological MMP9 inhibition reduced the apoptosis in the bovine retinal endothelial cell model induced by high-glucose treatment, suggesting MMP9 proteolytic activity drives apoptosis in diabetic conditions (340). Decreases in both HSP60 and HSP70 in diabetic wild-type compared to MMP9-null mice indicate that they may be MMP9 substrates as well as its chaperones, contributing to mitochondrial dysfunction (286). Connexin 43 may be another MMP9 mitochondrial substrate leading to cellular damage (286). To capitalize on mitochondrial MMP2 and MMP9 as drug targets, more research is required to reveal the mechanisms by which they cause cellular damage.

Nuclear localization and activity of MMP9 has been tied to research of MMP2 in brain tissue undergoing oxidative stress in animal models of cerebral ischemia (314–317, 319). Evidence of MMP9 cleavage of both poly-(ADP-ribose) polymerase-1 and X-ray cross-complementary factor 1 (Fig. 1.4A) *in vivo* and *in vitro* is provided by the same neuronal ischemic injury models which revealed nuclear MMP2 activity (317, 319). Unlike MMP2, no co-immunoprecipitation or other evidence of a direct interaction between MMP9 and the two DNA repair enzymes in the nucleus beyond observational data or proteolytic inhibition has been provided, emphasizing the need for well-designed studies focused on proving a direct MMP9-nuclear substrate interaction.

1.3.6 Cytosolic MMP10 and Huntington's disease

Recent research has identified mutant huntingtin protein as an intracellular MMP10 substrate (341). Huntingtin protein is associated with microtubules and organelle trafficking (342–344), has a multitude of intracellular binding partners and consequently has multiple functions. Expression of mutant huntingtin protein, caused by polyglutamine (poly Q)-encoding CAG expansion in the huntingtin gene, leads to Huntington's disease where protein aggregates form neurotoxic inclusion bodies in the nucleus and cytoplasm (341). Truncated mutant huntingtin protein and N-terminal mutant huntingtin protein fragments generated by proteolysis (345) contribute to toxicity by inducing apoptosis (346), whereas inhibiting huntingtin protein proteolysis ameliorates toxicity in certain models (345). This cleavage has been attributed to the intracellular cysteine proteases caspases (345, 347) and calpains (345), but an RNAi screen of all 514 known and predicted human proteases identified 3 MMPs (MMP10, 14, 23b) as generating N-terminal toxic huntingtin protein fragments linked to Huntington's disease pathogenesis (341). Only MMP10 cleaved huntingtin protein directly *in vitro* and co-localized with mutant huntingtin protein in an immortalized striatal cell line expressing transgenic mutant huntingtin protein. Knock down of MMP10 with siRNA in this cell line reduced huntingtin protein-mediated cell death and improved

the motor deficits of the Drosophila Huntington's disease model. As study into the normal function of huntingtin protein continues, its processing by MMP10 might yet reveal this MMP to regulate non-disease processes in addition to Huntington's disease (Fig. 1.2E).

1.3.7 Non-canonical roles of MMP12 as an immune regulator

1.3.7.1 Non-proteolytic MMP12 in the phagolysosome

Intracellular MMP functions discussed so far are dependent on proteolytic activity save for transcription factor activity of MMP3. MMP12, expressed by macrophages, has non-proteolytic roles in the nucleus (30) and phagolysosome (348). MMP12-null mice demonstrate impaired bacterial clearance and increased mortality in peritoneal and lung models of bacterial infection, suggesting that MMP12 contributes to the antibacterial function of macrophages (348). Unlike the bactericidal activity of MMP7, MMP12 achieves bacterial killing by direct, non-proteolytic action (Fig. 1.2F): MMP12 is localized within phagolysosomes of macrophages where it disrupts the bacterial cell wall by insertion of a 4 amino acid sequence on an exposed β-loop of the C-terminal hemopexin domain. This conserved sequence is unique to MMP12. As MMP12 can traffic to additional intracellular membranes and vesicles (258), it appears we have only just begun to elucidate the intracellular roles of MMP12 in macrophages.

1.3.7.2 Nuclear MMP12 as transcription factor in antiviral immunity

In an *in vivo* model, MMP12 was shown to regulate viral defense as both an extracellular protease and a transcription factor (30) (Fig. 1.4B). MMP12-null mice infected with coxsackievirus type B3 or respiratory syncytial virus had greater mortality and increased viral replication in their liver, pancreatic exocrine tissue, and heart muscle compared to their wild-type counterparts. IFNα, but not IFNβ and IFNγ, secretion is inhibited in *Mmp12*$^{-/-}$ cells, which was characterized as requiring IκBα. IFNα secretion and IκBα expression are reduced in MMP12 null mice, following pharmacological inhibition of IκBα-kinase or MMP12, or silencing of MMP12 by RNAi, but are restored upon transfection with MMP12 or addition of recombinant MMP12 protein. Chromatin immunoprecipitation, combined with whole genome sequence analysis, demonstrated that the catalytic domain of MMP12 binds directly to poly (AT) sequences in the NFKBIA promoter where luciferase reporter constructs revealed it drives IκBα expression and IFNα secretion. This IFNα promotion activity is balanced by extracellular MMP12 cleavage of IFNα after day 3 of infection that prevents inappropriate systemic IFNα production in a negative feedback mechanism (30), contrasting the positive feedback of MMP3 in the anti-viral response (327).

Macrophage MMP12 was shown to enter the nuclei and bind DNA of infected and non-infected cells including HeLa and the 1HAEo- human lung epithelial cell line in trans using 8 different antibodies to different MMP12 domains and Edman degradation of protein bands from nuclear extracts. Moreover, recombinant MMP12 entered several cells including *Mmp12*$^{-/-}$ cells: Upon binding exonal DNA sequences (vs. the promotor sequences that upregulate transcription), MMP12 inhibited gene expression of both proteasome activator complex subunit 3 and secreted protein, acidic and rich in cysteine-like among 177 similar targets, an effect lost upon silencing of MMP12 expression (30). MMP12 not only down regulates transcription of these genes, but also cleaves the proteasome activator complex subunit 3 intracellularly and secreted protein, acidic and rich in cysteine-like proteins extracellularly. Thus, MMP12 has “dual regulated substrates”, targeted at both transcriptional and post-translational levels. By shutting down transcription and then cleaving the protein, complete silencing of these dual regulated substrates is achieved—an important new concept in protease biology.

1.3.8 Moonlighting MMP14 proteolytic and non-proteolytic roles

A lack of survival (< 5 weeks postnatal) and postnatal growth defects in MMP14-null mice, but no other MMP-null mice, suggests that MMP14 has unique and critical functions in fetal and neonatal growth and development, many which remain to be discovered (349).

1.3.8.1 Cytoplasmic MMP14 proteolysis

Plasma membrane anchored MMP14, once internalized, traffics through the cytosol to the centrosome inside vesicles using the tubulin cytoskeleton (350). There, MMP14 reportedly cleaves pericentrin, an integral centrosomal protein that coordinates the mitotic spindle, leading to chromatin instability and malignant transformation (Fig. 1.2G). However, this study did not show cytosolic MMP14 or provide proof that MMP14 transited to the cytosol side of the vesicles to contact pericentrin. It also utilized the transmembrane deleted mutant form of the enzyme in some experiments which may not match results for membrane anchored MMP14. Thus cytosolic MMP14 requires further research into its role in malignant transformation.

1.3.8.2 A signal transducer in MMP14

Plasma membrane MMP14 acts as a cell-surface signaling receptor via its cytoplasmic tail (Fig. 1.2G). TIMP2 binds the hemopexin domain of certain MMPs (351–353). TIMP2, binding to the hemopexin domain of MMP14, rapidly activates extracellular signal-regulated kinase 1/2 leading

to proliferation and migration of human MCF-7 breast carcinoma cells, independent of MMP14 catalytic activity (354). While only 20 amino acids long, the MMP14 cytoplasmic tail is a hub for interaction with multiple proteins and is a target for various post-translational modifications (355). For example, $p130^{Cas}$ was identified as an adaptor protein of the MMP14 cytoplasmic tail (356), mediating membrane targeting and activation of the RacI G protein necessary for macrophage migration and fusion during osteoclast and giant cell formation. Impaired macrophage migration in the MMP14-null mouse is rescued by expression of a MMP14 mutant lacking the extracellular domain, thus MMP14 appears to have signal transduction activities that are independent of extracellular ligand binding or proteolytic activity (357).

In the Golgi, where MMP14 transiently interacts with furin during secretion and activation, the cytoplasmic tail of MMP14 binds factor inhibiting hypoxia-inducible factor-1 (355). During MMP14 secretion, factor inhibiting hypoxia-inducible factor-1 is transferred to Mint3 for sequestration in the Golgi. In MMP14 deficient macrophages, factor inhibiting hypoxia-inducible factor-1 escapes to the cytoplasm, hydroxylates hypoxia-inducible factor-1 and prevents hypoxia-inducible factor-1 stimulation of glycolysis leading to a decrease in ATP production and general impairment of macrophage activity (355).

1.3.8.3 Nuclear MMP14 as immune regulator modulator

Murine wild-type and MMP14-null macrophages have comparable tissue invasiveness, but the null macrophages exhibit a heightened proinflammatory phenotype, with increased pro-inflammatory markers (*e.g.* IL6) and reduced anti-inflammatory cytokines (*e.g.* IL10) (358). Chromatin immunoprecipitation and reporter vector analysis showed that MMP14 regulates the expression of > 100 genes, many directly linked to immune responses, independent of protease activity. For example, nuclear MMP14 binds to the p110ζ promoter and activates transcription of phosphatidyl-inositol 3 kinase (PI3K)ζ, a catalytic subunit of PI3K. PI3Kζ triggers an Akt/GSK3 signaling cascade, leading to formation of the Mi-2/NuRD complex of nucleosome remodeling enzymes that limits pro-inflammatory marker expression in response to triggers like LPS (Fig. 1.4B). Thus, MMP14 acts as a pro-inflammatory response brake, allowing macrophages to transition from defense to a resolution response. Deletion of the transmembrane domain of MMP14 eliminated MMP14 trafficking to the nucleus and prevented MMP14 mediated PI3Kζ expression. Expression of an MMP14 construct, possessing the extracellular domain tethered to the membrane using the glycophosphatidylinositol anchor of MMP25 replacing its transmembrane domain and cytoplasmic tail, in MMP14-null macrophages rescued their gene expression profile,

indicating that the membrane-anchored MMP14 extracellular domain possesses the necessary transcription control elements. The mechanism of nuclear trafficking of MMP14, the nuclear partners of MMP14, and the elements responsible for p110ζ promoter binding remain unknown.

1.3.9 Cytosolic MMP25 in tumorigenesis

Unlike other MMPs, MMP26 (matrilysin 2) accumulates within cells, auto-catalytically activating itself with only a fraction being secreted (359). MMP26 is induced by estrogen via an estrogen-response element in its promoter, suggesting a role for MMP26 in estrogen receptor positive breast cancer. In tissue microarrays of breast carcinoma, cytoplasmic estrogen receptor α–dependent expression of MMP26 is inversely correlated with intact ERβ in the cytoplasm: MMP26 cleaves estrogen receptor β *in vitro* in the N-terminal region that is responsible for ligand-independent transactivation, indicating a reduction in estrogen receptor β activation in these cells (360). The cytoplasmic estrogen receptor, estrogen receptor α, is resistant to MMP26 cleavage (360). Thus, MMP26 appears to participate in an anti-tumorigenic intracellular regulatory loop in breast cancer cells, degrading and inactivating estrogen receptor β and reducing the cellular response to estrogen stimulation (Fig. 1.2H). MMP26 can also be pro-tumorigenic, activating proMMP9 in the cytoplasm of human prostate cancer cells leading to increased extracellular MMP9 proteolysis and invasiveness (361) (Fig. 1.2H). Note that these findings suffer from the same inadequacies seen in most intracellular MMP studies, including lack of demonstrated direct interaction between MMP and its intracellular substrate beyond co-localisation observations.

1.3.10 Future directions and conclusions

As we unravel the multifunctional and moonlighting roles of MMPs in various biological processes, it becomes more obvious that broadly inhibiting MMPs in cancer would lead to failure in clinical trials (173, 362). At the time, some MMPs had yet to be characterized, and intracellular functions such as cleavage, activation/inactivation of intracellular substrates, signal transduction, and control of gene expression were not recognized. Our current knowledge of MMPs has already recognized them as more than just housekeeping proteases of ECM turnover, but also as regulators of bioactive signals (8, 16, 28). The coming years will likely give insight into the evolutionary advantages and functional plasticity that these enzymes grant our proteome by acting at multiple levels in diverse cellular locations.

Moonlighting MMPs will continue to be discovered in surprising locations performing unexpected roles. Covered in other reviews (73, 195), intracellular proteins released from cells are substrates

of extracellular MMPs in healthy and disease states, further expanding the processes that MMPs can modulate. The discovery of extracellular and intracellular non-matrix substrates is expanding the degradome of MMPs, and binding gene promoters brings MMPs into the realm of transcription factors. Thus, using increasingly powerful proteomic (8) and transcriptomic (30) technologies will become ever more crucial in filling the gaps in our knowledge. These studies into MMP moonlighting potential may reinstate these proteases as one of the most promising novel drug targets of this century and may present therapeutic options to target human diseases with previously limited options (30).

1.4 Aims and hypotheses

The focus of the research explored in this thesis are the bioactive roles MMPs play by processing extracellular moonlighting tRNA synthetases, specifically WRS and YRS. I am interested in the proinflammatory moonlighting activities that tRNA synthetases carry out once released into the extracellular milieu, which MMPs target these enzymes, and how MMP processing affects tRNA synthetase moonlighting activity. When this research began, little was known of tRNA synthetase moonlighting function in inflammation with the exception of full-length lysyl-tRNA synthetase (213) and YRS fragments (207), and even less in how proteolysis affected these moonlighting enzymes. Thus, little is known about the roles tRNA synthetases play in inflammation or about how MMPs might affect these roles by processing these enzymes in the extracellular environment.

While recent work that has developed parallel to this thesis has directly implicated both WRS (215, 217) and YRS (220) as moonlighting proinflammatory cytokines, not only do these works agree with the major findings of this thesis, they have yet to explore how proteolysis affects these novel functions. That includes proteolysis that has already been demonstrated by serine proteases let alone that which I hypothesize occurs by MMPs. If an intact tRNA synthetase possesses proinflammatory function, then MMPs may inactivate this moonlighting activity by cleavage. Conversely, if an intact tRNA synthetase lacks activity as a procytokine and requires proteolysis to acquire activity, similar to known CXC chemokine ligands (CXCL)5 and CXCL8 (25), I hypothesize that MMPs would release bioactive fragments thereby promoting an inflammatory response. In this thesis the following hypotheses will be reviewed and explored to understand the roles played by MMP processing.

i) In Chapter 2, I hypothesize that MMPs process and inactivate secreted proinflammatory WRS. After confirming the secretion of full-length WRS from multiple human cell-types

including macrophages in response to proinflammatory IFNγ, I expressed and purified full-length WRS to test MMP processing of WRS *in vitro*. Using proteomic and Edman degradation methods, the cleavage sites of MMPs in WRS were identified and determined that MMPs cleave off the N-terminus of WRS to generate stable C-terminal proteoforms. Full-length WRS was found to possess proinflammatory moonlighting activities in a variety of cell culture assays, owed to its N-terminal domain extensions. The receptors responsible for mediating these activities were identified to be TLR2 and TLR4, signaling through NF-κB inflammatory pathway. Finally, N-terminal truncations by MMPs of full-length WRS attenuated the proinflammatory moonlighting activities of WRS. These studies confirmed WRS as a substrate for multiple MMPs, strengthened emerging evidence that WRS is a crucial proinflammatory mediator, and identified a new role for MMPs to play in inflammation.

ii) In Chapter 3, I hypothesize that MMPs process and activate secreted YRS as a proinflammatory cytokine. First, the constitutive secretion of YRS from human cells was confirmed. I expressed and purified full-length YRS to test the cleavage of YRS by MMPs *in vitro*. Proteomic and Edman degradation methods were employed to determine the locations of MMP cleavage sites in YRS. These analyses demonstrated that MMPs cleave within the C-terminus of YRS to generate stable N-terminal proteoforms. Full-length YRS was found to possess proinflammatory moonlighting activities in cell culture assays. TLR2 was determined to be the receptor responsible for YRS proinflammatory activity, dependent on NF-κB activation. MMP processing potentiated the proinflammatory activities of YRS. Thus, these studies validated YRS as a substrate for multiple MMPs and demonstrated MMP processing enhances YRS proinflammatory cytokine activities. Moreover, it agrees with the most recent report that YRS and its truncated proteoforms engages TLR2 for moonlighting activity (220).

This thesis and the research presented herein advances our knowledge of the mechanisms MMPs use to regulate inflammatory responses. Owing to advances in proteomics, we now know proteases regulate many processes beyond accepted dogma. Investigating the significance of these substrates has now become a focus of research as more and more novel activities for moonlighting MMP substrates are discovered and exploited for therapeutic strategies. Understanding the functions of moonlighting proteins, including tRNA synthetases,

and how they are regulated by MMP processing will continue to reveal previously unknown pathogenic mediators and novel drug targets.

1.5 Tables, figures, and figure legends

Table 1.1 Degradomic identification of tRNA synthetases as candidate MMP substrates.

tRNA synthetase	1	2	3	4	5	6	7	Secreted (Ref.)
Alanyl-		X	X			X		
Arginyl-						X		
Asparaginyl-		X		X		X		
Aspartyl-					X	X		
Glutaminyl-						X		
Glutamyl/prolyl-					X			
Glycyl-		X		X	X	X		(216, 221)
Histidyl-						X		(223)
Isoleucyl-						X		
Leucyl-						X		
Lysyl-	X					X		(213)
Methionyl-						X		
Phenylalynyl-						X		
Seryl-		X	X	X				
Threonyl-							X	(214)
Tryptophanyl-	X					X	X	(215, 217, 222)
Tyrosyl-				X	X	X		(207, 224)
Valyl-						X		

*X denotes that the tRNA synthetase was identified as a substrate in numbered study specified above. Study secretomes or tissues were derived from: 1) iTRAQ labeled murine *Mmp2*$^{-/-}$ fibroblasts (186); 2) iTRAQ labelled TAILS analysis of murine *Mmp2*$^{-/-}$ fibroblast secretomes treated with recombinant MMP2 (177); 3) iTRAQ labeled TAILS analysis of murine *Mmp2*$^{-/-}$ fibroblast secretomes treated with recombinant MMP9 (177); 4) Dimethylation labeled TAILS analysis of murine *Mmp2*$^{-/-}$ fibroblasts (185); 5) iTRAQ labeled TAILS analysis of MMP2-null mouse skin inflammation model (189); 6) iTRAQ labeled TAILS analysis of TNFα-treated RAW264.7 murine macrophages (196); 7) ICAT labeled human MDA-MB-231 breast carcinoma cell line (39). ICAT, isotope-coded affinity tags; iTRAQ, isobaric tags for relative and absolute quantification; TAILS, Terminal Amine Isotopic Labeling of Substrates.

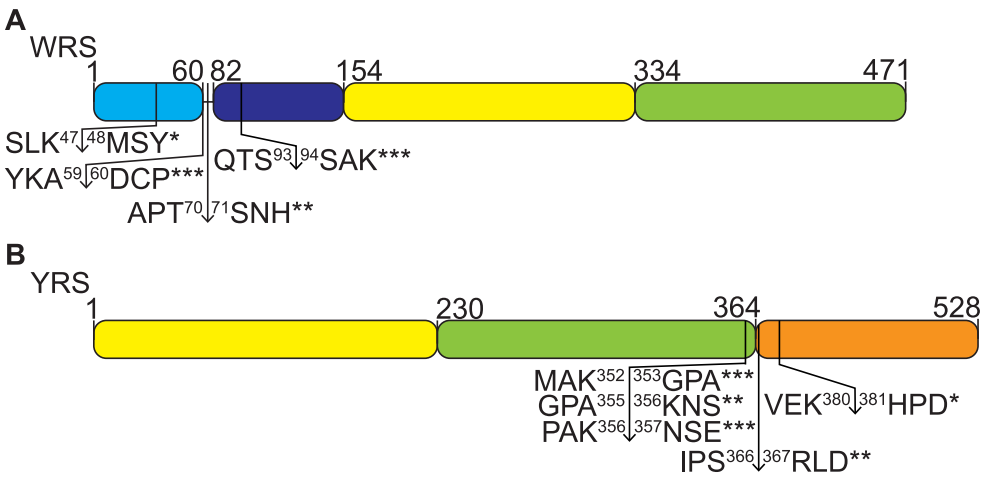

Figure 1.1 Known truncation sites in WRS and YRS by alternative splicing and serine proteases.

Truncation sites (↓) are shown in schematic diagrams of human WRS (A) or YRS (B) generated either at the transcriptional level by alternative splicing (*) or at the post-translational level by proteolysis with serine proteases neutrophil elastase (**) and plasmin (***). Light blue, vertebrate-specific extension (VSE) domain; dark blue, eukaryotic- specific extension (ESE) domain; yellow, Rossman fold catalytic domain; green, anticodon recognition domain; orange, endothelial monocyte-activating polypeptide II-like (EMAPII) domain. WRS truncation references: alternative splicing, (226); neutrophil elastase cleavage, (206); plasmin cleavage, (222). YRS truncation references: alternative splicing, (227); neutrophil elastase and plasmin cleavage, (229).

Table 1.2 Known proteolytic activities of moonlighting MMPs.

MMP	Location	Substrate	Cell-type	Proposed Role	Ref.
MMP2	Cytoplasm	α-actinin	Cardiomyocytes	Contractile dysfunction	(292)
		Tn1			(289)
		MLC-1			(293)
		Titin			(294)
		GSK-3β	Cardiomyoblasts	Apoptosis	(302)
		Talin	Platelets	Aggregation	(308)
	Mitochondria	HSP60, Cx43	Retinal endothelial cells	Apoptosis	(310)
		IκB-α	Myoblastic cells		(251)
	Nucleus	PARP1, XRCC1	Neurons	Apoptosis	(314, 319)
MMP3	Cytoplasm	?	Dopaminergic neurons	Apoptosis	(323, 324)
	Nucleus	?	Hepatocellular carcinoma cells, CHO cells, myofibroblasts	Genetic instability, apoptosis	(282)
MMP7	Cytoplasm	Pro-defensins	Paneth cells	Murine mucosal immunity	(330–333)
		SNAP-25	Neurons	Synaptic transmission loss	(266)
		Cx43	Cardiomyocytes	Gap junction loss	(334)
MMP9	Cytoplasm	AMPKα	Leukocytes	Innate immunity	(335)
	Mitochondria	Cx43, HSP60, HSP70	Retinal cells	Apoptosis	(286)
	Nucleus	PARP1, XRCC1	Neurons	Apoptosis	(314, 319)

MMP	Location	Substrate	Cell-type	Proposed Role	Ref.
MMP10	Cytoplasm	Mutant Htt	Striatal cells	Toxic fragment generation	(341)
MMP14	Cytoplasm	Pericentrin	Glioma, breast, colon carcinoma cells	Chromatin instability	(350)
MMP26	Cytoplasm	ERβ	Breast carcinoma cells	Anti-tumorigenic	(360)
		pro-MMP-9	Prostate cancer cells	Tumor invasion	(361)

*? denotes unknown substrate. AMPKα, 5′AMP-actviated protein kinase alpha; Cx43, connexin 43; ERβ, estrogen receptor beta; GSK-3β, glycogen synthase kinse-3 beta; HSP60, heat shock protein 60; HSP70, heat shock protein 70; Htt, huntingtin; IκB-α, inhibitor of kappa B-alpha; MLC-I, myosin light-chain I; MMP, matrix metalloproteinase; PARP1, poly-ADP-ribose polymerase1; SNAP-25, synaptosomal-associated protein of 25 kDa; TnI, troponin I; XRCC1, X-ray cross-complementary factor 1.

Table 1.3 Known non-proteolytic activities of moonlighting MMPs.

MMP	Location	Action	Domain	Cell-type	Proposed role	Ref.
MMP3	Nucleus	Transcription factor	Hemopexin + hinge	Chondrocytes	CCN2/CTFG expression	(282)
				RAW264.7 macrophages	NF-κB activation, DENV response	(327)
MMP12	Cytoplasm (phagolysosome)	Bactericidal	Hemopexin	Macrophages	Cell wall disruption	(348)
	Nucleus	Transcription factor	Catalytic or full length MMP12	Fibroblasts, myocytes, bronchial epithelial, macrophages	Anti-viral response	(30)
MMP14	Cytoplasm	Signaling	Cytoplasmic tail	MCF-7 cells	Proliferation	(354)
				Macrophages	Motility, fusion, energy regulation	(355–357)
	Nucleus	Transcription factor	Extracellular	Macrophages	Inflammation	(358)

CCN2/CTGF, connective tissue growth factor; DENV, Dengue virus; MMP, matrix metalloproteinase; NF-κB, nuclear factor-kappa B.

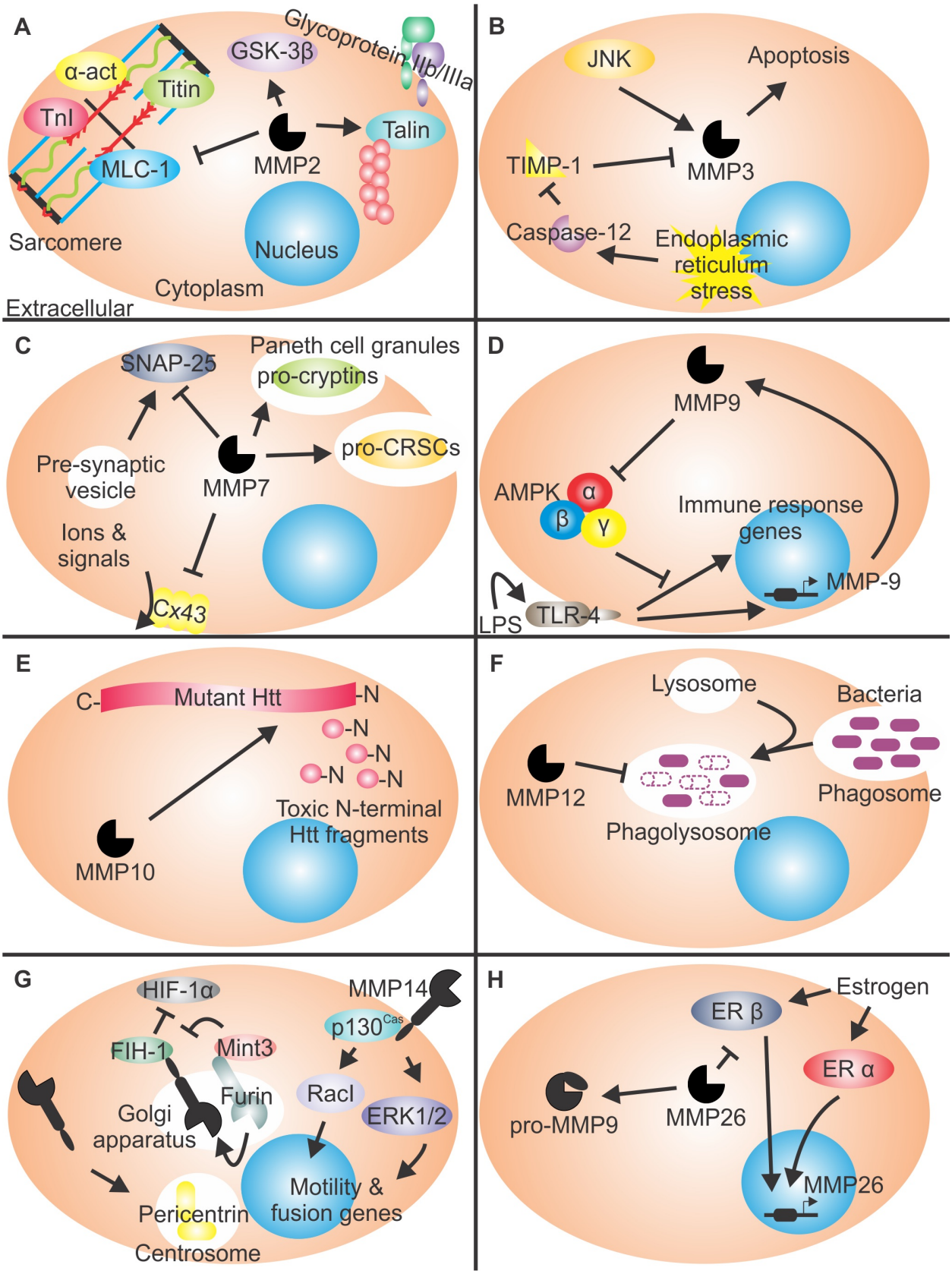
A
α-act
Titin
TnI
MLC-1
Sarcomere
GSK-3β
Glycoprotein IIb/IIIa
MMP2
Talin
Nucleus
Cytoplasm
Extracellular
B
JNK
Apoptosis
MMP3
TIMP-1
Caspase-12
Endoplasmic reticulum stress
C
SNAP-25
Paneth cell granules
pro-cryptins
Pre-synaptic vesicle
MMP7
pro-CRSCs
Ions & signals
Cx43
D
MMP9
AMPK
α
β
γ
Immune response genes
MMP-9
LPS
TLR-4
E
C-
Mutant Htt
-N
Toxic N-terminal Htt fragments
MMP10
F
Lysosome
Bacteria
MMP12
Phagosome
Phagolysosome
G
HIF-1α
MMP14
p130Cas
FIH-1
Mint3
Furin
Golgi apparatus
Racl
ERK1/2
Motility & fusion genes
Pericentrin
Centrosome
H
Estrogen
ER β
ER α
pro-MMP9
MMP26
MMP26

Figure 1.2 Activities of cytoplasmic MMPs.
Matrix metalloproteinases (MMPs) inactivate (flat head) or activate substrates (arrow head). (A) MMP2 cleaves α-actinin (α-act), (292), troponin I (TnI) (289), myosin light-chain I (MLC-I) (293), and glycogen synthase kinase 3β (GSK-3β) (302) in cardiomyocytes and talin (302) in platelets. (B) Both c-Jun N-terminal kinase (JNK) (323) and endoplasmic reticulum stress (324) (via caspase-12 cleaving tissue inhibitor of matrix metalloproteinases-1 (TIMP-1)) both activate neuronal MMP3 in apoptosis. (C) MMP7 activates mucosal innate immunity by cleaving pro-cryptins (330–332) and pro-cysteine-rich sequence 4C (CRS4C) peptides (333). MMP7 disrupts cell communication by cleaving synaptosomal-associated protein of 25 kDa (SNAP-25) (266) and connexin-43 (Cx43) (334). (D) MMP9 regulates the Toll-like receptor 4 (TLR4) response to lipopolysaccharide (LPS) by cleaving 5′AMP-actviated protein kinase (AMPK) (335). (E) MMP10 generates toxic Huntingtin (Htt) products by cleaving mutant Htt (341). (F) The phagolysosome kills bacteria using cell wall disrupting MMP12 (348). (G) MMP14 cleaves pericentrin (350) while its cytoplasmic tail acts a signal transducer through extracellular kinase ½ (ERK1/2) (354), Racl, $p130^{Cas}$ (356), and hypoxia-inducible factor-1 alpha (HIF-1α) via factor inhibiting HIF-1 (FIH-1) (357). (H) MMP26 inactivates its own transcription factor, estrogen receptor β (ERβ), in breast cancer (360) yet activates proMMP9 in prostate cancer cells (361).

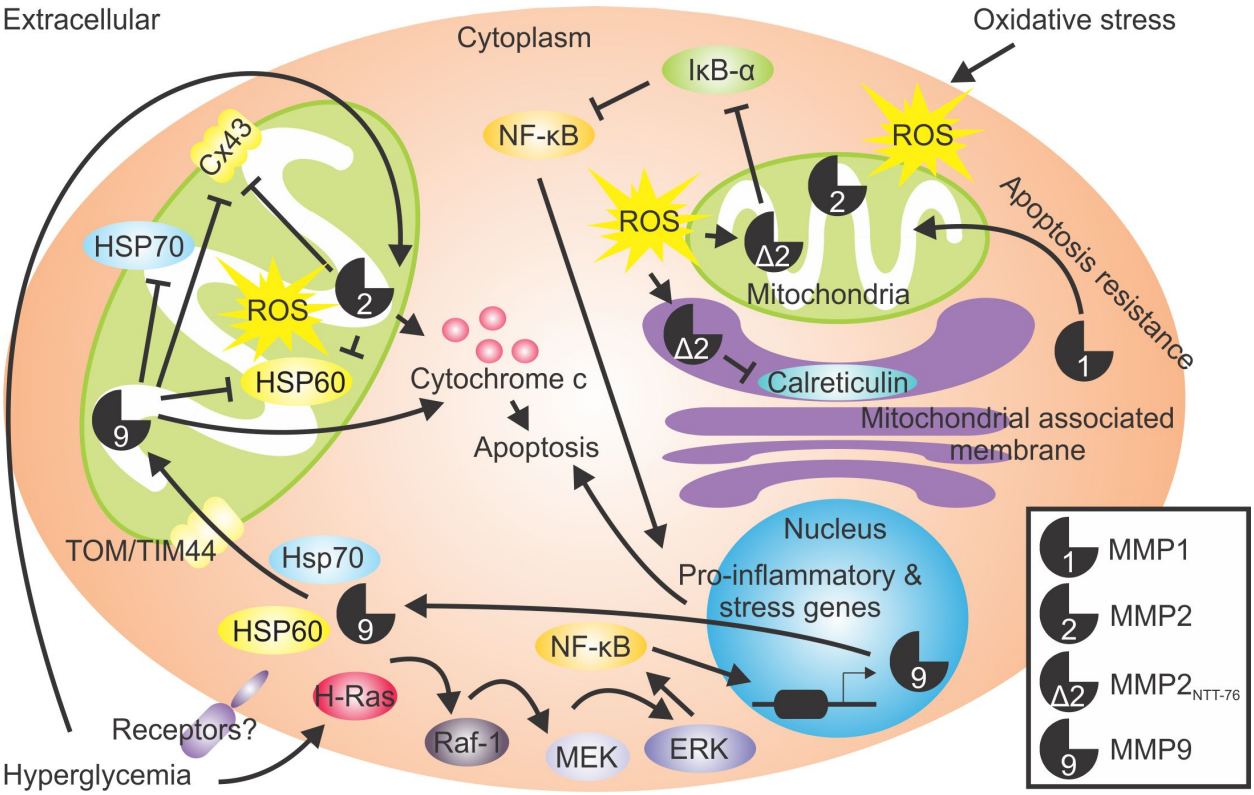

Figure 1.3 Mitochondrial MMPs and cellular damage.
Matrix metalloproteinases (MMPs) inactivate (flat head) or activate substrates (arrow head). 68 kDa active MMP2 and 65 kDa truncated MMP2 ($MMP2_{NTT-76}$) exist in both the mitochondria and mitochondrial associated membrane (290). Oxidative stress drives both $MMP2_{NTT-76}$ expression and reactive oxygen species (ROS) generation, leading to MMP2 proteolysis of heat shock protein 60 (HSP60) and connexin 43 (Cx43) (310). Hyperglycemia drives both MMP2 and 9 mitochondrial accumulation (311). Mitochondrial damage ensues, leading to cytochrome c release and apoptosis. $MMP2_{NTT-76}$, that cleaves inhibitor of kappa B-alpha (IκB-α), allows nuclear factor kappa B (NF-κB) to activate pro-inflammatory and mitochondrial stress gene expression (251). MMP9 enters mitochondria through the translocase of the outer membrane and translocase of the inner membrane receptor 44 complex (TOM/TIM44) chaperoned by HSP60 and 70 (286). Both hyperglycemia and oxidative stress induced ROS (339) drive mitochondrial MMP9 accumulation. Potential downstream substrates that induce mitochondrial dysfunction include Cx43, HSP60, and 70 (286).

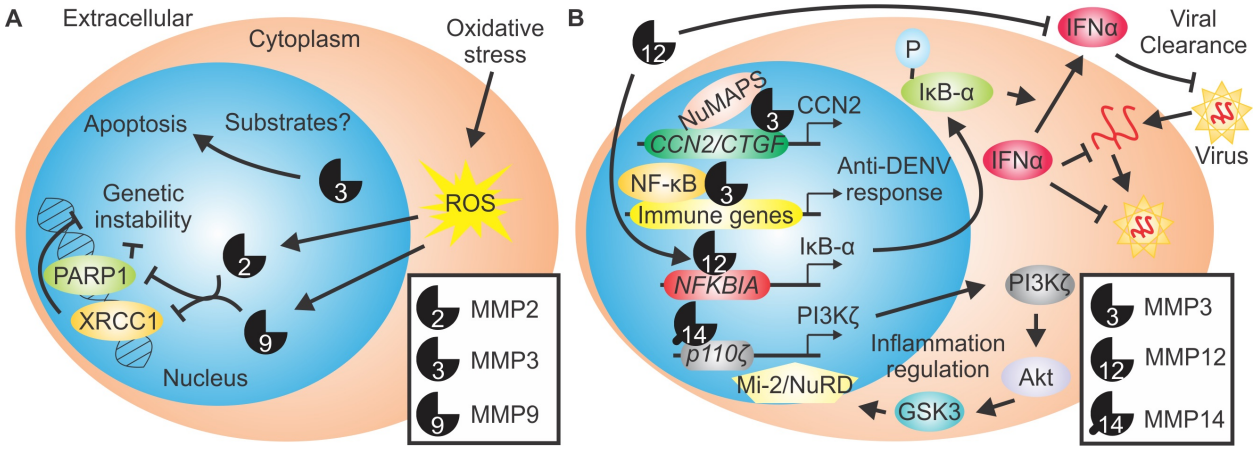

Figure 1.4 MMPs as nuclear proteins.
Matrix metalloproteinases (MMPs) inactivate (flat head) or activate substrates (arrow head). (A) MMPs act as nuclear proteases associated with genetic instability and apoptosis. MMP2 and 9, activated by oxidative stress induced reactive oxidative species (ROS), cleave DNA repair enzymes poly-ADP-ribose polymerase1 (PARP1) and X ray cross-complementary factor 1 (XRCC1) (314, 319), leading to genetic instability. MMP3 is found in multiple cell-type nuclei (248, 282, 323, 324) and is thought to contribute to apoptosis. (B) MMPs have multiple transcription factor activities. MMP3 associates with nuclear MMP3 associated proteins (NuMAPS) to drive the connective tissue growth factor (CCN2/CTGF) gene expression in chondrocytes (324) and binds nuclear factor-kappa B (NF-κB) in the anti-Dengue virus (DENV) response (327). Macrophage secreted MMP12 acts in trans on nearby cells, entering nuclei to drive the gene (NFKBIA) encoding inhibitor of kappa B-alpha (IκB-α) (30). Phosphorylated (P) IκB-α stimulates interferon α (IFNα) secretion, vital for viral clearance. MMP12 degrades secreted IFNα to limit systemic toxicity. Normally MMP14 drives phosphatidyl-inositol 3 kinase delta (PI3Kζ) expression using the p110ζ promoter in macrophage (358). This stimulates a PI3Kζ/Akt/glycogen synthase kinase 3 (GSK3) cascade to activate the Mi-2/NuRD complex of nucleosome remodeling enzymes, stopping an overactive pro-inflammatory response via gene control.

Chapter 2: Matrix metalloproteinases inactivate the proinflammatory functions of secreted moonlighting tryptophanyl-tRNA synthetase

2.1 Synopsis

Tryptophanyl-tRNA synthetase (WRS), a cytosolic aminoacyl-tRNA synthetase essential for protein synthesis, is one of a growing number of intracellular proteins that are attributed distinct non-canonical "moonlighting" functions in the extracellular milieu. We report that WRS was secreted from human macrophages, fibroblasts, and endothelial cells in response to proinflammatory interferon (IFN)γ and was a potent monocyte chemoattractant. WRS signaled primarily through Toll-like receptor 2 (TLR2) leading to TNFα and CXCL8 (IL8) secretion from macrophages and phosphorylation of the p65 subunit of NF-κB with associated loss of IκB-α protein. WRS increased matrix metalloproteinase (MMP) activity in the conditioned medium of macrophages in a TNFα-dependent manner. Multiple MMPs, but primarily macrophage MMP7 and neutrophil MMP8, cleaved secreted WRS at several sites. Notably, cleavage at ^{48}Met matched the N-terminus of a known alternatively spliced WRS proteoform. Designated Δ1-47 WRS, MMP-cleaved WRS lacked TLR signaling and proinflammatory activities. Thus, our data suggests that moonlighting WRS promotes IFNγ proinflammatory activities with MMPs providing negative feedback to later dampen these responses.

2.2 Introduction

Aminoacyl-tRNA synthetases perform the crucial task of ligating amino acids to their cognate tRNA molecules during protein translation. Unexpectedly, many aminoacyl tRNA synthetases are multifunctional proteins (8, 363) that perform additional cellular functions both within (210, 364) and outside the cell (5, 204). Despite the lack of traditional signal peptides, several tRNA synthetases are secreted by non-classical means (207, 213–215, 217, 221, 222, 224) and perform extracellular "moonlighting" roles — notably regulation of several processes including inflammation (204, 211, 212, 365).

The moonlighting functions of the aminoacyl-tRNA synthetases are primarily mediated by additional domains in higher eukaryotic tRNA synthetases (204, 227). Eukaryotic tryptophanyl-tRNA synthetase (WRS) (53 kDa, 471 residues) has N-terminal extensions known as the vertebrate-specific extension (VSE) (residues 1-60), also called the WHEP domain, and the eukaryotic-specific extension (ESE) (residues 82-154), which are not required for aminoacylation

and indeed are absent from its prokaryotic homologues (206, 366). WRS can be alternatively spliced to a proteoform lacking the N-terminal 47 residues, designated as Δ1-47 WRS (226, 367).

Interferon (IFN)γ is a proinflammatory cytokine that in human umbilical vein endothelial cells up-regulates the expression of cytosolic WRS and Δ1-47 WRS (222, 226, 367–371), as well as their secretion (222). WRS is also rapidly secreted from immune cells in response to both bacterial (215) and viral infections (217), suggesting its potential role in inflammation and immunity. Functional differences between WRS and alternatively spliced Δ1-47 WRS remain unclear. *In vitro*, neutrophil elastase generates stable WRS products, Δ1-70 WRS and Δ1-93 WRS (206), and WRS is also cleaved by plasmin (222). Unlike full-length WRS, elastase-truncated forms of WRS gain angiostatic properties through inhibition of endothelial cell migration, proliferation (206, 372), and angiogenesis (233). The effects of cleavage on inflammatory functions of WRS are unknown.

Macrophages adopt a spectrum of cellular phenotypes depending on their mode of activation (133, 137), ranging from the most polarized proinflammatory (M1) macrophages to anti-inflammatory (M2) macrophages that contribute to the resolution of inflammation, promote healing, and extracellular matrix reformation. Differentiation to M1 macrophages is induced by IFNγ, as well as tumor necrosis factor alpha (TNFα) (24, 131, 132). IFNγ-activated macrophages express several matrix metalloproteinases (MMPs), including MMP7 that has long been associated with macrophage function and is often stated to be destructive in inflammation (22, 330). M2 macrophage polarization is induced by interleukin 4 (IL4) (131, 132).

MMPs not only degrade extracellular matrix proteins, but also process virtually all chemokines and a multitude of other signaling factors (8, 21, 23, 24, 189, 196, 373). This has led to a shift in interest to their signaling roles, especially in dampening inflammation and that defines MMPs as anti-targets in many pathologies (362). We have previously identified WRS as a candidate MMP substrate using degradomics (39, 186, 196), *i.e.* proteomics techniques for the analysis of proteolysis, with quantification enabled by isotope-coded affinity tags (ICAT) (39), isobaric tags for relative and absolute quantification (iTRAQ) (186), or by Terminal Amine Isotopic Labeling of Substrates (TAILS) that identifies the cleavage-sites themselves (189, 196). Here, we report the effects of IFNγ on WRS expression and secretion from macrophages as well as proteolytic processing of WRS by MMPs. We describe how cleavage of the N-terminus of WRS to the Δ1-47

WRS proteoform by MMP7 and MMP8 abrogates its proinflammatory functions, aligning with other well documented anti-inflammatory activities of MMPs.

2.3 Results

2.3.1 Secretion of WRS was induced by IFNγ

To investigate potential inflammatory roles of WRS, we profiled the secretion of WRS in response to cytokine stimulation of macrophages. THP1 monocytes were differentiated to a macrophage-like phenotype (THP1 M0) using phorbol 12-myristate 13-acetate (PMA). After treatment with IFNγ (20 ng/mL), TNFα (40 ng/mL), or IL4 (40 ng/mL), we collected cytosolic, membrane, and conditioned media fractions. Immunoblot analysis using antibodies recognizing the N- or C-terminus of WRS (αN-WRS and αC-WRS, respectively) showed that only the pro-inflammatory IFNγ increased cytosolic WRS levels (*N* = 3; Fig. 2.1A). IFNγ also increased WRS in the cell membrane and conditioned medium fractions, indicating that WRS translocated to the plasma membrane and was secreted to the medium upon IFNγ stimulation in M1 macrophage polarization (Fig. 2.1A). Several lower molecular weight proteoforms of WRS were identified in the cytosol and conditioned medium following IFNγ stimulation. Predominant detection by the αC-WRS antibody revealed that these were N-terminally truncated. The effect on WRS was IFNγ-selective as IL4, TNFα (Fig. 2.1A), IFNα, and IFNβ (*N* = 3; Fig. 2.2A) had no effect on WRS protein levels or secretion. The absence of tubulin in the conditioned media supported secretion of WRS rather than cell lysis, and the absence of the plasma membrane protein Na^+/K^+ ATPase in the cytosolic fractions confirmed the fidelity of cell fractionation.

We isolated human monocytes from the peripheral blood mononuclear cells (PBMC) of three healthy human subjects. Monocytes were differentiated into primary M0 macrophages using monocyte-colony stimulating factor, and then cultured with IFNγ (20 ng/mL) or IL4 (40 ng/mL) to induce polarization to proinflammatory M1 or M2-type macrophages, respectively. Polarization was confirmed using the M1 marker indoleamine 2,3-dioxygenase and M2 marker transglutaminase 2 (Fig. 2.1B). Immunoblot analysis of cell lysates showed that, as with the THP1-derived macrophages, full-length WRS and additional smaller WRS proteoforms were markedly increased only in response to IFNγ. This included a form migrating like Δ1-47 WRS that was only detected by αC-WRS. Again, the absence of tubulin in the conditioned culture medium confirmed that there was little if any non-specific release of cytoplasmic proteins by cell lysis.

A time-dependent increase in WRS expression and secretion up to 48 h occurred in response to 20 ng/mL IFNγ in THP1 M0, endothelial cells (*N* = 3; Fig. 2.1C, D), and BJ human skin fibroblasts (*N* = 2; Fig. 2.1E), again with no change in tubulin protein. WRS secretion was dependent on IFNγ concentration, with 10 ng/mL inducing maximal WRS secretion (*N* = 3; Fig. 2.2B). The secreted proteoforms detected by each antibody were consistent in size between cell-types: αN-WRS, ~41, 39, and 32 kDa; αC-WRS, ~48 and 36 kDa, and these matched the electrophoretic migration of intracellular forms.

2.3.2 WRS stimulated proinflammatory monocyte and macrophage activities

Phosphorylation of the p65 subunit of NF-κB leads to upregulated transcription of multiple cytokines and chemokines, including TNFα, in macrophages and a variety of other cells (103). WRS (100 nM) treatment of THP1 M0 cells induced phosphorylation of p65 coincident with a decrease in protein levels of the NF-κB pathway inhibitor IκB-α (*N* = 3; Fig. 2.3A – C). Both responses were maximal at late time points indicating that NF-κB was activated by an indirect pathway.

ELISA showed that WRS (100 nM) also stimulated TNFα release from THP1 M0 cells, but Δ1-47 WRS or heat denatured WRS did not (*N* = 3; Fig. 2.3D), indicating that both the N-terminus and tertiary structure of WRS are important for signaling. We used an antibody-array to screen for the secretion of 36 different cytokines and chemokines from human PBMC-derived primary macrophages in response to 100 nM WRS (Fig. 2.4), which confirmed that WRS increased TNFα protein secretion, in addition to MIP-1α/β, CXCL8 (IL8), and CXCL1 (*N* = 2; Fig. 2.3E). Recombinant Δ1-47 WRS did not stimulate cytokine and chemokine release from PBMCs (Fig. 2.3E).

WRS displayed chemoattractant activity for monocytes in transwell migration assays (*N* = 3; Fig. 2.3F) (23). As with chemokine secretion, WRS chemoattractant activity was lost upon removal of the N-terminal 47 residues of WRS and heat denaturation (Fig. 2.3F). Thus, the N-terminal region of WRS in particular is essential for its signaling and proinflammatory responses.

2.3.3 WRS signaled via Toll-like receptors 2 and 4

Several pattern recognition receptors mediate innate immune signaling, including the Toll-like receptor (TLR) family in monocytes and macrophages (103, 374). We used HEK293 cells

transfected with a NF-κB alkaline phosphatase reporter linked to TLR2, TLR4, or TLR9, the intracellular DNA receptor as a negative control (Fig. 2.5A). We found that TLR2 and TLR4 were significantly stimulated by WRS, but not by Δ1-47 WRS (100 nM) (*N* = 3; Fig. 2.5A), consistent with the loss of activity of Δ1-47 WRS on TNFα release from THP1-derived M0 macrophages (Fig. 2.3D). Likewise, boiling of WRS led to loss of activity. Thus, the N-terminal sequence and fold of WRS are critical for TLR2 and TLR4 receptor engagement and signaling.

Next, we found that the NF-κB pathway inhibitor BAY11-7082 (10 μM), an IκB kinase inhibitor (375, 376), C29 (100 μM), a specific inhibitor of TLR2 signaling that disrupts the intracellular recruitment of myeloid differentiation primary response gene 88 to TLR2 (377), and 1 μg/mL CLI-095, a cyclohexane derivative that disrupts the intracellular domain of TLR4 (378, 379), all blocked TLR activation from the WRS-treated reporter cell lines (*N* = 2; Fig. 2.5B, C). This was confirmed using an antibody specific for TLR2 (αTLR2) or for TLR4 (αTLR4) before 100 nM WRS treatment (*N* = 2; Fig. 2.5D, E). Notably, the alkaline phosphatase readout for TLR2 was ~10-fold greater than for TLR4 indicating that signaling via TLR2 was the dominant pathway.

The effects of the signaling inhibitors in blocking TLR2 and TLR4 signaling at the concentrations used for the TLR reporter cells was confirmed using macrophages. We measured TNFα release from THP1-derived M0 macrophages incubated in the absence and presence of TLR signaling inhibitors and 100 nM WRS by ELISA. All inhibitors blocked TNFα release from WRS-treated THP1 M0 cells (*N* = 2; Fig. 2.6A). This was confirmed using the TLR2 and TLR4 blocking antibodies. TNFα release in THP1 M0 cells was reduced 40% by 5 μg/mL of αTLR2, 25% by αTLR4 antibody, and 80% by a combination of these antibodies, compared to antibody isotype controls (*N* = 2; Fig. 2.6B). Thus, these results and those from the reporter cells demonstrated that WRS triggers TLR2 especially, with a minor contribution by TLR4, to stimulate NF-κB activation and TNFα release in macrophages.

We had removed lipopolysaccharide (LPS), a potent heat-stable proinflammatory TLR stimulator, from our *E. coli*-expressed recombinant WRS using Triton X114 during bacterial cell lysis and using polymyxin B-agarose columns after purification. Furthermore, in all experiments 10 μg/mL polymyxin B was added to all cultures where WRS was used. To be fully confident that WRS, and not any contaminating LPS, drove the proinflammatory effects seen, the recombinant WRS and Δ1-47 WRS used for all presented experiments was expressed in *E. coli* ClearColi® BL21 (DE3)

cells, which produce a modified LPS lacking both the oligosaccharide chain and two of the six acyl chains required for endotoxin signaling in human cells (380, 381). As the limulus amoebocyte lysate test for endotoxin is ineffective for proteins prepared from ClearColi® (380), we further confirmed that the recombinant WRS proteins were free of LPS by demonstrating that the removal of 10 μg/mL polymyxin B from cell culture experiments did not increase TNFα secretion in response to 100 nM WRS, whereas addition of 100 ng/mL LPS did (*N* = 4; Fig. 2.7A). Heat-denaturation of WRS also eliminated TNFα release even in the absence of polymyxin B, confirming the absence of heat-stable LPS. (*N* = 4; Fig. 2.7B).

2.3.4 WRS was cleaved by MMPs

MMPs regulate inflammation by processing bioactive proteins to alter their function (22, 24, 382). MMP cleavage of WRS was explored using 9 recombinant MMPs (Fig. 2.8A), which generated stable cleavage products rather than degrading WRS (Figs. 2.8A, B): MMP7, MMP8 and MMP13 processed WRS most efficiently with little intact WRS remaining; MMP2, MMP3, MMP9, and MMP14 also cleaved WRS; whereas MMP1 and MMP10 cleaved WRS poorly. Activity for all MMPs was confirmed using quenched fluorescent peptide cleavage assays (not shown). Hence, the lack of activity on WRS by MMP1 and MMP10 was due to specificity differences. The spectrum of activity towards WRS was reflected by dose response digests (Fig. 2.8B), which showed that MMP8 and MMP7 cleaved WRS entirely at 1:10 MMP:WRS molar ratio compared to MMP14 which could not entirely digest WRS at a higher molar ratio of 1:5. Plasmin and neutrophil elastase were included as positive controls.

Edman N-terminal sequencing of the major MMP7 and MMP8 cleavage products (Fig. 2.9) revealed that WRS was cleaved at ^{48}Met by both MMPs to generate Δ1-47 WRS (~48 kDa), homologous to the Δ1-47 WRS alternatively-spliced proteoform, and by MMP8 at ^{90}Val to generate Δ1-90 WRS (~39 kDa). Both MMPs produced a smaller C-terminal WRS proteoform (Δ1-334 WRS) commencing at ^{335}Leu at the junction of the catalytic and anticodon recognition domains (Fig. 2.9). Peptide mapping using liquid chromatography tandem mass spectrometry (LC-MS/MS) analysis of SDS-PAGE-resolved MMP-cleaved WRS fragments confirmed both N- and C-terminal truncations of WRS (Fig. 2.10). Other members of the MMP family generated similar proteoforms of WRS: MMP2, MMP3, MMP7, MMP8, MMP9, MMP13, and MMP14 also produced a ~48-kDa fragment matching the Δ1-47 WRS alternatively-spliced mini-WRS. MMP2, MMP3, MMP8, MMP9, MMP13, and MMP14 generated a ~43-kDa proteoform; and MMP3,

MMP8, MMP9, MMP13, and MMP14 generated a ~39-kDa band comparable with the ∆1-93 WRS product of neutrophil elastase cleavage (Fig. 2.8B). Since peptide mapping by shotgun proteomics does not necessarily identify the actual neo N-terminal P1' residue of the cleavage site, Amino-Terminal Oriented Mass Spectrometry of Substrates (ATOMS), a sensitive targeted mass spectrometry sequencing method for identifying proteolytically generated N-termini (383, 384), was employed. Like Edman degradation, ATOMS identifies N-terminal residues without consideration of their relative abundances in a proteolytically digested mixture, but ATOMS is much more sensitive. ATOMS identified > 30 cleavage sites, including those characterized by Edman sequencing, many of which were common to several MMPs and resulted in N- and C-terminal deletions (Fig. 2.11).

2.3.5 MMP-cleavage attenuated the WRS-induced proinflammatory response

We tested how cleavage of WRS by MMP7 and MMP8 affected the WRS-induced proinflammatory responses of monocytes and macrophages (Fig. 2.12A, B). Cleavage of WRS by MMP7 or MMP8 decreased chemotaxis of THP1 monocytes by 87% and 76%, respectively, in Transwell migration assays (*N* = 3; Fig. 2.12A, C). Similarly, 100 nM WRS-induced TNFα release from THP1-derived M0 macrophages was reduced by 99% and 84% upon MMP7 or MMP8 cleavage, respectively (*N* = 4; Fig. 2.12D). Thus, the removal of the N-terminus of WRS by MMP7 and MMP8 abrogated both chemotaxis and TNFα stimulatory responses in THP1 monocytes/macrophages. In other words, proinflammatory TLR signaling by extracellular WRS was inactivated by N-terminal proteolytic processing.

TNFα is known to induce the expression of MMPs (44). Since we showed that WRS induced TNFα secretion from macrophages, we tested whether WRS promoted MMP expression via TNFα. Inflixamab (100 ng/mL), a monoclonal antibody inhibitor of TNFα, was added to THP1-derived M0 macrophages treated with 100 nM WRS, ∆1-47 WRS, or 40 ng/mL TNFα as a positive control. Using a quenched fluorescent peptide cleavage assay we assayed for MMP activity in the conditioned medium: WRS treatment increased MMP activity with similar potency to TNFα (*N* = 3; Fig. 2.13), but ∆1-47 WRS had no effect indicating that the increase in MMPs was dependent on the N-terminal domain of WRS. Furthermore, the inclusion of Inflixamab with WRS abrogated the increase in MMP activity. Therefore, WRS mediates increased MMP protein secretion and activity through the downstream mediator TNFα.

2.4 Discussion

Our study reveals that WRS, one of 37 nuclear- and mitochondrial-encoded tRNA synthetases (203), is specifically secreted from human macrophages and other cell types in response to IFNγ, a cytokine critical to both innate and adaptive immunity that is produced during in the initiation of immune responses (385, 386). The mechanism of secretion remains unclear, but may be similar to endothelial cells stimulated with IFNγ, where cytosolic WRS interacts with two known exocytosis-regulating proteins, cytoplasmic annexin A2 and S100A10 (222), to control WRS secretion.

We found several extracellular proinflammatory functions for WRS, including induction of monocyte chemotaxis and stimulation of the release of proinflammatory TNFα and several other chemokines from macrophages, most notably the potent neutrophil chemokine IL8. We also determined that WRS activated the TLR2, and to a lesser extent TLR4 pathways, followed by phosphorylation of NF-κB subunit p65 and loss of the NF-κB inhibitor IκB-α. This is consistent with two recent reports showing that WRS engages the TLR4-myeloid differentiation factor 2 complex to stimulate an innate immune response in murine bone marrow derived macrophages (215, 217). These authors found the first 154 residues of WRS was necessary to form the TLR4 complex (215). Our data refined this observation where we showed that recombinant Δ1-47 WRS, corresponding to the WRS splice form that was upregulated in the cytosol by IFNγ, and the major cleavage product of WRS generated by both MMP7 and MMP8, did not activate TLR2 or TLR4 and was inactive in all signaling and inflammatory pathways that we investigated.

In our study, the maximal NF-κB response occurred at 1 h, which is considerably later than is typical for an immediate direct response (387), suggesting a signaling relay, which we showed included TNFα. Indeed, TLR2- and TLR4-dependent release of TNFα into the medium led to increased MMP expression and activity. We showed that MMPs, particularly MMP7 and MMP8 that are secreted from macrophages and neutrophils, respectively, cleaved in the N-terminal domain of WRS to generate Δ1-47 WRS as one of their products. This major cleaved form of WRS was inactive on TLR2 and TLR4. In line with these observations, MMP cleavage of WRS reduced TNFα release and monocyte chemotaxis, revealing a negative feedback loop mediated by MMPs that suppresses the proinflammatory actions of WRS (Fig. 2.14). Thus, MMPs in this context dampen inflammatory responses.

The distinct activities of full-length WRS and truncated proteoforms suggested that MMPs modulate IFNγ induced inflammatory processes through proteolysis of WRS. It is interesting that both MMPs and serine proteases (neutrophil elastase (206) and plasmin (222)) from different cellular and tissue sources generate similar lower molecular weight forms through extracellular proteolysis as alternative splicing does within cells, namely the N-terminal truncation of WRS to Δ1-47 WRS. Redundancy of proteases cleaving WRS would afford different cell-types the ability to control the resolution of innate immune responses, further indicating the importance of WRS in host defense. As initially proposed by Jin (365), and since both alternatively spliced Δ1-47 WRS and neutrophil elastase-generated WRS proteoforms exhibit anti-angiogenic activity (206), we hypothesize that increased secretion of WRS and accumulation of MMP-generated N-terminally truncated anti-angiogenic WRS proteoforms could pause angiogenesis at a site of injury to allow proper resolution of inflammation prior to angiogenesis. Furthermore, neutrophils, that quickly infiltrate a site of tissue injury along IL8 chemoattractant gradients and play an important role in wound healing, secrete neutrophil elastase and MMP8, which potently truncate the N-terminus of WRS terminating its proinflammatory function and promoting angiogenesis (206). Therefore, cleavage of WRS by immune cell MMPs to generate Δ1-47 WRS expands the potential functions of MMPs in regulating angiogenesis and wound healing.

In conclusion, our study shows that in human cells, MMPs exert post-translational control over moonlighting WRS to down-regulate inflammation. Our degradomics analyses previously indicated that MMPs cleave WRS in secretomes of human MDA-MB-231 cells expressing MMP14 (39) and murine MMP2$^{-/-}$ fibroblasts (186), and we have now elucidated a new MMP–WRS–TNFα axis for regulating inflammation. MMPs process a variety of substrates to regulate inflammation (22, 382), and our data here shows that WRS is another such substrate, and also confirms a new class of MMP substrate. It would be interesting to examine WRS processing in inflammatory disease — for example, both WRS and MMPs are increased in the blood of sepsis patients (199, 215), so it is possible that processing of WRS by MMPs during sepsis has a role in regulating systemic inflammation. To establish the significance of WRS proteolysis by MMPs in the immune response, non-cleavable mutant WRS animal models would be valuable, since knocking out MMPs would likely be ineffective due to proteolytic redundancy. Overall, our data reveal that WRS is an MMP substrate that is entwined in inflammation due to its moonlighting functions, eclipsing mere matrix modelling roles for MMPs.

2.5 Material and methods

2.5.1 WRS expression and purification

Human full-length WRS and Δ1-47 WRS with a C-terminal His-tag in pET28a were expressed in ClearColi® BL21 (DE3) (Lucigen) in Lennox Broth under kanamycin (20 µg/mL) selection. Cell pellets were resuspended in ice-cold column buffer (20 mM KH_2PO_4, 500 mM NaCl, 10 mM imidazole, 2 mM β-mercaptoethanol, pH 7.8) supplemented with protease inhibitors (1 mM AEBSF, 1 mM EDTA, 10 µM E-64, 10 µM leupeptin, and 1 µM pepstatin A). Clarified cell lysates were treated with Triton X114 as previously described (388). Treated lysates were loaded onto a Ni-NTA Perfect Pro (Qiagen) column, washed with column buffer at pH 7.8, pH 6 and then pH 5.2, before elution using a 25-250 mM imidazole gradient. Fractions containing WRS were pooled, dialysed against PBS/15 % glycerol, passed through a polymyxin B-agarose column (Millipore-Sigma) and stored at –80 °C. Protein concentrations were determined by bicinchoinic acid assay (Thermo-Fisher Scientific).

2.5.2 Cell culture

The human skin fibroblast cell line, BJ (ATCC #CRL-2522), was cultured in DMEM, 4.5 g/L glucose, 10% (*v*/*v*) cosmic calf serum (CCS, Hyclone), 50 µg/mL streptomycin, and 50 U/mL penicillin. Human primary umbilical vein endothelial cells (HUVEC) (Lonza #C2519A) were cultured in Vascular Cell Basal medium plus Endothelial Cell Growth kit-VEGF (both from ATCC).

Blood was donated by healthy volunteers using University of British Columbia Clinical Research Ethics Board approved protocol (#H06-00047). Informed consent was obtained from all donors and research was conducted in accordance with the Declaration of Helsinki. PBMCs were prepared from buffy coats obtained using Ficoll-Pacque™ PLUS (GE Healthcare). Monocytes were isolated from PBMCs using an EasySep™ Human Monocyte Isolation Kit (Stemcell) following the manufacturer's instructions. Monocytes (2×10^5/mL) were differentiated into primary macrophages (M0) by culturing in 50 ng/mL monocyte-colony stimulating factor in ImmunoCult™-SF Macrophage Medium (both Stemcell) for 4 days. For cytokine/chemokine array analysis, PBMC-derived M0 were serum-starved and treated for 3 h in serum free growth medium, 10 µg/mL polymyxin B (Millipore-Sigma) with 100 nM WRS, Δ1-47 WRS, or PBS. Clarified conditioned media was assayed using a Human Cytokine Array® (#ARY005B, R&D Systems) as per manufacturer's instructions. Membranes were blocked with Odyssey Blocking Buffer (LI-COR) for 20 min and detected with Alexa Fluor® 680-Streptavidin (Thermo-Fisher Scientific). Imaging

was conducted with a LI-COR Odyssey infrared imager (LI-COR). Spots were quantified by densitometry using ImageJ software (NIH).

THP1 cells (human monocytic cell line, ATCC #TIB-202) were cultured in RPMI growth medium: RPMI-1640, 4.5 g/L glucose, 10% (*v*/*v*) CCS, 50 µg/mL streptomycin, and 50 U/mL penicillin. THP1 M0 macrophages were differentiated from THP1 monocytes (1 x 10^6 cells/mL) using 100 ng/mL phorbol 12-myristate 13-acetate (PMA) as previously described (24). Experiments were performed in serum-free growth medium containing 10 µg/mL polymyxin B on PMA-differentiated THP1 M0 cells synchronized by serum-starvation. For NF-κB pathway analyses, cells were treated with 100 nM WRS for up to 3 h. PBS-washed cells were lysed with 50 mM Tris-HCl, 150 mM NaCl, 10 mM EDTA, 0.2 % (*w*/*v*) Zwittergent, pH 8 supplemented with a protease and phosphatase inhibitor cocktail (Biotool). Cleared lysates were analysed by immunoblotting (see below). For TNFα release, THP1 M0 were treated for 3 h with 100 nM WRS, heat-denatured WRS (boiled for 5 min), Δ1-47 WRS, *E. coli* 0111:B4 lipopolysaccharide (LPS) (Millipore-Sigma), or PBS. TNFα in conditioned media was quantified using a human TNFα ELISA kit (Duoset® ELISA, R&D Systems). For TLR inhibitor experiments, 5 µg/mL TLR2 blocking antibody (#maba2-htlr2, InvivoGen), IgA2 (#maba2-ctrl, InvivoGen) isotype control antibody, TLR4 blocking antibody (#mabg-htlr4, InvivoGen), IgG1 isotype control (#mabg1-crtlm, InvivoGen), 1% (*v*/*v*) DMSO vehicle, 100 µM C29 (MedChemExpress), 1 µg/mL CLI-095 (InvivoGen), 10 µM BAY11-7082 (Selleckchem) or combination thereof were added to THP1 M0 1 h prior to treatment with 100 nM WRS for 3 h.

For chemotaxis, 100 nM WRS, heat-denatured WRS, Δ1-47 WRS, 50 nM CCL7, or PBS in chemotaxis buffer (RPMI-1640, 20 mM HEPES, 0.1% BSA, 10 µg/mL polymyxin B) was dispensed into the lower reservoir of chemotaxis chambers (Neuroprobe). A 5 µm membrane was placed over the wells. Serum-starved THP1 monocytes were resuspended (1 x 10^6 cells/mL) in chemotaxis buffer and cells (2 x 10^5 cells) were added to the top reservoir. After 90 min at 37 °C, cells were collected from the bottom chamber and quantified using CyQUANT® (Thermo-Fisher Scientific). CCL7 was synthesized as previously described (168).

HEK-Blue™ (human embryonic kidney 293) cells co-expressing the NF-κB reporter system and TLR2, TLR4, TLR9 or receptor-null counterparts (Null1 and Null2) were cultured in DMEM growth medium with selective antibiotics. Cells and reagents were from InvivoGen and assays were carried out according to their instructions. For TLR reporter assays, 96 well plates were seeded

with TLR2 and Null1, TLR4 and Null2, or TLR9 and Null1 HEK-Blue™ cells and incubated with 100 nM WRS, Δ1-47 WRS, heat-denatured WRS, or PBS with 10 μg/mL polymyxin B for 18 h. Conditioned media were assayed for NF-κB activation in QUANTI-Blue™ detection medium. For TLR inhibitor experiments, cells were incubated with antibodies and inhibitors for 1 h prior to treatment with 100 nM WRS for 18 h as for THP1 M0 above.

2.5.3 WRS secretion assays

Serum-free media containing various concentrations of human IFNα (Cedarlane), IFNβ, IFNγ, IL4 (all Peprotech), TNFα (Millipore-Sigma), or combinations thereof were added to PBMC-derived M0, PMA-differentiated THP1 M0, HUVEC, and fibroblasts at 80% confluence. Clarified conditioned media were harvested at times shown and protease inhibitor cocktail (Biotool) and 1 mM EDTA were added. PBS-washed cells were lysed with Zwittergent buffer containing protease inhibitor cocktail as above. Membrane and cytosolic fractions were isolated from THP1 M0 using a Mem-PER™ Plus membrane protein extraction kit (Thermo-Fisher Scientific) as per manufacturer's instructions.

To precipitate proteins, 15% (*v*/*v*) trichloroacetic acid was added to conditioned media samples, centrifuged, and the protein pellet was washed with 100% acetone. Pellets were air-dried, re-solubilized by boiling for 5 min in 4 x SDS-PAGE loading buffer (0.5 M Tris, 8 M urea, 8% (*w*/*v*) SDS, pH 6.8), and diluted 4-fold. Protein concentrations were determined by A_{280}nm.

2.5.4 Immunoblotting

Samples were diluted in SDS-PAGE loading buffer with DTT and denatured by boiling before separation using 10% SDS-PAGE and transfer to PVDF membrane (Immobilon-FL, Millipore-Sigma). After blocking with Odyssey Blocking Buffer (LICOR) for 20 min, primary antibodies (at concentrations recommended by manufacturers) were incubated overnight at 4 °C. Primary antibodies: Affinity-purified polyclonal antibodies against WRS (N-terminal, #A304-274A) (C-terminal, #A304-275A) Bethyl Laboratories; monoclonal antibodies IDO (#86630), TGM2 (#3557), total NF-κB p65 (#4764), phospho-NF-κB p65 (Ser 536; #3033), and total IκB-α (#4814) all Cell Signaling Technology; α-tubulin (#sc-53646) Santa Cruz Biotechnology; Na^+/K^+ ATPase (ab76020) Abcam. Secondary antibodies, goat anti-mouse IgG conjugated to IRDye 800CW (LI-COR) and goat anti-rabbit IgG conjugated to Alexa Fluor® 680 (Thermo-Fisher Scientific), were

applied for 1 h at 25 °C. Imaging was conducted with an Odyssey infrared imager. Where indicated, bands were quantified by densitometry using ImageJ software (NIH).

2.5.5 MMP expression and purification

Human MMP7 cDNA was subcloned into pGW1GH, both generously provided by J. M. Clements (British Biotech Pharmaceuticals, Oxford, UK). The MMP7–pGW1GH was electroporated into CHO-K1 cells (ATCC #CCL-61) grown in DMEM, 4.5 g/L glucose, 10% (*v*/*v*) CCS, 50 µg/mL streptomycin, 50 U/mL penicillin. Stable clones were selected with 25 µg/mL mycophenolic acid, cultured to 80% confluency in flasks, transferred to 1,700 cm^2 roller bottles (Corning), and grown with rotation in serum-free medium (1:1 *v*/*v* CHO-SFM (Thermo-Fisher Scientific):DMEM). One tenth volume of buffer (500 mM 2-(*N*-morpholino)ethanesulfonic acid, 1 M NaCl, 50 mM $CaCl_2$, pH 6)) was added to clarified conditioned medium and loaded onto a green Sepharose column (Millipore-Sigma). After washing, bound protein was eluted using a 1-2 M NaCl gradient. The eluate, dialysed against 20 mM Tris, 5 mM $CaCl_2$, pH 7.4, was loaded onto a Q-Sepharose (Millipore-Sigma) column. After washing, bound protein was eluted with 20 mM Tris, 200 mM NaCl, 5 mM $CaCl_2$, pH 7.4. Fractions containing MMP7 were assayed for activity as below and stored at –80 °C.

C-terminally FLAG-tagged murine MMP10 in pGW1GH was expressed and purified from CHO-K1 cells. Conditioned medium was loaded onto a green Sepharose (Millipore-Sigma) column and eluted as described for MMP7. Eluate, dialysed against 50 mM Tris, 150 mM NaCl, pH 7.4, was loaded onto an αFLAG-agarose column (Millipore-Sigma), washed with dialysis buffer and MMP10 was eluted with 100 mM glycine, pH 3.5 into tubes containing 50 µL 1 M Tris, pH 8. Fractions containing MMP10 were exchanged into 50 mM HEPES, 150 mM NaCl, 5 mM $CaCl_2$, pH 7.2 using Ultra-4 Centrifugal Filter Units (Amicon). Activity was assayed as below and aliquots were stored at –80 °C.

We expressed and purified recombinant human MMP1, MMP2, MMP3, MMP8, MMP9, MMP13, and soluble MMP14 (lacking the transmembrane domain) as previously described (389). MMP activity was validated by quenched fluorescence synthetic peptide substrate cleavage assays using Mca-Pro-Leu-Gly↓Leu-Dpa-Ala-Arg-NH_2 (R&D systems) as previously described (389, 390).

To assess MMP activity in conditioned medium, THP1 M0 were cultured in phenol red-free, serum-free growth medium for 24 h with 10 µg/mL polymyxin B plus 100 nM WRS, TNFα 40 µg/mL, or PBS ± 100 µg/mL Inflixamab (#NBP2-52655, Novus Biologicals). Clarified conditioned medium was concentrated 20 x using Ultra-4 Centrifugal Filter Units and 40 µg protein was assayed for MMP activity using the quenched fluorescence peptide cleavage activity as above.

2.5.6 WRS cleavage assays

ProMMPs were activated for 20 min at 25 °C with 1 mM *p*-aminophenylmercuric acetate (APMA) in HEPES buffer (50 mM HEPES, 150 mM NaCl, 5 mM $CaCl_2$, pH 7.2). APMA was removed by dialysis against HEPES buffer at 4 °C for 1 h. WRS cleavage assays were performed at protease:WRS molar ratios described in the figures. Human serine proteases neutrophil elastase (Millipore-Sigma) and plasmin (Biovision) were reconstituted in 50 mM HEPES, 150 mM NaCl, 5 mM $CaCl_2$, pH 7.2.

2.5.7 LC-MS/MS analysis of MMP cleavage of WRS

WRS (1 µg) was digested at 37 °C ± MMP for 18 h at molar ratios selected from prior digests. Reactions were diluted 3 in 4 into sample buffer (0.5 M Tris, 8% (*w*/*v*) SDS, pH 6.8, 20% (*v*/*v*) β-mercaptoethanol), boiled for 5 min, and were resolved by 10% SDS-PAGE. Gels were stained with Coomassie brilliant Blue G-250. Cleaved WRS bands were excised, destained, lyophilized, and rehydrated in 15 µL MS-grade trypsin (12 ng/µL in 50 mM ammonium bicarbonate) for 45 min at 4 °C. Excess buffer was removed, and the gel plugs were resuspended in 15 µL ammonium bicarbonate for 18 h at 37 °C. Centrifuged plugs were discarded and supernatants were desalted using StageTips (391). Samples were run on an Easy nLC-1000 (Thermo-Fisher Scientific) online coupled to an UHR Q-TOF Impact II mass spectrometer (Bruker-Daltonics) with a CaptiveSpray nanoBooster ionization interface. Peptides (1 µg) were loaded on to a 75 µm × 400 mm analytical column containing ReproSil-Pur C18 1.8 µm stationary phase resin (packed in house; Dr Maisch GmbH) and the column temperature was maintained at 50 °C. Samples were automatically loaded onto the analytical column at 800 Bar using buffer A (0.1% formic acid) and 8 µL injection flush volume. Peptides were eluted using a 125 min gradient established with the nLC at 200 nL/min from 2% to 24% buffer B (99.9% acetonitrile, 0.1% formic acid) over 90 min, then increased to 30% over 10 min period, further increased to 95% buffer B over 5 min and finally held at 95% for 15 min. Alternatively, a 60 min gradient with 20 min separation was utilized with similar washing parameters. Peptides were ionized by electrospray ionization (2.2 kV), and MS analysis was

performed in positive ion polarity with precursor ions detected from 150 *m*/*z* to 1750 *m*/*z*. Spectra were acquired using a Top17 data-dependent method with precursor intensity-adjusted MS/MS summation time (Compass oTOF control 1.9, Bruker).

For database searching, Bruker .d files were converted to .mgf using DataAnalysis v4.3 (Bruker Daltonics) and searched with the Mascot search algorithm (MatrixScience) using the following parameters: 25 ppm MS1 tolerance, 0.08 Da MS2 tolerance, semi-tryptic enzyme specificity, variable modifications: oxidation (M), propionamide (C), N-terminal ammonia loss and N-terminal cyclization at glutamine and glutamic acid against the reverse concatenated *H. sapiens* Uniprot database (downloaded 2014-10-01; 69,085 sequences). Result files were imported into Scaffold v4.8.7 (Proteome Software) and searched with X!Tandem (392). Search results were filtered for 1% FDR at the peptide and protein level. The N-terminal residue of the most N-terminal semi-tryptic peptide detected and C-terminal residue of the most C-terminal semi-tryptic peptide detected were defined as the N- and C-termini of the excised band respectively. The mass spectrometry proteomics data have been deposited with the ProteomeXchange Consortium (393) via the PRIDE partner repository (394) with the dataset identifier PXD013217.

2.5.8 Determination of WRS cleavage sites

WRS cleavage sites were determined by Edman degradation (performed by Tufts University Core Facility) as previously described (383, 384) and by positional mass spectrometry using ATOMS (383, 384). Briefly, WRS (100 µg) was incubated ± MMP (at molar ratios selected from prior digests) for 18 h, 37 °C. Digests were denatured with 4 M guanidine-HCl. Cysteines were reduced with 5 mM DTT, 1 h, 37 °C and alkylated with 15 mM iodoacetamide, 15 min at room temperature in the dark. Excess iodoacetamide was quenched with 15 mM DTT, 30 min, 37 °C. Lysine and N-termini were labeled with 40 mM heavy ($C^{13}D_2O$) (+ MMP) or light (CH_2O) (control) formaldehyde with 20 mM sodium cyanoborohydride, 18 h, 37 °C. Excess formaldehyde was quenched with 50 mM ammonium bicarbonate, 2 h, 37 °C. Samples were mixed, split in half, and digested for 16 h, 37 °C with either MS-grade trypsin (1 µg/mL, Thermo-Fisher Scientific) or GluC (*Staphylococcus aureus* protease V8, 1 µg/mL, Worthington). Samples were desalted and analysed by LC-MS/MS as above.

Data were analyzed using MaxQuant software v1.6.0.1 (395) and searched against a custom protein database including WRS, all proteases used, and 247 protein contaminants frequently observed in MS experiments. Enzyme specificity was set as semi-specific free N-terminus.

Quantitation of peptides was performed using the MS1 signal from heavy ($C^{13}{}_2D_4$, 34.063 Da) and light (C_2H_4, 28.031 Da) dimethylated peptides. Carbamidomethylation on cysteine was set as a fixed modification, methionine oxidation and asparagine deamidation were set as variable modifications. Delta score-based false discovery rates of 1% and 5% were set for peptide and protein identification respectively. Peptide-spectrum matches corresponding to N-terminal dimethylated peptides from WRS were manually validated. P1' residues of the cleavage site were identified from peptides dimethylated at the N-terminus that can only be labeled after a cleavage event, with a heavy to light ratio > 2, and identified: i) in both trypsin and GluC analyses, ii) in either trypsin and GluC analyses based on three or more peptide spectrum matches; iii) or by Edman degradation. Cleavage sites beginning at the P1' position with a charged or a hydrophilic residue with the exception of glutamine and cysteine were excluded due to known substrate preferences for MMPs (389). The data have been deposited as above under the dataset identifier PXD013367.

2.5.9 Statistics

All statistical tests were performed using GraphPad Prism version 5.0b software.

2.6 Figures and figure legends

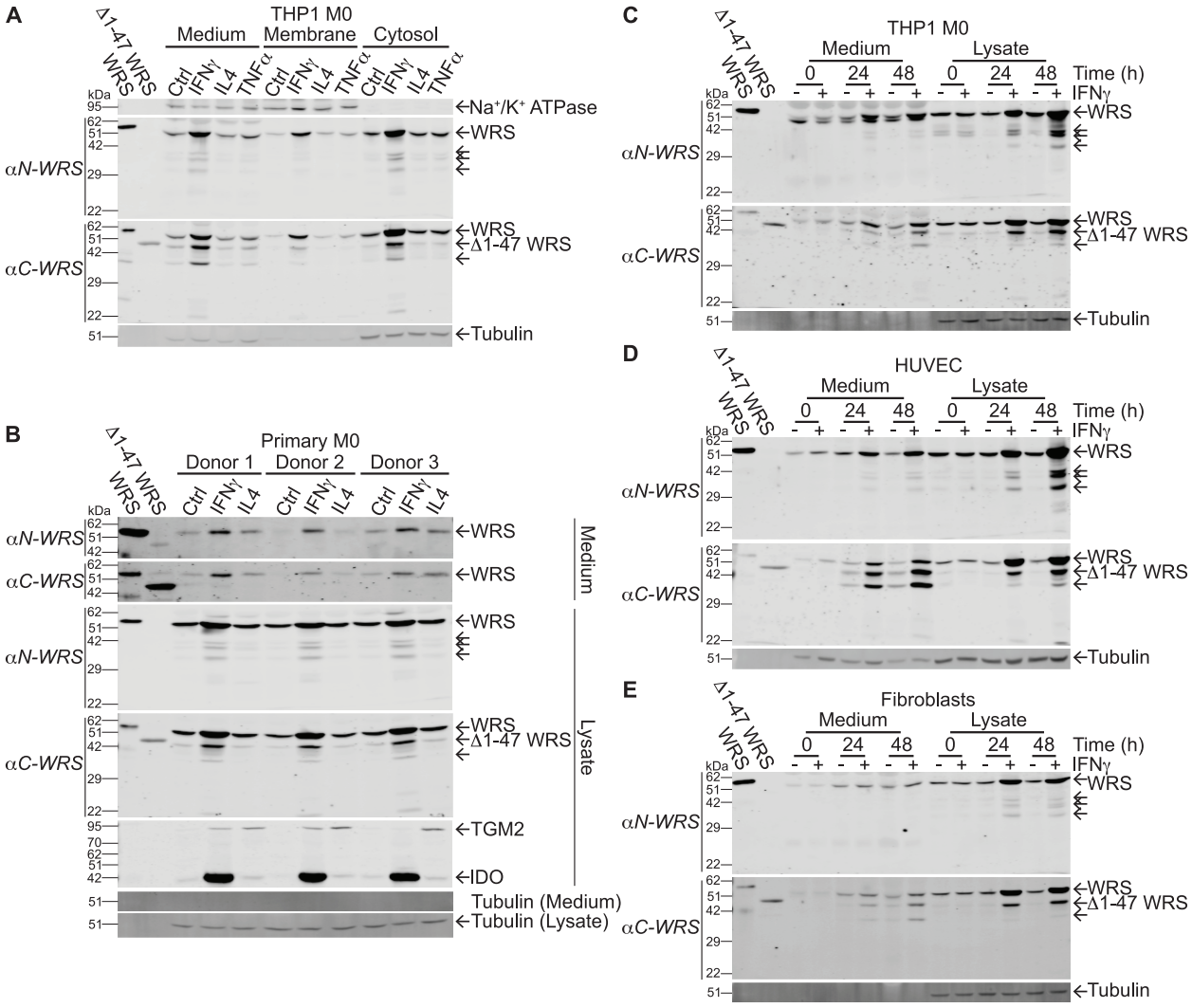

Figure 2.1 IFNγ stimulated WRS expression and secretion from human cells.
Immunoblots of PMA-differentiated (A,C) PMA-differentiated THP1-derived macrophages (THP1 M0), (B) human peripheral blood mononuclear-derived macrophages (Primary M0), (D) human umbilical vein endothelial cells (HUVEC), and (E) skin fibroblasts (BJ). Cells were treated for 24 h or for times shown with IFNγ (20 ng/mL), IL4 (40 ng/mL), or TNFα (40 ng/mL) as indicated. Antibodies specific to the N-terminus or C-terminus of WRS (α*N-WRS* and α*C-WRS*, respectively) identified WRS and proteoforms (arrows). Controls and standards were: Recombinant human WRS and Δ1-47 WRS (~58 and 48 kDa, respectively); α-tubulin, loading control; Na^+/K^+ ATPase, membrane protein loading control; polarization markers: indoleamine 2,3-dioxygenase (IDO), IFNγ stimulation to M1 macrophage polarization; transglutaminase 2 (TGM2), IL4 stimulation to M2 macrophage polarization. Representative immunoblots after 10% SDS-PAGE are shown from *N* = 3 independent experiments, *N* = 2 for fibroblasts.

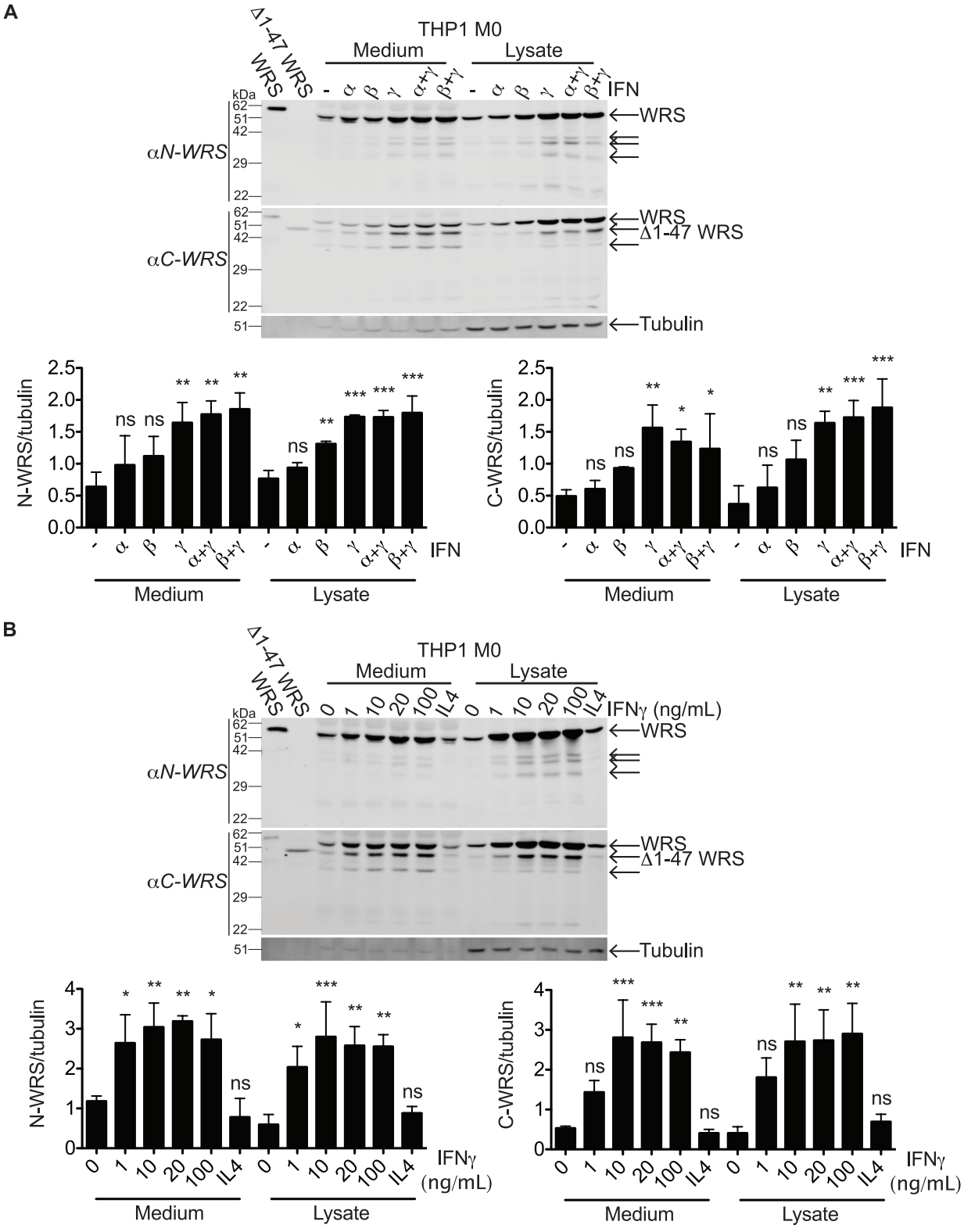
A
THP1 M0
Medium
Lysate
Δ1-47 WRS
WRS
IFN
kDa
αN-WRS
αC-WRS
WRS
Δ1-47 WRS
Tubulin
N-WRS/tubulin
C-WRS/tubulin
B
IFNγ (ng/mL)
IL4
(ng/mL)

Figure 2.2 WRS expression and secretion in THP1 macrophages was IFNγ-specific and concentration-dependent.
(A) Immunoblot analysis of PMA-differentiated THP1-derived macrophages (THP1 M0) treated for 48 h with interferons (IFN) α, β, or γ (100 ng/mL), combinations thereof, or buffer control (–). Antibodies specific to the N-terminus or C-terminus of WRS (α*N-WRS* and α*C-WRS*, respectively) identified WRS cleaved proteoforms in conditioned media and cell lysates (arrows). Recombinant human WRS and Δ1-47 WRS were loaded as standards (~58 and 48 kDa, respectively) and α-tubulin serves as a loading control. (B) Immunoblot analysis of THP1 M0 treated with 1 – 100 ng/mL IFNγ (M1 macrophage inducer), or 100 ng/mL IL4 (M2 inducer) for 48 h. Immunoreactive bands were analyzed by densitometry and relative amounts of WRS were normalized to tubulin. Graphs of means ± S.D. of $N = 3$ independent experiments are shown. Statistical significance was determined against the controls: buffer in *A* and 0 ng/mL IFNγ in *B* using a one-way ANOVA with Dunnett's multiple comparison posttests. Representative immunoblots are shown of $N = 3$ independent experiments. *, $p < 0.05$; **, $p < 0.01$; *** $p < 0.001$; ns, not significant.

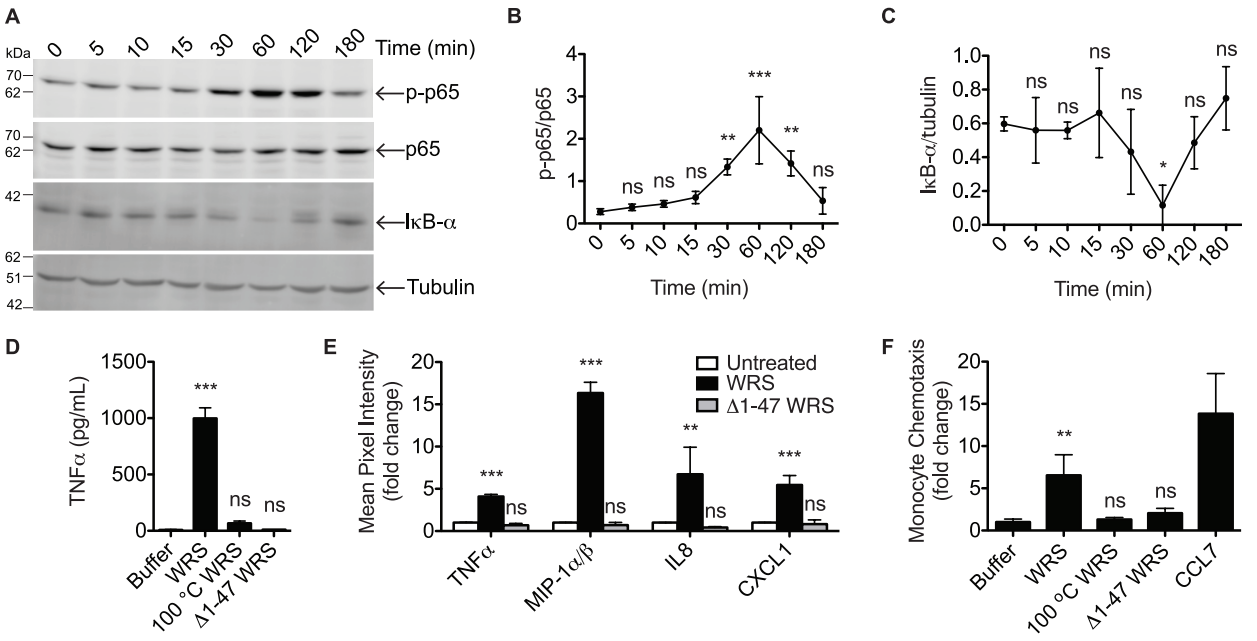

Figure 2.3 Inflammatory signaling responses were activated by WRS, but not Δ1-47 WRS. Representative immunoblots (A) and quantification (B, C) of NF-κB p65, phosphorylated p65 (p-p65), and inhibitor of NF-κB (IκB-α) protein levels in response to recombinant human WRS (100 nM) incubated with PMA-differentiated THP1-derived macrophages (THP1 M0) for the times shown. α-tubulin was the loading control. Relative band densities are plotted as means ± S.D. of *N* = 3 independent experiments. (D) TNFα protein levels in the conditioned media of THP1 M0 treated for 3 h with WRS versus Δ1-47 WRS (100 nM each), or as controls heat-denatured WRS (100 °C WRS) and buffer (means ± S.D., *n* = 4) determined by ELISA, *N* = 2 independent experiments. (E) Human cytokine protein array analysis of conditioned media of human peripheral blood mononuclear-derived macrophages treated for 3 h with WRS, Δ1-47 WRS (100 nM each), or buffer control. Mean pixel intensities were measured by densitometric analysis of the cytokine protein array shown in Fig. 2.4 and plotted as fold change compared to untreated cells (mean ± S.D., *n* = 4) of *N* = 2 independent experiments. (F) Transwell chemotaxis migration assay of THP1 monocytes towards WRS, Δ1-47 WRS (100 nM each) *versus* heat-denatured WRS or buffer over 90 min, with CCL7 (MCP-3) (50 nM) used as a positive control. Migrated cell numbers were plotted as fold changes compared to buffer (mean ± S.D., *n* = 3) of *N* = 3 independent experiments. Statistical significance was determined against controls: 0 h for *B, C*; buffer for *D, F*; and untreated for *E* using a one-way ANOVA with Dunnett's multiple comparison posttests. *, $p < 0.05$; ** $p < 0.01$; *** $p < 0.001$; ns, not significant.

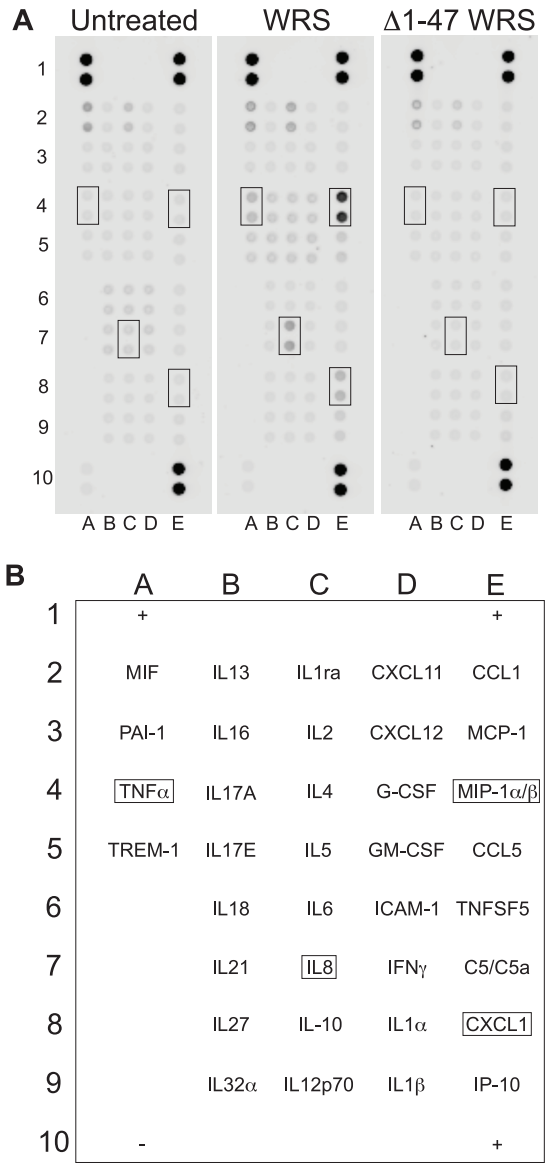

Figure 2.4 Cytokine protein array analysis of conditioned media from human peripheral blood mononuclear-derived macrophages following stimulation by WRS or Δ1-47 WRS. (A) The cytokines and chemokines reported in Fig. 2.3E are shown boxed on the Human Cytokine Array® above. (B) Grid showing the identity of cytokines and chemokines spotted on each array in *A* (each cytokine or control is spotted in duplicate). +, positive control spots; –, negative control spots.

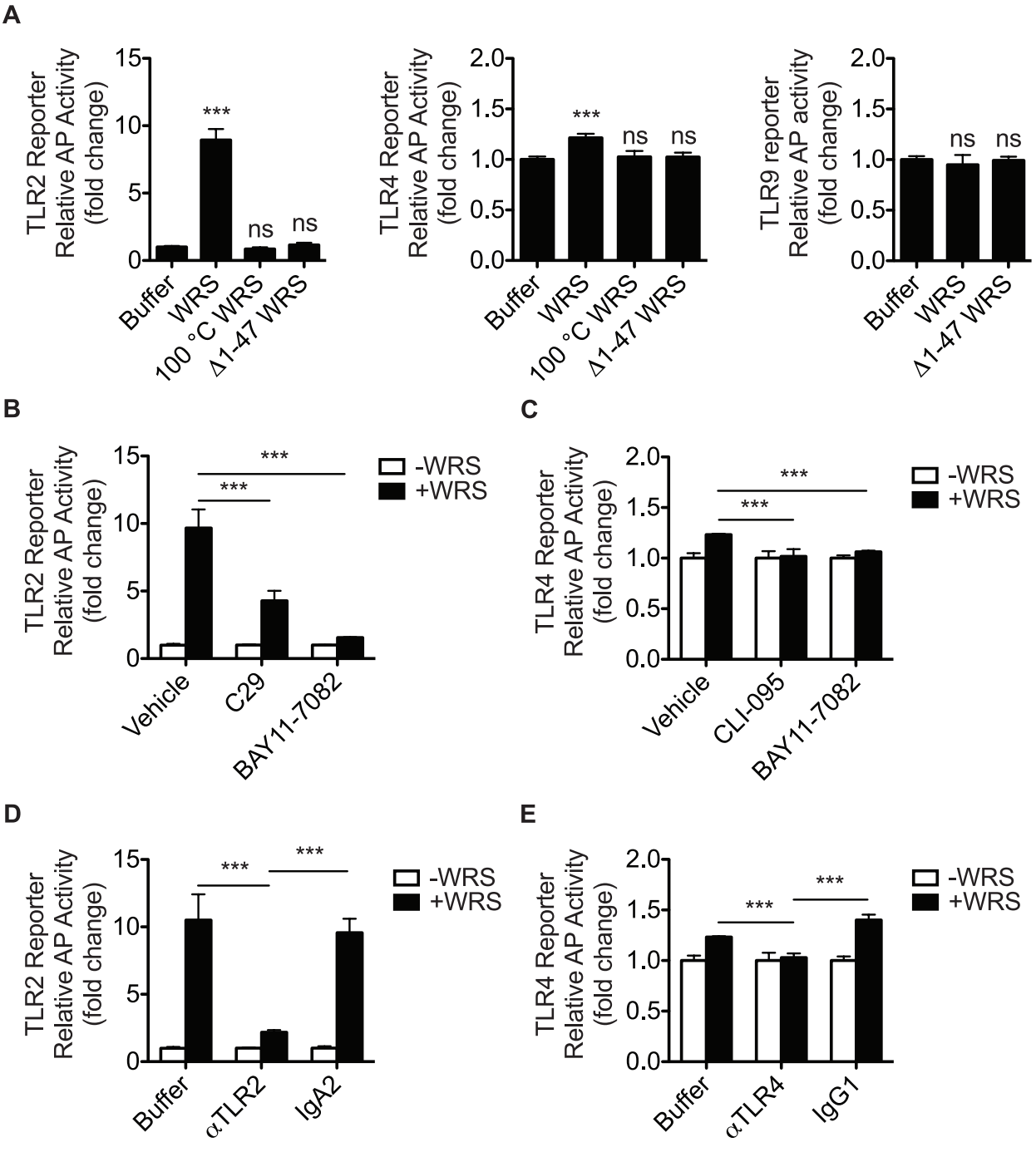
A
TLR2 Reporter Relative AP Activity (fold change)
15
10
5
0
***
ns
ns
Buffer
WRS
100 °C WRS
Δ1-47 WRS
TLR4 Reporter Relative AP Activity (fold change)
2.0
1.5
1.0
0.5
0.0
***
ns
ns
Buffer
WRS
100 °C WRS
Δ1-47 WRS
TLR9 reporter Relative AP activity (fold change)
2.0
1.5
1.0
0.5
0.0
ns
ns
Buffer
WRS
Δ1-47 WRS
B
TLR2 Reporter Relative AP Activity (fold change)
15
10
5
0
***
***
-WRS
+WRS
Vehicle
C29
BAY11-7082
C
TLR4 Reporter Relative AP Activity (fold change)
2.0
1.5
1.0
0.5
0.0
***
***
-WRS
+WRS
Vehicle
CLI-095
BAY11-7082
D
TLR2 Reporter Relative AP Activity (fold change)
15
10
5
0
***
***
-WRS
+WRS
Buffer
αTLR2
IgA2
E
TLR4 Reporter Relative AP Activity (fold change)
2.0
1.5
1.0
0.5
0.0
***
***
-WRS
+WRS
Buffer
αTLR4
IgG1

Figure 2.5 TLR2 and TLR4-mediated signaling responses to WRS.
(A) HEK293 cells co-expressing TLRs 2, 4, or 9 with a NF-κB alkaline phosphatase (AP) reporter system as indicated were treated for 18 h with 100 nM each of recombinant human WRS, Δ1-47 WRS, heat-denatured WRS (100 °C WRS), or buffer. (B, C) Reporter cells were pre-treated for 1 h with TLR2 inhibitor C29 (100 μM), IκB kinase inhibitor BAY11-7082 (10 μM), TLR4 inhibitor CLI095 (1 μg/mL), or vehicle (1% (*v*/*v*) DMSO) prior to treatment ± WRS (100 nM) for 18 h. (D, E) Reporter cells were pre-treated for 1 h with antibody (5 μg/mL) or buffer prior to treatment ± recombinant human WRS (100 nM) for 18 h: (D) TLR2–blocking antibody (αTLR2) and isotype control antibody IgA2; (E) TLR4–blocking antibody (αTLR4) or isotype control antibody IgG1.The relative activity of alkaline phosphatase was plotted as: *A*, fold change for each TLR compared to buffer (mean ± S.D., $n = 4$) of $N = 2$ independent experiments; TLR9, $N = 1$; *B* – *E*, fold change compared to the – WRS control for each treatment (mean ± S.D., $n = 4$) of $N = 2$ independent experiments. Statistical significance was determined as follows: *A*, against buffer by a one-way ANOVA with Dunnett's multiple comparison posttests; *B* – *E*, between vehicle (or buffer) and inhibitor (or antibody) treatment in the presence of WRS (+ WRS) using a two-tailed unpaired Student's *t*-test. *** $p < 0.001$; ns, not significant.

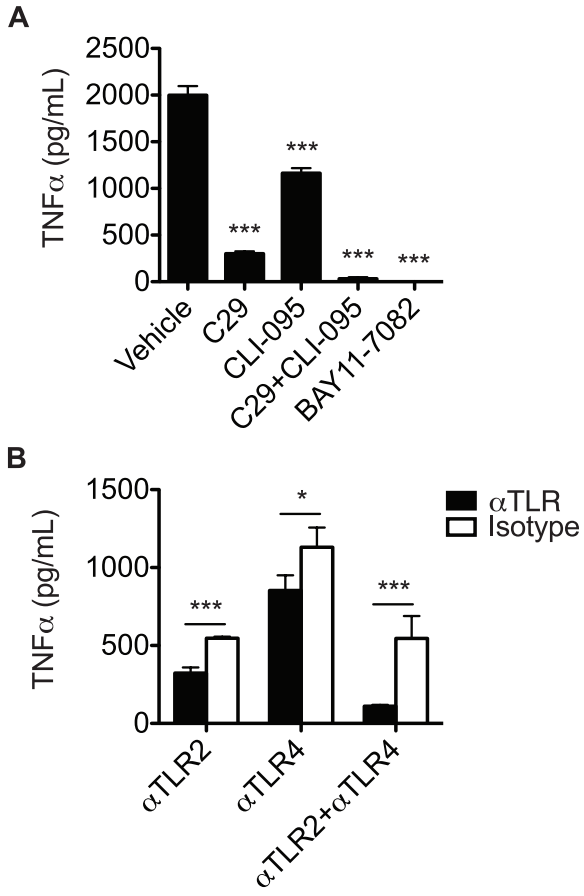

Figure 2.6 Inhibition of TLR2 and TLR4 signaling reduced WRS-mediated TNFα release from THP1 macrophages.

(A) ELISA analysis of TNFα released into the conditioned media of PMA-differentiated THP1-derived macrophages in response to treatment with recombinant human WRS (100 nM) in vehicle (1% (*v*/*v*) DMSO) for 3 h and after pre-treatment for 1 h with TLR2 inhibitor C29 (100 μM), TLR4 inhibitor CLI-095 (1 μg/mL), or IκB kinase inhibitor BAY11-7082 (10 μM). (B) TNFα levels in the conditioned media of THP1 M0 cells treated with recombinant human WRS (100 nM) for 3 h after pre-treatment for 1 h with TLR2- or TLR4-blocking antibodies (αTLR2, αTLR4), or isotype controls (5 μg/mL). Data are presented as means ± S.D. (n = 4) of N = 2 independent experiments. Statistical significance was determined against vehicle using a one-way ANOVA with Dunnett's multiple comparison posttests in *A* and between each isotype control and antibody using a two-tailed unpaired Student's *t*-test in *B*. *, $p < 0.05$; ***, $p < 0.001$; ns, not significant.

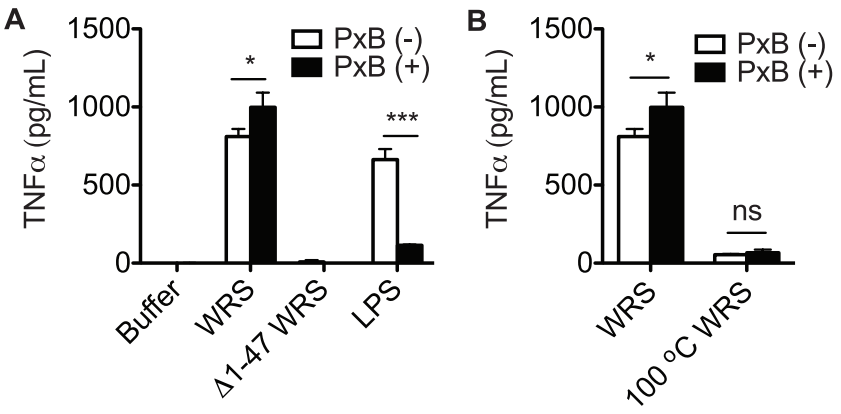

Figure 2.7 Confirmation of the absence of lipopolysaccharide in recombinant WRS and Δ1-47 WRS preparations expressed in ClearColi® BL21 (DE3).
TNFα in the conditioned media of PMA-differentiated THP1-derived macrophages treated for 3 h ± polymyxin B (PxB) (10 μg/mL) with (A) recombinant human WRS (100 nM), Δ1-47 WRS (100 nM), lipopolysaccharide (LPS) (100 ng/mL), or buffer, or (B) heat-denatured WRS (100 °C WRS) (100 nM), was measured by ELISA. Data were plotted as means ± S.D., $n = 4$, $N = 3$ independent experiments. Statistical significance was determined between the – polymyxin B and + polymyxin B conditions using a two-tailed unpaired Student's *t*-test. *, $p < 0.05$; *** $p < 0.001$; ns, not significant.

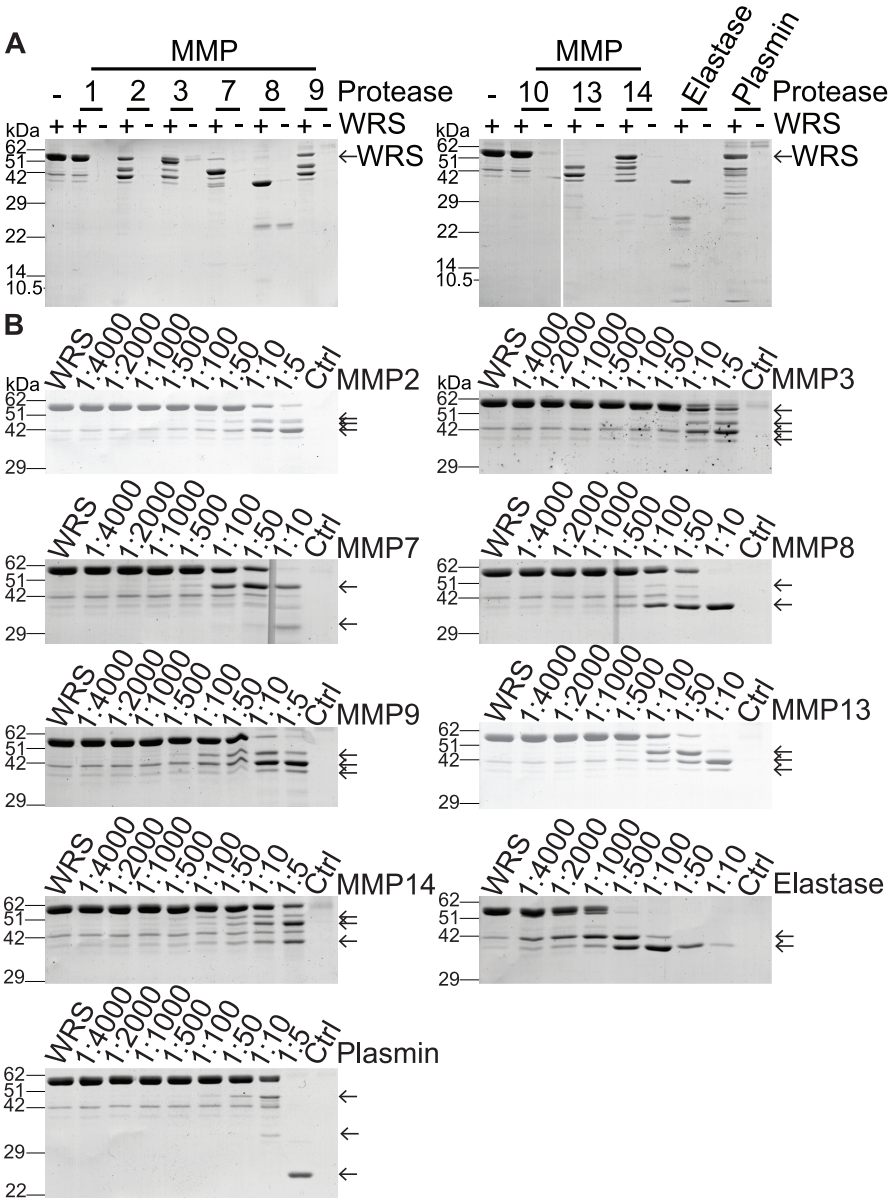

Figure 2.8 SDS-PAGE analysis of WRS cleavage by recombinant MMPs *in vitro*.
(A) Recombinant human WRS (~58 kDa) was incubated with recombinant MMPs, neutrophil elastase, or plasmin (1:10 molar ratio protease:WRS) for 18 h at 37 °C and analysed by 12% SDS-PAGE, *N* = 2 independent experiments. (B) WRS was incubated at the protease:WRS molar ratios shown for 18 h at 37 °C and the cleavage products were analysed by 10% SDS-PAGE and Coomassie Brilliant Blue G-250–staining. Controls (Ctrl), highest concentration of protease without WRS. Cleavage products are indicated by arrows. Vertical line artefacts on the MMP7 and MMP8 images are reflections caused by the scanner.

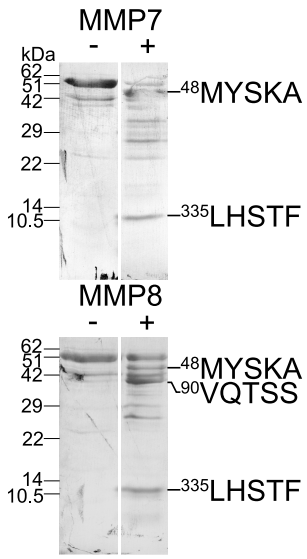

Figure 2.9 MMP-cleaved WRS protein bands sequenced by Edman degradation.
Recombinant human WRS was incubated ± MMP7 or MMP8 at 1:10 protease:WRS molar ratios for 18 h at 37 °C. Cleavage products were resolved by 16.5% SDS-PAGE and transferred to PVDF membrane for Edman degradation. Bands sequenced are shown with the 5 N-terminal residues.

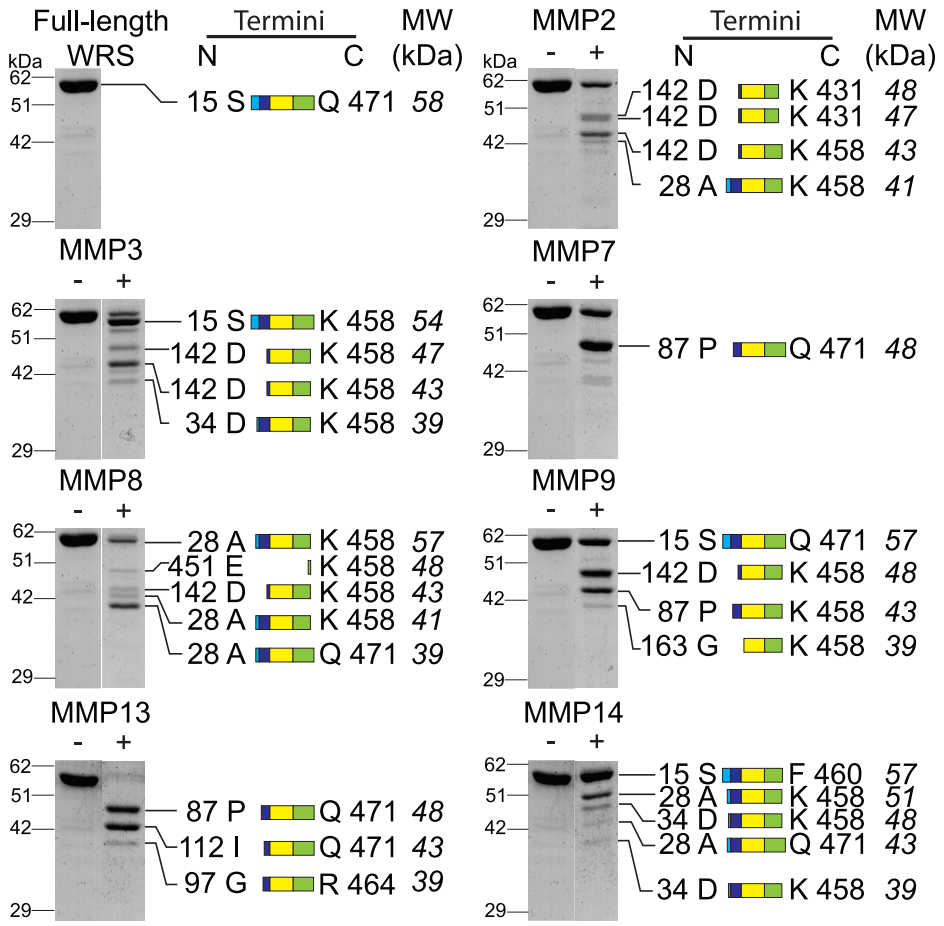

Figure 2.10 LC-MS/MS identified N- and C-terminal boundaries of MMP-cleaved WRS bands.

After MMP digestion of recombinant human WRS for 18 h at 37 °C, cleavage products were resolved by 10% SDS-PAGE and stained with Coomassie Brilliant Blue G-250. Bands were excised, digested with trypsin, and analyzed by LC-MS/MS. Semi-tryptic peptides (*i.e.* cleaved by MMP at one end and trypsin at the other) were detected from all WRS domains. Cleaved proteoforms of WRS are represented by color-coded domain cartoons where the N- and C-terminal residues of the most N- and C-terminal semi-tryptic peptides are shown. The absence of detected peptides either side of these residues suggest that cleavage had occurred nearby, resulting in the fragments shown on the gel. Molecular weights were determined from the relative migration distance (R_f analysis). Light blue, vertebrate-specific extension (VSE) domain; dark blue, eukaryotic-specific extension (ESE) domain; yellow, Rossman fold catalytic domain; green, anticodon recognition domain. The N-terminus of full-length recombinant WRS (~58 kDa) was ^{15}Ser, shown at the top left.

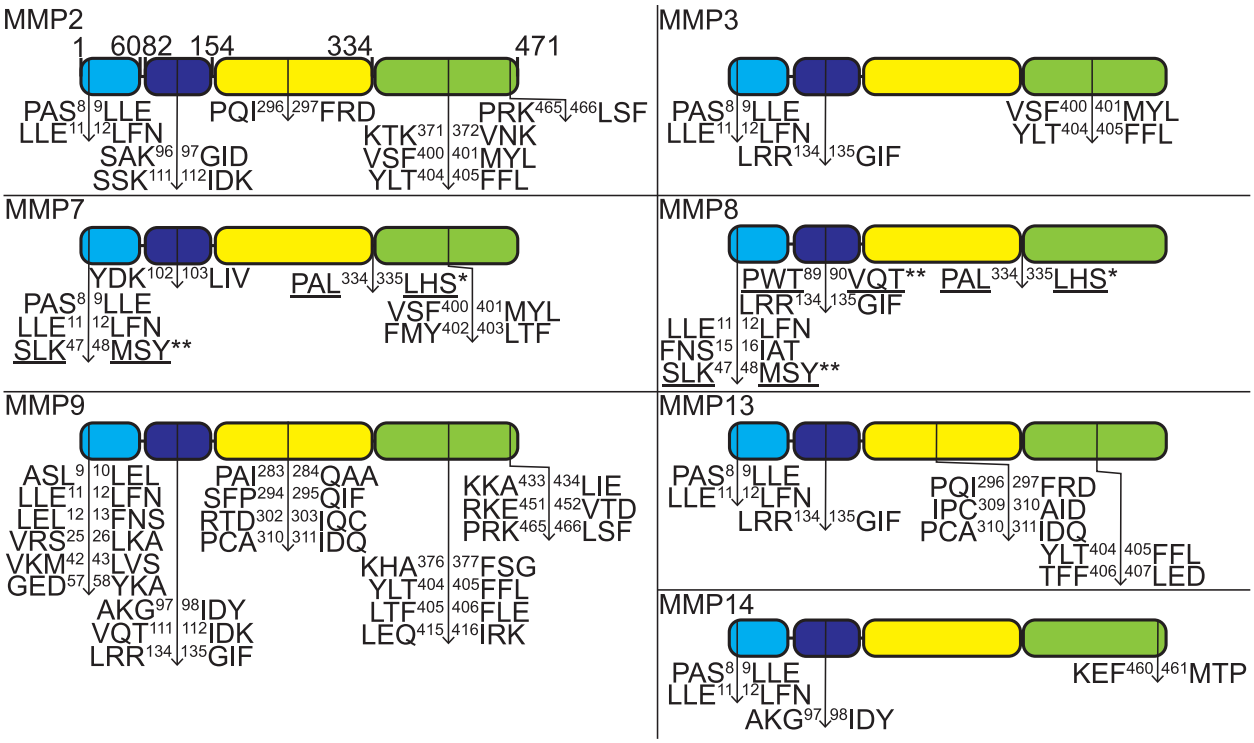

Figure 2.11 Identification of MMP cleavage sites in WRS.
After cleavage of recombinant human WRS by human MMPs, the cleavage sites of all MMPs were identified by ATOMS N-terminal positional proteomics and for MMP7 and MMP8 also by N-terminal sequencing by Edman degradation (WRS cleavage product bands sequenced are shown in Fig. 2.9). Schematic diagrams of WRS with the MMP cleavage sites identified by ATOMS (↓), Edman degradation (*, underlined), or by both (**). Only MMP7 and MMP8 cleaved at the exact site as the Δ1-47 WRS alternate spliced form. Light blue, vertebrate-specific extension (VSE) domain; dark blue, eukaryotic-specific extension (ESE) domain; yellow, Rossman fold catalytic domain; green, anticodon recognition domain.

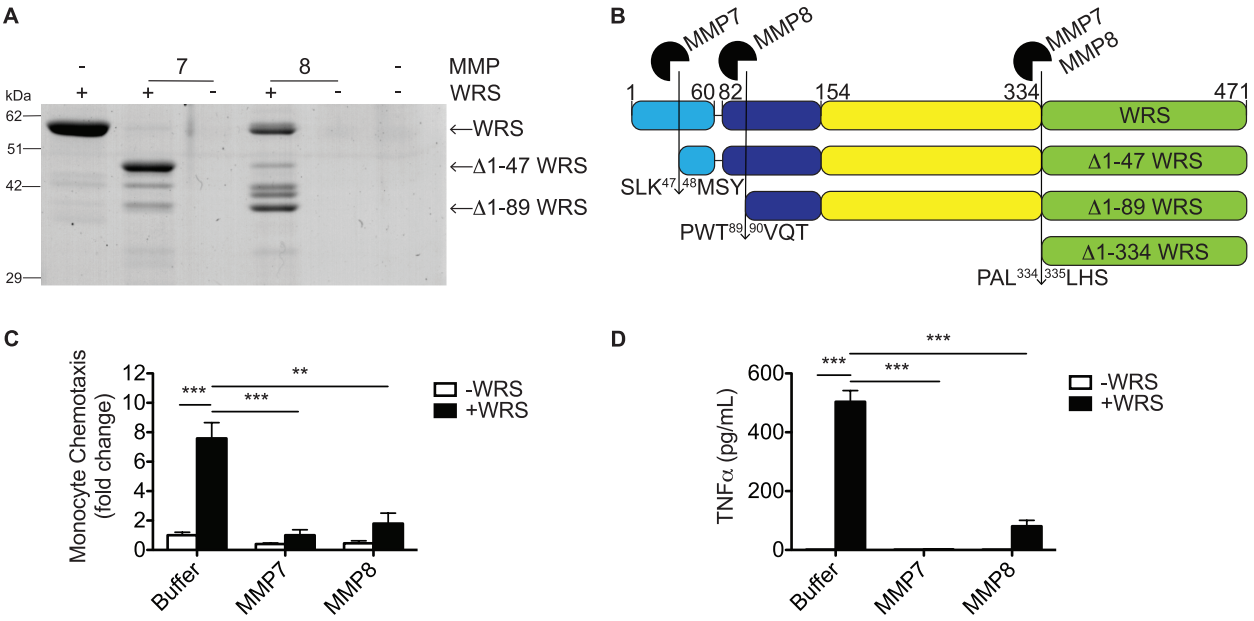

Figure 2.12 WRS cleavage by MMP7 and MMP8 reduced chemotaxis and TNFα release. (A) Cleavage of recombinant human WRS (~58 kDa) by MMP7 and MMP8 (1:10 protease:WRS molar ratio) for 18 h at 37 °C visualized by Coomassie Brilliant Blue G-250–stained 10% SDS-PAGE gels. (B) Schematic diagrams of WRS with the MMP7 and MMP8 cleavage sites identified by Edman degradation (↓) (shown in Fig. 2.9). Light blue, vertebrate-specific extension (VSE) domain; dark blue, eukaryotic-specific extension (ESE) domain; yellow, Rossman fold catalytic domain; green, anticodon recognition domain. (C) Transwell chemotaxis assay of THP1 monocytes in response to WRS, WRS cleaved by MMP7 or MMP8 (100 nM each), buffer, or MMPs alone (shown in *A*) over 90 min. Data are presented as fold-change compared to buffer – WRS (means ± S.D., $n = 3$) of $N = 3$ independent experiments. (D) TNFα released to the conditioned media of PMA-differentiated THP1-derived macrophages treated for 3 h with intact or MMP-cleaved WRS (100 nM each) was measured by ELISA (plotted as means ± S.D., $n = 4$) of $N = 3$ independent experiments. Statistical significance was determined between WRS treated with buffer and WRS treated with each MMP as well as between buffer ± WRS conditions using a two-tailed unpaired Student's *t*-test. **, $p < 0.01$; ***, $p < 0.001$; ns, not significant.

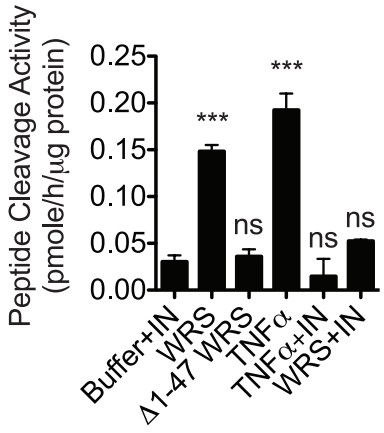

Figure 2.13 WRS increased MMP activity in macrophage-conditioned media by a TNFα-dependent pathway.

PMA-differentiated THP1-derived macrophages were treated for 24 h with recombinant human WRS (100 nM), Δ1-47 WRS (100 nM) as an analogue of the MMP7 and MMP8 cleavage product, TNFα (40 ng/mL), or buffer, with or without a monoclonal antibody inhibitor of TNFα (Inflixamab, IN) (100 ng/mL). MMPs in 20-fold concentrated conditioned media were activated with 1 mM *p*-aminophenylmercuric acetate (APMA) and cleavage of the quenched fluorescence peptide substrate Mca-Pro-Leu-Gly↓Leu-Dpa-Ala-Arg-NH_2 was measured (mean ± S.D., $n = 3$) in $N = 3$ independent experiments. Statistical significance was determined against buffer + Inflixamab using a one-way ANOVA with Dunnett's multiple comparison posttests. ***, $p < 0.001$; ns, not significant.

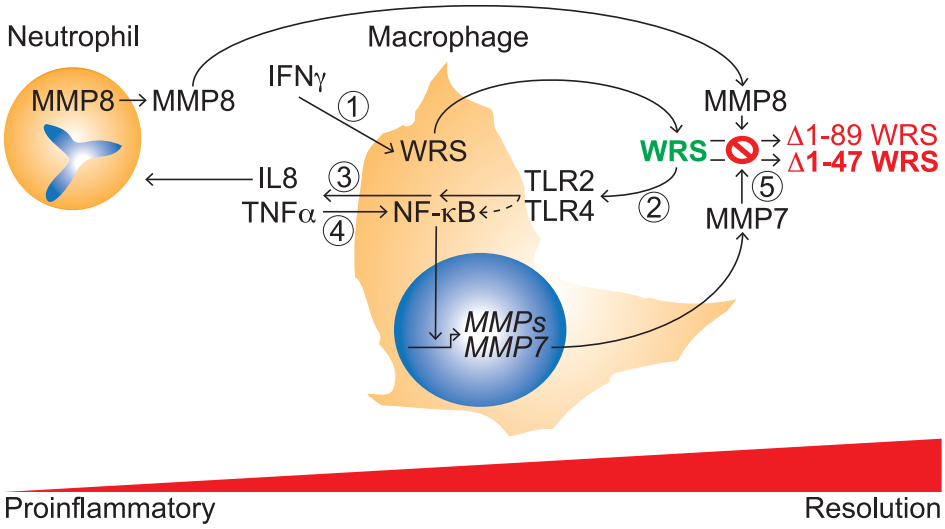

Figure 2.14 Model of the WRS – MMP temporal relationship and feedback loops regulating IFNγ responses in inflammation.
(1) IFNγ activation of M1 macrophage polarization including IFNγ-induced secretion of WRS. (2) WRS activation of TLR2 (and to a lesser extent, TLR4) signaling to induce monocyte/macrophage chemotaxis, and cytokine and chemokine release, notably of the neutrophil chemoattractant IL8 (3). (4) TNFα activation of NF-κB and upregulation of MMP expression, notably of MMP7, in macrophages. (5) With time, MMP cleavage of WRS, particularly by macrophage MMP7 and neutrophil-specific MMP8, inactivates proinflammatory activities of WRS, and so dampens these inflammatory pathways.

Chapter 3: Matrix metalloproteinases activate the proinflammatory functions of extracellular moonlighting tyrosyl-tRNA synthetase

3.1 Synopsis

Tyrosyl-tRNA synthetase ligates tyrosine to its cognate tRNA in the cytoplasm and is secreted through a non-canonical pathway. We investigated the extracellular activities of YRS and found when moonlighting outside the cell, this “intracellular” protein was proinflammatory: As well as acting as a monocyte chemoattractant, YRS initiated signaling through Toll-like receptor 2 (TLR2), resulting in NF-κB activation and release of TNFα and multiple chemokines including MIP-1α/β, CXCL8 (IL8), and CXCL1 (KC) from macrophages. Furthermore, YRS upregulated macrophage matrix metalloproteinase (MMP) extracellular activity in a TNFα-dependent manner. Since MMPs process a variety of intracellular proteins with extracellular moonlighting functions, we profiled 10 MMPs for YRS cleavage and identified 55 cleavage sites by ATOMS positional proteomics and Edman degradation—all of which were within or near to the beginning of the YRS C-terminal domain. All MMPs tested shared two common cleavage sites at $ADS^{386}\downarrow^{387}LYV$ and $VSG^{405}\downarrow^{406}LVQ$, with MMP7, which is highly expressed by monocytes and macrophages, and neutrophil-specific MMP8 exhibiting the highest catalytic efficiency for YRS. The 41 kDa cleaved proteoform enhanced activation of TLR2 signaling, increased TNFα secretion from macrophages, and amplified monocyte chemotaxis compared to unprocessed YRS. We propose that the proinflammatory activity of YRS is enhanced by MMP cleavage in a feed-forward mechanism that drives inflammation.

3.2 Introduction

Matrix metalloproteinases (MMPs), a family of 23 secreted and membrane-anchored proteases, regulate diverse processes including inflammation (16, 21–24, 196, 363) by cleaving a variety of signaling molecules in addition to extracellular matrix components. MMP substrates include chemokines such as CC chemokine ligand (CCL)7 (23), cytokines such as interferon (IFN)α (30) and γ (24), and complement proteins including mannose-binding lectin (171), C1q (170), C3, C3a, C3b, and C5a (196). MMP processing of multiple bioactive substrates such as these dampens inflammation and so rather than being detrimental proteases leading to pathology, MMPs possess beneficial roles in inflammation essential for terminating inflammatory responses (23, 362). Especially notable are the innate immune cell MMPs: neutrophil-specific MMP8 (25), and

macrophage-expressed MMP7 (330) and MMP12 [14], which coordinate leukocyte chemotaxis during inflammation by activating and inactivating cleavages of chemokines.

To further elucidate the roles of MMPs in physiological and pathological processes, we developed targeted proteomic technologies known as “degradomics” (39, 175, 185) to identify protease substrates in cell culture systems (39, 177, 187, 396), animal models (189, 196), and human tissues (397–400). Our Terminal Amine Isotopic Labeling of Substrates (TAILS) method identifies actual cleavage sites (185, 190) and quantification is incorporated by differential isotopic labelling, for example, with isobaric tags for relative and absolute quantification (iTRAQ) (183). In degradomic screens, we identified tyrosyl-tRNA synthetase (YRS) as a candidate MMP substrate.

YRS (~59 kDa, 528 residues) ligates tyrosine to tRNA(Tyr) for protein synthesis in the cytoplasm. In addition to the N-terminal Rossman fold catalytic domain (residues 1-230) and tRNA anticodon binding domain (residues 231-364), eukaryotic YRS has a C-terminal endothelial monocyte-activating polypeptide II-like (EMAPII) domain (residues 365-528). The EMAPII domain is absent from prokaryotic YRS and is not necessary for translation (207, 401). Several eukaryotic tRNA synthetases have roles within the cell in addition to aminoacylation (208, 210, 364) and, despite lacking a canonical signal sequence, YRS and other tRNA synthetases (207, 213, 215, 216, 220) are reported to have extracellular “moonlighting” functions (204, 212). YRS has been detected in human plasma (242), in exosomes (402), and is abundant in platelets compared to other tRNA synthetases (220, 242). YRS is secreted from the human histiocytic lymphoma cell line U-937 in culture (228) and from apoptotic *Drosophila melanogaster* cells (224). Truncated proteoforms of YRS, arising from alternative splicing (220) or plasmin and elastase cleavage (207, 229), have immune cell chemoattractant activities and also induce secretion of tumor necrosis factor (TNF)α from macrophages (207, 229).

Since YRS was found as a candidate substrate in our degradomics screens we assessed whether MMPs process YRS to modulate inflammation. Here we describe how the proinflammatory activities of YRS are *enhanced* by MMP cleavage in the C-terminal domain and show that YRS can induce MMP activity which could potentiate inflammation.

3.3 Results

3.3.1 Proinflammatory activities of YRS on monocytes and macrophages

The recruitment of monocytes is a key component of the inflammatory response (128). Using an *in vitro* Transwell chemotaxis assay, we found that the chemotaxis of THP1 monocytes in response YRS (50 nM) was significantly enhanced compared with the buffer control (*N* = 3; Fig. 3.1A). Chemotaxis was abrogated by heat-denaturation of YRS. Thus, YRS is a chemoattractant for monocytes, a function that depends upon the tertiary structure of YRS.

Once at a site of inflammation, monocytes and macrophages secrete cytokines and chemokines that potentiate the inflammatory response by recruiting additional inflammatory cells (22). We found that THP1 monocyte-derived macrophages (THP1 M0), differentiated using phorbol 12-myristate 13-acetate (PMA), constitutively secreted YRS and secretion appeared to be unaffected by treatment with IFNα, IFNβ, IFNγ or interleukin (IL)4 (Fig. 3.2A, B). A TNFα ELISA revealed that treatment of THP1 M0 macrophages with recombinant YRS (50 nM) for 3 h induced the release of TNFα into the medium (*N* = 2; Fig. 3.1B). TNFα was not released when YRS had been heat-denatured, revealing a requirement for native tertiary structure of YRS. The stimulation of cytokine and chemokine production by YRS (50 nM) from human peripheral blood mononuclear cell (PBMC)-derived macrophages was measured using a protein array of 36 cytokines and chemokines (Fig. 3.1C, Fig. 3.3). Thereby, we confirmed that YRS increased the secretion of TNFα from human PBMC, as well as CCL3 and CCL4 (MIP-1α/β), CXCL1 (KC), and CXCL8 (IL8) (*N* = 2; Fig. 3.1C, D).

3.3.2 YRS signaled through Toll-like receptor 2

The transcription and release of cytokines such as TNFα from a variety of cells involves the NF-κB signaling pathway that leads to coordination of proinflammatory responses (103). Therefore, we investigated whether the NF-κB pathway is involved in the YRS-mediated stimulation of cytokine and chemokine secretion from macrophages. Treatment of PMA-derived THP1 macrophages with YRS led to phosphorylation of the p65 subunit of NF-κB within 10 min, with maximal levels of phosphorylated (p)-p65 (*N* = 3; Fig. 3.4A, B) at 30 min. This rapid increase in active p-p65 corresponded to maximal reduction of the NF-κB inhibitor, IκB-α (*N* = 3; Fig. 3.4A, C), indicating that YRS directly activates the NF-κB signaling pathway in macrophages.

NF-κB signaling occurs after pattern recognition receptors are triggered, including Toll-like receptors (TLR) 2 and TLR4 on macrophages and monocytes that stimulate innate immune responses (215, 217). We screened for YRS activation of TLRs using HEK293 TLR NF-κB reporter cell lines: YRS (50 nM) stimulated NF-κB reporter signaling through TLR2, but not TLR4 or the cytosolic DNA receptor TLR9 (*N* = 2; Fig. 3.4D). TLR2 signaling was abolished by heat-denaturation of YRS, consistent with the effect of heat-denaturation on chemotaxis of monocytes (Fig. 3.1A) and TNFα release from macrophages (Fig. 3.1B).

To confirm that YRS initiates NF-κB signaling through TLR2 in macrophages, we treated THP1-derived macrophages with a TLR2 neutralizing antibody and TLR2 pathway inhibitors that we confirmed blocked TLR2-mediated signaling in the HEK293 TLR2 reporter cells (*N* = 2; Fig. 3.4E, F). In THP1-derived macrophages, the TLR2-blocking antibody (5 μg/mL) reduced TNFα production by 95% compared to its isotype control, while a TLR4-blocking antibody failed to reduce TNFα production compared to its isotype control (*N* = 3; Fig. 3.5A). TNFα production by THP1 M0 was also reduced by 74% by C29 (100 μM), a small molecule TLR2 signaling inhibitor that inhibits myeloid differentiation primary response gene 88 recruitment to TLR2 (377), and completely by BAY11-7082 (10 μM), a NF-κB nuclear translocation inhibitor that targets IκB kinase (375, 376) (*N* = 2; Fig. 3.5B). Thus, blocking either the extracellular domain of TLR2 with an αTLR2 antibody, or interfering with intracellular components of the NF-κB signaling pathway using chemical inhibitors disrupted YRS induced TNFα secretion, demonstrating that TLR2 mediates this proinflammatory response to YRS in macrophages.

As recombinant proteins expressed in *E. coli* can be contaminated with lipopolysaccharide (LPS), a heat-stable activator of TLR signaling, the recombinant YRS used in all of the experiments presented herein were expressed in *E. coli* ClearColi® BL21 (DE3) cells (380, 381). This strain of *E. coli* produces a lipid variant LPS that does not trigger an endotoxic response in human cells. Additional measures were taken to eliminate any LPS contamination: inclusion of Triton X114 during YRS purification, polymyxin B-agarose extraction of purified recombinant YRS, and inclusion of polymyxin B in cell culture experiments to scavenge any contaminating endotoxin. To validate the efficacy of our strategy in eliminating any endotoxin contamination of YRS, we assessed TNFα release from THP1-derived macrophages: 10 μg/mL polymyxin B blocked TNFα release from M0 macrophages in response to LPS (100 ng/mL), but did not reduce TNFα release

stimulated by YRS (50 nM) (*N* = 3; Fig. 3.5C). Heat-denaturation of YRS eliminated TNFα release in the absence of polymyxin B, confirming the absence of endotoxin (*N* = 3; Fig. 3.5D).

3.3.3 MMPs induced by TNFα cleaved YRS

TNFα is known to increase MMP expression (44). Since YRS stimulated TNFα secretion from macrophages, we assessed whether YRS could induce MMP expression. THP1-derived macrophages were treated with YRS (50 nM) or TNFα (50 ng/mL) (*N* = 3; Fig. 3.6A) with or without the TNFα inhibitory antibody Inflixamab (100 ng/mL). Treatment of the macrophages with YRS markedly increased MMP activity (measured by cleavage of a quenched fluorescent MMP peptide substrate) in the medium to a level comparable with that induced by TNFα. Inflixamab negated the YRS-stimulated increase in MMP activity, suggesting that YRS stimulated MMP production through TNFα.

Our previous results identified YRS as a candidate MMP substrate (177, 185, 186, 196). Hence, we explored whether the MMPs induced by YRS treatment of macrophages could cleave YRS. Conditioned medium was harvested from TNFα-treated M0 macrophages and treated with 1 mM *p*-aminophenylmercuric acetate (APMA) to activate MMPs (27) prior to incubation with recombinant human YRS. Incubation led to a strong reduction in the YRS protein band at 62 kDa (*N* = 3; Fig. 3.6B), which was abrogated by Marimastat (10 μM), a broad-spectrum metalloproteinase inhibitor (403), demonstrating that metalloproteinase activity in the conditioned media was involved in YRS cleavage. This suggests a feedback mechanism where YRS drives MMP expression through TNFα, and these proteases can cleave YRS.

3.3.4 YRS was cleaved by MMPs

To further elucidate which MMPs can cleave YRS, we conducted *in vitro* cleavage assays with ten MMPs. Serine proteases neutrophil elastase and plasmin were included as positive controls as they have been reported to cleave YRS (207, 229). Before incubation, the activity of each MMP was confirmed using quenched fluorescent peptide cleavage assays (not shown). At a 1:10 molar ratio MMP:YRS, MMP2, MMP7, MMP8, MMP9, MMP12, and MMP13 completely processed 62 kDa YRS to a major ~41 kDa form (*N* = 2; Fig. 3.7A). MMP8, MMP9 and MMP13 produced a doublet, similar to that produced by plasmin. MMP1, MMP3 and MMP10 incompletely cleaved YRS, whereas MMP14 cleavage resulted in multiple bands indicative of degradation. Neutrophil elastase completely degraded YRS.

We compared cleavage efficiencies and potential differences in specificity by incubating YRS at a range of molar ratios and calculated kinetic parameters using densitometry (Fig. 3.7B). Four MMPs with the highest cleavage efficiency of YRS, MMP7, MMP8, MMP12, and MMP13 generated the stable fragment comigrating at ~41 kDa all at 1:100 molar ratio MMP:YRS. At higher molar ratios, MMP7 failed to degrade the ~41 kDa fragment, whereas increasing concentrations of the serine proteases neutrophil elastase and plasmin, resulted in complete degradation of YRS (Fig. 5B). The efficiency of the MMPs varied considerably: MMP7 was more efficient, processing YRS almost entirely at a 1:100 molar ratio MMP:YRS compared to MMP10 which did not process YRS entirely even at a greater molar ratio of 1:5.

To identify the cleavage sites for MMPs in YRS, we excised YRS and MMP-generated fragments from SDS-PAGE gels and performed in gel trypsin digests followed by liquid chromatography tandem MS (LC-MS/MS) (Fig. 3.8A). Since trypsin cuts after arginine and lysine residues, any peptide resulting from proteases with different cleavage specificity are identified as “semi-tryptic” peptides. Peptide mapping of cleavage fragments confirmed that the 41 kDa fragment and additional major cleavage products were either the original N-terminus of YRS, or were processed at ^{16}Arg↓^{17}Asn. Thus, we concluded that the conversion of YRS from 62 k Da to 41 kDa was mediated by C-terminal cleavages. Indeed, Edman degradation sequencing confirmed that the 41 kDa band generated by MMP8 contained the N-terminus of YRS, whereas N-terminal sequencing of lower molecular weight cleavage products generated by MMP7 and MMP12 indicated cleavage within the YRS catalytic domain by MMP7 at ^{163}Gly↓^{164}Leu and MMP12 at ^{203}Gly↓^{204}Tyr, and a C-terminal cleavage by MMP12 at ^{405}Gly↓^{406}Leu (Fig. 3.8B).

We also used Amino-Terminal Oriented Mass Spectrometry of Substrates (ATOMS) (383, 384), a highly sensitive targeted approach for identifying N-termini generated by proteolysis to identify MMP cleavage sites in YRS (Fig. 3.9). In accordance with the N-terminal sequence for MMP12 identified by Edman sequencing suggesting a cleavage site at VSG^{405}↓^{406}LVQ (Fig. 3.8B), ATOMS indicated that all the MMPs tested cleaved in this region, *i.e.* close to the beginning of the C-terminal EMAPII-like domain at VSG^{405}↓^{406}LVQ, and within this domain at ADS^{386}↓^{387}LYV, or at DSL^{387}↓^{388}YVE (MMP3) (Fig. 3.9). N-terminal fragments generated by these cleavages, (1 – 386)YRS and (1 – 405)YRS, have predicted molecular weights of 43 kDa and 45 kDa, respectively (Fig. 3.10), that are comparable to the major YRS cleavage products identified by SDS-PAGE (Fig. 3.8A, Fig. 3.10). Thus, MMPs cleave YRS at the C-terminus at ADS^{386}↓^{387}LYV and VSG^{405}↓^{406}LVQ (Fig. 3.10).

3.3.5 MMP-cleavage enhanced the YRS-induced proinflammatory responses

Proteolytic processing by MMPs can alter protein function to modulate inflammation (22–25). Therefore, we investigated whether MMP cleavage affects the proinflammatory activities of YRS. We focused on MMP7 and MMP8, since they are secreted by immune cells and showed relatively high cleavage efficiency for YRS (Fig. 3.7B). Cleavage of YRS with MMP7 and MMP8 (Fig. 3.11A) *increased* THP1 monocyte chemotaxis in the Transwell assay 1.6-fold and 1.9-fold, respectively, compared to full-length YRS (50 nM) (N = 2; Fig. 3.11B). Activation of NF-κB in the HEK293 TLR2 reporter system was enhanced 2.0-fold and 2.4-fold by MMP7 and MMP8 cleavage respectively compared to intact YRS (50 nM) (N = 2; Fig. 3.11C). Additionally, TNFα release from THP1-derived macrophages increased 1.6-fold and 2.3-fold after treatment with MMP7 and MMP8-cleaved YRS respectively compared to intact YRS (50 nM) (N = 3; Fig. 3.11D). Thus, MMP cleavage of YRS potentiates the proinflammatory activity of YRS.

3.4 Discussion

MMPs are key regulators of inflammation (16, 21–24, 196, 363): These metalloproteases achieve such regulation through cleavage of a wide range of signaling molecules that alters their activity, for example, turning off activity to dampen inflammation such as with IFNγ (24) and the monocyte chemoattractant protein (MCP) chemokines (23, 168), or enhancing activity to promote inflammation as with neutrophil chemokines like IL8 (25) and monocyte chemokines like CCL15 and CCL23 (404). Recently we demonstrated that the proinflammatory activities of tryptophanyl-tRNA synthetase, secreted in response to IFNγ, are abrogated by MMP cleavage [Jobin *et al.* unpublished]. Conversely, here we show that MMP7 and MMP8 cleavages within the C-terminal EMAPII domain at $Ser^{386}\downarrow^{387}Leu$ and $Gly^{405}\downarrow^{406}Leu$ that generate stable proteoforms of YRS, (1-386)YRS and (1-405)YRS *potentiate* proinflammatory activities of YRS, namely monocyte chemotaxis, TLR2/NF-κB signaling, and TNFα release from macrophages. These cleavage sites are supported by our previous TAILS degradomic screens that revealed MMP-dependent cleavage of YRS *in vivo* and *in vitro*; in murine *Mmp2*$^{-/-}$ vs. wild-type mouse models of PMA-induced skin inflammation (186); in the secretomes of murine *Mmp2*$^{-/-}$ fibroblasts treated with recombinant MMP2, where cleavage at $Gly^{405}\downarrow^{406}Leu$ (185) was also found in the present study; and in the secretomes of murine RAW264.7 macrophages treated with TNFα (cleavage at $Leu^{387}\downarrow^{388}Tyr$, a site matching one we found *in vitro* here for MMP3) (196). Here we confirmed that multiple MMPs cleave YRS at sites in the C-terminal EMAPII domain including $ADS^{386}\downarrow^{387}LYV$

and VSG$^{405}\downarrow^{406}$LVQ, with these and other sites identified *in vivo* that are often up or down stream by one residue due to exopeptidase activity known as peptide “ragging”.

MMP regulation of the cytokine activity of YRS has previously been reported for the *D. melanogaster* homologue of MMP2: YRS secreted from apoptotic *D. melanogaster* hemocytes acted as a chemoattractant of hemocytes as did MMP2-generated YRS fragments, both promoting clearance of the dying cells (224). Proteoforms of YRS lacking the C-terminus are generated by alternative splicing and by serine proteases: An alternatively spliced form of intracellular YRS, (1-380)YRS, was identified by transcript analyses in leukocytes and spleen (205). Neutrophil elastase is reported to cleave YRS in or near the C-terminal EMAPII domain at Ala$^{355}\downarrow^{356}$Lys and Ser$^{366}\downarrow^{367}$Arg to generate (1-355)YRS and (1-366)YRS respectively, whereas plasmin cuts at Lys$^{352}\downarrow^{353}$Gly and Lys$^{356}\downarrow^{357}$Gln yielding (1-352)YRS and (1-356)YRS, respectively (229). Previously, neutrophil elastase was shown to produce (1-364)YRS from recombinant YRS that was a leukocyte chemoattractant (235), and studies have shown that conformational changes induced by alternative splicing (220), serine protease cleavage (207, 229), or in a gain of function mutation (Y341A) are responsible for initiating cytokine activity (229). We determined that intact YRS activated NF-κB signaling through TLR2, and that MMP cleavage enhanced this signaling, presumably due to conformational change induced by truncation similar to that caused by alternative splicing (220) and serine protease cleavage (207, 229). Native YRS was previously found to bind directly but not stimulate TLR4 (220), whereas YRS with a conformation-changing Y341A mutation activated TLR2 and TLR4 signaling in human and murine leukocytes (220). Future research should address which elements of YRS are necessary to engage and activate TLR signaling.

TNFα induces MMP expression and activity from macrophages through signaling pathways including NF-κB (44). We demonstrated that YRS, through the release of TNFα, promoted an increase in macrophage metalloproteinase activity. We propose a positive-feedback mechanism where proteoforms of YRS generated by MMP cleavage are involved in the recruitment of monocytes that differentiate into macrophages once at the site of inflammation. As macrophages release MMPs that cleave and activate further the inflammatory properties of YRS (Fig. 3.12), we suggest this would accentuate the inflammatory response, analogous to the MMP8/elastase-mediated feed-forward mechanism of IL8 activation for neutrophil chemotaxis (25, 174). Interestingly, neutrophil elastase and plasmin completely degraded YRS at higher molar ratios, whereas MMPs generated stable products. MMP8 is a neutrophil-specific protease that activates

IL8 (25) and inactivates α_1-antitrypsin, a potent elastase inhibitor, and so removes the block *in vivo* for the highly efficient activating cleavage of IL8 by elastase (174). As MMPs cleave and inactivate several serine protease inhibitors, including α_2-antiplasmin (405), by relieving serine protease inhibition at different phases of the inflammatory process, serine protease activity could further regulate net YRS activity. The challenge now is to assess the mechanism of YRS regulation by MMPs in the context of healthy and diseased states *in vivo* to now assess the depth of this proteolytic tuning of the highly regulated inflammatory response.

3.5 Material and methods

3.5.1 YRS expression and purification

Human YRS (residues 1-528) with a C-terminal His-tag in pET28a was expressed in ClearColi® BL21(DE3) (Lucigen) in Lennox Broth under kanamycin (20 µg/mL) selection. Harvested cell pellets were resuspended in ice-cold column buffer (20 mM KH_2PO_4, 500 mM NaCl, 10 mM imidazole, 2 mM β-mercaptoethanol, pH 7.8) with protease inhibitors (1 mM AEBSF, 1 mM EDTA, 10 µM E-64, 10 µM leupeptin, and 1 µM pepstatin A). Clarified cell lysates were treated with Triton X114 as previously described (388). Treated lysates were applied to a Ni-NTA Perfect Pro (Qiagen) column that was washed with column buffer at pH 7.8, pH 6, then pH 5.2, and bound protein was eluted with a 25 – 250 mM imidazole gradient in column buffer. Protein-containing fractions were pooled and dialyzed against PBS/15% glycerol. Pooled fractions were passed through a polymyxin B-agarose column (Millipore-Sigma) before aliquoting and storage at –80 °C. Protein concentration was determined by bicinchoinic acid assay (Thermo-Fisher Scientific).

3.5.2 Cell culture

The human monocytic cell line THP1 (ATCC #TIB-202) was cultured in RPMI growth medium: RPMI-1640, 4.5 g/L glucose, 10% (*v*/*v*) cosmic calf serum (CCS), 50 µg/mL streptomycin, and 50 U/mL penicillin. THP1 M0 macrophages were generated by differentiation of THP1 monocytes (1 x 10^6 cells/mL) with 100 ng/mL phorbol 12-myristate 13-acetate (PMA) as previously described (24). Experiments were performed using PMA-differentiated THP1 M0 macrophages synchronized for 24 h growth in serum-free medium containing 10 µg/mL polymyxin B. For NF-κB pathway analyses, THP1 M0 cells were treated with 50 nM YRS for various times. Cells were washed with PBS and lysed with 50 mM Tris-HCl, 150 mM NaCl, 10 mM EDTA, 0.2% (*w*/*v*) Zwittergent, pH 8 containing a protease and phosphatase inhibitor cocktail (Biotool). Centrifugated cell lysates were assessed using immunoblotting as described below. For TNFα

experiments, THP1 M0 cells were treated for 3 h with 50 nM YRS, heat-denatured YRS (boiled for 5 min), *E. coli* 0111:B4 lipopolysaccharide (LPS) (Millipore-Sigma), or PBS. TNFα in conditioned media was measured using a human TNFα ELISA kit (Duoset® ELISA, R&D Systems). 5 µg/mL TLR2-blocking antibody (#maba2-htlr2, InvivoGen), TLR4 blocking antibody (#mabg-htlr4, InvivoGen), IgA2 isotype control antibody (#maba2-ctrl, InvivoGen), IgG1 isotype control antibody (#mabgl-ctrlm, InvivoGen), 1% (*v*/*v*) DMSO (vehicle), 100 µM C29 (MedChemExpress), 10 µM BAY11-7082 (Selleckchem), or a combination thereof were added 1 h prior to treatment with 50 nM YRS for 3 h for TLR inhibitor experiments.

Human peripheral blood mononuclear cells (PBMC) were obtained from Ficoll-Pacque™ PLUS (GE Healthcare) separated blood samples. Healthy volunteers donated blood according to a University of British Columbia Clinical Research Ethics Board approved protocol (#H06-00047). All donors provided informed consent and research was conducted in accordance with the Declaration of Helsinki. Monocytes were isolated from the human PBMCs using an EasySep™ Human Monocyte Isolation Kit (Stemcell) according to manufacturer's instructions. Monocytes (2 x 10^5/mL) were differentiated into primary macrophages (M0) by culturing in ImmunoCult™-SF Macrophage Medium containing 50 ng/mL monocyte-colony stimulating factor (both Stemcell) for 4 days. For cytokine and chemokine array analysis, serum-starved PBMC-derived M0 were treated for 3 h in serum-free growth medium, 10 µg/mL polymyxin B with 50 nM YRS or PBS. Conditioned media, cleared by centrifugation, were assayed using a Human Cytokine Array® (#ARY005B, R&D Systems) as per manufacturer's instructions. Membranes were blocked with Odyssey Blocking Buffer (LI-COR) for 20 min, before incubation 1 h at 25 °C with Streptavidin conjugated to Alexa Fluor® 680 (Thermo-Fisher Scientific). A LI-COR Odyssey infrared imager (LI-COR) was used for imaging. Spots were quantified by densitometry using ImageJ software (NIH).

3.5.3 Monocyte chemotaxis

YRS, heat-denatured YRS, CCL7 (all 50 nM), or PBS in RPMI-1640, 20 mM HEPES, 0.1% BSA, 10 µg/mL polymyxin B (chemotaxis buffer) was added to the lower wells of chemotaxis chambers (Neuroprobe). THP1 monocytes, synchronized by serum-starvation, were resuspended in chemotaxis buffer (1 x 10^6 cells/mL) and 2 x 10^5 cells were placed in the top wells separated by a 5-µm membrane. After incubation for 90 min at 37 °C, cells were harvested from the lower well

and quantified using CyQUANT® (Thermo-Fisher Scientific). CCL7 was synthesized as previously described (168).

3.5.4 TLR reporter assays

Human embryonic kidney 293 (HEK)-Blue™ cells co-expressing the NF-κB reporter system and receptors TLR2, TLR4, TLR9 or receptor-null counterparts (Null1 and Null2) (all InvivoGen) were cultured in DMEM growth medium (DMEM, 4.5 g/L glucose, 10% (*v*/*v*) CCS, 50 µg/mL streptomycin, and 50 U/mL penicillin) with selective antibiotics. Cell maintenance and assays were conducted according to manufacturer's instructions. For reporter assays, 96-well plates were seeded with TLR2 and Null1, TLR4 and Null2, or TLR9 and Null1 HEK-Blue™ cells and treated with 50 nM YRS, heat-denatured YRS, or PBS with 10 µg/mL polymyxin B for 18 h. NF-κB activation was assayed using conditioned medium and QUANTI-Blue™ detection medium (InvivoGen). For TLR inhibitor experiments, cells were incubated with antibodies and inhibitors for 1 h before treatment with 50 nM YRS for 18 h as for THP1-derived macrophages above.

3.5.5 YRS secretion assays

PMA-differentiated THP1 M0 macrophages were transferred to serum-free media with 100 ng/mL human IFNα (Cedarlane), 100 ng/mL IFNβ, 20 ng/mL IFNγ, or 40 ng/mL IL4 (all Peprotech). Clarified conditioned media were harvested at times shown and protease inhibitor cocktail (Biotool) and 1 mM EDTA were added. Cells were washed with PBS and lysed in buffer containing protease inhibitor cocktail and 1 mM EDTA as above.

Proteins in conditioned media were precipitated by 15% (*v*/*v*) trichloroacetic acid and the resulting protein pellets were washed with 100% acetone. Air-dried pellets were re-solubilized by boiling for 5 min in 4 x SDS-PAGE loading buffer (0.5 M Tris, 8 M urea, 8% (*w*/*v*) SDS, pH 6.8), and then diluted 1 in 4 in water. Protein concentrations were determined by absorbance measurements at A_{280} nm.

3.5.6 Immunoblotting

Reduced samples were separated using 10% SDS-PAGE and transferred to PVDF membranes (Immobilon-FL, Millipore-Sigma). Membranes were blocked with Odyssey Blocking Buffer for 20 min, after which primary antibodies (at concentrations recommended by manufacturers) in 5% BSA with 0.05% Tween 20 were added and incubated overnight at 4 °C. Primary antibodies were: Affinity-purified polyclonal antibody for the N-terminus of YRS (#A305-064A, Bethyl Laboratories);

monoclonal antibodies phospho-NF-κB p65 (Ser 536; #3033) and total IκB-α (#4814) (both Cell Signaling Technology); α-tubulin (#sc-53646, Santa Cruz Biotechnology). After washing the membranes in PBS with 0.05% Tween 20, secondary antibodies were incubated (at concentrations recommended by manufacturers) in 1% BSA with 0.05% Tween 20 for 1 h at 25 °C. Secondary antibodies were: goat anti-mouse IgG conjugated to IRDye 800CW (LI-COR) and goat anti-rabbit IgG conjugated to Alexa Fluor® 680 (Thermo-Fisher Scientific). Immunoblots were washed and analyzed using a LI-COR Odyssey infrared imager and immunoreactive bands were quantified by densitometry using ImageJ software (NIH).

3.5.7 MMP expression, purification, and activity assays

Recombinant human MMP1, MMP2, MMP3, MMP8, MMP9, MMP12, MMP13, MMP14 without the transmembrane helix, MMP7 and murine MMP10 were produced as previously described (389). A quenched fluorescence synthetic peptide substrate cleavage assay using Mca-Pro-Leu-Gly↓Leu-Dpa-Ala-Arg-NH_2 (R&D systems) was used to confirm MMP activation as previously described (389, 390). THP1-derived M0 macrophages were cultured in phenol red-free RPMI-1640 serum-free growth medium with 10 µg/mL polymyxin B (Millipore-Sigma) incubated with 50 nM YRS, heat-denatured YRS, 40 µg/mL TNFα, or PBS ± 100 µg/mL Inflixamab (#NBP2-52655, Novus Biologicals). Conditioned medium, clarified by centrifugation, was concentrated 20x using Ultra-4 Centrifugal Filter Units (Amicon). MMP activity in 40 µg conditioned medium protein was quantified by quenched fluorescence peptide cleavage activity as above.

3.5.8 YRS cleavage assays

YRS was incubated for 18 h at 37 °C in HEPES buffer: 50 mM HEPES, 150 mM NaCl, 5 mM $CaCl_2$, pH 7.2 at various protease:YRS molar ratios. Human neutrophil elastase (Millipore-Sigma) and plasmin (Biovision) were reconstituted in 50 mM HEPES, 150 mM NaCl, 5 mM $CaCl_2$, pH 7.2. All proMMPs were activated in HEPES buffer containing 1 mM *p*-aminophenylmercuric acetate (APMA) for 20 min at 22 °C. APMA was removed by dialysis against HEPES buffer at 4 °C.

Clarified conditioned media from THP1 M0 cells cultured in serum-free growth medium with 40 µg/mL TNFα for 24 h was concentrated 20x as above. Concentrated media were treated with 1 mM APMA for 20 min at 25 °C and APMA was removed as before. YRS was added at a medium:YRS total protein ratio of 5:1 and incubated for 18 h at 37 °C. YRS cleavage products

were visualized by SDS-PAGE analysis and Coomassie Brilliant Blue-250 staining and western blotting.

3.5.9 LC-MS/MS analysis of MMP cleavage of YRS

YRS (1 µg) was digested ± MMPs for 18 h 37 °C using molar ratios MMP:YRS: MMP2, 1:10; MMP3, 1:10; MMP7, 1:50; MMP8, 1:50; MMP9, 1:50; MMP10, 1:5; MMP12, 1:50; MMP13, 1:50; and MMP14, 1:10. Reactions were diluted into 3 in 4 in buffer (0.5 M Tris, 8% (*w*/*v*) SDS, pH 6.8, 20% (*v*/*v*) β-mercaptoethanol) and boiled for 5 min before resolving by 10% SDS-PAGE. MMP-digested YRS bands were stained with Coomassie brilliant Blue G-250 and excised from the gels, destained with methanol and lyophilized. Gel slices were rehydrated in15 µL MS-grade trypsin (12 ng/µL in 50 mM ammonium bicarbonate) for 45 min at 4 °C. After pulse-centrifugation, buffer was removed, and the gel plugs were resuspended in 50 mM ammonium bicarbonate and incubated at 37 °C for 18 h. After centrifugation as above, polyacrylamide plugs were discarded and supernatants were desalted using StageTips (391). Samples were analyzed by LC-MS/MS as previously described (Chapter 2). The N-terminal peptides of MMP cleaved YRS proteoforms excised from the gels were determined by peptide mapping. The mass spectrometry data has been deposited with the ProteomeXchange Consortium (393) via the PRIDE partner repository (394) with the dataset identifier PXD013197.

3.5.10 MMP cleavage site determination

YRS cleavage sites were determined by Edman degradation (performed by the Tufts University Core Facility) as previously described (383, 384) and by ATOMS (383, 384). Briefly, YRS (100 µg) was incubated ± MMP (at molar ratios detailed in the previous section) at 37 °C for 18 h. Proteins were denatured in 4 M guanidine-HCl, cysteines were reduced using 5 mM DTT for 1 h at 37 °C and alkylated using 15 mM iodoacetamide for 15 min at room temperature in the dark. Excess iodoacetamide was quenched with 15 mM DTT for 30 min at 37 °C. Lysine and N-terminal amine groups in MMP-digested samples were labeled using 40 mM heavy formaldehyde ($C^{13}D_2O$) (+ MMP), and in samples without MMPs using light formaldehyde (CH_2O), both in the presence of 20 mM sodium cyanoborohydride at 37 °C for 18 h. Excess formaldehyde was quenched with 50 mM ammonium bicarbonate at 37 °C for 2 h. Samples were mixed, split equally between 2 tubes, and digested with either 1 µg/mL MS-grade trypsin (Thermo-Fisher Scientific) or 1 µg/mL GluC (*Staphylococcus aureus* protease V8, Worthington) for 16 h at 37 °C. Samples were desalted using StageTips (391), analyzed by LC-MS/MS and cleavage sites were analyzed as

described previously (Chapter 2). Cleavage sites with a charged or hydrophilic residue in the P1' position except for cysteine and glutamine were not further considered as they did not match the major substrate preferences derived from > 4,000 MMP cleavage sites (389). The ATOMS mass spectrometry data have been deposited as above with the dataset identifier PXD013366.

3.5.11 Statistics

GraphPad Prism version 5.0b software was used to perform all statistical testing as detailed in the figure legends.

3.6 Figures and figure legends

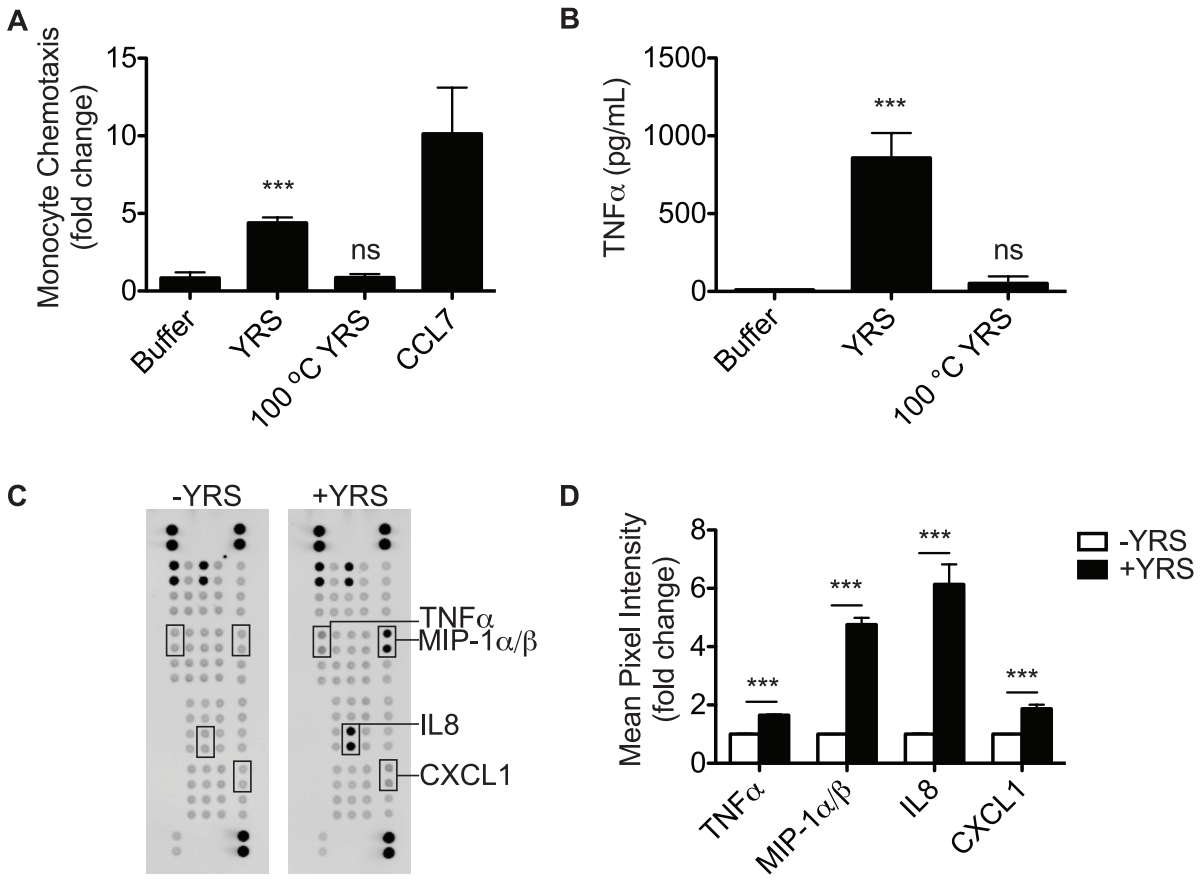

Figure 3.1 Increased THP1 monocyte chemotaxis, TNFα secretion, and chemokine secretion induced by YRS.
(A) Transwell chemotaxis assay of THP1 monocytes in response to 50 nM recombinant human YRS, 50 nM heat-denatured YRS (100 °C YRS), or buffer. CCL7 (50 nM) was used as a positive control. After 90 min, cells in the lower chamber were counted. Data was plotted as fold change compared to buffer (mean ± S.D., $n = 3$) of $N = 3$ independent experiments. (B) ELISA of TNFα protein levels in THP1 M0 macrophage conditioned media after treatment for 3 h with 50 nM YRS, heat-denatured YRS (100 °C YRS), or buffer control (mean ± S.D., $n = 4$) of $N = 2$ independent experiments. (C) Cytokine protein levels in the conditioned media of human peripheral blood mononuclear-derived macrophages treated for 3 h ± 50 nM YRS detected by a human cytokine array. The cytokines and chemokines with significant changes in expression ± YRS are boxed. The identity of all the cytokines and chemokines blotted is shown in Fig. 3.3. (D) Mean pixel intensities were measured by densitometric analysis and plotted as fold changes + YRS compared to – YRS (mean ± S.D., $n = 4$) of $N = 2$ independent experiments. Statistical significance was determined: against buffer for *A, B* using a one-way ANOVA with Dunnett's multiple comparison posttests; between ± YRS conditions for *D* using an unpaired two tailed Student's *t*-test. *** $p < 0.001$, ns, not significant.

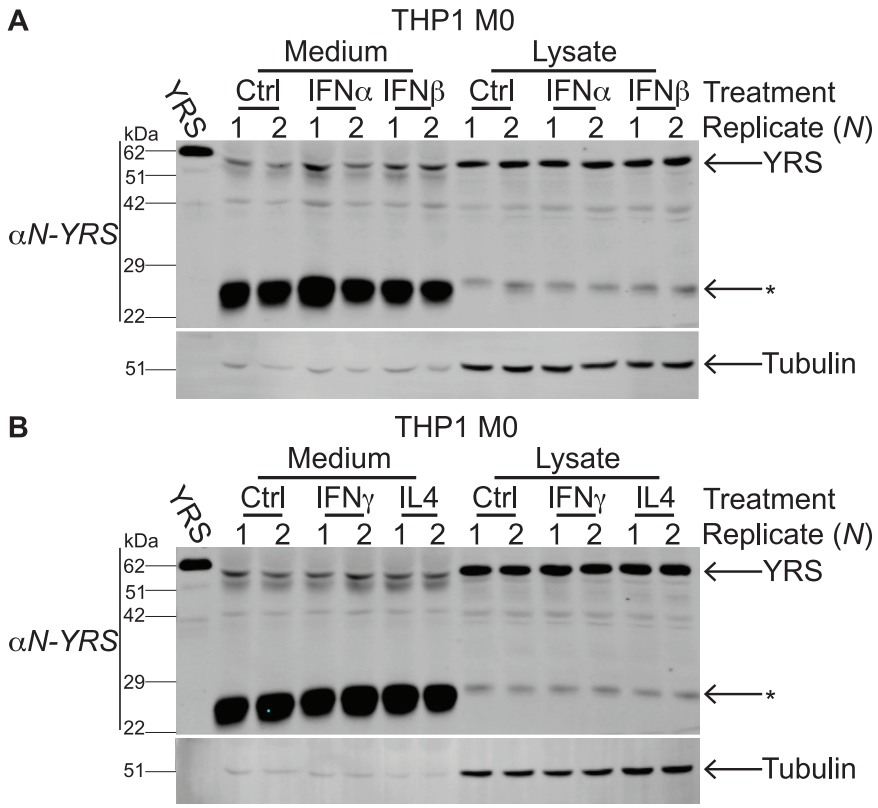

Figure 3.2 YRS expression and secretion in THP1 cells was constitutive.
Immunoblots of replicate samples (1 and 2) of PMA-differentiated THP1-derived macrophages (THP1 M0) treated for 48 h with buffer (Ctrl), (A) IFNα, IFNβ (100 ng/mL each), or (B) IFNγ (20 ng/mL), or IL4 (40 ng/mL). An antibody specific to the N-terminus of YRS (α*N-YRS*) was used to identify YRS in conditioned media and cell lysates. *, nonspecific immunoreactive band. Standards: YRS: Recombinant human YRS (band ~62 kDa); tubulin, loading control. Representative immunoblots after 10% SDS-PAGE are shown of $N = 2$ independent experiments.

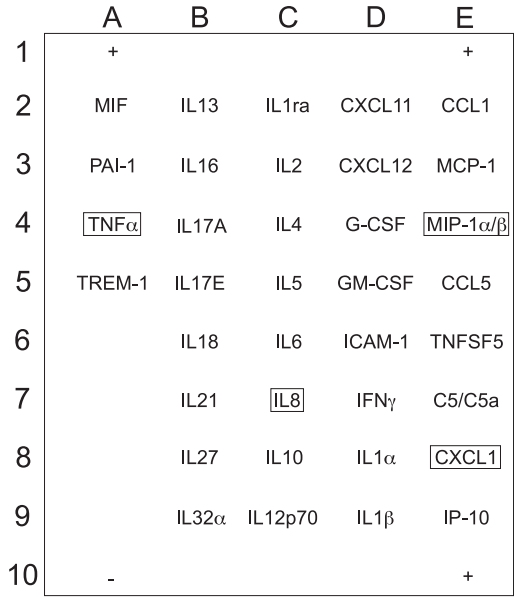

Figure 3.3 Grid showing layout of the cytokine protein array used to analyze conditioned media of human peripheral blood mononuclear-derived macrophages following stimulation by YRS.
The cytokines and chemokines with significant changes in expression in Fig. 3.1C are boxed. +, positive control spots; –, negative control protein spots.

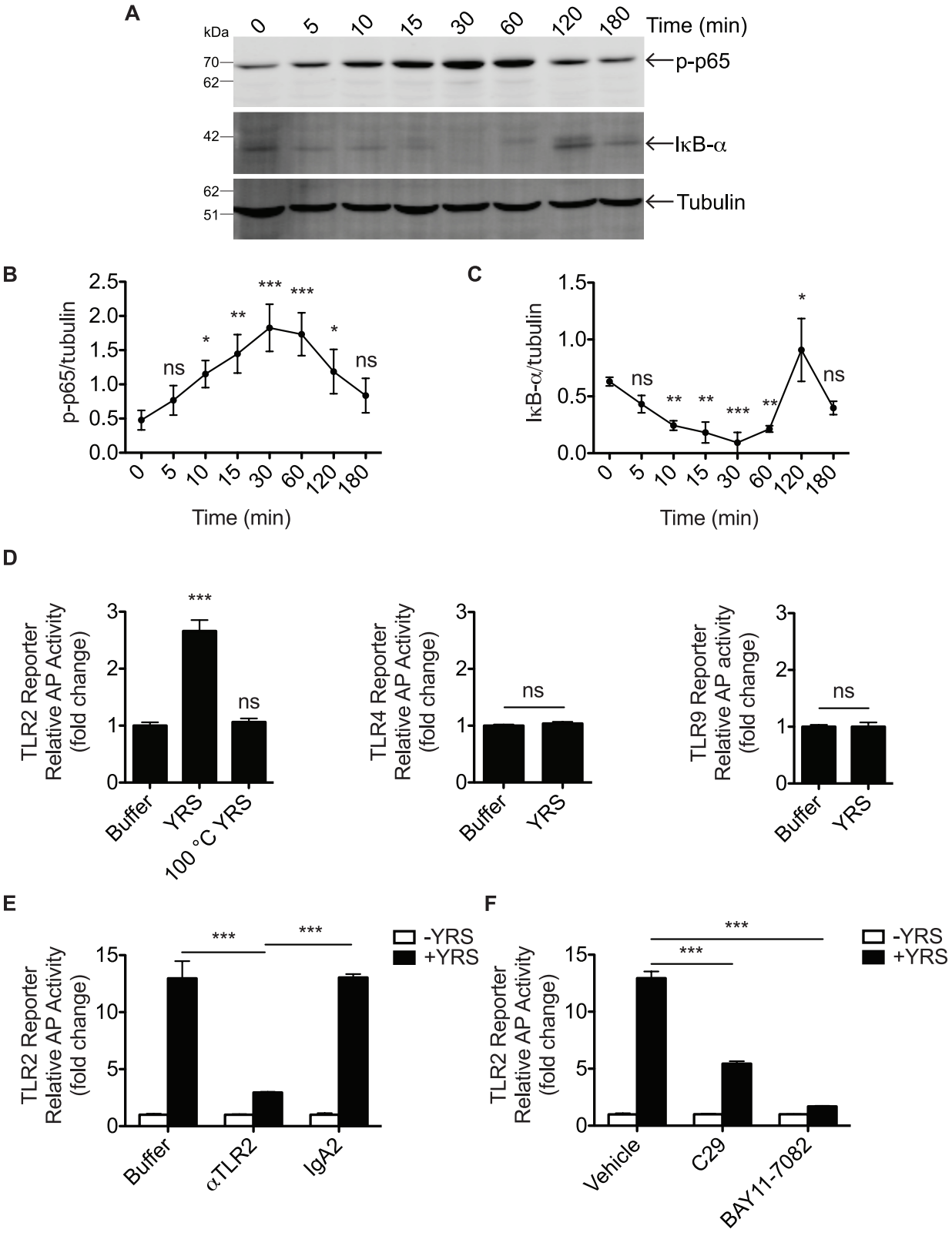
A
kDa
0
5
10
15
30
60
120
180
Time (min)
70
62
p-p65
42
IκB-α
62
51
Tubulin
B
p-p65/tubulin
Time (min)
C
IκB-α/tubulin
Time (min)
D
TLR2 Reporter Relative AP Activity (fold change)
Buffer
YRS
100 °C YRS
TLR4 Reporter Relative AP Activity (fold change)
TLR9 Reporter Relative AP activity (fold change)
E
TLR2 Reporter Relative AP Activity (fold change)
-YRS
+YRS
Buffer
αTLR2
IgA2
F
TLR2 Reporter Relative AP Activity (fold change)
Vehicle
C29
BAY11-7082

Figure 3.4 YRS stimulated NF-κB signaling through TLR2.
(A) Representative immunoblots of phosphorylated (p)-p65 NF-κB and inhibitor of NF-κB (IκB-α) following treatment of PMA-differentiated THP1-derived human macrophages with 50 nM recombinant human YRS for the times shown. An immunoblot of α-tubulin is shown as the loading control. (B, C) Quantification of relative band densities of p-p65 NF-κB and IκB-α plotted as mean ± S.D. of *N* = 3 independent experiments. (D) HEK293 cells expressing TLR2, 4, or 9 with a NF-κB alkaline phosphatase (AP) reporter system, were treated for 18 h with 50 nM recombinant human YRS, heat-denatured YRS (100 °C YRS), or buffer. (E) TLR2 reporter cells were pre-treated for 1 h with 5 μg/mL TLR2–blocking antibody (αTLR2), isotype control IgA2, or buffer prior to treatment ± 50 nM YRS for 18 h. (F) TLR2 reporter cells were pre-treated for 1 h with 100 μM TLR2 inhibitor C29, 10 μM NF-κB activation inhibitor BAY11-7082 that targets IκB kinase, or vehicle (1% (*v*/*v*) DMSO) prior to treatment ± 50 nM YRS for 18 h. The relative activity of alkaline phosphatase was plotted: *A*, fold changes compared to buffer (means ± S.D., *n* = 4) of *N* = 2 independent experiments; TLR9, *N* = 1; *B* – *C*, TLR2 fold change compared to the – YRS control for each treatment (means ± S.D., *n* = 4) of *N* = 2 independent experiments. Statistical significance was determined: *B* – *C*, against 0 h using a one-way ANOVA with Dunnett's multiple comparison posttests; *D*, against buffer using a one-way ANOVA with Dunnett's multiple comparison posttests for TLR2 and an unpaired two-tailed Student's *t*-test for TLR4/9; *E* – *F*, against buffer (or vehicle) and antibody (or inhibitor) treatment in the presence of YRS (+ YRS) using a two-tailed unpaired Student's *t*-test. *, $p < 0.05$; ** $p < 0.01$; *** $p < 0.001$; ns, not significant.

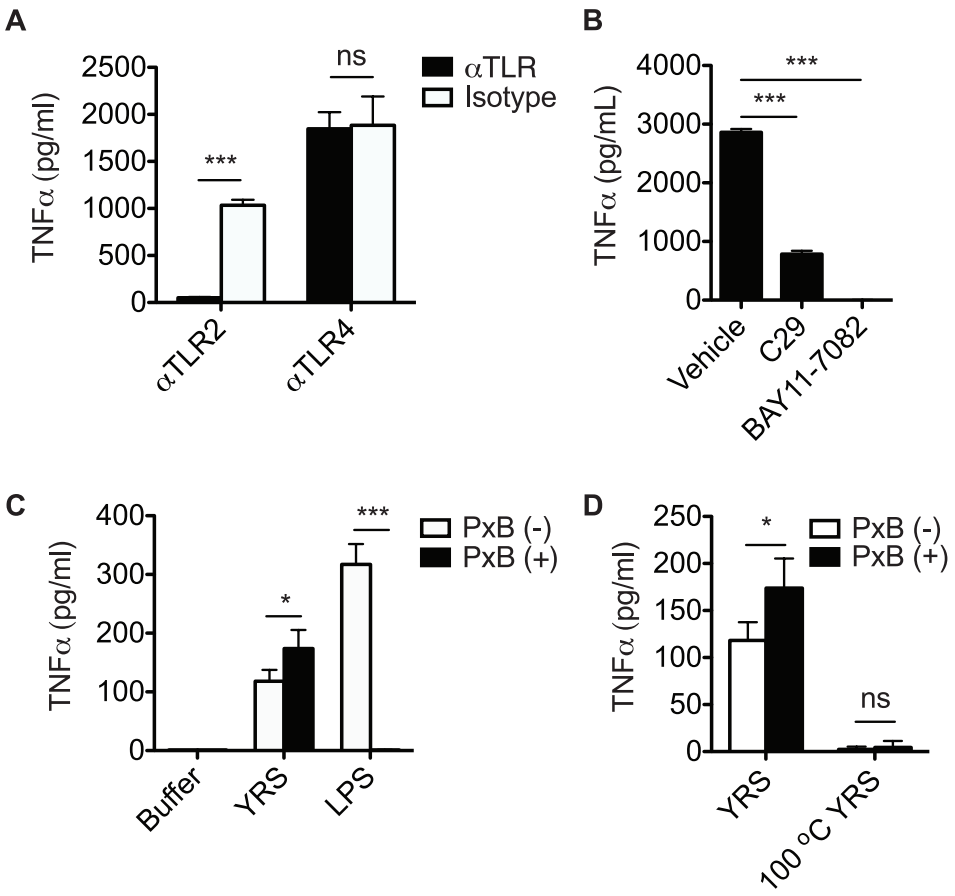

Figure 3.5 Inhibition of TLR2 signaling reduced YRS-mediated TNFα release from THP1 macrophages.

TNFα released to the conditioned media of PMA-differentiated THP1-derived macrophages in response to treatment with 50 nM recombinant human YRS for 3 h after pre-treatment for 1 h with (A) 5 μg/mL TLR2- or TLR4-blocking antibodies (αTLR2, αTLR4) or isotype controls (mean ± S.D., *n* = 4) of *N* = 3 independent experiments), or (B) TLR2 inhibitor 100 μM C29, 10 μM IκB kinase inhibitor BAY11-7082, or vehicle (1% (*v*/*v*) DMSO) (mean ± S.D., *n* = 4) of *N* = 2 independent experiments). (C) TNFα in the conditioned media of PMA-differentiated THP1-derived macrophages treated for 3 h ± 10 μg/mL polymyxin B (PxB) with 50 nM YRS, 100 ng/mL lipopolysaccharide (LPS), or buffer, or (D) 50 nM heat-denatured YRS (100 °C YRS), was measured by ELISA. Data were plotted as means ± S.D. (*n* = 4) of *N* = 3 independent experiments. Statistical significance was determined: *A*, between each isotype control and antibody using a two-tailed unpaired Student's *t*-test; *B*, against vehicle using a one-way ANOVA with Dunnett's multiple comparison posttests; *C* – *D*, between the – polymyxin B and + polymyxin B conditions using a two-tailed unpaired Student's *t*-test. *, $p < 0.05$; *** $p < 0.001$; ns, not significant.

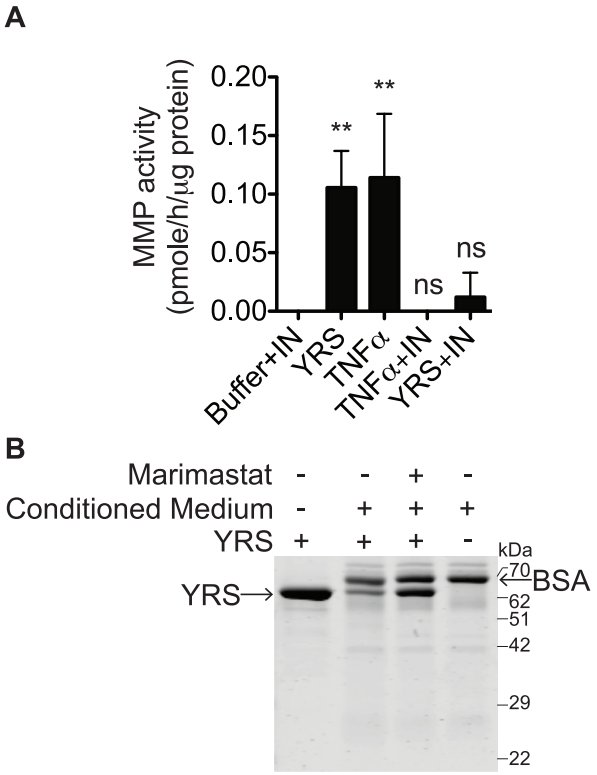

Figure 3.6 YRS increased macrophage MMP activity in a TNFα-dependent pathway.
(A) PMA-differentiated THP1-derived macrophages were treated for 24 h with 50 nM recombinant human YRS, 40 ng/mL TNFα, or buffer, with or without a monoclonal antibody inhibitor of TNFα (100 ng/mL Inflixamab, IN). MMPs in concentrated conditioned media (20x) were activated with 1 mM *p*-aminophenylmercuric acetate (APMA) and cleavage of a quenched fluorescence peptide substrate Mca-Pro-Leu-Gly↓Leu-Dpa-Ala-Arg-NH_2 was measured (mean ± S.D., n = 3) in N = 3 independent experiments. Statistical significance was determined against 'buffer + Inflixamab' using a one-way ANOVA with Dunnett's multiple comparison posttest. **, $p < 0.01$; ns, not significant. (B) To induce MMP expression, PMA-differentiated THP1-derived macrophages were treated for 24 h with 40 ng/mL TNFα MMPs in the concentrated conditioned media (20x) were activated with 1 mM APMA for 20 min at 22 °C prior to addition of YRS (~62 kDa) ± MMP inhibitor (10 μM Marimastat), at a protein ratio of 5:1 media:YRS, for 18 h at 37 °C. Samples were resolved by 10% SDS-PAGE and stained with Coomassie Brilliant Blue G-250. The ~66 kDa band is BSA in the concentrated conditioned medium. A representative gel of N = 3 independent experiments is shown.

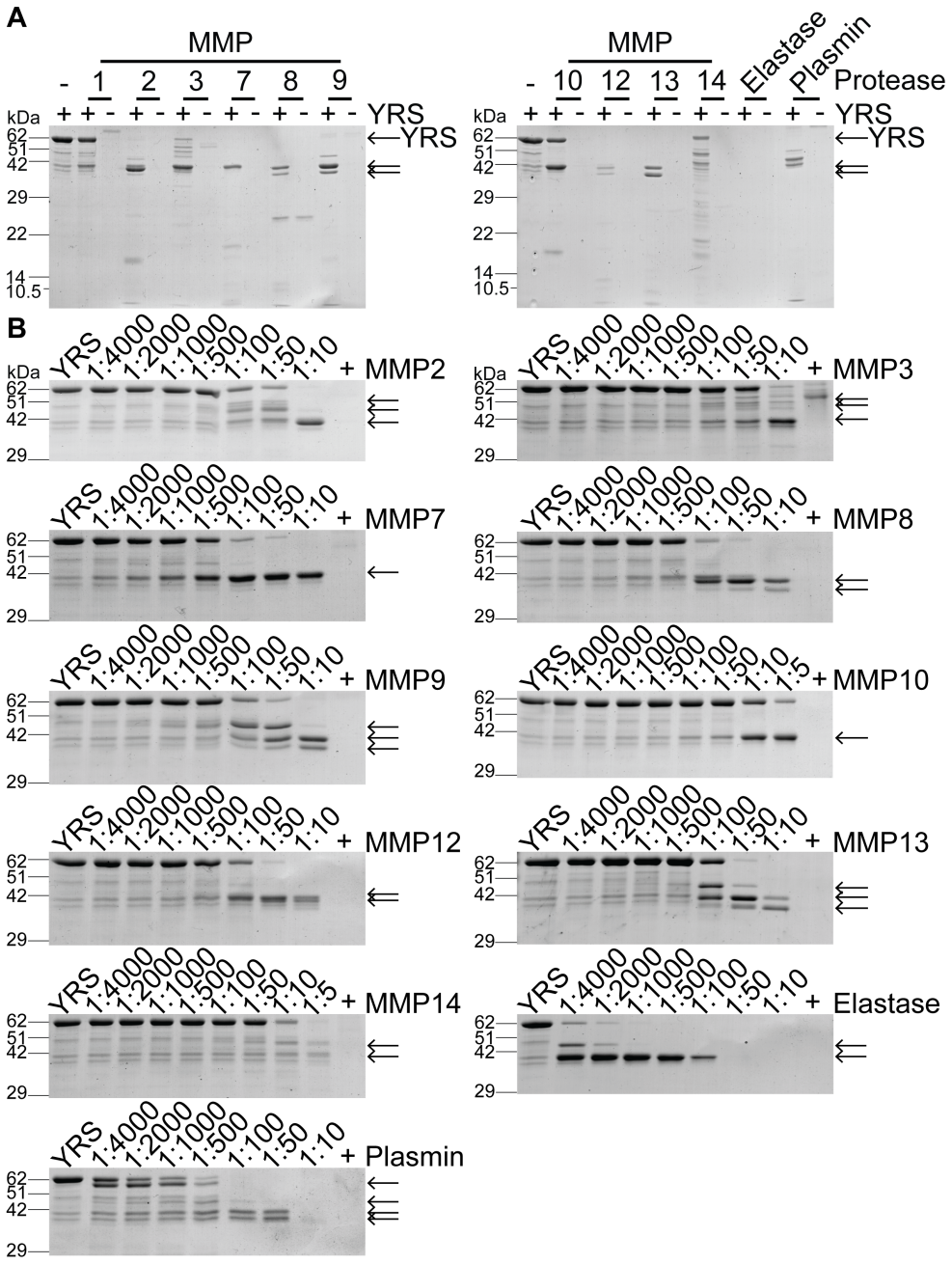

Figure 3.7 Coomassie blue-stained SDS-PAGE analysis of YRS cleavage by recombinant MMPs *in vitro*.

(A) Recombinant human YRS (~62 kDa) was incubated for 18 h at 37 °C with recombinant MMPs, neutrophil elastase or plasmin (1:10 molar ratio protease:YRS), *N* = 2 independent experiments. (B) YRS was incubated for 18 h at 37 °C at the protease:YRS molar ratios shown. Cleavage products were analyzed by (A) 12% or (B) 10% SDS-PAGE with Coomassie Brilliant Blue G-250 staining. Controls (+) are the highest concentration of protease without YRS. Cleavage products are indicated by arrows.

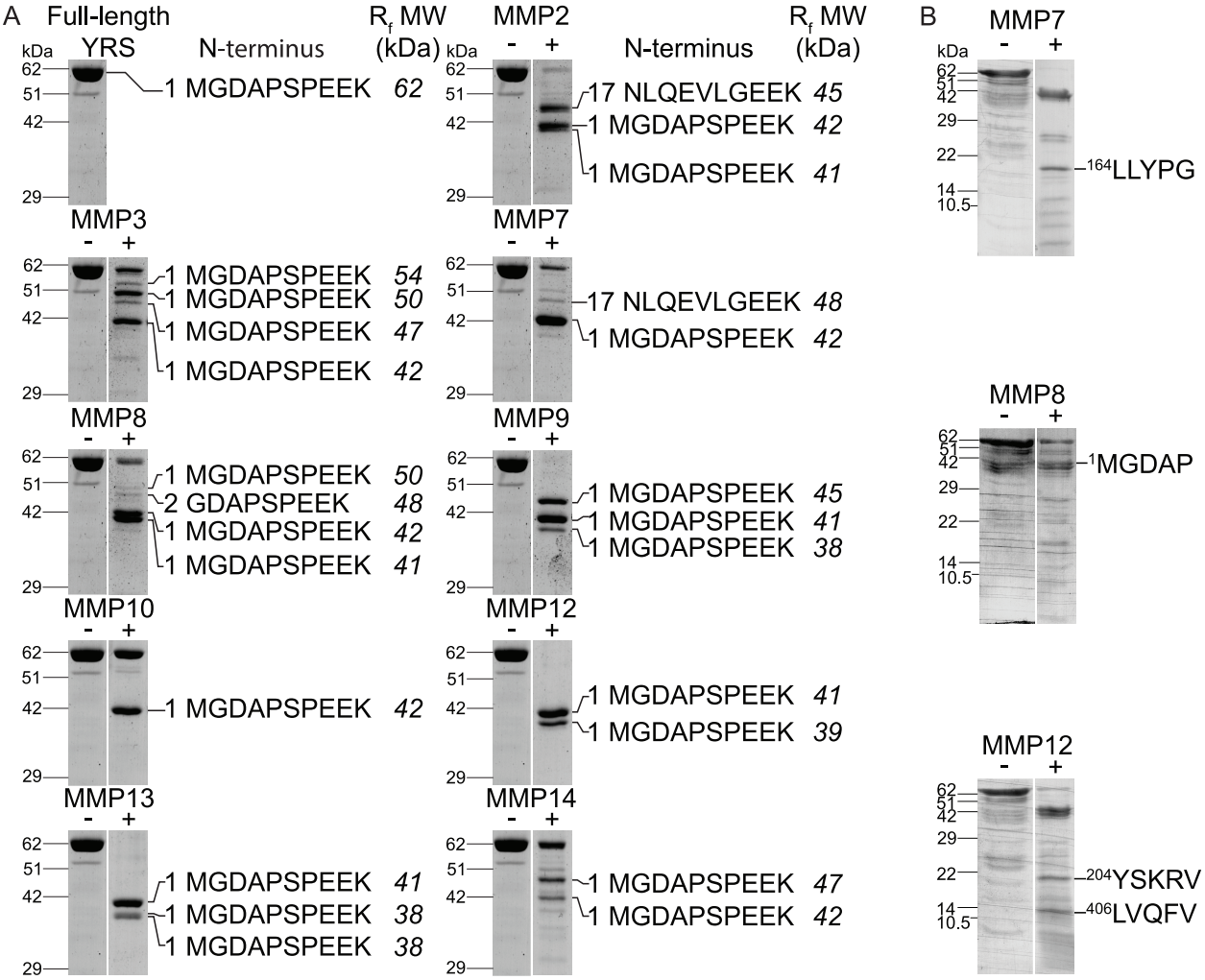

Figure 3.8 MMP-cleaved YRS protein bands sequenced by LC-MS/MS and Edman degradation.

(A) LC-MS/MS was used to identify the N-terminal peptide of MMP-cleaved YRS bands. After MMP digestion of 2 μM recombinant human YRS for 18 h at 37 °C (MMP:YRS molar ratios used were guided by results shown in Fig. 3.7B), cleavage products or the full-length ~62 kDa YRS (top left) were resolved by 10% SDS-PAGE and stained with Coomassie Brilliant Blue G-250. Bands were excised, digested with trypsin for analysis by LC-MS/MS. N-terminal semi-tryptic peptides identified from YRS cleavage products are shown (*i.e.* resulting from MMP cleavage before SDS-PAGE and trypsin digestion). Molecular weights shown were estimated from R_f values. (B) YRS was incubated for 18 h at 37 °C ± MMP7, MMP8, or MMP12 at 1:10 MMP:YRS molar ratios. Cleavage products were resolved by 16.5% SDS-PAGE, transferred to PVDF membrane and subjected to Edman degradation. N-terminal sequences are shown.

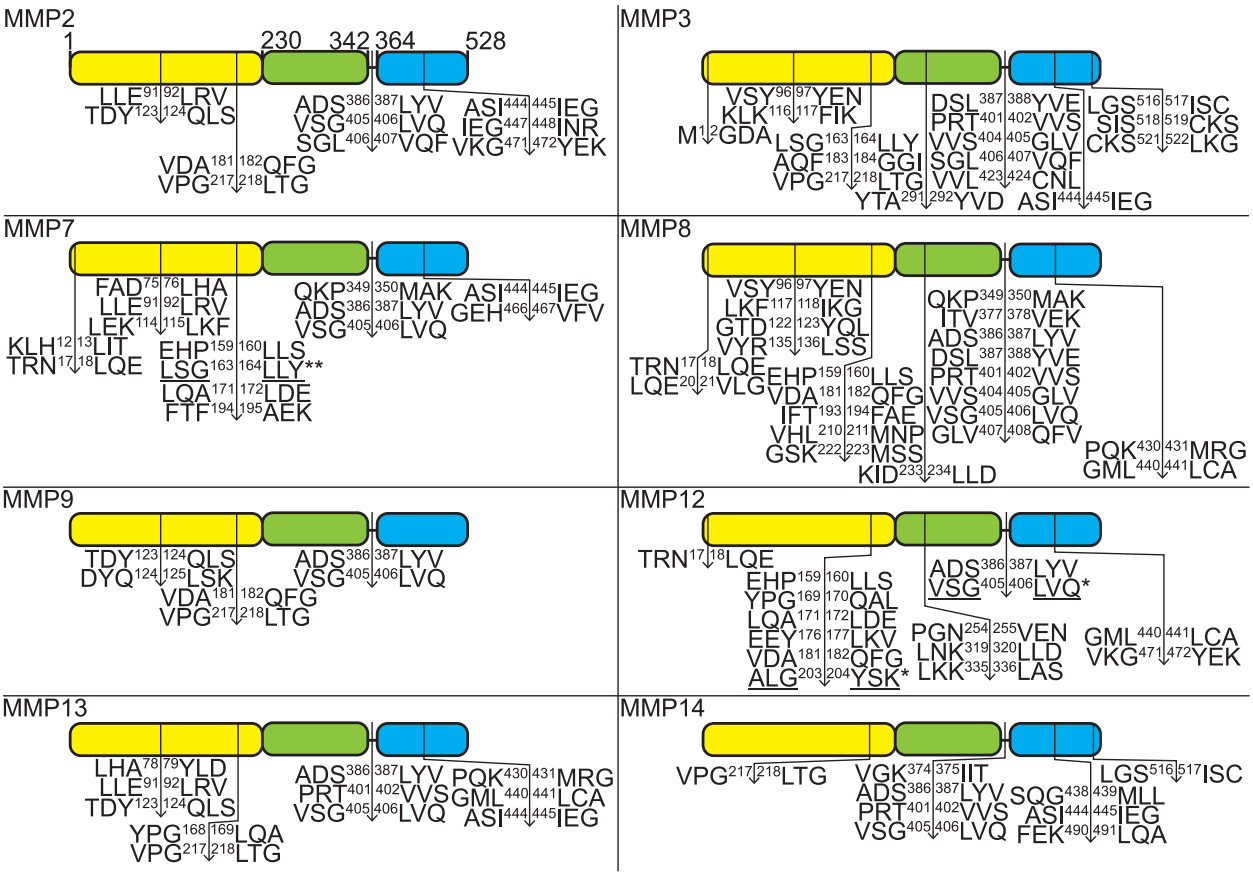

Figure 3.9 Identification of MMP cleavage sites in YRS.
MMP cleavage sites in recombinant human YRS were determined by ATOMS N-terminal positional proteomics, or by Edman degradation of proteins blotted to PVDF membranes as shown in Fig. 3.8B. Cleavage sites identified by ATOMS (↓), Edman degradation (*, underlined), or by both (**) are shown. Yellow, Rossman fold catalytic domain; green, anticodon recognition domain; blue, endothelial monocyte-activating polypeptide II-like (EMAPII) domain.

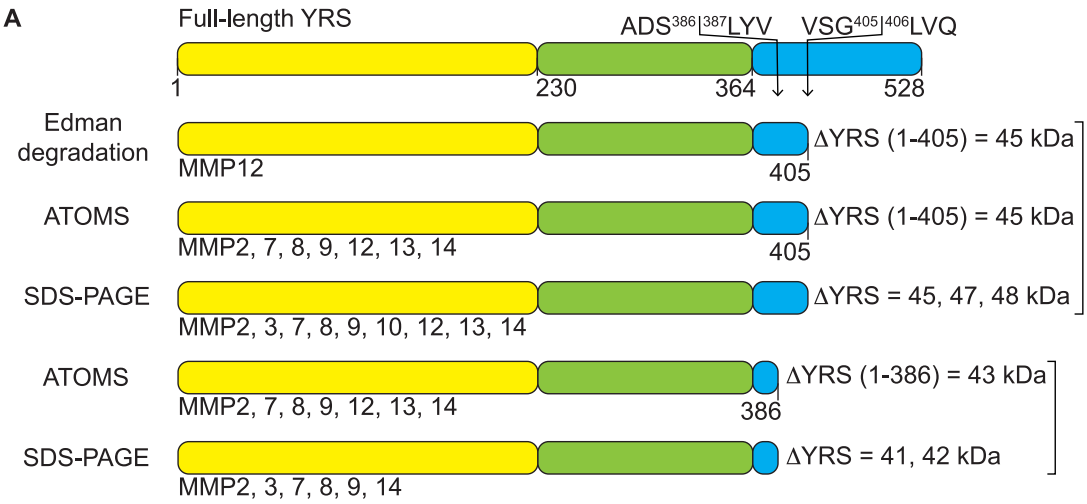

B

Cleavage site	MMP	Predicted MW	R_f MW	MMP
ADS$^{386}\downarrow^{387}$LYV	2, 7, 8, 9, 12, 13, 14	ΔYRS (1-386) = 43 kDa	41, 42 kDa	2, 3, 7, 8, 9, 10,
DSL$^{387}\downarrow^{388}$YVE	3			12, 13, 14
VSG$^{405}\downarrow^{406}$LVQ	2, 7, 8, 9, 12, 13, 14	ΔYRS (1-405) = 45 kDa	45, 47, 48 kDa	2, 3, 7, 8, 9, 14
SGL$^{406}\downarrow^{407}$VQF	3			

Figure 3.10 Major YRS proteoforms generated by MMP cleavage of YRS.
(A) Human MMP cleavage sites in YRS were determined by N-terminal sequencing by Edman degradation of proteins shown in Fig. 3.8B or by ATOMS N-terminal positional proteomics shown in Fig. 3.9. Schematic diagrams of YRS with the MMP cleavage sites leading to predicted N-terminal fragments of YRS (ΔYRS) are shown. Fragments predicted from cleavage sites are aligned by molecular weight with fragments observed on SDS-PAGE gels in Fig 3.8A. Molecular weights of predicted fragments were determined using the ExPASy pI/MW tool (https://web.expasy.org/compute_pi/), and the molecular weight of YRS fragments observed by SDS-PAGE were determined from relative migration distances compared with molecular weight standards (R_f). MMPs generating each fragment are indicated. Yellow, Rossman fold catalytic domain; green, anticodon recognition domain; blue, endothelial monocyte-activating polypeptide II-like (EMAPII) domain. (B) Table of cleavage sites common to predicted and measured molecular weights, and the MMPs responsible.

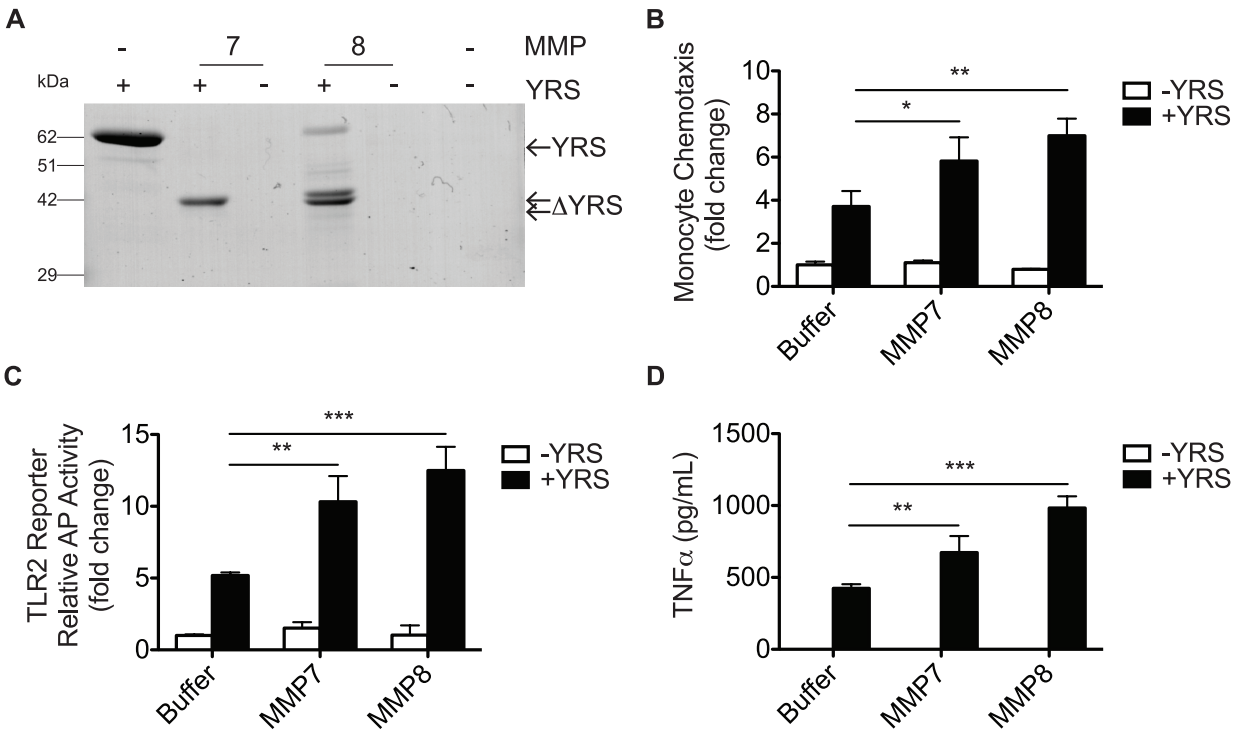

Figure 3.11 MMP7 and MMP8 cleavage of YRS increased monocyte chemotaxis, TLR2 signaling, NF-κB activation, and TNFα release by macrophages.
(A) Cleavage of recombinant human YRS (~62 kDa) by MMP7 and MMP8 (1:10 protease:YRS molar ratio) for 18 h at 37 °C visualized by Coomassie Brilliant Blue G-250–stained 10% SDS-PAGE. (B) Transwell chemotaxis assay (90 min) of THP1 monocytes towards 50 nM YRS, YRS cleaved by MMP7 or MMP8, MMPs alone or buffer. Data are presented as fold change compared to buffer alone (mean ± S.D., n = 3) of N = 3 independent experiments. (C) HEK293 cells co-expressing TLR2 and a NF-κB alkaline phosphatase (AP) reporter system were treated for 18 h with 50 nM YRS, YRS cleaved by MMP7 or MMP8, MMPs alone or buffer. The relative activity of alkaline phosphatase is plotted as fold change for TLR2 compared to buffer alone (mean ± S.D., n = 4) of N = 2 independent experiments. (D) ELISA measurement of TNFα released to the conditioned media of PMA-differentiated THP1-derived macrophages treated for 3 h with 50 nM intact YRS or MMP7 or MMP8-cleaved YRS (plotted as mean ± S.D., n = 4) of N = 3 independent experiments. Statistical significance was determined between YRS treated with buffer and YRS cleaved by MMP7 and MMP8 using a two-tailed unpaired Student's t-test. *, $p < 0.05$; **, $p < 0.01$; ***, $p < 0.001$.

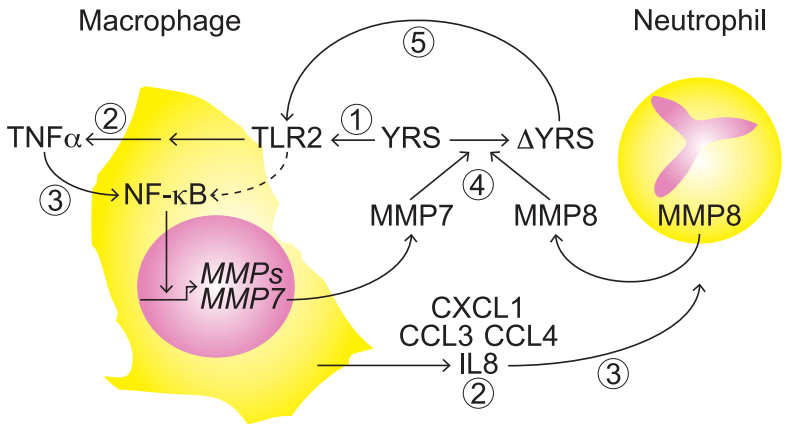

Figure 3.12 Feed-forward model of the YRS-MMP temporal relationship in first inducing and then potentiating proinflammatory pathways.

1. Extracellular YRS activation of TLR2 signaling (2) triggering TNFα and chemokine release. 3. TNFα and NF-κB activation upregulates MMP expression. Chemokine release recruits neutrophils. 4. Macrophage MMP7 and neutrophil MMP8 processing of YRS generates truncated proteoforms of YRS (ΔYRS). 5. ΔYRS drives inflammation by enhanced activation of TLR2 signaling in a feed-forward mechanism.

Chapter 4: Conclusion and Outlook

My studies showed that MMPs process two tRNA synthetases and thereby modulate tRNA synthetase moonlighting activities in regulating inflammation.

The aims of this thesis were to assess the bioactive roles MMPs play by targeting and processing tRNA synthetases as moonlighting substrates, specifically WRS and YRS. Where WRS was found to possess proinflammatory cytokine activity, MMP processing inactivated this function by cleavage of the N-terminus of WRS (Chapter 2). Conversely, the novel proinflammatory activity of YRS was found to be potentiated by MMP processing by cleavage in the C-terminus (Chapter 3). Together, these results reveal two tRNA synthetases, WRS and YRS, as extracellular substrates of MMPs. MMPs modulate the moonlighting activities of WRS and YRS, but the relative potency of the activities of WRS and YRS in modulating inflammation remains unknown. It is open to speculation that MMPs attenuate inflammation through processing of WRS and potentiate inflammation through processing of YRS, suggesting divergent roles for MMPs in inflammation depending on the substrate present. By modulating the proinflammatory moonlighting activities of WRS and YRS, the functional network of MMP protease web is further expanded to encompass a new class of multifunctional signaling cytokines, the tRNA synthetase family.

The studies performed in Chapters 2 and 3 showed that WRS and YRS both possessed proinflammatory activities. While these studies were limited by their *in vitro* nature, the use of protein antibody arrays as a screen for 36 different cytokines and chemokines produced from macrophages is comparable to other modern approaches for screening for inflammatory stimuli. Luminex magnetic bead-based immunoassays compare a similar number of cytokine analytes to the membranes used in this thesis, and both methods are effective in determining the cytokine response to stimuli (406). Nonetheless, future *in vivo* models of different inflammatory conditions will be useful in determining the depth of the relationship of WRS and YRS in inflammation.

I showed mechanisms to describe the relationship of WRS and YRS to MMPs (Chapter 2, 3). Secreted WRS stimulates TNFα release leading to the production of MMPs that process WRS and reduce the proinflammatory activities of WRS (Chapter 2). Conversely, secreted YRS stimulates TNFα release leading to the production of MMPs that process YRS and enhance the proinflammatory activities of YRS (Chapter 3). Furthermore, this work represents the first evidence of MMPs regulating tRNA synthetase moonlighting activities and provides insight on how these novel functions depend upon appended domains unique to the eukaryotic versions of

these enzymes. This sheds new light on how tRNA synthetases have been adapted by cells to influence cell-cell signaling and how proteolysis has been adapted as a post-translational process to afford cells control over signaling even after secretion.

While I focused on WRS and YRS, the discovery that MMP processing modulates extracellular tRNA synthetase moonlighting activities is likely to extend to other cellular processes beyond the inflammatory signaling explored here. Given that 18 tRNA synthetases (Table 1.1) have been detected as candidate MMP substrates in degradomic screens (177, 185, 186, 189, 193, 196) – it follows that the tRNA synthetase family represents an new pool of MMP substrates. As these degradomic studies focus on different MMPs, a family-wide strategy to approach MMP-processing of tRNA synthetases might prove useful to generate insight how proteolysis affects moonlighting tRNA synthetase activity. Such an approach also provides clues to the cellular processes, like inflammation, that these cleavage events might be relevant to. Not only did MMP2 and MMP14 cleave WRS and MMP2 and MMP12 cleave YRS, validating prior degradomic screens, I found 5 and 8 additional MMPs cleave WRS and YRS respectively (Chapter 2, 3). The discovery of additional MMPs processing of these proteins hints at the wider relevance that MMPs might play in regulating moonlighting protein activities.

Understanding the wider relevance of MMP regulation requires contextualizing the sources and timing of MMPs. The inflammatory response presents an excellent example for this context-based outlook, not only because it is directly related to the moonlighting activities explored in the previous two chapters but because inflammation requires a time-layered response of cells to inflammatory triggers. This temporal response depends on different MMPs being produced by distinct immune cell-types responding at specific times. In this way, the appropriate timing of both negative and positive feedback mechanisms is controlled to promote appropriate leukocyte recruitment early in inflammation and to terminate recruitment later to prevent chronic inflammation.

I showed that full-length WRS is secreted from cells in response to IFNγ, which also induces M1 macrophage polarization (Chapter 2). WRS potentially favours/enhances this by stimulating monocyte migration and TNFα release from macrophages (Chapter 2). Others have shown WRS is released rapidly from immune cells exposed to bacterial infection (215). I speculate that early in the immune response, neutrophil-specific proteases, such as neutrophil elastase and MMP8, process extracellular full-length WRS to attenuate the response to WRS as a negative feedback

mechanism. As inflammation progresses, the number of macrophages starts increasing at the site of injury due to monocyte invasion and differentiation while the number of neutrophils decrease. Macrophage-driven phagocytosis and clearance of dying cells changes the cytokine profile at the site of inflammation (407–409). This shift in cell-type also changes the proteases regulating inflammation. Macrophage proteases, such as MMP7, accumulate as the number of macrophages increase, which can inactivate full-length WRS. However, to validate this hypothesis, *in vivo* models are needed to assess the potency of MMPs in down-regulating proinflammatory WRS.

WRS and MMP processing may play a role in macrophage polarization. Only briefly described in Chapter 1 and Chapter 2, macrophages possess a range of phenotypes (131–133, 410, 411). Different cytokines and conditions drive "activation" of macrophages into M1 and M2 populations which loosely exhibit pro- and anti-inflammatory phenotypes respectively (131, 132). IFNγ, secreted from Type 1 helper T cells and natural killer cells during an immune response, is a major driver of the M1 phenotype (132, 385, 386). IFNγ drove expression and secretion of proinflammatory WRS from macrophages accompanied by increased expression of the M1 phenotype intracellular marker indoleamine 2,3-dioxygenase (Chapter 2). WRS may be a marker of the M1 phenotype, however assigning WRS as such a marker would require the same level of scrutiny other macrophage markers have undergone and is beyond this scope of the work presented in Chapter 2 (reviewed in (131, 132)).

M1 and M2 phenotypes are also temporally regulated during inflammation. During inflammation resolution, Type 2 helper T cells produced cytokines including IL4 drive macrophages towards the anti-inflammatory M2 phenotype (132, 385). MMPs affect macrophage phenotype (24, 412, 413). MMP12 regulates macrophage activation by processing IFNγ, cleaving it once to initially activate IFNγ before inactivating IFNγ with a second cleavage (24). MMP12 activation and subsequent inactivation of IFNγ is an example of negative feedback control of macrophage populations (24). Although WRS and MMP12 cleavage was not explored here, WRS is a candidate MMP12 substrate (196). Thus I speculate that not only do macrophages regulate a M1 stimulus in IFNγ through MMP regulation, but also a M1 marker in WRS. Future research of the relationship between MMP12 and WRS that models the approach of Dufour *et al.* (24) would be useful in assessing this hypothesis.

The feed-forward mechanism of MMP regulation of YRS that I presented in Chapter 3 is supported by recent research (207, 220, 224, 228). This recent work has proposed that YRS has been adapted by cells as a signal for chemotaxis (224). To build on the proposed feed-forward mechanism of YRS-MMP regulation, I speculate that extracellular YRS first stimulates leukocyte migration towards the site of injury as a "find-me" signal. Second, MMP processing of YRS generates YRS proteoforms with increased proinflammatory activities, leading to an amplified or more finely-tuned chemotactic gradient to recruit cells. CXCL8 is activated by MMP8 cleavage to fine-tune chemotactic gradients (25). It is exciting to learn that moonlighting activities of YRS may resemble the function of chemokines like CXCL8, thus the relationship of YRS to MMPs warrants further investigation in *in vivo* studies beyond the scope of the work presented herein.

The secretion of WRS and YRS into the extracellular environment provides clues as to the relevance of these tRNA synthetases in cell-cell signaling processes. These enzymes are crucial to protein synthesis. Thus tRNA synthetases likely serve as intrinsic sensors of cellular viability and amino acid availability that have been adapted by cells using secretion to convey cellular viability status to nearby cells. For WRS, its moonlighting activity and its secretion induced by IFNγ appears to have some connection to the status of tryptophan as the least represented amino acid in human proteins (~1%) (414). Tryptophan doubles in immune-related proteins such as human major histocompatibility antigens and immunoglobulins (~2%) (415). Perhaps tryptophan is underrepresented in non-immune related proteins to ensure WRS is primed to respond in inflammation, increasing tryptophan incorporation into immune-related proteins while being secreted rapidly in response to pathogen associated molecular pattern molecules and IFNγ. Despite Kapoor *et al.* previously determining only a fraction of subcellular WRS is secreted in response to IFNγ (~1.3%) (222), the elevation of WRS in the blood of sepsis patients with systemic infection (215) demonstrates just how important this secreted fraction is.

A newly discovered role of extracellular WRS in mediating high-affinity uptake of tryptophan into human cells further ties WRS to inflammation regulation (219). Miyanokoshi *et al*. demonstrated a second, novel tryptophan import system alternative to the ubiquitously expressed neutral amino acid transporter System L that imports tryptophan into cells (416–418). The tryptophan-selective importer was identified as WRS, boasting a tryptophan uptake rate (K_m = 150 nM) 100 x greater than System L transporter (K_m = 20 – 60 μM), making WRS a far more sensitive importer of lower tryptophan concentrations characteristic in immune responses (419) (normal tryptophan concentration in blood is ~50 μM (420)). Relevant to proteolysis, both WRS and Δ1-47 WRS are

capable of importing tryptophan into cells while Δ1-93 WRS (a proteoform produced by neutrophil elastase processing) does not. This result suggests that the N-terminus of WRS is necessary for tryptophan import function and that proteases can inactivate this activity depending how much of the sequence of the N-terminus of WRS the protease cuts off. Thus, proteases might regulate tryptophan uptake into cells by inactivating WRS importation of tryptophan, making this a topic for future research. This would further tie MMPs into inflammation regulation using WRS as a substrate. Kynurenine, a byproduct of tryptophan catabolism, arrests T cell proliferation except that of regulatory T cells, leading to immunosuppression (219). If sufficient WRS is processed into a non-tryptophan importing proteoform by MMPs, dysregulation of T cell populations might occur leading to dysregulated immunosuppression. Future study is needed to understand if this regulation of tryptophan import by proteases occurs *in vivo*.

The physiological relevance of YRS secretion remains unclear. Only serum-starvation (207) and apoptosis (224) induce YRS secretion. Research into the roles YRS plays in cellular stress has revealed YRS might behave as a general stress transducer, mediating responses to starvation, heat shock, endoplasmic reticulum stress (240), and oxidative stress (421). However, these studies focused on the translocation of YRS into the nucleus where it activates poly-(ADP-ribose) polymerase-1, not on the secretion of YRS. Future work should attempt to elucidate how YRS is secreted from cells to circulate in in extracellular compartments like plasma (242).

The challenge is now to understand what forms of WRS and YRS are present when – as we learn more about the activities of these moonlighting proteins in cellular processes, detecting them may provide an avenue for the improvement of diagnostics and prognostics in relevant diseases. Elevated levels of WRS in both the serum of sepsis patients with systemic infections (215) and patients with chronic kidney disease (218) detected by antibodies indicates that WRS is a marker of pathology. YRS circulates in human plasma (242), but nothing is known if YRS levels in plasma change in disease states. Other moonlighting proteins, like HMGB1, are already being capitalized on as clinical prognostic biomarkers (62, 422–424) and as therapeutic targets (63–66, 198, 425, 426) using sepsis as an example. Combining our knowledge that both WRS and MMP levels increase in serum during sepsis (199, 215) suggests that tRNA synthetases like WRS are likely targeted and processed by MMPs into different proteoforms exhibiting distinct activities from their full-length forms.

The promise of tRNA synthetases as prognostic biomarkers hinges on the capability of direct approaches to recognize and distinguish active proteoforms from inactive counterparts. Using WRS and YRS as examples, their moonlighting activities are affected by their N- and C-terminal domains respectively (Chapter 2, 3). One direct approach, the development of neo-epitope antibodies (23, 427), is particularly amenable to distinguishing proteoforms of signaling proteins generated by MMP cleavage (428). Neo-epitope antibodies recognize the N- and C-terminal epitopes generated by proteolysis but do not recognize the peptide chain of the intact cleavage site in the full-length substrate that possesses the same sequence. This discrimination is due to the peptides used to generate these neo-epitope antibodies, which are based on the terminal sequences of both sides of the cleavage site that have free amino (N)- or carboxy (C)-terminal groups to replace the peptide bond present in the intact protein substrate (427, 428). This allows unequivocal identification of processed cytokines. Affinity-purified and highly specific, these antibodies have been used to identify truncated chemokines such as CCL7 (23) and CXCL12 (429) in diseased fluid and tissue samples. Previous reports of WRS and YRS in healthy and diseased tissues have relied on antibodies unable to discriminate between the different proteoforms of these tRNA synthetases, thus not providing information about the presence of active from inactive proteoforms. To address this, neo-epitope antibodies might be useful in evaluating the WRS and YRS proteoforms that are present in disease states.

Mass spectrometry represents a more useful direct approach of tRNA synthetase proteoform detection. More sensitive than antibodies, mass spectrometry would be more useful as it can quantify the levels of proteoforms in a sample. Within a determined mass to charge ratio window, specific peptides can be analyzed and quantified using selected reaction monitoring (430–432) or multiple reaction monitoring (433, 434) type assays in readily available biofluids like plasma, urine, or saliva (176). These technologies can quantify the reduction in full-length protein and generation of truncated protein all in the same biological sample when translated into targeted methods for proteolytic signatures using proteolytic signature peptides (176, 435). Proteolytic signature peptides use tryptic peptides spanning known cleavage sites in full-length proteins and semi-tryptic peptides of proteolytically generated neo-N- and C-termini to quantify the reduction in full-length proteins and the generation of truncated proteins (176, 435). Mass spectrometry-based assays could be designed to quantify which WRS and YRS proteoforms are present in biological samples. As an example, such an assay might be designed to detect full-length WRS as a marker of sepsis in blood. While this technology has never been applied to moonlighting

proteins, it has been used to detect a proteolytic signature of cell death in the plasma of cancer patients undergoing chemotherapy (436), making it a candidate technology for detecting biomarkers affected by proteolysis.

Clinical applications of using WRS and YRS and their proteolytic truncations as biomarkers derives from proteoform moonlighting function. Hypothesized by Jin (365), low levels of proinflammatory full-length WRS in early responses to systemic infections in sepsis patients might indicate a poor prognosis, yet increased serum levels of WRS proteoforms might serve as an "all-clear" signal later in sepsis. Although Ahn *et al.* did not find serum levels of WRS elevated in sterile inflammatory disorders (215), its elevation in chronic kidney disease suggests WRS might be a detectable marker of chronic inflammation (218). Interestingly, high WRS expression levels are linked to favorable prognosis in gastric adenocarcinoma (437). Perhaps the angiostatic roles of N-terminally truncated WRS prevent neovascularization of growing tumors and hinder metastasis (438). This is reflected by low WRS expression levels being associated with increase lymph node metastasis in colorectal cancer (439). Excitingly, WRS has been used as a predictive biomarker for adjuvant chemotherapy following gastric cancer resection (440). However, this clinical promise is marred by the paradoxical effect WRS has in promoting the invasiveness of other cancers such as oral squamous cell carcinoma (441) where researchers proposed WRS induces cancer cell migration. Thus WRS must be evaluated as a biomarker on a case by case basis.

For clinical applications of YRS and its proteoforms, therapy innovations have already outpaced its potential as a biomarker. The development of a YRS variant with a gain of function mutation (Y341A) (220, 243, 442), that recapitulates the moonlighting activities of both YRS N- and C-terminal domains, has been touted as a novel therapy for thrombocytopenia (220). This variant may complement or replace second-line treatment standard thrombopoietin mimetics without carrying the same risks that come with thrombopoietin mimetic use such as thrombosis and acute myelogenous leukemia (443, 444). For vascular health, systemic treatment of recombinant N-terminal YRS fragments (mini-YRS) increases cardiac function post myocardial infarction in mice (445) and decreases infarction size in rats (372). Adenoviral vector administration containing mini-YRS into rhesus monkey myocardium following acute myocardial infarction increases cardiac function while decreasing infarction size (446), suggesting N-terminal YRS truncations are candidates for angiogenic and myocardial infarction therapy.

Adapting WRS and its proteoforms into therapeutic strategies remains in its infancy. Proposals for applications in sepsis have been made for patients in acute phase sepsis with high WRS serum levels, who might benefit from WRS antagonist strategies, and for immunocompromised patients who might benefit from WRS systemic administration to prime a weakened immune response (215, 365). In contrast to N-terminal fragments of YRS, C-terminal fragments of WRS inhibit recovery from myocardial infarctions in animal models (237, 372, 446), suggesting WRS truncations could serve as a counter strategy for angiogenesis. As exogenous single agent therapy, WRS truncations have proven stable to produce effects far distal to the site of entry (206) and have been proposed, based on murine models of macular degeneration (233, 447) and cancer (447), as therapy for pathological angiogenesis in diabetes, age related macular degeneration, and cancer (212, 233). Additionally, as WRS truncations have been found to stabilize endothelial cells to shear stress seen in high blood pressure, inflammation, and atherosclerosis (232), WRS truncation administration may be beneficial in maintaining of vascular homeostasis during vascular events like sepsis, restenosis, and stent replacement.

The moonlighting tryptophan import activity of WRS may also be an area for clinical application. As an adjuvant therapy, administration of WRS proteoforms such as Δ1-47 WRS, that would theoretically not induce a proinflammatory response like full-length WRS, might increase kynurenine production in transplanted tissue. This would lead to regulatory T cell upregulation leading to immunotolerance. Evaluating WRS proteoforms as biomarkers in transplant patients might also indicate probability of transplant rejection. Unfortunately, much of this novel tryptophan importing activity remains unclear and more research is needed to determine the what proteoforms can carry it out.

Genetically, mutations in 31 tRNA synthetase genes of the 37 member gene family (reviewed in (448, 449)) have been linked to a broad variety of human inherited disorders. The inheritance patterns of these disorders are both recessive and dominant. With both late and early onset phenotypes ranging from tissue specific diseases or multi-system developmental syndromes, the heterogeneity of these disorders makes teasing apart the mechanisms responsible that much more important. The only known WRS variant, H257R WRS, found in three separate families all with autosomal dominant neuropathy (450), negatively affected aminoacylation *in vitro* but potentiated angiostatic function when tested in a truncated WRS proteoform. Autosomal dominant variants G41R, V153_V156del, E196K, E196Q (451), and D81I YRS (452) are all located in the catalytic domain of YRS and are associated to dominant intermediate Charcot-Marie-Tooth

neuropathy. Autosomal recessive variants P213L, G525R (453), P167T (454), and P213L (455) YRS can be found inside and outside the catalytic domain of YRS and have been linked to failure to thrive and multiple organ abnormalities. Although none of these mutations affect the identified P1' position of MMP cleavage sites in WRS (Chapter 2) or YRS (Chapter 3), there is little evidence into what extent the canonical and non-canonical functions of these proteins contribute to these diseases and future work may reveal a role for proteolysis in these phenotypes.

Annotating extracellular activities for WRS and YRS helps fill the signaling network these proteins are responsible for. Given multiple members of the tRNA synthetase family have been found as MMP substrates (Table 1.1) and knowing glycyl- (216, 221), lysyl- (213, 456–458), histidyl- (223), and threonyl- (214, 459) tRNA synthetases are also secreted in response to stimuli with distinct extracellular activities, it is exciting to think what other cellular processes might be regulated by MMP processing of these enzymes. Although not the focus of this thesis, it is interesting to consider if intracellular MMP moonlighting proteolysis (Chapter 1) might target and regulate non-canonical functions of tRNA synthetases within the cell. The N-terminus of WRS is required for WRS to activate p53 in the nucleus in response to IFNγ stimulation (460), while only full-length YRS can interact with poly-(ADP-ribose) polymerase-1 (poly-(ADP-ribose) polymerase-1 is also processed by MMPs in the nucleus) in the nucleus to induce stress signaling during serum-starvation (240). MMPs process these proteins and thus might affect these processes.

Future studies aiming at determining the physiological significance of MMP processing of these moonlighting proteins will require clever use of animal models. While murine models are useful for determining functional effects of MMPs (22, 140), multiple MMPs cleaved tRNA synthetases, and in WRS and YRS several MMP cleavage sites were shared by other MMPs. Thus studying tRNA synthetase cleavage in a single or even double *Mmp*$^{-/-}$ null mouse might prove difficult considering proteolytic redundancy. However, developing non-cleavable mutant variants of tRNA synthetases might generate phenotypes that inform us of the role proteolysis plays in processing these moonlighting enzymes.

In conclusion, my thesis presents evidence to advance our knowledge of the functions and mechanisms MMPs use to contribute to inflammation by processing moonlighting tRNA synthetases. I have expanded information from previous degradomic studies to generate evidence that MMPs can activate or inactivate extracellular activities of tRNA synthetases. Using WRS and YRS, I have not only confirmed findings of novel moonlighting activities for these

proteins in parallel with other research groups but also found WRS and YRS to be direct substrates of MMPs. MMP processing regulated WRS and YRS moonlighting functions by generating new proteoforms of each, suggesting MMPs regulate WRS and YRS activity. Furthermore, I have expanded understanding that these proteins are secreted by multiple different cell-types, identified extracellular receptors for these proteins, and explored the mechanisms how MMPs might influence inflammation by targeting them. This research is only a first step towards understanding tRNA synthetases as MMP substrates, exposing a previously unknown regulatory network of diverse cellular processes that may be useful to applications for therapeutic research.

Bibliography

1. Henderson, B., and Martin, A. C. R. (2014) Protein moonlighting: a new factor in biology and medicine. *Biochem. Soc. Trans.* **42**, 1671–1678
2. Consortium, I. H. G. S., Lander, E. S., Linton, L. M., Birren, B., Nusbaum, C., Zody, M. C., Baldwin, J., Devon, K., Dewar, K., Doyle, M., FitzHugh, W., Funke, R., Gage, D., Harris, K., Heaford, A., Howland, J., Kann, L., Lehoczky, J., LeVine, R., McEwan, P., McKernan, K., Meldrim, J., Mesirov, J. P., Miranda, C., Morris, W., Naylor, J., Raymond, C., Rosetti, M., Santos, R., Sheridan, A., Sougnez, C., Stange-Thomann, N., Stojanovic, N., Subramanian, A., Wyman, D., Rogers, J., Sulston, J., Ainscough, R., Beck, S., Bentley, D., Burton, J., Clee, C., Carter, N., Coulson, A., Deadman, R., Deloukas, P., Dunham, A., Dunham, I., Durbin, R., French, L., Grafham, D., Gregory, S., Hubbard, T., Humphray, S., Hunt, A., Jones, M., Lloyd, C., McMurray, A., Matthews, L., Mercer, S., Milne, S., Mullikin, J. C., Mungall, A., Plumb, R., Ross, M., Shownkeen, R., Sims, S., Waterston, R. H., Wilson, R. K., Hillier, L. W., McPherson, J. D., Marra, M. A., Mardis, E. R., Fulton, L. A., Chinwalla, A. T., Pepin, K. H., Gish, W. R., Chissoe, S. L., Wendl, M. C., Delehaunty, K. D., Miner, T. L., Delehaunty, A., Kramer, J. B., Cook, L. L., Fulton, R. S., Johnson, D. L., Minx, P. J., Clifton, S. W., Hawkins, T., Branscomb, E., Predki, P., Richardson, P., Wenning, S., Slezak, T., Doggett, N., Cheng, J.-F., Olsen, A., Lucas, S., Elkin, C., Uberbacher, E., Frazier, M., Gibbs, R. A., Muzny, D. M., Scherer, S. E., Bouck, J. B., Sodergren, E. J., Worley, K. C., Rives, C. M., Gorrell, J. H., Metzker, M. L., Naylor, S. L., Kucherlapati, R. S., Nelson, D. L., Weinstock, G. M., Sakaki, Y., Fujiyama, A., Hattori, M., Yada, T., Toyoda, A., Itoh, T., Kawagoe, C., Watanabe, H., Totoki, Y., Taylor, T., Weissenbach, J., Heilig, R., Saurin, W., Artiguenave, F., Brottier, P., Bruls, T., Pelletier, E., Robert, C., Wincker, P., Rosenthal, A., Platzer, M., Nyakatura, G., Taudien, S., Rump, A., Smith, D. R., Doucette-Stamm, L., Rubenfield, M., Weinstock, K., Lee, H. M., Dubois, J., Yang, H., Yu, J., Wang, J., Huang, G., Gu, J., Hood, L., Rowen, L., Madan, A., Qin, S., Davis, R. W., Federspiel, N. A., Abola, A. P., Proctor, M. J., Roe, B. A., Chen, F., Pan, H., Ramser, J., Lehrach, H., Reinhardt, R., McCombie, W. R., de la Bastide, M., Dedhia, N., Blöcker, H., Hornischer, K., Nordsiek, G., Agarwala, R., Aravind, L., Bailey, J. A., Bateman, A., Batzoglou, S., Birney, E., Bork, P., Brown, D. G., Burge, C. B., Cerutti, L., Chen, H.-C., Church, D., Clamp, M., Copley, R. R., Doerks, T., Eddy, S. R., Eichler, E. E., Furey, T. S., Galagan, J., Gilbert, J. G. R., Harmon, C., Hayashizaki, Y., Haussler, D., Hermjakob, H., Hokamp, K., Jang, W., Johnson, L. S., Jones, T. A., Kasif, S., Kaspryzk, A., Kennedy, S., Kent, W. J., Kitts, P., Koonin, E. V, Korf, I., Kulp, D., Lancet, D., Lowe, T. M., McLysaght, A., Mikkelsen, T., Moran, J. V, Mulder, N., Pollara, V. J., Ponting, C. P., Schuler, G., Schultz, J., Slater, G., Smit, A. F. A., Stupka, E., Szustakowki, J., Thierry-Mieg, D., Thierry-Mieg, J., Wagner, L., Wallis, J., Wheeler, R., Williams, A., Wolf, Y. I., Wolfe, K. H., Yang, S.-P., Yeh, R.-F., Collins, F., Guyer, M. S., Peterson, J., Felsenfeld, A., Wetterstrand, K. A., Myers, R. M., Schmutz, J., Dickson, M., Grimwood, J., Cox, D. R., Olson, M. V, Kaul, R., Raymond, C., Shimizu, N., Kawasaki, K., Minoshima, S., Evans, G. A., Athanasiou, M., Schultz, R., Patrinos, A., and Morgan, M. J. (2001) Initial sequencing and analysis of the human genome. *Nature*. **409**, 860
3. Omenn, G. S., Lane, L., Lundberg, E. K., Beavis, R. C., Overall, C. M., and Deutsch, E. W. (2016) Metrics for the Human Proteome Project 2016: Progress on Identifying and Characterizing the Human Proteome, Including Post-Translational Modifications. *J. Proteome Res.* **15**, 3951–3960
4. neXtProt [online] https://www.nextprot.org (Accessed March 6, 2017)
5. Jeffery, C. J. (1999) Moonlighting proteins. *Trends Biochem. Sci.* **24**, 8–11

6. Pal, S., Gupta, R., and Davuluri, R. V (2012) Alternative transcription and alternative splicing in cancer. *Pharmacol. Ther.* **136**, 283–294
7. Piatigorsky, J. (1998) Gene sharing in lens and cornea: facts and implications. *Prog. Retin. Eye Res.* **17**, 145–174
8. Butler, G. S., and Overall, C. M. (2009) Proteomic identification of multitasking proteins in unexpected locations complicates drug targeting. *Nat. Rev. Drug Discov.* **8**, 935
9. Jeffery, C. J. (2003) Moonlighting proteins: old proteins learning new tricks. *Trends Genet.* **19**, 415–417
10. Jeffery, C. J. (2005) Mass spectrometry and the search for moonlighting proteins. *Mass Spectrom. Rev.* **24**, 772–782
11. Jeffery, C. J. (2004) Molecular mechanisms for multitasking: recent crystal structures of moonlighting proteins. *Curr. Opin. Struct. Biol.* **14**, 663–668
12. Jeffery, C. J. (2009) Moonlighting proteins—an update. *Mol. Biosyst.* **5**, 345–350
13. Jeffery, C. J. (2011) Proteins with neomorphic moonlighting functions in disease. *IUBMB Life*. **63**, 489–494
14. Jeffery, C. J. (2014) An introduction to protein moonlighting. *Biochem. Soc. Trans.* **42**, 1679–1683
15. Jeffery, C. J. (2015) Why study moonlighting proteins? *Front. Genet.* **6**, 211
16. Butler, G. S., and Overall, C. M. (2009) Updated Biological Roles for Matrix Metalloproteinases and New “Intracellular” Substrates Revealed by Degradomics. *Biochemistry*. **48**, 10830–10845
17. Chen, C., Mani, M., Jeffery, C. J., Patel, B., Zwicke, G., Thakkar, J., Mathur, T., Amblee, V., Liu, H., and Zabad, S. (2014) MoonProt: a database for proteins that are known to moonlight. *Nucleic Acids Res.* **43**, D277–D282
18. Mozo-Villarias, A., Ferragut, G., Amela, I., Piñol, J., Perez-Pons, J., Hernández, S., Cedano, J., and Querol, E. (2013) MultitaskProtDB: a database of multitasking proteins. *Nucleic Acids Res.* **42**, D517–D520
19. Sirover, M. A. (2011) On the functional diversity of glyceraldehyde-3-phosphate dehydrogenase: Biochemical mechanisms and regulatory control. *Biochim. Biophys. Acta - Gen. Subj.* **1810**, 741–751
20. Kang, R., Chen, R., Zhang, Q., Hou, W., Wu, S., Cao, L., Huang, J., Yu, Y., Fan, X., Yan, Z., Sun, X., Wang, H., Wang, Q., Tsung, A., Billiar, T. R., Zeh, H. J., Lotze, M. T., and Tang, D. (2014) HMGB1 in health and disease. *Mol. Aspects Med.* **40**, 1–116
21. Rodriguez, D., Morrison, C. J., and Overall, C. M. (2010) Matrix metalloproteinases: what do they not do? New substrates and biological roles identified by murine models and proteomics. *Biochim. Biophys. Acta*. **1803**, 39–54
22. Parks, W. C., Wilson, C. L., and Lopez-Boado, Y. S. (2004) Matrix metalloproteinases as modulators of inflammation and innate immunity. *Nat. Rev. Immunol.* **4**, 617–629
23. McQuibban, G. A., Gong, J. H., Tam, E. M., McCulloch, C. A., Clark-Lewis, I., and Overall, C. M. (2000) Inflammation dampened by gelatinase A cleavage of monocyte chemoattractant protein-3. *Science*. **289**, 1202–1206
24. Dufour, A., Bellac, C. L., Eckhard, U., Solis, N., Klein, T., Kappelhoff, R., Fortelny, N., Jobin, P., Rozmus, J., Mark, J., Pavlidis, P., Dive, V., Barbour, S. J., and Overall, C. M. (2018) C-terminal truncation of IFN-gamma inhibits proinflammatory macrophage responses and is deficient in autoimmune disease. *Nat. Commun.* **9**, 2416
25. Tester, A. M., Cox, J. H., Connor, A. R., Starr, A. E., Dean, R. A., Puente, X. S., López-Otín, C., and Overall, C. M. (2007) LPS Responsiveness and Neutrophil Chemotaxis In Vivo Require PMN MMP-8 Activity. *PLoS One*. **2**, e312
26. Bonnans, C., Chou, J., and Werb, Z. (2014) Remodelling the extracellular matrix in

development and disease. *Nat. Rev. Mol. Cell Biol.* **15**, 786
27. Klein, T., and Bischoff, R. (2011) Physiology and pathophysiology of matrix metalloproteases. *Amino Acids*. **41**, 271–290
28. Morrison, C. J., Butler, G. S., Rodríguez, D., and Overall, C. M. (2009) Matrix metalloproteinase proteomics: substrates, targets, and therapy. *Curr. Opin. Cell Biol.* **21**, 645–653
29. Khokha, R., Murthy, A., and Weiss, A. (2013) Metalloproteinases and their natural inhibitors in inflammation and immunity. *Nat. Rev. Immunol.* **13**, 649
30. Marchant, D. J., Bellac, C. L., Moraes, T. J., Wadsworth, S. J., Dufour, A., Butler, G. S., Bilawchuk, L. M., Hendry, R. G., Robertson, A. G., Cheung, C. T., Ng, J., Ang, L., Luo, Z., Heilbron, K., Norris, M. J., Duan, W., Bucyk, T., Karpov, A., Devel, L., Georgiadis, D., Hegele, R. G., Luo, H., Granville, D. J., Dive, V., McManus, B. M., and Overall, C. M. (2014) A new transcriptional role for matrix metalloproteinase-12 in antiviral immunity. *Nat. Med.* **20**, 493
31. Gross, J., and Lapiere, C. M. (1962) Collagenolytic activity in amphibian tissues: a tissue culture assay. *Proc. Natl. Acad. Sci. U. S. A.* **48**, 1014–1022
32. Hynes, R. O., and Naba, A. (2012) Overview of the matrisome--an inventory of extracellular matrix constituents and functions. *Cold Spring Harb. Perspect. Biol.* **4**, a004903
33. Overall, C. M. (2002) Molecular determinants of metalloproteinase substrate specificity: matrix metalloproteinase substrate binding domains, modules, and exosites. *Mol. Biotechnol.* **22**, 51–86
34. Rohani, M. G., and Parks, W. C. (2015) Matrix remodeling by MMPs during wound repair. *Matrix Biol.* **44**–**46**, 113–121
35. Overall, C. M. (2001) Matrix metalloproteinase substrate binding domains, modules and exosites. Overview and experimental strategies. *Methods Mol. Biol.* **151**, 79–120
36. Nagase, H. (1997) Activation mechanisms of matrix metalloproteinases. *Biol. Chem.* **378**, 151–160
37. Overall, C. M., and Butler, G. S. (2007) Protease Yoga: Extreme Flexibility of a Matrix Metalloproteinase. *Structure*. **15**, 1159–1161
38. Wallon, U. M., and Overall, C. M. (1997) The hemopexin-like domain (C domain) of human gelatinase A (matrix metalloproteinase-2) requires Ca2+ for fibronectin and heparin binding. Binding properties of recombinant gelatinase A C domain to extracellular matrix and basement membrane components. *J. Biol. Chem.* **272**, 7473–7481
39. Tam, E. M., Morrison, C. J., Wu, Y. I., Stack, M. S., and Overall, C. M. (2004) Membrane protease proteomics: Isotope-coded affinity tag MS identification of undescribed MT1-matrix metalloproteinase substrates. *Proc. Natl. Acad. Sci. U. S. A.* **101**, 6917–6922
40. Steffensen, B., Wallon, U. M., and Overall, C. M. (1995) Extracellular matrix binding properties of recombinant fibronectin type II-like modules of human 72-kDa gelatinase/type IV collagenase. High affinity binding to native type I collagen but not native type IV collagen. *J. Biol. Chem.* **270**, 11555–11566
41. Steffensen, B., Bigg, H. F., and Overall, C. M. (1998) The involvement of the fibronectin type II-like modules of human gelatinase A in cell surface localization and activation. *J. Biol. Chem.* **273**, 20622–20628
42. Page-McCaw, A., Ewald, A. J., and Werb, Z. (2007) Matrix metalloproteinases and the regulation of tissue remodelling. *Nat. Rev. Mol. Cell Biol.* **8**, 221
43. Nagase, H., and Woessner, J. F. J. (1999) Matrix metalloproteinases. *J. Biol. Chem.* **274**, 21491–21494
44. Vincenti, M. P. (2001) The matrix metalloproteinase (MMP) and tissue inhibitor of

metalloproteinase (TIMP) genes. Transcriptional and posttranscriptional regulation, signal transduction and cell-type-specific expression. *Methods Mol. Biol.* **151**, 121–148
45. Ra, H.-J., and Parks, W. C. (2007) Control of matrix metalloproteinase catalytic activity. *Matrix Biol.* **26**, 587–596
46. Marchenko, N. D., Marchenko, G. N., and Strongin, A. Y. (2002) Unconventional activation mechanisms of MMP-26, a human matrix metalloproteinase with a unique PHCGXXD cysteine-switch motif. *J. Biol. Chem.* **277**, 18967–18972
47. Pei, D., and Weiss, S. J. (1995) Furin-dependent intracellular activation of the human stromelysin-3 zymogen. *Nature*. **375**, 244–247
48. Baker, A. H., Edwards, D. R., and Murphy, G. (2002) Metalloproteinase inhibitors: biological actions and therapeutic opportunities. *J. Cell Sci.* **115**, 3719–3727
49. Tytell, M., Greenberg, S. G., and Lasek, R. J. (1986) Heat shock-like protein is transferred from glia to axon. *Brain Res.* **363**, 161–164
50. Tagaya, Y., Maeda, Y., Mitsui, A., Kondo, N., Matsui, H., Hamuro, J., Brown, N., Arai, K., Yokota, T., and Wakasugi, H. (1989) ATL-derived factor (ADF), an IL-2 receptor/Tac inducer homologous to thioredoxin; possible involvement of dithiol-reduction in the IL-2 receptor induction. *EMBO J.* **8**, 757–764
51. Sherry, B., Yarlett, N., Strupp, A., and Cerami, A. (1992) Identification of cyclophilin as a proinflammatory secretory product of lipopolysaccharide-activated macrophages. *Proc. Natl. Acad. Sci. U. S. A.* **89**, 3511–3515
52. Morton, H., Rolfe, B., and Clunie, G. J. (1977) An early pregnancy factor detected in human serum by the rosette inhibition test. *Lancet (London, England)*. **1**, 394–397
53. Noonan, F. P., Halliday, W. J., Morton, H., and Clunie, G. J. (1979) Early pregnancy factor is immunosuppressive. *Nature*. **278**, 649–651
54. Cavanagh, A. C., and Morton, H. (1994) The purification of early-pregnancy factor to homogeneity from human platelets and identification as chaperonin 10. *Eur. J. Biochem.* **222**, 551–560
55. Vanags, D., Williams, B., Johnson, B., Hall, S., Nash, P., Taylor, A., Weiss, J., and Feeney, D. (2006) Therapeutic efficacy and safety of chaperonin 10 in patients with rheumatoid arthritis: a double-blind randomised trial. *Lancet (London, England)*. **368**, 855–863
56. Williams, B., Vanags, D., Hall, S., McCormack, C., Foley, P., Weiss, J., Johnson, B., Latz, E., and Feeney, D. (2008) Efficacy and safety of chaperonin 10 in patients with moderate to severe plaque psoriasis: evidence of utility beyond a single indication. *Arch. Dermatol.* **144**, 683–685
57. van Eden, W. (2008) XToll, a recombinant chaperonin 10 as an anti-inflammatory immunomodulator. *Curr. Opin. Investig. Drugs*. **9**, 523–533
58. Broadley, S. A., Vanags, D., Williams, B., Johnson, B., Feeney, D., Griffiths, L., Shakib, S., Brown, G., Coulthard, A., Mullins, P., and Kneebone, C. (2009) Results of a phase IIa clinical trial of an anti-inflammatory molecule, chaperonin 10, in multiple sclerosis. *Mult. Scler.* **15**, 329–336
59. Rossotto, P., and Ruffo, A. (1958) Prognostic significance of the study of certain enzymes of anaerobic glycolysis (aldolase, phosphoglucoisomerase) in the blood of malignant tumor patients. *Minerva Med.* **49**, 2145–2150
60. Gurney, M. E., Heinrich, S. P., Lee, M. R., and Yin, H. S. (1986) Molecular cloning and expression of neuroleukin, a neurotrophic factor for spinal and sensory neurons. *Science*. **234**, 566–574
61. Niinaka, Y., Paku, S., Haga, A., Watanabe, H., and Raz, A. (1998) Expression and secretion of neuroleukin/phosphohexose isomerase/maturation factor as autocrine

motility factor by tumor cells. *Cancer Res.* **58**, 2667–2674
62. Sunden-Cullberg, J., Norrby-Teglund, A., Rouhiainen, A., Rauvala, H., Herman, G., Tracey, K. J., Lee, M. L., Andersson, J., Tokics, L., and Treutiger, C. J. (2005) Persistent elevation of high mobility group box-1 protein (HMGB1) in patients with severe sepsis and septic shock. *Crit. Care Med.* **33**, 564–573
63. Karlsson, S., Pettila, V., Tenhunen, J., Laru-Sompa, R., Hynninen, M., and Ruokonen, E. (2008) HMGB1 as a predictor of organ dysfunction and outcome in patients with severe sepsis. *Intensive Care Med.* **34**, 1046–1053
64. Gamez-Diaz, L. Y., Enriquez, L. E., Matute, J. D., Velasquez, S., Gomez, I. D., Toro, F., Ospina, S., Bedoya, V., Arango, C. M., Valencia, M. L., De La Rosa, G., Gomez, C. I., Garcia, A., Patino, P. J., and Jaimes, F. A. (2011) Diagnostic accuracy of HMGB-1, sTREM-1, and CD64 as markers of sepsis in patients recently admitted to the emergency department. *Acad. Emerg. Med.* **18**, 807–815
65. Yu, H., Qi, Z., Zhao, L., Shao, R., Fang, Y., and Li, C. (2016) Prognostic Value of Dynamic Monitoring of Cellular Immunity and HMGB1 in Severe Sepsis: Delayed Chronic Inflammation may be the Leading Cause of Death in Late Severe Sepsis. *Clin. Lab.* **62**, 2379–2385
66. Stevens, N. E., Chapman, M. J., Fraser, C. K., Kuchel, T. R., Hayball, J. D., and Diener, K. R. (2017) Therapeutic targeting of HMGB1 during experimental sepsis modulates the inflammatory cytokine profile to one associated with improved clinical outcomes. *Sci. Rep.* **7**, 5850
67. Kirkham, B., Chaabo, K., Hall, C., Garrood, T., Mant, T., Allen, E., Vincent, A., Vasconcelos, J. C., Prevost, A. T., Panayi, G. S., and Corrigall, V. M. (2016) Safety and patient response as indicated by biomarker changes to binding immunoglobulin protein in the phase I/IIA RAGULA clinical trial in rheumatoid arthritis. *Rheumatology (Oxford).* **55**, 1993–2000
68. Bodman-Smith, M. D., Corrigall, V. M., Kemeny, D. M., and Panayi, G. S. (2003) BiP, a putative autoantigen in rheumatoid arthritis, stimulates IL-10-producing CD8-positive T cells from normal individuals. *Rheumatology (Oxford).* **42**, 637–644
69. Corrigall, V. M., Bodman-Smith, M. D., Brunst, M., Cornell, H., and Panayi, G. S. (2004) Inhibition of antigen-presenting cell function and stimulation of human peripheral blood mononuclear cells to express an antiinflammatory cytokine profile by the stress protein BiP: relevance to the treatment of inflammatory arthritis. *Arthritis Rheum.* **50**, 1164–1171
70. Brownlie, R. J., Myers, L. K., Wooley, P. H., Corrigall, V. M., Bodman-Smith, M. D., Panayi, G. S., and Thompson, S. J. (2006) Treatment of murine collagen-induced arthritis by the stress protein BiP via interleukin-4-producing regulatory T cells: a novel function for an ancient protein. *Arthritis Rheum.* **54**, 854–863
71. Rabouille, C. (2017) Pathways of Unconventional Protein Secretion. *Trends Cell Biol.* **27**, 230–240
72. Ferro-Novick, S., and Brose, N. (2013) Traffic control system within cells. *Nature*. **504**, 98
73. Cauwe, B., and Opdenakker, G. (2010) Intracellular substrate cleavage: a novel dimension in the biochemistry, biology and pathology of matrix metalloproteinases. *Crit. Rev. Biochem. Mol. Biol.* **45**, 351–423
74. Lu, B., Wang, C., Wang, M., Li, W., Chen, F., Tracey, K. J., and Wang, H. (2014) Molecular mechanism and therapeutic modulation of high mobility group box 1 release and action: an updated review. *Expert Rev. Clin. Immunol.* **10**, 713–727
75. Green, E. R., and Mecsas, J. (2016) Bacterial Secretion Systems: An Overview. *Microbiol. Spectr.* **4**, 10.1128/microbiolspec.VMBF-0012–2015
76. Prudovsky, I., Tarantini, F., Landriscina, M., Neivandt, D., Soldi, R., Kirov, A., Small, D.,

Kathir, K. M., Rajalingam, D., and Kumar, T. K. S. (2008) Secretion without Golgi. *J. Cell. Biochem.* **103**, 1327–1343
77. Steringer, J. P., Bleicken, S., Andreas, H., Zacherl, S., Laussmann, M., Temmerman, K., Contreras, F. X., Bharat, T. A. M., Lechner, J., Muller, H.-M., Briggs, J. A. G., Garcia-Saez, A. J., and Nickel, W. (2012) Phosphatidylinositol 4,5-bisphosphate (PI(4,5)P2)-dependent oligomerization of fibroblast growth factor 2 (FGF2) triggers the formation of a lipidic membrane pore implicated in unconventional secretion. *J. Biol. Chem.* **287**, 27659–27669
78. Zeitler, M., Steringer, J. P., Muller, H.-M., Mayer, M. P., and Nickel, W. (2015) HIV-Tat Protein Forms Phosphoinositide-dependent Membrane Pores Implicated in Unconventional Protein Secretion. *J. Biol. Chem.* **290**, 21976–21984
79. Adamczyk, M., Griffiths, R., Dewitt, S., Knäuper, V., and Aeschlimann, D. (2015) P2X7 receptor activation regulates rapid unconventional export of transglutaminase-2. *J. Cell Sci.* **128**, 4615–4628
80. Prudovsky, I., Kumar, T. K. S., Sterling, S., and Neivandt, D. (2013) Protein-phospholipid interactions in nonclassical protein secretion: problem and methods of study. *Int. J. Mol. Sci.* **14**, 3734–3772
81. Landriscina, M., Soldi, R., Bagala, C., Micucci, I., Bellum, S., Tarantini, F., Prudovsky, I., and Maciag, T. (2001) S100A13 participates in the release of fibroblast growth factor 1 in response to heat shock in vitro. *J. Biol. Chem.* **276**, 22544–22552
82. Ford, R. C., and Beis, K. (2019) Learning the ABCs one at a time: structure and mechanism of ABC transporters. *Biochem. Soc. Trans.* **1**, BST20180147
83. Neul, C., Schaeffeler, E., Sparreboom, A., Laufer, S., Schwab, M., and Nies, A. T. (2016) Impact of Membrane Drug Transporters on Resistance to Small-Molecule Tyrosine Kinase Inhibitors. *Trends Pharmacol. Sci.* **37**, 904–932
84. Meldolesi, J. (2018) Exosomes and Ectosomes in Intercellular Communication. *Curr. Biol.* **28**, R435–R444
85. Thery, C., Boussac, M., Veron, P., Ricciardi-Castagnoli, P., Raposo, G., Garin, J., and Amigorena, S. (2001) Proteomic analysis of dendritic cell-derived exosomes: a secreted subcellular compartment distinct from apoptotic vesicles. *J. Immunol.* **166**, 7309–7318
86. Fevrier, B., and Raposo, G. (2004) Exosomes: endosomal-derived vesicles shipping extracellular messages. *Curr. Opin. Cell Biol.* **16**, 415–421
87. Keller, S., Sanderson, M. P., Stoeck, A., and Altevogt, P. (2006) Exosomes: from biogenesis and secretion to biological function. *Immunol. Lett.* **107**, 102–108
88. Simpson, R. J., Jensen, S. S., and Lim, J. W. E. (2008) Proteomic profiling of exosomes: current perspectives. *Proteomics*. **8**, 4083–4099
89. Vega, V. L., Rodriguez-Silva, M., Frey, T., Gehrmann, M., Diaz, J. C., Steinem, C., Multhoff, G., Arispe, N., and De Maio, A. (2008) Hsp70 translocates into the plasma membrane after stress and is released into the extracellular environment in a membrane-associated form that activates macrophages. *J. Immunol.* **180**, 4299–4307
90. Thery, C., Ostrowski, M., and Segura, E. (2009) Membrane vesicles as conveyors of immune responses. *Nat. Rev. Immunol.* **9**, 581–593
91. Cocucci, E., Racchetti, G., and Meldolesi, J. (2009) Shedding microvesicles: artefacts no more. *Trends Cell Biol.* **19**, 43–51
92. Cocucci, E., and Meldolesi, J. (2015) Ectosomes and exosomes: shedding the confusion between extracellular vesicles. *Trends Cell Biol.* **25**, 364–372
93. Blott, E. J., and Griffiths, G. M. (2002) Secretory lysosomes. *Nat. Rev. Mol. Cell Biol.* **3**, 122–131
94. Raposo, G., Tenza, D., Murphy, D. M., Berson, J. F., and Marks, M. S. (2001) Distinct

protein sorting and localization to premelanosomes, melanosomes, and lysosomes in pigmented melanocytic cells. *J. Cell Biol.* **152**, 809–824
95. Gardella, S., Andrei, C., Ferrera, D., Lotti, L. V, Torrisi, M. R., Bianchi, M. E., and Rubartelli, A. (2002) The nuclear protein HMGB1 is secreted by monocytes via a non-classical, vesicle-mediated secretory pathway. *EMBO Rep.* **3**, 995–1001
96. Kerr, J. F., Wyllie, A. H., and Currie, A. R. (1972) Apoptosis: a basic biological phenomenon with wide-ranging implications in tissue kinetics. *Br. J. Cancer.* **26**, 239–257
97. Taylor, R. C., Cullen, S. P., and Martin, S. J. (2008) Apoptosis: controlled demolition at the cellular level. *Nat. Rev. Mol. Cell Biol.* **9**, 231–241
98. Gardai, S. J., McPhillips, K. A., Frasch, S. C., Janssen, W. J., Starefeldt, A., Murphy-Ullrich, J. E., Bratton, D. L., Oldenborg, P.-A., Michalak, M., and Henson, P. M. (2005) Cell-surface calreticulin initiates clearance of viable or apoptotic cells through trans-activation of LRP on the phagocyte. *Cell*. **123**, 321–334
99. Bianchi, M. E. (2007) DAMPs, PAMPs and alarmins: all we need to know about danger. *J. Leukoc. Biol.* **81**, 1–5
100. Kono, H., and Rock, K. L. (2008) How dying cells alert the immune system to danger. *Nat. Rev. Immunol.* **8**, 279–289
101. DeMarco, R. A., Fink, M. P., and Lotze, M. T. (2005) Monocytes promote natural killer cell interferon gamma production in response to the endogenous danger signal HMGB1. *Mol. Immunol.* **42**, 433–444
102. Anderson, K. M., Srivastava, P. K., Binder, R. J., Suto, R., and Basu, S. (2000) Necrotic but not apoptotic cell death releases heat shock proteins, which deliver a partial maturation signal to dendritic cells and activate the NF-κB pathway. *Int. Immunol.* **12**, 1539–1546
103. Kawai, T., and Akira, S. (2007) Signaling to NF- k B by Toll-like receptors. *Trends Mol. Med.* **13**, 460–469
104. Brinkmann, V., Reichard, U., Goosmann, C., Fauler, B., Uhlemann, Y., Weiss, D. S., Weinrauch, Y., and Zychlinsky, A. (2004) Neutrophil extracellular traps kill bacteria. *Science*. **303**, 1532–1535
105. Yousefi, S., and Simon, H.-U. (2016) NETosis - Does It Really Represent Nature's "Suicide Bomber"? *Front. Immunol.* **7**, 328
106. Yousefi, S., Stojkov, D., Germic, N., Simon, D., Wang, X., Benarafa, C., and Simon, H.-U. (2019) Untangling "NETosis" from NETs. *Eur. J. Immunol.* **49**, 221–227
107. Yousefi, S., Mihalache, C., Kozlowski, E., Schmid, I., and Simon, H. U. (2009) Viable neutrophils release mitochondrial DNA to form neutrophil extracellular traps. *Cell Death Differ.* **16**, 1438–1444
108. Giuliani, F., Grieve, A., and Rabouille, C. (2011) Unconventional secretion: a stress on GRASP. *Curr. Opin. Cell Biol.* **23**, 498–504
109. Chovatiya, R., and Medzhitov, R. (2014) Stress, inflammation, and defense of homeostasis. *Mol. Cell*. **54**, 281–288
110. Nissinen, L., and Kahari, V.-M. (2014) Matrix metalloproteinases in inflammation. *Biochim. Biophys. Acta*. **1840**, 2571–2580
111. McCawley, L. J., and Matrisian, L. M. (2001) Matrix metalloproteinases: they're not just for matrix anymore! *Curr. Opin. Cell Biol.* **13**, 534–540
112. Overall, C. M., and Blobel, C. P. (2007) In search of partners: linking extracellular proteases to substrates. *Nat. Rev. Mol. Cell Biol.* **8**, 245–257
113. Vong, L., D'Acquisto, F., Pederzoli-Ribeil, M., Lavagno, L., Flower, R. J., Witko-Sarsat, V., and Perretti, M. (2007) Annexin 1 cleavage in activated neutrophils: a pivotal role for proteinase 3. *J. Biol. Chem.* **282**, 29998–30004

114. Lawrence, T., Willoughby, D. A., and Gilroy, D. W. (2002) Anti-inflammatory lipid mediators and insights into the resolution of inflammation. *Nat. Rev. Immunol.* **2**, 787
115. Medzhitov, R. (2008) Origin and physiological roles of inflammation. *Nature*. **454**, 428–435
116. Tomazella, G. G., da Silva, I., Laure, H. J., Rosa, J. C., Chammas, R., Wiker, H. G., de Souza, G. A., and Greene, L. J. (2009) Proteomic analysis of total cellular proteins of human neutrophils. *Proteome Sci.* **7**, 32
117. Nicolás-Ávila, J. Á., Adrover, J. M., and Hidalgo, A. (2017) Neutrophils in Homeostasis, Immunity, and Cancer. *Immunity*. **46**, 15–28
118. Belaaouaj, A. azzaq, Kim, K. S., and Shapiro, S. D. (2000) Degradation of Outer Membrane Protein A in Escherichia coli Killing by Neutrophil Elastase. *Science*. **289**, 1185–1187
119. Lominadze, G., Powell, D. W., Luerman, G. C., Link, A. J., Ward, R. A., and McLeish, K. R. (2005) Proteomic analysis of human neutrophil granules. *Mol. Cell. Proteomics*. **4**, 1503–1521
120. Cederlund, A., Agerberth, B., and Bergman, P. (2010) Specificity in killing pathogens is mediated by distinct repertoires of human neutrophil peptides. *J. Innate Immun.* **2**, 508–521
121. Lee, C., Miura, K., Liu, X., and Zweier, J. L. (2000) Biphasic regulation of leukocyte superoxide generation by nitric oxide and peroxynitrite. *J. Biol. Chem.* **275**, 38965–38972
122. Eiserich, J. P., Hristova, M., Cross, C. E., Jones, A. D., Freeman, B. A., Halliwell, B., and van der Vliet, A. (1998) Formation of nitric oxide-derived inflammatory oxidants by myeloperoxidase in neutrophils. *Nature*. **391**, 393–397
123. Haniffa, M., Bigley, V., and Collin, M. (2015) Human mononuclear phagocyte system reunited. *Semin. Cell Dev. Biol.* **41**, 59–69
124. Becker, S., Warren, M. K., and Haskill, S. (1987) Colony-stimulating factor-induced monocyte survival and differentiation into macrophages in serum-free cultures. *J. Immunol.* **139**, 3703–3709
125. Zhou, L. J., and Tedder, T. F. (1996) CD14+ blood monocytes can differentiate into functionally mature CD83+ dendritic cells. *Proc. Natl. Acad. Sci.* **93**, 2588–2592
126. Murray, P. J. (2018) Immune regulation by monocytes. *Semin. Immunol.* **35**, 12–18
127. Geissmann, F., Jung, S., and Littman, D. R. (2003) Blood Monocytes Consist of Two Principal Subsets with Distinct Migratory Properties. *Immunity*. **19**, 71–82
128. Auffray, C., Fogg, D., Garfa, M., Elain, G., Join-Lambert, O., Kayal, S., Sarnacki, S., Cumano, A., Lauvau, G., and Geissmann, F. (2007) Monitoring of blood vessels and tissues by a population of monocytes with patrolling behavior. *Science*. **317**, 666–670
129. Nahrendorf, M., Swirski, F. K., Aikawa, E., Stangenberg, L., Wurdinger, T., Figueiredo, J.-L., Libby, P., Weissleder, R., and Pittet, M. J. (2007) The healing myocardium sequentially mobilizes two monocyte subsets with divergent and complementary functions. *J. Exp. Med.* **204**, 3037–3047
130. Soehnlein, O., Zernecke, A., Eriksson, E. E., Rothfuchs, A. G., Pham, C. T., Herwald, H., Bidzhekov, K., Rottenberg, M. E., Weber, C., and Lindbom, L. (2008) Neutrophil secretion products pave the way for inflammatory monocytes. *Blood*. **112**, 1461–1471
131. Martinez, F. O., and Gordon, S. (2014) The M1 and M2 paradigm of macrophage activation: time for reassessment. *F1000Prime Rep.* **6**, 1–13
132. Murray, P. J., Allen, J. E., Biswas, S. K., Fisher, E. A., Gilroy, D. W., Goerdt, S., Gordon, S., Hamilton, J. A., Ivashkiv, L. B., Lawrence, T., Locati, M., Mantovani, A., Martinez, F. O., Mege, J. L., Mosser, D. M., Natoli, G., Saeij, J. P., Schultze, J. L., Shirey, K. A., Sica, A., Suttles, J., Udalova, I., vanGinderachter, J. A., Vogel, S. N., and Wynn, T. A. (2014)

Macrophage Activation and Polarization: Nomenclature and Experimental Guidelines. *Immunity*. **41**, 14–20
133. Mantovani, A., Sica, A., Sozzani, S., Allavena, P., Vecchi, A., and Locati, M. (2004) The chemokine system in diverse forms of macrophage activation and polarization. *Trends Immunol.* **25**, 677–686
134. Varin, A., Mukhopadhyay, S., Herbein, G., and Gordon, S. (2010) Alternative activation of macrophages by IL-4 impairs phagocytosis of pathogens but potentiates microbial-induced signalling and cytokine secretion. *Blood*. **115**, 353–362
135. Schroder, K., Hertzog, P. J., Ravasi, T., and Hume, D. A. (2004) Interferon-gamma: an overview of signals, mechanisms and functions. *J. Leukoc. Biol.* **75**, 163–189
136. Wynn, T. A., Chawla, A., and Pollard, J. W. (2013) Macrophage biology in development, homeostasis and disease. *Nature*. **496**, 445–455
137. Gordon, S. (2003) Alternative activation of macrophages. *Nat. Rev. Immunol.* **3**, 23
138. Fernandez-Boyanapalli, R. F., Frasch, S. C., McPhillips, K., Vandivier, R. W., Harry, B. L., Riches, D. W. H., Henson, P. M., and Bratton, D. L. (2009) Impaired apoptotic cell clearance in CGD due to altered macrophage programming is reversed by phosphatidylserine-dependent production of IL-4. *Blood*. **113**, 2047–2055
139. Kessenbrock, K., Plaks, V., and Werb, Z. (2010) Matrix metalloproteinases: regulators of the tumor microenvironment. *Cell*. **141**, 52–67
140. Fanjul-Fernandez, M., Folgueras, A. R., Cabrera, S., and Lopez-Otin, C. (2010) Matrix metalloproteinases: evolution, gene regulation and functional analysis in mouse models. *Biochim. Biophys. Acta*. **1803**, 3–19
141. Corry, D. B., Rishi, K., Kanellis, J., Kiss, A., Song, L., Xu, J., Feng, L., Werb, Z., and Kheradmand, F. (2002) Decreased allergic lung inflammatory cell egression and increased susceptibility to asphyxiation in MMP2-deficiency. *Nat. Immunol.* **3**, 347
142. Rajasekhar, L., Liou, L. B., Chan, C. Y., Tsai, W. P., and Cheng, C. Y. (2004) Matrix metalloproteinase-8 in sera and from polymorphonuclear leucocytes in rheumatoid arthritis: in vitro characterization and correlation with disease activity. *Clin. Exp. Rheumatol.* **22**, 597–602
143. Liu, J., Shue, E., Ewalt, K. L., and Schimmel, P. (2004) A new γ-interferon-inducible promoter and splice variants of an anti-angiogenic human tRNA synthetase. *Nucleic Acids Res.* **32**, 719–727
144. Molet, S., Belleguic, C., Lena, H., Germain, N., Bertrand, C. P., Shapiro, S. D., Planquois, J.-M., Delaval, P., and Lagente, V. (2005) Increase in macrophage elastase (MMP-12) in lungs from patients with chronic obstructive pulmonary disease. *Inflamm. Res.* **54**, 31–36
145. Marcaccini, A. M., Novaes, A. B., Meschiari, C. A., Souza, S. L., Palioto, D. B., Sorgi, C. A., Faccioli, L. H., Tanus-Santos, J. E., and Gerlach, R. F. (2009) Circulating matrix metalloproteinase-8 (MMP-8) and MMP-9 are increased in chronic periodontal disease and decrease after non-surgical periodontal therapy. *Clin. Chim. Acta*. **409**, 117–122
146. Linder, R., Ronmark, E., Pourazar, J., Behndig, A., Blomberg, A., and Lindberg, A. (2015) Serum metalloproteinase-9 is related to COPD severity and symptoms - cross-sectional data from a population based cohort-study. *Respir. Res.* **16**, 28
147. Balli, U., Cetinkaya, B. O., Keles, G. C., Keles, Z. P., Guler, S., Sogut, M. U., and Erisgin, Z. (2016) Assessment of MMP-1, MMP-8 and TIMP-2 in experimental periodontitis treated with kaempferol. *J. Periodontal Implant Sci.* **46**, 84–95
148. Martignetti, J. A., Aqeel, A. Al, Sewairi, W. Al, Boumah, C. E., Kambouris, M., Mayouf, S. Al, Sheth, K. V, Eid, W. Al, Dowling, O., Harris, J., Glucksman, M. J., Bahabri, S., Meyer, B. F., and Desnick, R. J. (2001) Mutation of the matrix metalloproteinase 2 gene (MMP2) causes a multicentric osteolysis and arthritis syndrome. *Nat. Genet.* **28**, 261

149. Zankl, A., Bonafé, L., Calcaterra, V., Di Rocco, M., and Superti-Furga, A. (2005) Winchester syndrome caused by a homozygous mutation affecting the active site of matrix metalloproteinase 2. *Clin. Genet.* **67**, 261–266
150. Zankl, A., Pachman, L., Poznanski, A., Bonafé, L., Wang, F., Shusterman, Y., Fishman, D. A., and Superti-Furga, A. (2007) Torg Syndrome Is Caused by Inactivating Mutations in MMP2 and Is Allelic to NAO and Winchester Syndrome. *J. Bone Miner. Res.* **22**, 329–333
151. Kukkonen, M. K., Tiili, E., Vehmas, T., Oksa, P., Piirila, P., and Hirvonen, A. (2013) Association of genes of protease-antiprotease balance pathway to lung function and emphysema subtypes. *BMC Pulm. Med.* **13**, 36
152. Gilowska, I., Majorczyk, E., Kasper, Ł., Bogacz, K., Szczegielniak, J., Kasper, M., Kaczmarski, J., Skomudek, A., Czerwinski, M., and Sładek, K. (2019) The role of MMP-12 gene polymorphism - 82 A-to-G (rs2276109) in immunopathology of COPD in polish patients: a case control study. *BMC Med. Genet.* **20**, 19
153. Pei, D. (1999) Leukolysin/MMP25/MT6-MMP: a novel matrix metalloproteinase specifically expressed in the leukocyte lineage. *Cell Res.* **9**, 291–303
154. Shapiro, S. D., Kobayashi, D. K., and Ley, T. J. (1993) Cloning and characterization of a unique elastolytic metalloproteinase produced by human alveolar macrophages. *J. Biol. Chem.* **268**, 23824–23829
155. Rothenberg, M. L., Nelson, A. R., and Hande, K. R. (1999) New drugs on the horizon: matrix metalloproteinase inhibitors. *Stem Cells*. **17**, 237–240
156. Zucker, S., Cao, J., and Chen, W. T. (2000) Critical appraisal of the use of matrix metalloproteinase inhibitors in cancer treatment. *Oncogene*. **19**, 6642–6650
157. Coussens, L. M., Fingleton, B., and Matrisian, L. M. (2002) Matrix metalloproteinase inhibitors and cancer: trials and tribulations. *Science*. **295**, 2387–2392
158. Overall, C. M., and Lopez-Otin, C. (2002) Strategies for MMP inhibition in cancer: innovations for the post-trial era. *Nat. Rev. Cancer*. **2**, 657–672
159. Fingleton, B. (2008) MMPs as therapeutic targets--still a viable option? *Semin. Cell Dev. Biol.* **19**, 61–68
160. Autelitano, D. J., Rajic, A., Smith, A. I., Berndt, M. C., Ilag, L. L., and Vadas, M. (2006) The cryptome: a subset of the proteome, comprising cryptic peptides with distinct bioactivities. *Drug Discov. Today*. **11**, 306–314
161. O'Reilly, M. S., Holmgren, L., Shing, Y., Chen, C., Rosenthal, R. A., Moses, M., Lane, W. S., Cao, Y., Sage, E. H., and Folkman, J. (1994) Angiostatin: a novel angiogenesis inhibitor that mediates the suppression of metastases by a Lewis lung carcinoma. *Cell*. **79**, 315–328
162. O'Reilly, M. S., Boehm, T., Shing, Y., Fukai, N., Vasios, G., Lane, W. S., Flynn, E., Birkhead, J. R., Olsen, B. R., and Folkman, J. (1997) Endostatin: an endogenous inhibitor of angiogenesis and tumor growth. *Cell*. **88**, 277–285
163. Watanabe, K., Takahashi, H., Habu, Y., Kamiya-Kubushiro, N., Kamiya, S., Nakamura, H., Yajima, H., Ishii, T., Katayama, T., Miyazaki, K., and Fukai, F. (2000) Interaction with heparin and matrix metalloproteinase 2 cleavage expose a cryptic anti-adhesive site of fibronectin. *Biochemistry*. **39**, 7138–7144
164. Gearing, A. J., Beckett, P., Christodoulou, M., Churchill, M., Clements, J., Davidson, A. H., Drummond, A. H., Galloway, W. A., Gilbert, R., and Gordon, J. L. (1994) Processing of tumour necrosis factor-alpha precursor by metalloproteinases. *Nature*. **370**, 555–557
165. Ochieng, J., Fridman, R., Nangia-Makker, P., Kleiner, D. E., Liotta, L. A., Stetler-Stevenson, W. G., and Raz, A. (1994) Galectin-3 is a novel substrate for human matrix metalloproteinases-2 and -9. *Biochemistry*. **33**, 14109–14114

166. Ito, A., Mukaiyama, A., Itoh, Y., Nagase, H., Thogersen, I. B., Enghild, J. J., Sasaguri, Y., and Mori, Y. (1996) Degradation of interleukin 1beta by matrix metalloproteinases. *J. Biol. Chem.* **271**, 14657–14660
167. McQuibban, G. A., Butler, G. S., Gong, J. H., Bendall, L., Power, C., Clark-Lewis, I., and Overall, C. M. (2001) Matrix metalloproteinase activity inactivates the CXC chemokine stromal cell-derived factor-1. *J. Biol. Chem.* **276**, 43503–43508
168. McQuibban, G. A., Gong, J.-H., Wong, J. P., Wallace, J. L., Clark-Lewis, I., and Overall, C. M. (2002) Matrix metalloproteinase processing of monocyte chemoattractant proteins generates CC chemokine receptor antagonists with anti-inflammatory properties in vivo. *Blood*. **100**, 1160–1167
169. Fowlkes, J. L., Enghild, J. J., Suzuki, K., and Nagase, H. (1994) Matrix metalloproteinases degrade insulin-like growth factor-binding protein-3 in dermal fibroblast cultures. *J. Biol. Chem.* **269**, 25742–25746
170. Ruiz, S., Henschen-Edman, A. H., Nagase, H., and Tenner, A. J. (1999) Digestion of C1q collagen-like domain with MMPs-1, -2, -3, and -9 further defines the sequence involved in the stimulation of neutrophil superoxide production. *J. Leukoc. Biol.* **66**, 416–422
171. Butler, G. S., Sim, D., Tam, E., Devine, D., and Overall, C. M. (2002) Mannose-binding lectin (MBL) mutants are susceptible to matrix metalloproteinase proteolysis: potential role in human MBL deficiency. *J. Biol. Chem.* **277**, 17511–17519
172. Mast, A. E., Enghild, J. J., Nagase, H., Suzuki, K., Pizzo, S. V, and Salvesen, G. (1991) Kinetics and physiologic relevance of the inactivation of alpha 1-proteinase inhibitor, alpha 1-antichymotrypsin, and antithrombin III by matrix metalloproteinases-1 (tissue collagenase), -2 (72-kDa gelatinase/type IV collagenase), and -3 (stromelysin). *J. Biol. Chem.* **266**, 15810–15816
173. Overall, C. M., and Kleifeld, O. (2006) Tumour microenvironment - opinion: validating matrix metalloproteinases as drug targets and anti-targets for cancer therapy. *Nat. Rev. Cancer*. **6**, 227–239
174. Fortelny, N., Cox, J. H., Kappelhoff, R., Starr, A. E., Lange, P. F., Pavlidis, P., and Overall, C. M. (2014) Network analyses reveal pervasive functional regulation between proteases in the human protease web. *PLoS Biol.* **12**, e1001869
175. López-Otín, C., and Overall, C. M. (2002) Protease degradomics: A new challenge for proteomics. *Nat. Rev. Mol. Cell Biol.* **3**, 509–519
176. Eckhard, U., Marino, G., Butler, G. S., and Overall, C. M. (2016) Positional proteomics in the era of the human proteome project on the doorstep of precision medicine. *Biochimie*. **122**, 110–118
177. Prudova, A., Butler, G. S., and Overall, C. M. (2010) Multiplex N-terminome analysis of MMP-2 and MMP-9 substrate degradomes by iTRAQ-TAILS quantitative proteomics. *Mol. Cell. Proteomics*. **9**, 894–911
178. Kappelhoff, R., Puente, X. S., Wilson, C. H., Seth, A., Lopez-Otin, C., and Overall, C. M. (2017) Overview of transcriptomic analysis of all human proteases, non-proteolytic homologs and inhibitors: Organ, tissue and ovarian cancer cell line expression profiling of the human protease degradome by the CLIP-CHIP DNA microarray. *Biochim. Biophys. acta. Mol. cell Res.* **1864**, 2210–2219
179. J. Pennington, C., K. Nuttall, R., Sampieri-Ramirez, C., Wallard, M., Pilgrim, S., and Edwards, D. (2008) Quantitative Real-Time PCR Analysis of Degradome Gene Expression. in *The Cancer Degradome: Proteases and Cancer Biology*, pp. 49–65, Springer US
180. Fonovic, M., and Bogyo, M. (2008) Activity-based probes as a tool for functional proteomic analysis of proteases. *Expert Rev. Proteomics*. **5**, 721–730

181. Mann, M. (2006) Functional and quantitative proteomics using SILAC. *Nat. Rev. Mol. Cell Biol.* **7**, 952–958
182. Hsu, J.-L., Huang, S.-Y., Chow, N.-H., and Chen, S.-H. (2003) Stable-isotope dimethyl labeling for quantitative proteomics. *Anal. Chem.* **75**, 6843–6852
183. Gygi, S. P., Rist, B., Gerber, S. A., Turecek, F., Gelb, M. H., and Aebersold, R. (1999) Quantitative analysis of complex protein mixtures using isotope-coded affinity tags. *Nat. Biotechnol.* **17**, 994–999
184. Ross, P. L., Huang, Y. N., Marchese, J. N., Williamson, B., Parker, K., Hattan, S., Khainovski, N., Pillai, S., Dey, S., Daniels, S., Purkayastha, S., Juhasz, P., Martin, S., Bartlet-Jones, M., He, F., Jacobson, A., and Pappin, D. J. (2004) Multiplexed protein quantitation in Saccharomyces cerevisiae using amine-reactive isobaric tagging reagents. *Mol. Cell. Proteomics*. **3**, 1154–1169
185. Kleifeld, O., Doucet, A., Auf Dem Keller, U., Prudova, A., Schilling, O., Kainthan, R. K., Starr, A. E., Foster, L. J., Kizhakkedathu, J. N., and Overall, C. M. (2010) Isotopic labeling of terminal amines in complex samples identifies protein N-termini and protease cleavage products. *Nat. Biotechnol.* **28**, 281–288
186. Dean, R. A., and Overall, C. M. (2007) Proteomics Discovery of Metalloproteinase Substrates in the Cellular Context by iTRAQ™ Labeling Reveals a Diverse MMP-2 Substrate Degradome. *Mol. Cell. Proteomics*. **6**, 611–623
187. Butler, G. S., Dean, R. A., Tam, E. M., and Overall, C. M. (2008) Pharmacoproteomics of a Metalloproteinase Hydroxamate Inhibitor in Breast Cancer Cells: Dynamics of Membrane Type 1 Matrix Metalloproteinase-Mediated Membrane Protein Shedding. *Mol. Cell. Biol.* **28**, 4896–4914
188. Greenlee, K. J., Corry, D. B., Engler, D. A., Matsunami, R. K., Tessier, P., Cook, R. G., Werb, Z., and Kheradmand, F. (2006) Proteomic identification of in vivo substrates for matrix metalloproteinases 2 and 9 reveals a mechanism for resolution of inflammation. *J. Immunol.* **177**, 7312–7321
189. auf dem Keller, U., Prudova, A., Eckhard, U., Fingleton, B., and Overall, C. M. (2013) Systems-Level Analysis of Proteolytic Events in Increased Vascular Permeability and Complement Activation in Skin Inflammation. *Sci. Signal.* **6**, rs2
190. Doucet, A., Kleifeld, O., Kizhakkedathu, J. N., and Overall, C. M. (2011) Identification of Proteolytic Products and Natural Protein N-Termini by Terminal Amine Isotopic Labeling of Substrates (TAILS). *Methods Mol Biol*. **753**, 273–287
191. Gevaert, K., Impens, F., Van Damme, P., Ghesquiere, B., Hanoulle, X., and Vandekerckhove, J. (2007) Applications of diagonal chromatography for proteome-wide characterization of protein modifications and activity-based analyses. *FEBS J.* **274**, 6277–6289
192. Staes, A., Van Damme, P., Helsens, K., Demol, H., Vandekerckhove, J., and Gevaert, K. (2008) Improved recovery of proteome-informative, protein N-terminal peptides by combined fractional diagonal chromatography (COFRADIC). *Proteomics*. **8**, 1362–1370
193. Overall, C. M., Tam, E. M., Kappelhoff, R., Connor, A., Ewart, T., Morrison, C. J., Puente, X., López-Otín, C., and Seth, A. (2004) Protease degradomics: Mass spectrometry discovery of protease substrates and the CLIP-CHIP, a dedicated DNA microarray of all human proteases and inhibitors. *Biol. Chem.* **385**, 493–504
194. Cauwe, B., Martens, E., Van den Steen, P. E., Proost, P., Van Aelst, I., Blockmans, D., and Opdenakker, G. (2008) Adenylyl cyclase-associated protein-1/CAP1 as a biological target substrate of gelatinase B/MMP-9. *Exp. Cell Res.* **314**, 2739–2749
195. Cauwe, B., Martens, E., Proost, P., and Opdenakker, G. (2009) Multidimensional degradomics identifies systemic autoantigens and intracellular matrix proteins as novel

gelatinase B/MMP-9 substrates. *Integr. Biol. (Camb).* **1**, 404–426
196. Bellac, C. L., Dufour, A., Krisinger, M. J., Loonchanta, A., Starr, A. E., auf dem Keller, U., Lange, P. F., Goebeler, V., Kappelhoff, R., Butler, G. S., Burtnick, L. D., Conway, E. M., Roberts, C. R., and Overall, C. M. (2014) Macrophage matrix metalloproteinase-12 dampens inflammation and neutrophil influx in arthritis. *Cell Rep.* **9**, 618–632
197. Ito, T., Kawahara, K., Okamoto, K., Yamada, S., Yasuda, M., Imaizumi, H., Nawa, Y., Meng, X., Shrestha, B., Hashiguchi, T., and Maruyama, I. (2008) Proteolytic cleavage of high mobility group box 1 protein by thrombin-thrombomodulin complexes. *Arterioscler. Thromb. Vasc. Biol.* **28**, 1825–1830
198. Wang, H., Ward, M. F., and Sama, A. E. (2014) Targeting HMGB1 in the treatment of sepsis. *Expert Opin. Ther. Targets*. **18**, 257–268
199. Yazdan-Ashoori, P., Liaw, P., Toltl, L., Webb, B., Kilmer, G., Carter, D. E., and Fraser, D. D. (2011) Elevated plasma matrix metalloproteinases and their tissue inhibitors in patients with severe sepsis. *J. Crit. Care*. **26**, 556–565
200. Mor-Vaknin, N., Punturieri, A., Sitwala, K., and Markovitz, D. M. (2003) Vimentin is secreted by activated macrophages. *Nat. Cell Biol.* **5**, 59–63
201. Starr, A. E., Bellac, C. L., Dufour, A., Goebeler, V., and Overall, C. M. (2012) Biochemical characterization and N-terminomics analysis of leukolysin, the membrane-type 6 matrix metalloprotease (MMP25): chemokine and vimentin cleavages enhance cell migration and macrophage phagocytic activities. *J. Biol. Chem.* **287**, 13382–13395
202. Han, J. M., Kim, J. Y., and Kim, S. (2003) Molecular network and functional implications of macromolecular tRNA synthetase complex. *Biochem. Biophys. Res. Commun.* **303**, 985–993
203. Antonellis, A., and Green, E. D. (2008) The role of aminoacyl-tRNA synthetases in genetic diseases. *Annu. Rev. Genomics Hum. Genet.* **9**, 87–107
204. Guo, M., Yang, X.-L., and Schimmel, P. (2010) New functions of aminoacyl-tRNA synthetases beyond translation. *Nat. Rev. Mol. Cell Biol.* **11**, 668
205. Lo, W. S., Gardiner, E., Xu, Z., Lau, C. F., Wang, F., Zhou, J. J., Mendlein, J. D., Nangle, L. A., Chiang, K. P., Yang, X. L., Au, K. F., Wong, W. H., Guo, M., Zhang, M., and Schimmel, P. (2014) Human tRNA synthetase catalytic nulls with diverse functions. *Science*. **345**, 328–332
206. Wakasugi, K., Slike, B. M., Hood, J., Otani, A., Ewalt, K. L., Friedlander, M., Cheresh, D. A., and Schimmel, P. (2002) A human aminoacyl-tRNA synthetase as a regulator of angiogenesis. *Proc. Natl. Acad. Sci.* **99**, 173–177
207. Wakasugi, K., and Schimmel, P. (1999) Two distinct cytokines released from a human aminoacyl-tRNA synthetase. *Science*. **284**, 147–151
208. Cerini, C., Kerjan, P., Astier, M., Gratecos, D., Mirande, M., and Sémériva, M. (1991) A component of the multisynthetase complex is a multifunctional aminoacyl-tRNA synthetase. *EMBO J.* **10**, 4267–77
209. Ko, Y. G., Kim, E. Y., Kim, T., Park, H., Park, H. S., Choi, E. J., and Kim, S. (2001) Glutamine-dependent antiapoptotic interaction of human glutaminyl-tRNA synthetase with apoptosis signal-regulating kinase 1. *J. Biol. Chem.* **276**, 6030–6036
210. Han, J. M., Jeong, S. J., Park, M. C., Kim, G., Kwon, N. H., Kim, H. K., Ha, S. H., Ryu, S. H., and Kim, S. (2012) Leucyl-tRNA synthetase is an intracellular leucine sensor for the mTORC1-signaling pathway. *Cell*. **149**, 410–424
211. Kim, S., You, S., and Hwang, D. (2011) Aminoacyl-tRNA synthetases and tumorigenesis: More than housekeeping. *Nat. Rev. Cancer*. **11**, 708–718
212. Guo, M., and Schimmel, P. (2013) Essential nontranslational functions of tRNA synthetases. *Nat. Chem. Biol.* **9**, 145

213. Park, S. G., Kim, H. J., Min, Y. H., Choi, E.-C., Shin, Y. K., Park, B.-J., Lee, S. W., and Kim, S. (2005) Human lysyl-tRNA synthetase is secreted to trigger proinflammatory response. *Proc. Natl. Acad. Sci.* **102**, 6356–6361
214. Williams, T. F., Mirando, A. C., Wilkinson, B., Francklyn, C. S., and Lounsbury, K. M. (2013) Secreted Threonyl-tRNA synthetase stimulates endothelial cell migration and angiogenesis. *Sci. Rep.* **3**, 1–7
215. Ahn, Y. H., Park, S., Choi, J. J., Park, B.-K., Rhee, K. H., Kang, E., Ahn, S., Lee, C.-H., Lee, J. S., Inn, K.-S., Cho, M.-L., Park, S.-H., Park, K., Park, H. J., Lee, J.-H., Park, J.-W., Kwon, N. H., Shim, H., Han, B. W., Kim, P., Lee, J.-Y., Jeon, Y., Huh, J. W., Jin, M., and Kim, S. (2016) Secreted tryptophanyl-tRNA synthetase as a primary defence system against infection. *Nat. Microbiol.* **2**, 16191
216. Park, S.-R., Kim, H.-J., Yang, S.-R., Park, C. H., Lee, H.-Y., and Hong, I.-S. (2018) A novel endogenous damage signal, glycyl tRNA synthetase, activates multiple beneficial functions of mesenchymal stem cells. *Cell Death Differ.* **25**, 2023–2036
217. Lee, H.-C., Lee, E.-S., Uddin, M. B., Kim, T.-H., Kim, J.-H., Chathuranga, K., Chathuranga, W. A. G., Jin, M., Kim, S., Kim, C.-J., and Lee, J.-S. (2018) Released tryptophanyl-tRNA synthetase stimulates innate immune responses against viral infection. *J. Virol.* **93**, e01291-18
218. Bao, Y. S., Ji, Y., Zhao, S. L., Ma, L. L., Xie, R. J., and Na, S. P. (2013) Serum levels and activity of indoleamine2,3-dioxygenase and tryptophanyl-tRNA synthetase and their association with disease severity in patients with chronic kidney disease. *Biomarkers*. **18**, 379–385
219. Miyanokoshi, M., Yokosawa, T., and Wakasugi, K. (2018) Tryptophanyl-tRNA synthetase mediates high-affinity tryptophan uptake into human cells. *J. Biol. Chem.* **293**, 8428–8438
220. Kanaji, T., Vo, M.-N., Kanaji, S., Zarpellon, A., Shapiro, R., Morodomi, Y., Yuzuriha, A., Eto, K., Belani, R., Do, M.-H., Yang, X.-L., Ruggeri, Z. M., and Schimmel, P. (2018) Tyrosyl-tRNA synthetase stimulates thrombopoietin-independent hematopoiesis accelerating recovery from thrombocytopenia. *Proc. Natl. Acad. Sci.* **115**, 201807000
221. Park, M. C., Kang, T., Jin, D., Han, J. M., Kim, S. B., Park, Y. J., Cho, K., Park, Y. W., Guo, M., He, W., Yang, X.-L., Schimmel, P., and Kim, S. (2012) Secreted human glycyl-tRNA synthetase implicated in defense against ERK-activated tumorigenesis. *Proc. Natl. Acad. Sci.* **109**, E640–E647
222. Kapoor, M., Zhou, Q., Otero, F., Myers, C. A., Bates, A., Belani, R., Liu, J., Luo, J. K., Tzima, E., Zhang, D. E., Yang, X. L., and Schimmel, P. (2008) Evidence for annexin II-S100A10 complex and plasmin in mobilization of cytokine activity of human TrpRS. *J. Biol. Chem.* **283**, 2070–2077
223. Zhou, J. J., Wang, F., Xu, Z., Lo, W. S., Lau, C. F., Chiang, K. P., Nangle, L. A., Ashlock, M. A., Mendlein, J. D., Yang, X. L., Zhang, M., and Schimmel, P. (2014) Secreted histidyl-tRNA synthetase splice variants elaborate major epitopes for autoantibodies in inflammatory myositis. *J. Biol. Chem.* **289**, 19269–19275
224. Casas-Tintó, S., Lolo, F. N., and Moreno, E. (2015) Active JNK-dependent secretion of Drosophila Tyrosyl-tRNA synthetase by loser cells recruits haemocytes during cell competition. *Nat. Commun.* **6**, 1–12
225. Yang, X. L., Schimmel, P., and Ewalt, K. L. (2004) Relationship of two human tRNA synthetases used in cell signaling. *Trends Biochem. Sci.* **29**, 250–256
226. Tolstrup, A. B., Bejder, A., Fleckner, J., and Justesen, J. (1995) Transcriptional regulation of the interferon-gamma-inducible tryptophanyl-tRNA synthetase includes alternative splicing. *J. Biol. Chem.* **270**, 397–403
227. Lo, W.-S., Gardiner, E., Xu, Z., Lau, C.-F., Wang, F., Zhou, J. J., Mendlein, J. D., Nangle,

L. A., Chiang, K. P., Yang, X.-L., Au, K.-F., Wong, W. H., Guo, M., Zhang, M., and Schimmel, P. (2014) Human tRNA synthetase catalytic nulls with diverse functions. *Science*. **345**, 328–332
228. Wakasugi, K., and Schimmel, P. (1999) Highly differentiated motifs responsible for two cytokine activities of a split human tRNA synthetase. *J. Biol. Chem.* **274**, 23155–23159
229. Yang, X. L., Kapoor, M., Otero, F. J., Slike, B. M., Tsuruta, H., Frausto, R., Bates, A., Ewalt, K. L., Cheresh, D. A., and Schimmel, P. (2007) Gain-of-Function Mutational Activation of Human tRNA Synthetase Procytokine. *Chem. Biol.* **14**, 1323–1333
230. Kise, Y., Lee, S. W., Park, S. G., Fukai, S., Sengoku, T., Ishii, R., Yokoyama, S., Kim, S., and Nureki, O. (2004) A short peptide insertion crucial for angiostatic activity of human tryptophanyl-tRNA synthetase. *Nat. Struct. Mol. Biol.* **11**, 149–156
231. Tzima, E., Reader, J. S., Irani-Tehrani, M., Ewalt, K. L., Schwartz, M. A., and Schimmel, P. (2005) VE-cadherin links tRNA synthetase cytokine to anti-angiogenic function. *J. Biol. Chem.* **280**, 2405–2408
232. Tzima, E., Reader, J. S., Irani-Tehrani, M., Ewalt, K. L., Schwartz, M. A., and Schimmel, P. (2003) Biologically active fragment of a human tRNA synthetase inhibits fluid shear stress-activated responses of endothelial cells. *Proc. Natl. Acad. Sci.* **100**, 14903–14907
233. Otani, A., Slike, B. M., Dorrell, M. I., Hood, J., Kinder, K., Ewalt, K. L., Cheresh, D., Schimmel, P., and Friedlander, M. (2002) A fragment of human TrpRS as a potent antagonist of ocular angiogenesis. *Proc. Natl. Acad. Sci.* **99**, 178–183
234. Greenberg, Y., King, M., Kiosses, W. B., Ewalt, K., Yang, X., Schimmel, P., Reader, J. S., and Tzima, E. (2007) The novel fragment of tyrosyl tRNA synthetase, mini-TyrRS, is secreted to induce an angiogenic response in endothelial cells. *FASEB J.* **22**, 1597–1605
235. Kapoor, M., Otero, F. J., Slike, B. M., Ewalt, K. L., and Yang, X. L. (2009) Mutational Separation of Aminoacylation and Cytokine Activities of Human Tyrosyl-tRNA Synthetase. *Chem. Biol.* **16**, 531–539
236. Cheng, G., Zhang, H., Yang, X., Tzima, E., Ewalt, K. L., Schimmel, P., and Faber, J. E. (2008) Effect of mini-tyrosyl-tRNA synthetase on ischemic angiogenesis, leukocyte recruitment, and vascular permeability. *Am. J. Physiol. Integr. Comp. Physiol.* **295**, R1138–R1146
237. Zeng, R., Chen, Y.-C., Zeng, Z., Liu, W.-Q., Liu, X.-X., Liu, R., Qiang, O., and Li, X. (2010) Different angiogenesis effect of mini-TyrRS/mini-TrpRS by systemic administration of modified siRNAs in rats with acute myocardial infarction. *Heart Vessels*. **25**, 324–332
238. Zeng, R., Chen, Y., Zeng, Z., Liu, W., Jiang, X., Liu, R., Qiang, O., and Li, X. (2011) Effect of mini-tyrosyl-tRNA synthetase/mini-tryptophanyl-tRNA synthetase on ischemic angiogenesis in rats: proliferation and migration of endothelial cells. *Heart Vessels*. **26**, 69–80
239. Zeng, R., Chen, Y. C., Zeng, Z., Liu, X. X., Liu, R., Qiang, O., and Li, X. (2012) Inhibition of mini-TyrRS-induced angiogenesis response in endothelial cells by VE-cadherin-dependent mini-TrpRS. *Heart Vessels*. **27**, 193–201
240. Sajish, M., and Schimmel, P. (2015) A human tRNA synthetase is a potent PARP1-activating effector target for resveratrol. *Nature*. **519**, 370–373
241. Cao, X., Li, C., Xiao, S., Tang, Y., Huang, J., Zhao, S., Li, X., Li, J., Zhang, R., and Yu, W. (2017) Acetylation promotes TyrRS nuclear translocation to prevent oxidative damage. *Proc. Natl. Acad. Sci. U. S. A.* **114**, 687–692
242. Marcus, K., Immler, D., Sternberger, J., and Meyer, H. E. (2000) Identification of platelet proteins separated by two-dimensional gel electrophoresis and analyzed by matrix assisted laser desorption/ionization-time of flight-mass spectrometry and detection of tyrosine-phosphorylated proteins. *Electrophoresis*. **21**, 2622–2636

243. Jinchao, Y., Yanling, Z., Xu, W., Bing, Z., Yuhao, Y., Weiran, Z., Shaoyang, S., Liyun, M., Yun, S., Ling, Z., Min, Y., and Wei, M. (2017) Thrombopoietic stimulating activity of rhTyrRS (Y341A). *Sci. Rep.* **7**, 12184
244. Wakasugi, K., Slike, B. M., Hood, J., Ewalt, K. L., Cheresh, D. A., and Schimme, P. (2002) Induction of angiogenesis by a fragment of human tyrosyl-tRNA synthetase. *J. Biol. Chem.* **277**, 20124–20126
245. Wakasugi, K., Slike, B. M., Hood, J., Ewalt, K. L., Cheresh, D. A., and Schimme, P. (2002) Induction of angiogenesis by a fragment of human tyrosyl-tRNA synthetase. *J. Biol. Chem.* **277**, 20124–20126
246. Warner, J. R., and McIntosh, K. B. (2009) How Common Are Extraribosomal Functions of Ribosomal Proteins? *Mol. Cell*. **34**, 3–11
247. Hegde, R. S., and Bernstein, H. D. (2006) The surprising complexity of signal sequences. *Trends Biochem. Sci.* **31**, 563–571
248. Eguchi, T., Kubota, S., Kawata, K., Mukudai, Y., Uehara, J., Ohgawara, T., Ibaragi, S., Sasaki, A., Kuboki, T., and Takigawa, M. (2008) Novel transcription-factor-like function of human matrix metalloproteinase 3 regulating the CTGF/CCN2 gene. *Mol. Cell. Biol.* **28**, 2391–2413
249. Shaffer, K. L., Sharma, A., Snapp, E. L., and Hegde, R. S. (2005) Regulation of Protein Compartmentalization Expands the Diversity of Protein Function. *Dev. Cell*. **9**, 545–554
250. Ali, M. A. M., Chow, A. K., Kandasamy, A. D., Fan, X., West, L. J., Crawford, B. D., Simmen, T., and Schulz, R. (2012) Mechanisms of cytosolic targeting of matrix metalloproteinase-2. *J. Cell. Physiol.* **227**, 3397–3404
251. Lovett, D. H., Mahimkar, R., Raffai, R. L., Cape, L., Maklashina, E., Cecchini, G., and Karliner, J. S. (2012) A novel intracellular isoform of matrix metalloproteinase-2 induced by oxidative stress activates innate immunity. *PLoS One*. **7**, e34177
252. DeCoux, A., Lindsey, M. L., Villarreal, F., Garcia, R. A., and Schulz, R. (2014) Myocardial matrix metalloproteinase-2: inside out and upside down. *J. Mol. Cell. Cardiol.* **77**, 64–72
253. Yu, W.-H., Woessner, J. F. J., McNeish, J. D., and Stamenkovic, I. (2002) CD44 anchors the assembly of matrilysin/MMP-7 with heparin-binding epidermal growth factor precursor and ErbB4 and regulates female reproductive organ remodeling. *Genes Dev.* **16**, 307–323
254. Yamamoto, K., Higashi, S., Kioi, M., Tsunezumi, J., Honke, K., and Miyazaki, K. (2006) Binding of active matrilysin to cell surface cholesterol sulfate is essential for its membrane-associated proteolytic action and induction of homotypic cell adhesion. *J. Biol. Chem.* **281**, 9170–9180
255. Yang, Z., Strickland, D. K., and Bornstein, P. (2001) Extracellular matrix metalloproteinase 2 levels are regulated by the low density lipoprotein-related scavenger receptor and thrombospondin 2. *J. Biol. Chem.* **276**, 8403–8408
256. Emonard, H., Bellon, G., Troeberg, L., Berton, A., Robinet, A., Henriet, P., Marbaix, E., Kirkegaard, K., Patthy, L., Eeckhout, Y., Nagase, H., Hornebeck, W., and Courtoy, P. J. (2004) Low density lipoprotein receptor-related protein mediates endocytic clearance of pro-MMP-2.TIMP-2 complex through a thrombospondin-independent mechanism. *J. Biol. Chem.* **279**, 54944–54951
257. Traub, L. M. (2009) Tickets to ride: selecting cargo for clathrin-regulated internalization. *Nat. Rev. Mol. Cell Biol.* **10**, 583
258. Koppisetti, R. K., Fulcher, Y. G., Jurkevich, A., Prior, S. H., Xu, J., Lenoir, M., Overduin, M., and Van Doren, S. R. (2014) Ambidextrous binding of cell and membrane bilayers by soluble matrix metalloproteinase-12. *Nat. Commun.* **5**, 5552
259. Nisato, R. E., Hosseini, G., Sirrenberg, C., Butler, G. S., Crabbe, T., Docherty, A. J. P.,

Wiesner, M., Murphy, G., Overall, C. M., Goodman, S. L., and Pepper, M. S. (2005) Dissecting the role of matrix metalloproteinases (MMP) and integrin alpha(v)beta3 in angiogenesis in vitro: absence of hemopexin C domain bioactivity, but membrane-type 1-MMP and alpha(v)beta3 are critical. *Cancer Res.* **65**, 9377–9387

260. Hahn-Dantona, E., Ruiz, J. F., Bornstein, P., and Strickland, D. K. (2001) The low density lipoprotein receptor-related protein modulates levels of matrix metalloproteinase 9 (MMP-9) by mediating its cellular catabolism. *J. Biol. Chem.* **276**, 15498–15503
261. Van den Steen, P. E., Van Aelst, I., Hvidberg, V., Piccard, H., Fiten, P., Jacobsen, C., Moestrup, S. K., Fry, S., Royle, L., Wormald, M. R., Wallis, R., Rudd, P. M., Dwek, R. A., and Opdenakker, G. (2006) The hemopexin and O-glycosylated domains tune gelatinase B/MMP-9 bioavailability via inhibition and binding to cargo receptors. *J. Biol. Chem.* **281**, 18626–18637
262. Yamamoto, K., Okano, H., Miyagawa, W., Visse, R., Shitomi, Y., Santamaria, S., Dudhia, J., Troeberg, L., Strickland, D. K., Hirohata, S., and Nagase, H. (2016) MMP-13 is constitutively produced in human chondrocytes and co-endocytosed with ADAMTS-5 and TIMP-3 by the endocytic receptor LRP1. *Matrix Biol.* **56**, 57–73
263. Chow, A. K., Cena, J., El-Yazbi, A. F., Crawford, B. D., Holt, A., Cho, W. J., Daniel, E. E., and Schulz, R. (2007) Caveolin-1 inhibits matrix metalloproteinase-2 activity in the heart. *J. Mol. Cell. Cardiol.* **42**, 896–901
264. Cho, W. J., Chow, A. K., Schulz, R., and Daniel, E. E. (2007) Matrix metalloproteinase-2, caveolins, focal adhesion kinase and c-Kit in cells of the mouse myocardium. *J. Cell. Mol. Med.* **11**, 1069–1086
265. Berton, A., Selvais, C., Lemoine, P., Henriet, P., Courtoy, P. J., Marbaix, E., and Emonard, H. (2007) Binding of matrilysin-1 to human epithelial cells promotes its activity. *Cell. Mol. Life Sci.* **64**, 610–620
266. Szklarczyk, A., Oyler, G., McKay, R., Gerfen, C., and Conant, K. (2007) Cleavage of neuronal synaptosomal-associated protein of 25 kDa by exogenous matrix metalloproteinase-7. *J. Neurochem.* **102**, 1256–1263
267. Ganguly, B., Banerjee, J., Elegbede, A. I., Klocke, D. J., Mallik, S., and Srivastava, D. K. (2007) Intrinsic selectivity in binding of matrix metalloproteinase-7 to differently charged lipid membranes. *FEBS Lett.* **581**, 5723–5726
268. Monferran, S., Paupert, J., Dauvillier, S., Salles, B., and Muller, C. (2004) The membrane form of the DNA repair protein Ku interacts at the cell surface with metalloproteinase 9. *EMBO J.* **23**, 3758–3768
269. Sbai, O., Ould-Yahoui, A., Ferhat, L., Gueye, Y., Bernard, A., Charrat, E., Mehanna, A., Risso, J.-J., Chauvin, J.-P., Fenouillet, E., Rivera, S., and Khrestchatisky, M. (2010) Differential vesicular distribution and trafficking of MMP-2, MMP-9, and their inhibitors in astrocytes. *Glia*. **58**, 344–366
270. Jiang, A., Lehti, K., Wang, X., Weiss, S. J., Keski-Oja, J., and Pei, D. (2001) Regulation of membrane-type matrix metalloproteinase 1 activity by dynamin-mediated endocytosis. *Proc. Natl. Acad. Sci.* **98**, 13693–13698
271. Uekita, T., Itoh, Y., Yana, I., Ohno, H., and Seiki, M. (2001) Cytoplasmic tail–dependent internalization of membrane-type 1 matrix metalloproteinase is important for its invasion-promoting activity. *J. Cell Biol.* **155**, 1345–1356
272. Remacle, A., Murphy, G., and Roghi, C. (2003) Membrane type I-matrix metalloproteinase (MT1-MMP) is internalised by two different pathways and is recycled to the cell surface. *J. Cell Sci.* **116**, 3905–3916
273. Gálvez, B. G., Matías-Román, S., Yáñez-Mó, M., Vicente-Manzanares, M., Sánchez-Madrid, F., and Arroyo, A. G. (2003) Caveolae Are a Novel Pathway for Membrane-Type

1 Matrix Metalloproteinase Traffic in Human Endothelial Cells. *Mol. Biol. Cell*. **15**, 678–687
274. Golubkov, V. S., Chekanov, A. V, Doxsey, S. J., and Strongin, A. Y. (2005) Centrosomal pericentrin is a direct cleavage target of membrane type-1 matrix metalloproteinase in humans but not in mice: potential implications for tumorigenesis. *J. Biol. Chem.* **280**, 42237–42241
275. Golubkov, V. S., Chekanov, A. V, Savinov, A. Y., Rozanov, D. V, Golubkova, N. V, and Strongin, A. Y. (2006) Membrane Type-1 Matrix Metalloproteinase Confers Aneuploidy and Tumorigenicity on Mammary Epithelial Cells. *Cancer Res.* **66**, 10460–10465
276. Remacle, A. G., Rozanov, D. V, Baciu, P. C., Chekanov, A. V, Golubkov, V. S., and Strongin, A. Y. (2005) The transmembrane domain is essential for the microtubular trafficking of membrane type-1 matrix metalloproteinase (MT1-MMP). *J. Cell Sci.* **118**, 4975–4984
277. Ip, Y. C., Cheung, S. T., Lee, Y. T., Ho, J. C., and Fan, S. T. (2007) Inhibition of hepatocellular carcinoma invasion by suppression of claudin-10 in HLE cells. *Mol. Cancer Ther.* **6**, 2858–2867
278. Grant, B. D., and Donaldson, J. G. (2009) Pathways and mechanisms of endocytic recycling. *Nat. Rev. Mol. Cell Biol.* **10**, 597
279. Emonard, H., Bellon, G., de Diesbach, P., Mettlen, M., Hornebeck, W., and Courtoy, P. J. (2005) Regulation of matrix metalloproteinase (MMP) activity by the low-density lipoprotein receptor-related protein (LRP). A new function for an “old friend.” *Biochimie*. **87**, 369–376
280. Szklarczyk, A., Conant, K., Owens, D. F., Ravin, R., McKay, R. D., and Gerfen, C. (2007) Matrix metalloproteinase-7 modulates synaptic vesicle recycling and induces atrophy of neuronal synapses. *Neuroscience*. **149**, 87–98
281. Mannello, F., and Medda, V. (2012) Nuclear localization of Matrix metalloproteinases. *Prog. Histochem. Cytochem.* **47**, 27–58
282. Si-Tayeb, K., Monvoisin, A., Mazzocco, C., Lepreux, S., Decossas, M., Cubel, G., Taras, D., Blanc, J.-F., Robinson, D. R., and Rosenbaum, J. (2006) Matrix Metalloproteinase 3 Is Present in the Cell Nucleus and Is Involved in Apoptosis. *Am. J. Pathol.* **169**, 1390–1401
283. Kwan, J. A., Schulze, C. J., Wand, W., Leon, H., Sariahmetoglu, M., Sung, M., Sawicka, J., Sims, D. E., Sawicki, G., and Schulze, R. (2004) Matrix metalloproteinase-2 (MMP-2) is present in the nucleus of cardiac myocytes and is capable of cleaving poly (ADP-ribose) polymerase (PARP) in vitro. *FASEB J.* **18**, 690–692
284. Benmerah, A., Scott, M., Poupon, V., and Marullo, S. (2003) Nuclear Functions for Plasma Membrane-Associated Proteins? *Traffic*. **4**, 503–511
285. Lee, K.-W., Liu, B., Ma, L., Li, H., Bang, P., Koeffler, H. P., and Cohen, P. (2004) Cellular internalization of insulin-like growth factor binding protein-3: distinct endocytic pathways facilitate re-uptake and nuclear localization. *J. Biol. Chem.* **279**, 469–476
286. Kowluru, R. A., Mohammad, G., dos Santos, J. M., and Zhong, Q. (2011) Abrogation of MMP-9 gene protects against the development of retinopathy in diabetic mice by preventing mitochondrial damage. *Diabetes*. **60**, 3023–3033
287. Schulz, R. (2007) Intracellular Targets of Matrix Metalloproteinase-2 in Cardiac Disease: Rationale and Therapeutic Approaches. *Annu. Rev. Pharmacol. Toxicol.* **47**, 211–242
288. Solli, A. I., Fadnes, B., Winberg, J.-O., Uhlin-Hansen, L., and Hadler-Olsen, E. (2013) Tissue- and cell-specific co-localization of intracellular gelatinolytic activity and matrix metalloproteinase 2. *J. Histochem. Cytochem.* **61**, 444–461
289. Wenjie, W., J., S. C., L., S.-P. W., R.B., D. J., Grzegorz, S., and Richard, S. (2002)

Intracellular Action of Matrix Metalloproteinase-2 Accounts for Acute Myocardial Ischemia and Reperfusion Injury. *Circulation*. **106**, 1543–1549
290. Hughes, B. G., Fan, X., Cho, W. J., and Schulz, R. (2013) MMP-2 is localized to the mitochondria-associated membrane of the heart. *Am. J. Physiol. Circ. Physiol.* **306**, H764–H770
291. Coker, M. L., Doscher, M. A., Thomas, C. V, Galist, Z. S., and Spinale, F. G. (1998) Matrix metalloproteinase synthesis and expression in isolated LV myocyte preparations. *J. Card. Fail.* **4**, 16
292. Sung, M. M., Schulz, C. G., Wang, W., Sawicki, G., Bautista-López, N. L., and Schulz, R. (2007) Matrix metalloproteinase-2 degrades the cytoskeletal protein α-actinin in peroxynitrite mediated myocardial injury. *J. Mol. Cell. Cardiol.* **43**, 429–436
293. Grzegorz, S., Hernando, L., Jolanta, S., Meltem, S., J., S. C., G., S. P., Danuta, S.-C., and Richard, S. (2005) Degradation of Myosin Light Chain in Isolated Rat Hearts Subjected to Ischemia-Reperfusion Injury. *Circulation*. **112**, 544–552
294. A.M., A. M., Jung, C. W., Bryan, H., Zamaneh, K., Henk, G., and Richard, S. (2010) Titin is a Target of Matrix Metalloproteinase-2. *Circulation*. **122**, 2039–2047
295. J., S. C., Wenjie, W., L., S.-P. W., Jolanta, S., Grzegorz, S., and Richard, S. (2003) Imbalance Between Tissue Inhibitor of Metalloproteinase-4 and Matrix Metalloproteinases During Acute Myoctardial Ischemia-Reperfusion Injury. *Circulation*. **107**, 2487–2492
296. Kandasamy, A. D., Chow, A. K., Ali, M. A. M., and Schulz, R. (2009) Matrix metalloproteinase-2 and myocardial oxidative stress injury: beyond the matrix. *Cardiovasc. Res.* **85**, 413–423
297. Sariahmetoglu, M., Crawford, B. D., Leon, H., Sawicka, J., Li, L., Ballermann, B. J., Holmes, C., Berthiaume, L. G., Holt, A., Sawicki, G., and Schulz, R. (2007) Regulation of matrix metalloproteinase-2 (MMP-2) activity by phosphorylation. *FASEB J.* **21**, 2486–2495
298. Viappiani, S., Nicolescu, A. C., Holt, A., Sawicki, G., Crawford, B. D., León, H., van Mulligen, T., and Schulz, R. (2009) Activation and modulation of 72kDa matrix metalloproteinase-2 by peroxynitrite and glutathione. *Biochem. Pharmacol.* **77**, 826–834
299. Linask, K. K., Han, M., Cai, D. H., Brauer, P. R., and Maisastry, S. M. (2005) Cardiac morphogenesis: Matrix metalloproteinase coordination of cellular mechanisms underlying heart tube formation and directionality of looping. *Dev. Dyn.* **233**, 739–753
300. Strynadka, K. D., Schulz, R., and Yasmin, W. (1997) Generation of peroxynitrite contributes to ischemia-reperfusion injury in isolated rat hearts. *Cardiovasc. Res.* **33**, 422–432
301. A., L. W. (2010) Molecular Giant Vulnerable to Oxidative Damage. *Circulation*. **122**, 2002–2004
302. Kandasamy, A. D., and Schulz, R. (2009) Glycogen synthase kinase-3β is activated by matrix metalloproteinase-2 mediated proteolysis in cardiomyoblasts. *Cardiovasc. Res.* **83**, 698–706
303. Hadler-Olsen, E., Solli, A. I., Hafstad, A., Winberg, J.-O., and Uhlin-Hansen, L. (2015) Intracellular MMP-2 Activity in Skeletal Muscle Is Associated With Type II Fibers. *J. Cell. Physiol.* **230**, 160–169
304. Paul, J., W.Y., C. A., Anna, R., and W., R. M. (2002) Nonremodeling Properties of Matrix Metalloproteinases. *Circ. Res.* **90**, 1041–1043
305. Galt, W. S., Stephan, L., Loren, A., Medd, J. D., Falk, M. J., McIntyre, M. T., Prescott, M. S., Kraiss, W. L., Zimmerman, A. G., and Weyrich, S. A. (2002) Outside-In Signals Delivered by Matrix Metalloproteinase-1 Regulate Platelet Function. *Circ. Res.* **90**, 1093–1099

306. Sheu, J. R., Fong, T. H., Liu, C. M., Shen, M. Y., Chen, T. L., Chang, Y., Lu, M. S., and Hsiao, G. (2004) Expression of matrix metalloproteinase-9 in human platelets: regulation of platelet activation in in vitro and in vivo studies. *Br. J. Pharmacol.* **143**, 193–201
307. Schoenwaelder, S. M., Yuan, Y., Cooray, P., Salem, H. H., and Jackson, S. P. (1997) Calpain cleavage of focal adhesion proteins regulates the cytoskeletal attachment of integrin alphaIIbbeta3 (platelet glycoprotein IIb/IIIa) and the cellular retraction of fibrin clots. *J. Biol. Chem.* **272**, 1694–1702
308. Soslau, G., Mason, C., Lynch, S., Benjamin, J., Ashak, D., Prakash, J. M., Moore, A., Bagsiyao, P., Albert, T., Mathew, L. M., and Jost, M. (2014) Intracellular matrix metalloproteinase-2 (MMP-2) regulates human platelet activation via hydrolysis of talin. *Thromb. Haemost.* **111**, 140–153
309. Zhou, H.-Z., Ma, X., Gray, M. O., Zhu, B., Nguyen, A. P., Baker, A. J., Simonis, U., Cecchini, G., Lovett, D. H., and Karliner, J. S. (2007) Transgenic MMP-2 expression induces latent cardiac mitochondrial dysfunction. *Biochem. Biophys. Res. Commun.* **358**, 189–195
310. Mohammad, G., and Kowluru, R. A. (2011) Novel Role of Mitochondrial Matrix Metalloproteinase-2 in the Development of Diabetic Retinopathy. *Invest. Ophthalmol. Vis. Sci.* **52**, 3832–3841
311. Santos, J. M., Tewari, S., Lin, J. Y., and Kowluru, R. A. (2013) Interrelationship between activation of matrix metalloproteinases and mitochondrial dysfunction in the development of diabetic retinopathy. *Biochem. Biophys. Res. Commun.* **438**, 760–764
312. De Bock, M., Wang, N., Decrock, E., Bultynck, G., and Leybaert, L. (2015) Intracellular Cleavage of the Cx43 C-Terminal Domain by Matrix-Metalloproteases: A Novel Contributor to Inflammation? *Mediators Inflamm.* **2015**, 257471
313. Ruta, A., Mark, B., Edward, B., Jawaharlal, P., and Jianliang, Z. (2009) Nuclear localization of active matrix metalloproteinase-2 in cigarette smoke-exposed apoptotic endothelial cells. *Exp. Lung Res.* **35**, 59–75
314. Gasche, Y., Copin, J. C., Sugawara, T., Fujimura, M., and Chan, P. H. (2001) Matrix metalloproteinase inhibition prevents oxidative stress-associated blood-brain barrier disruption after transient focal cerebral ischemia. *J. Cereb. Blood Flow Metab.* **21**, 1393–1400
315. Amantea, D., Corasaniti, M. T., Mercuri, N. B., Bernardi, G., and Bagetta, G. (2008) Brain regional and cellular localization of gelatinase activity in rat that have undergone transient middle cerebral artery occlusion. *Neuroscience*. **152**, 8–17
316. Cuadrado, E., Rosell, A., Borrell-Pages, M., Garcia-Bonilla, L., Hernandez-Guillamon, M., Ortega-Aznar, A., and Montaner, J. (2009) Matrix metalloproteinase-13 is activated and is found in the nucleus of neural cells after cerebral ischemia. *J. Cereb. Blood Flow Metab.* **29**, 398–410
317. Hill, J. W., Poddar, R., Thompson, J. F., Rosenberg, G. A., and Yang, Y. (2012) Intranuclear matrix metalloproteinases promote DNA damage and apoptosis induced by oxygen–glucose deprivation in neurons. *Neuroscience*. **220**, 277–290
318. Ohtaki, H., Takeda, T., Dohi, K., Yofu, S., Nakamachi, T., Satoh, K., Hiraizumi, Y., Miyaoka, H., Matsunaga, M., and Shioda, S. (2007) Increased mitochondrial DNA oxidative damage after transient middle cerebral artery occlusion in mice. *Neurosci. Res.* **58**, 349–355
319. Yang, Y., Candelario-Jalil, E., Thompson, J. F., Cuadrado, E., Estrada, E. Y., Rosell, A., Montaner, J., and Rosenberg, G. A. (2010) Increased intranuclear matrix metalloproteinase activity in neurons interferes with oxidative DNA repair in focal cerebral ischemia. *J. Neurochem.* **112**, 134–149

320. Yang, Y., and Rosenberg, G. A. (2015) Matrix metalloproteinases as therapeutic targets for stroke. *Brain Res.* **1623**, 30–38
321. Kimura-Ohba, S., and Yang, Y. (2016) Oxidative DNA Damage Mediated by Intranuclear MMP Activity Is Associated with Neuronal Apoptosis in Ischemic Stroke. *Oxid. Med. Cell. Longev.* **2016**, 6927328
322. Köhrmann, A., Kammerer, U., Kapp, M., Dietl, J., and Anacker, J. (2009) Expression of matrix metalloproteinases (MMPs) in primary human breast cancer and breast cancer cell lines: New findings and review of the literature. *BMC Cancer*. **9**, 188
323. Choi, D. H., Kim, E.-M., Son, H. J., Joh, T. H., Kim, Y. S., Kim, D., Flint Beal, M., and Hwang, O. (2008) A novel intracellular role of matrix metalloproteinase-3 during apoptosis of dopaminergic cells. *J. Neurochem.* **106**, 405–415
324. Kim, E.-M., Shin, E.-J., Choi, J. H., Son, H. J., Park, I.-S., Joh, T. H., and Hwang, O. (2010) Matrix metalloproteinase-3 is increased and participates in neuronal apoptotic signaling downstream of caspase-12 during endoplasmic reticulum stress. *J. Biol. Chem.* **285**, 16444–16452
325. Sung, J. Y., Park, S. M., Lee, C.-H., Um, J. W., Lee, H. J., Kim, J., Oh, Y. J., Lee, S.-T., Paik, S. R., and Chung, K. C. (2005) Proteolytic cleavage of extracellular secreted {alpha}-synuclein via matrix metalloproteinases. *J. Biol. Chem.* **280**, 25216–25224
326. Levin, J., Giese, A., Boetzel, K., Israel, L., Högen, T., Nübling, G., Kretzschmar, H., and Lorenzl, S. (2009) Increased α-synuclein aggregation following limited cleavage by certain matrix metalloproteinases. *Exp. Neurol.* **215**, 201–208
327. Zuo, X., Pan, W., Feng, T., Shi, X., and Dai, J. (2014) Matrix metalloproteinase 3 promotes cellular anti-dengue virus response via interaction with transcription factor NFkappaB in cell nucleus. *PLoS One*. **9**, e84748
328. Woo, M.-S., Park, J.-S., Choi, I.-Y., Kim, W.-K., and Kim, H.-S. (2008) Inhibition of MMP-3 or -9 suppresses lipopolysaccharide-induced expression of proinflammatory cytokines and iNOS in microglia. *J. Neurochem.* **106**, 770–780
329. Li, C. K. F., Pender, S. L. F., Pickard, K. M., Chance, V., Holloway, J. A., Huett, A., Gonçalves, N. S., Mudgett, J. S., Dougan, G., Frankel, G., and MacDonald, T. T. (2004) Impaired Immunity to Intestinal Bacterial Infection in Stromelysin-1 (Matrix Metalloproteinase-3)-Deficient Mice. *J. Immunol.* **173**, 5171–5179
330. Wilson, C. L., Ouellette, A. J., Satchell, D. P., Ayabe, T., López-Boado, Y. S., Stratman, J. L., Hultgren, S. J., Matrisian, L. M., and Parks, W. C. (1999) Regulation of Intestinal α-Defensin Activation by the Metalloproteinase Matrilysin in Innate Host Defense. *Science*. **286**, 113–117
331. Ayabe, T., Satchell, D. P., Pesendorfer, P., Tanabe, H., Wilson, C. L., Hagen, S. J., and Ouellette, A. J. (2002) Activation of Paneth cell alpha-defensins in mouse small intestine. *J. Biol. Chem.* **277**, 5219–5228
332. Shirafuji, Y., Tanabe, H., Satchell, D. P., Henschen-Edman, A., Wilson, C. L., and Ouellette, A. J. (2003) Structural determinants of procryptdin recognition and cleavage by matrix metalloproteinase-7. *J. Biol. Chem.* **278**, 7910–7919
333. Shanahan, M. T., Vidrich, A., Shirafuji, Y., Dubois, C. L., Henschen-Edman, A., Hagen, S. J., Cohn, S. M., and Ouellette, A. J. (2010) Elevated expression of Paneth cell CRS4C in ileitis-prone SAMP1/YitFc mice: regional distribution, subcellular localization, and mechanism of action. *J. Biol. Chem.* **285**, 7493–7504
334. Lindsey, L. M., Patricia, E. G., Rupak, M., Goshorn, K. D., Sheats, J. N., Bruce, A. J., Matthew, M. I., Hendrick, K. J., Hewett, W. K., Gourdie, G. R., Matrisian, M. L., and Spinale, G. F. (2006) Matrix Metalloproteinase-7 Affects Connexin-43 Levels, Electrical Conduction, and Survival After Myocardial Infarction. *Circulation*. **113**, 2919–2928

335. Zhang, Z., Amorosa, L. F., Coyle, S. M., Macor, M. A., Lubitz, S. E., Carson, J. L., Birnbaum, M. J., Lee, L. Y., and Haimovich, B. (2015) Proteolytic Cleavage of AMPKα and Intracellular MMP9 Expression Are Both Required for TLR4-Mediated mTORC1 Activation and HIF-1α Expression in Leukocytes. *J. Immunol.* **195**, 2452–2460
336. Sans-Fons, M. G., Sole, S., Sanfeliu, C., and Planas, A. M. (2010) Matrix Metalloproteinase-9 and Cell Division in Neuroblastoma Cells and Bone Marrow Macrophages. *Am. J. Pathol.* **177**, 2870–2885
337. Rouet-Benzineb, P., Buhler, J.-M., Dreyfus, P., Delcourt, A., Dorent, R., Perennec, J., Crozatier, B., Harf, A., and Lafuma, C. (1999) Altered balance between matrix gelatinases (MMP-2 and MMP-9) and their tissue inhibitors in human dilated cardiomyopathy: potential role of MMP-9 in myosin-heavy chain degradation. *Eur. J. Heart Fail.* **1**, 337–352
338. Kowluru, R. A., Zhong, Q., and Santos, J. M. (2012) Matrix metalloproteinases in diabetic retinopathy: potential role of MMP-9. *Expert Opin. Investig. Drugs*. **21**, 797–805
339. Moshal, K. S., Tipparaju, S. M., Vacek, T. P., Kumar, M., Singh, M., Frank, I. E., Patibandla, P. K., Tyagi, N., Rai, J., Metreveli, N., Rodriguez, W. E., Tseng, M. T., and Tyagi, S. C. (2008) Mitochondrial matrix metalloproteinase activation decreases myocyte contractility in hyperhomocysteinemia. *Am. J. Physiol. Heart Circ. Physiol.* **295**, H890-7
340. Mohammad, G., and Kowluru, R. A. (2012) Diabetic retinopathy and signaling mechanism for activation of matrix metalloproteinase-9. *J. Cell. Physiol.* **227**, 1052–1061
341. Miller, J. P., Holcomb, J., Al-Ramahi, I., de Haro, M., Gafni, J., Zhang, N., Kim, E., Sanhueza, M., Torcassi, C., Kwak, S., Botas, J., Hughes, R. E., and Ellerby, L. M. (2010) Matrix Metalloproteinases Are Modifiers of Huntingtin Proteolysis and Toxicity in Huntington's Disease. *Neuron*. **67**, 199–212
342. Kahlem, P., Green, H., and Djian, P. (1998) Transglutaminase Action Imitates Huntington's Disease: Selective Polymerization of Huntingtin Containing Expanded Polyglutamine. *Mol. Cell*. **1**, 595–601
343. Velier, J., Kim, M., Schwarz, C., Kim, T. W., Sapp, E., Chase, K., Aronin, N., and DiFiglia, M. (1998) Wild-Type and Mutant Huntingtins Function in Vesicle Trafficking in the Secretory and Endocytic Pathways. *Exp. Neurol.* **152**, 34–40
344. Lehrach, H., Lurz, R., Gauss, C., Scherzinger, E., Nordhoff, E., Wanker, E. E., Bates, G. P., Goehler, H., Sathasivam, K., Hasenbank, R., and Waelter, S. (2001) The huntingtin interacting protein HIP1 is a clathrin and α-adaptin-binding protein involved in receptor-mediated endocytosis. *Hum. Mol. Genet.* **10**, 1807–1817
345. Gafni, J., Hermel, E., Young, J. E., Wellington, C. L., Hayden, M. R., and Ellerby, L. M. (2004) Inhibition of calpain cleavage of huntingtin reduces toxicity: accumulation of calpain/caspase fragments in the nucleus. *J. Biol. Chem.* **279**, 20211–20220
346. Martindale, D., Hackam, A., Wieczorek, A., Ellerby, L., Wellington, C., McCutcheon, K., Singaraja, R., Kazemi-Esfarjani, P., Devon, R., Kim, S. U., Bredesen, D. E., Tufaro, F., and Hayden, M. R. (1998) Length of huntingtin and its polyglutamine tract influences localization and frequency of intracellular aggregates. *Nat. Genet.* **18**, 150–154
347. Doty, C. N., Carroll, J. B., Hayden, M. R., Graham, R. K., Singaraja, R. R., Warby, S. C., Yang, Y.-Z., and Overall, C. M. (2008) Activated caspase-6 and caspase-6-cleaved fragments of huntingtin specifically colocalize in the nucleus. *Hum. Mol. Genet.* **17**, 2390–2404
348. Houghton, A. M., Hartzell, W. O., Robbins, C. S., Gomis-Rüth, F. X., and Shapiro, S. D. (2009) Macrophage elastase kills bacteria within murine macrophages. *Nature*. **460**, 637
349. Holmbeck, K., Bianco, P., Caterina, J., Yamada, S., Kromer, M., Kuznetsov, S. A., Mankani, M., Gehron Robey, P., Poole, A. R., Pidoux, I., Ward, J. M., and Birkedal-

Hansen, H. (1999) MT1-MMP-Deficient Mice Develop Dwarfism, Osteopenia, Arthritis, and Connective Tissue Disease due to Inadequate Collagen Turnover. *Cell*. **99**, 81–92
350. Golubkov, V. S., Boyd, S., Savinov, A. Y., Chekanov, A. V, Osterman, A. L., Remacle, A., Rozanov, D. V, Doxsey, S. J., and Strongin, A. Y. (2005) Membrane type-1 matrix metalloproteinase (MT1-MMP) exhibits an important intracellular cleavage function and causes chromosome instability. *J. Biol. Chem.* **280**, 25079–25086
351. Overall, C. M., King, A. E., Sam, D. K., Ong, A. D., Lau, T. T., Wallon, U. M., DeClerck, Y. A., and Atherstone, J. (1999) Identification of the tissue inhibitor of metalloproteinases-2 (TIMP-2) binding site on the hemopexin carboxyl domain of human gelatinase A by site-directed mutagenesis. The hierarchical role in binding TIMP-2 of the unique cationic clusters of hemopexin . *J. Biol. Chem.* **274**, 4421–4429
352. Overall, C. M., King, A. E., Bigg, H. F., McQuibban, A., Atherstone, J., Sam, D. K., Ong, A. D., Lau, T. T. Y., Wallon, U. M., DeClerck, Y. A., and Tam, E. (1999) Identification of the TIMP-2 Binding Site on the Gelatinase A Hemopexin C-Domain by Site-Directed Mutagenesis and the Yeast Two-Hybrid System. *Ann. N. Y. Acad. Sci.* **878**, 747–753
353. Bigg, H. F., Morrison, C. J., Butler, G. S., Bogoyevitch, M. A., Wang, Z., Soloway, P. D., and Overall, C. M. (2001) Tissue Inhibitor of Metalloproteinases-4 Inhibits But Does Not Support the Activation of Gelatinase A via Efficient Inhibition of Membrane Type 1-Matrix Metalloproteinase. *Cancer Res.* **61**, 3610–3618
354. D'Alessio, S., Ferrari, G., Cinnante, K., Scheerer, W., Galloway, A. C., Roses, D. F., Rozanov, D. V, Remacle, A. G., Oh, E.-S., Shiryaev, S. A., Strongin, A. Y., Pintucci, G., and Mignatti, P. (2008) Tissue inhibitor of metalloproteinases-2 binding to membrane-type 1 matrix metalloproteinase induces MAPK activation and cell growth by a non-proteolytic mechanism. *J. Biol. Chem.* **283**, 87–99
355. Sakamoto, T., and Seiki, M. (2010) A membrane protease regulates energy production in macrophages by activating hypoxia-inducible factor-1 via a non-proteolytic mechanism. *J. Biol. Chem.* **285**, 29951–29964
356. Gonzalo, P., Guadamillas, M. C., Hernández-Riquer, M. V., Pollán, Á., Grande-García, A., Bartolomé, R. A., Vasanji, A., Ambrogio, C., Chiarle, R., Teixidó, J., Risteli, J., Apte, S. S., del Pozo, M. A., and Arroyo, A. G. (2010) MT1-MMP Is Required for Myeloid Cell Fusion via Regulation of Rac1 Signaling. *Dev. Cell*. **18**, 77–89
357. Sakamoto, T., and Seiki, M. (2009) Cytoplasmic tail of MT1-MMP regulates macrophage motility independently from its protease activity. *Genes to Cells*. **14**, 617–626
358. Shimizu-Hirota, R., Xiong, W., Baxter, B. T., Kunkel, S. L., Maillard, I., Chen, X.-W., Sabeh, F., Liu, R., Li, X.-Y., and Weiss, S. J. (2012) MT1-MMP regulates the PI3Kdelta.Mi-2/NuRD-dependent control of macrophage immune function. *Genes Dev.* **26**, 395–413
359. Strongin, A. Y. (2006) Mislocalization and unconventional functions of cellular MMPs in cancer. *Cancer Metastasis Rev.* **25**, 87–98
360. Savinov, A. Y., Remacle, A. G., Golubkov, V. S., Krajewska, M., Kennedy, S., Duffy, M. J., Rozanov, D. V, Krajewski, S., and Strongin, A. Y. (2006) Matrix Metalloproteinase 26 Proteolysis of the NH_2-Terminal Domain of the Estrogen Receptor β Correlates with the Survival of Breast Cancer Patients. *Cancer Res.* **66**, 2716–2724
361. Zhao, Y.-G., Xiao, A.-Z., Newcomer, R. G., Park, H. I., Kang, T., Chung, L. W. K., Swanson, M. G., Zhau, H. E., Kurhanewicz, J., and Sang, Q.-X. A. (2003) Activation of pro-gelatinase B by endometase/matrilysin-2 promotes invasion of human prostate cancer cells. *J. Biol. Chem.* **278**, 15056–15064
362. Dufour, A., and Overall, C. M. (2013) Missing the target: matrix metalloproteinase antitargets in inflammation and cancer. *Trends Pharmacol. Sci.* **34**, 233–242

363. Jobin, P. G., Butler, G. S., and Overall, C. M. (2017) New intracellular activities of matrix metalloproteinases shine in the moonlight. *Biochim. Biophys. acta. Mol. cell Res.* **1864**, 2043–2055
364. Ko, Y. G., Kim, E. K., Kim, T., Park, H., Park, H. S., Choi, E. J., and Kim, S. (2001) Glutamine-dependent Antiapoptotic Interaction of Human Glutaminyl-tRNA Synthetase with Apoptosis Signal-regulating Kinase 1. *J. Biol. Chem.* **276**, 6030–6036
365. Jin, M. (2019) Unique roles of tryptophanyl-tRNA synthetase in immune control and its therapeutic implications. *Exp. Mol. Med.* **51**, 1
366. Xu, X., Zhou, H., Zhou, Q., Hong, F., Vo, M.-N., Niu, W., Wang, Z., Xiong, X., Nakamura, K., Wakasugi, K., Schimmel, P., and Yang, X.-L. (2018) An alternative conformation of human TrpRS suggests a role of zinc in activating non-enzymatic function. *RNA Biol.* **15**, 649–658
367. Turpaev, K. T., Zakhariev, V. M., Sokolova, I. V, Narovlyansky, A. N., Amchenkova, A. M., Justesen, J., and Frolova, L. Y. (1996) Alternative Processing of the Tryptophanyl-tRNA Synthetase mRNA from Interferon-Treated Human Cells. *Eur. J. Biochem.* **240**, 732–737
368. Rubin, B. Y., Anderson, S. L., Xing, L., Powell, R. J., and Tate, W. P. (1991) Interferon induces tryptophanyl-tRNA synthetase expression in human fibroblasts. *J. Biol. Chem.* **266**, 24245–24248
369. Fleckner, J., and Rasmussent, H. H. (1991) Human interferon y potently induces the synthesis of a 55-kDa protein (y2) highly homologous to rabbit peptide chain release factor and bovine tryptophanyl-tRNA synthetase. *Biochemistry*. **88**, 11520–11524
370. Reano, A., Richard, M. H., Denoroy, L., Viac, J., Benedetto, J. P., and Schmitt, D. (1993) Gamma interferon potently induces tryptophanyl-tRNA synthetase expression in human keratinocytes. *J. Invest. Dermatol.* **100**, 775–779
371. Fleckner, J., Martensen, P. M., Tolstrup, A. B., Kjeldgaard, N. O., and Justesen, J. (1995) Differential regulation of the human, interferon inducible tryptophanyl-tRNA synthetase by various cytokines in cell lines. *Cytokine*. **7**, 70–77
372. Zeng, R., Chen, Y. C., Zeng, Z., Liu, W. Q., Jiang, X. F., Liu, R., Qiang, O., and Li, X. (2011) Effect of mini-tyrosyl-tRNA synthetase/mini-tryptophanyl-tRNA synthetase on ischemic angiogenesis in rats: Proliferation and migration of endothelial cells. *Heart Vessels*. **26**, 69–80
373. Dean, R. A., Cox, J. H., Bellac, C. L., Doucet, A., Starr, A. E., and Overall, C. M. (2008) Macrophage-specific metalloelastase (MMP-12) truncates and inactivates ELR+ CXC chemokines and generates CCL2, -7, -8, and -13 antagonists: potential role of the macrophage in terminating polymorphonuclear leukocyte influx. *Blood*. **112**, 3455–3464
374. Henning, L. N., Azad, A. K., Parsa, K. V. L., Joy, E., Tridandapani, S., and Schlesinger, L. S. (2018) Pulmonary Surfactant Protein A Regulates TLR Expression and Activity in Human Macrophages. *J. Immunol.* **180**, 7847–7858
375. Pierce, J. W., Schoenleber, R., Jesmok, G., Best, J., Moore, S. A., Collins, T., and Gerritsen, M. E. (1997) Novel inhibitors of cytokine-induced IkappaBalpha phosphorylation and endothelial cell adhesion molecule expression show anti-inflammatory effects in vivo. *J. Biol. Chem.* **272**, 21096–21103
376. Melisi, D., and Chiao, P. J. (2007) NF-kappa B as a target for cancer therapy. *Expert Opin. Ther. Targets*. **11**, 133–144
377. Mistry, P., Laird, M. H. W., Schwarz, R. S., Greene, S., Dyson, T., Snyder, G. A., Xiao, T. S., Chauhan, J., Fletcher, S., Toshchakov, V. Y., MacKerell, A. D., and Vogel, S. N. (2015) Inhibition of TLR2 signaling by small molecule inhibitors targeting a pocket within the TLR2 TIR domain. *Proc. Natl. Acad. Sci.* **112**, 5455 LP – 5460

378. Ii, M., Matsunaga, N., Hazeki, K., Nakamura, K., Takashima, K., Seya, T., Hazeki, O., Kitazaki, T., and Iizawa, Y. (2006) A novel cyclohexene derivative, ethyl (6R)-6-[N-(2-Chloro-4-fluorophenyl)sulfamoyl]cyclohex-1-ene-1-carboxylate (TAK-242), selectively inhibits toll-like receptor 4-mediated cytokine production through suppression of intracellular signaling. *Mol. Pharmacol.* **69**, 1288–1295
379. Kawamoto, T., Ii, M., Kitazaki, T., Iizawa, Y., and Kimura, H. (2008) TAK-242 selectively suppresses Toll-like receptor 4-signaling mediated by the intracellular domain. *Eur. J. Pharmacol.* **584**, 40–48
380. Mamat, U., Wilke, K., Bramhill, D., Schromm, A. B., Lindner, B., Kohl, T. A., Corchero, J. L., Villaverde, A., Schaffer, L., Head, S. R., Souvignier, C., Meredith, T. C., and Woodard, R. W. (2015) Detoxifying Escherichia coli for endotoxin-free production of recombinant proteins. *Microb. Cell Fact.* **14**, 57
381. Planesse, C., Nativel, B., Iwema, T., Gasque, P., Silva, C. R., and Viranaïcken, W. (2015) Recombinant human HSP60 produced in ClearColi BL21(DE3) does not activate the NFkappaB pathway. *Cytokine*. **73**, 190–195
382. Butler, G. S., and Overall, C. M. (2013) Matrix metalloproteinase processing of signaling molecules to regulate inflammation. *Periodontol. 2000*. **63**, 123–148
383. Doucet, A., and Overall, C. M. (2011) Broad Coverage Identification of Multiple Proteolytic Cleavage Site Sequences in Complex High Molecular Weight Proteins Using Quantitative Proteomics as a Complement to Edman Sequencing. *Mol. Cell. Proteomics*. **10**, M110.003533
384. Doucet, A., and Overall, C. M. (2011) Amino-Terminal Oriented Mass Spectrometry of Substrates (ATOMS): N-Terminal Sequencing of Proteins and Proteolytic Cleavage Sites by Quantitative Mass Spectrometry. *Methods Enzymol.* **501**, 275–293
385. Schroder, K., Hertzog, P. J., Ravasi, T., and Hume, D. A. (2004) Interferon-gamma: an overview of signals, mechanisms and functions. *J. Leukoc. Biol.* **75**, 163–189
386. Hu, X., and Ivashkiv, L. B. (2009) Review Cross-regulation of Signaling Pathways by Interferon- g : Implications for Immune Responses and Autoimmune Diseases. *Immunity*. **31**, 539–550
387. Klein, T., Fung, S.-Y., Renner, F., Blank, M. A., Dufour, A., Kang, S., Bolger-Munro, M., Scurll, J. M., Priatel, J. J., Schweigler, P., Melkko, S., Gold, M. R., Viner, R. I., Regnier, C. H., Turvey, S. E., and Overall, C. M. (2015) The paracaspase MALT1 cleaves HOIL1 reducing linear ubiquitination by LUBAC to dampen lymphocyte NF-kappaB signalling. *Nat. Commun.* **6**, 8777
388. Aida, Y., and Pabst, M. J. (1990) Removal of endotoxin from protein solutions by phase separation using Triton X-114. *J. Immunol. Methods*. **132**, 191–195
389. Eckhard, U., Huesgen, P. F., Schilling, O., Bellac, C. L., Butler, G. S., Cox, J. H., Dufour, A., Goebeler, V., Kappelhoff, R., Klein, T., Lange, P. F., Marino, G., Morrison, C. J., Prudova, A., Rodriguez, D., Starr, A. E., Wang, Y., and Overall, C. M. (2016) Active site specificity profiling of the matrix metalloproteinase family : Proteomic identification of 4300 cleavage sites by nine MMPs explored with structural and synthetic peptide cleavage analyses. *Matrix Biol.* **49**, 37–60
390. Knight, C. G., Willenbrock, F., and Murphy, G. (1992) A novel coumarin-labelled peptide for sensitive continuous assays of the matrix metalloproteinases. *FEBS Lett.* **296**, 263–266
391. Rappsilber, J., Mann, M., and Ishihama, Y. (2007) Protocol for micro-purification , enrichment , pre-fractionation and storage of peptides for proteomics using StageTips. *Nat. Protoc.* **2**, 1896–1906
392. Craig, R., and Beavis, R. C. (2004) TANDEM: matching proteins with tandem mass

spectra. *Bioinformatics*. **20**, 1466–1467
393. Deutsch, E. W., Csordas, A., Sun, Z., Jarnuczak, A., Perez-Riverol, Y., Ternent, T., Campbell, D. S., Bernal-Llinares, M., Okuda, S., Kawano, S., Moritz, R. L., Carver, J. J., Wang, M., Ishihama, Y., Bandeira, N., Hermjakob, H., and Vizcaino, J. A. (2017) The ProteomeXchange consortium in 2017: supporting the cultural change in proteomics public data deposition. *Nucleic Acids Res.* **45**, D1100–D1106
394. Perez-Riverol, Y., Csordas, A., Bai, J., Bernal-Llinares, M., Hewapathirana, S., Kundu, D. J., Inuganti, A., Griss, J., Mayer, G., Eisenacher, M., Perez, E., Uszkoreit, J., Pfeuffer, J., Sachsenberg, T., Yilmaz, S., Tiwary, S., Cox, J., Audain, E., Walzer, M., Jarnuczak, A. F., Ternent, T., Brazma, A., and Vizcaino, J. A. (2019) The PRIDE database and related tools and resources in 2019: improving support for quantification data. *Nucleic Acids Res.* **47**, D442–D450
395. Cox, J., and Mann, M. (2008) MaxQuant enables high peptide identification rates, individualized p.p.b.-range mass accuracies and proteome-wide protein quantification. *Nat. Biotechnol.* **26**, 1367–1372
396. Dean, R. A., Butler, G. S., Hamma-Kourbali, Y., Delbe, J., Brigstock, D. R., Courty, J., and Overall, C. M. (2007) Identification of candidate angiogenic inhibitors processed by matrix metalloproteinase 2 (MMP-2) in cell-based proteomic screens: disruption of vascular endothelial growth factor (VEGF)/heparin affin regulatory peptide (pleiotrophin) and VEGF/Connective . *Mol. Cell. Biol.* **27**, 8454–8465
397. Eckhard, U., Marino, G., Abbey, S. R., Tharmarajah, G., Matthew, I., and Overall, C. M. (2015) The Human Dental Pulp Proteome and N-Terminome: Levering the Unexplored Potential of Semitryptic Peptides Enriched by TAILS to Identify Missing Proteins in the Human Proteome Project in Underexplored Tissues. *J. Proteome Res.* **14**, 3568–3582
398. Abbey, S. R., Eckhard, U., Solis, N., Marino, G., Matthew, I., and Overall, C. M. (2018) The Human Odontoblast Cell Layer and Dental Pulp Proteomes and N-Terminomes. *J. Dent. Res.* **97**, 338–346
399. Prudova, A., Serrano, K., Eckhard, U., Fortelny, N., Devine, D. V, and Overall, C. M. (2014) TAILS N-terminomics of human platelets reveals pervasive metalloproteinase-dependent proteolytic processing in storage. *Blood*. **124**, e49-60
400. Eckhard, U., Marino, G., Abbey, S. R., Matthew, I., and Overall, C. M. (2015) TAILS N-terminomic and proteomic datasets of healthy human dental pulp. *Data Br.* **5**, 542–548
401. Yang, X.-L., Skene, R. J., McRee, D. E., and Schimmel, P. (2002) Nonlinear partial differential equations and applications: Crystal structure of a human aminoacyl-tRNA synthetase cytokine. *Proc. Natl. Acad. Sci.* **99**, 15369–15374
402. ExoCarta [online] http://exocarta.org/gene_summary?gene_id=8565 (Accessed June 2, 2017)
403. Millar, A. W., Brown, P. D., Moore, J., Galloway, W. A., Cornish, A. G., Lenehan, T. J., and Lynch, K. P. (1998) Results of single and repeat dose studies of the oral matrix metalloproteinase inhibitor marimastat in healthy male volunteers. *Br. J. Clin. Pharmacol.* **45**, 21–26
404. Starr, A. E., Dufour, A., Maier, J., and Overall, C. M. (2012) Biochemical analysis of matrix metalloproteinase activation of chemokines CCL15 and CCL23 and increased glycosaminoglycan binding of CCL16. *J. Biol. Chem.* **287**, 5848–5860
405. Lijnen, H. R., Van Hoef, B., and Collen, D. (2001) Inactivation of the serpin alpha(2)-antiplasmin by stromelysin-1. *Biochim. Biophys. Acta*. **1547**, 206–213
406. Ying, Z., Huang, X. F., Xiang, X., Liu, Y., Kang, X., Song, Y., Guo, X., Liu, H., Ding, N., Zhang, T., Duan, P., Lin, Y., Zheng, W., Wang, X., Lin, N., Tu, M., Xie, Y., Zhang, C., Liu, W., Deng, L., Gao, S., Ping, L., Wang, X., Zhou, N., Zhang, J., Wang, Y., Lin, S., Mamuti,

M., Yu, X., Fang, L., Wang, S., Song, H., Wang, G., Jones, L., Zhu, J., and Chen, S.-Y. (2019) A safe and potent anti-CD19 CAR T cell therapy. *Nat. Med.* 10.1038/s41591-019-0421-7

407. Fadok, V. A., Bratton, D. L., Konowal, A., Freed, P. W., Westcott, J. Y., and Henson, P. M. (1998) Macrophages that have ingested apoptotic cells in vitro inhibit proinflammatory cytokine production through autocrine/paracrine mechanisms involving TGF-beta, PGE2, and PAF. *J. Clin. Invest.* **101**, 890–898
408. Huynh, M.-L. N., Fadok, V. A., and Henson, P. M. (2002) Phosphatidylserine-dependent ingestion of apoptotic cells promotes TGF-beta1 secretion and the resolution of inflammation. *J. Clin. Invest.* **109**, 41–50
409. Lucas, M., Stuart, L. M., Savill, J., and Lacy-Hulbert, A. (2003) Apoptotic cells and innate immune stimuli combine to regulate macrophage cytokine secretion. *J. Immunol.* **171**, 2610–2615
410. Doulatov, S., Notta, F., Eppert, K., Nguyen, L. T., Ohashi, P. S., and Dick, J. E. (2010) Revised map of the human progenitor hierarchy shows the origin of macrophages and dendritic cells in early lymphoid development. *Nat. Immunol.* **11**, 585–593
411. Geissmann, F., Manz, M. G., Jung, S., Sieweke, M. H., Merad, M., and Ley, K. (2010) Development of monocytes, macrophages, and dendritic cells. *Science*. **327**, 656–661
412. Weaver, A., Goncalves da Silva, A., Nuttall, R. K., Edwards, D. R., Shapiro, S. D., Rivest, S., and Yong, V. W. (2005) An elevated matrix metalloproteinase (MMP) in an animal model of multiple sclerosis is protective by affecting Th1/Th2 polarization. *FASEB J. Off. Publ. Fed. Am. Soc. Exp. Biol.* **19**, 1668–1670
413. Vieira, A. T., Fagundes, C. T., Alessandri, A. L., Castor, M. G. M., Guabiraba, R., Borges, V. O., Silveira, K. D., Vieira, E. L. M., Goncalves, J. L., Silva, T. A., Deruaz, M., Proudfoot, A. E. I., Sousa, L. P., and Teixeira, M. M. (2009) Treatment with a novel chemokine-binding protein or eosinophil lineage-ablation protects mice from experimental colitis. *Am. J. Pathol.* **175**, 2382–2391
414. Collins, D. W., and Jukes, T. H. (1993) Relationship between G + C in silent sites of codons and amino acid composition of human proteins. *J. Mol. Evol.* **36**, 201–213
415. Xue, H., and Wong, J. T. F. (1995) Interferon induction of human tryptophanyl-tRNA synthetase safeguards the synthesis of tryptophan-rich immune-system proteins: a hypothesis. *Gene*. **165**, 335–339
416. Fukasawa, Y., Segawa, H., Kim, J. Y., Chairoungdua, A., Kim, D. K., Matsuo, H., Cha, S. H., Endou, H., and Kanai, Y. (2000) Identification and Characterization of a Na ⁺ -independent Neutral Amino Acid Transporter That Associates with the 4F2 Heavy Chain and Exhibits Substrate Selectivity for Small Neutral D - and L -Amino Acids *. **275**, 9690–9698
417. Yanagida, O., Kanai, Y., Chairoungdua, A., and Kyung, D. (2001) Human L-type amino acid transporter 1 (LAT1): characterization of function and expression in tumor cell lines. *Biochim Biophys Acta*. **1514**, 291–302
418. Eva, M., Urtti, A., and Yliperttula, M. (2008) Pharmacokinetic role of L-type amino acid transporters LAT1 and LAT2. *Eur J Pharm Sci*. **5**, 161–174
419. Kudo, Y., Boyd, C. A. R., Sargent, I. L., and Redman, C. W. G. (2003) Decreased tryptophan catabolism by placental indoleamine 2 , 3-dioxygenase in preeclampsia. *Am. J. Obstet. Gynecol.* **188**, 719–726
420. Kudo, Y., Boyd, C. A. R., Sargent, I. L., and Redman, C. W. G. (2003) Decreased tryptophan catabolism by placental indoleamine 2,3-dioxygenase in preeclampsia. *Am. J. Obstet. Gynecol.* **188**, 719–726
421. Cao, X., Li, C., Xiao, S., Tang, Y., Huang, J., Zhao, S., Li, X., Li, J., Zhang, R., and Yu,

W. (2017) Acetylation promotes TyrRS nuclear translocation to prevent oxidative damage. *Proc. Natl. Acad. Sci.* **114**, 687–692
422. Wang, H., Zhu, S., Zhou, R., Li, W., and Sama, A. E. (2008) Therapeutic potential of HMGB1-targeting agents in sepsis. *Expert Rev. Mol. Med.* **10**, 1–20
423. Andersson, U., and Tracey, K. J. (2011) HMGB1 is a therapeutic target for sterile inflammation and infection. *Annu. Rev. Immunol.* **29**, 139–162
424. Charoensup, J., Sermswan, R. W., Paeyao, A., Promakhejohn, S., Punasee, S., Chularari, C., Krabkraikaew, S., Lertanekawattana, S., and Wongratanacheewin, S. (2014) High HMGB1 level is associated with poor outcome of septicemic melioidosis. *Int. J. Infect. Dis.* **28**, 111–116
425. Yang, H., Ochani, M., Li, J., Qiang, X., Tanovic, M., Harris, H. E., Susarla, S. M., Ulloa, L., Wang, H., DiRaimo, R., Czura, C. J., Wang, H., Roth, J., Warren, H. S., Fink, M. P., Fenton, M. J., Andersson, U., and Tracey, K. J. (2004) Reversing established sepsis with antagonists of endogenous high-mobility group box 1. *Proc. Natl. Acad. Sci. U. S. A.* **101**, 296–301
426. Gaini, S., Pedersen, S. S., Koldkjaer, O. G., Pedersen, C., and Moller, H. J. (2007) High mobility group box-1 protein in patients with suspected community-acquired infections and sepsis: a prospective study. *Crit. Care*. **11**, R32
427. Hughes, C. E., Caterson, B., White, R. J., Roughley, P. J., and Mort, J. S. (1992) Monoclonal antibodies recognizing protease-generated neoepitopes from cartilage proteoglycan degradation. Application to studies of human link protein cleavage by stromelysin. *J. Biol. Chem.* **267**, 16011–16014
428. Starr, A. E., and Overall, C. M. (2009) Chapter 13 Characterizing Proteolytic Processing of Chemokines by Mass Spectrometry, Biochemistry, Neo-Epitope Antibodies and Functional Assays. *Methods Enzymol.* **461**, 281–307
429. Vergote, D., Butler, G. S., Ooms, M., Cox, J. H., Silva, C., Hollenberg, M. D., Jhamandas, J. H., Overall, C. M., and Power, C. (2006) Proteolytic processing of SDF-1alpha reveals a change in receptor specificity mediating HIV-associated neurodegeneration. *Proc. Natl. Acad. Sci. U. S. A.* **103**, 19182–19187
430. Huttenhain, R., Malmstrom, J., Picotti, P., and Aebersold, R. (2009) Perspectives of targeted mass spectrometry for protein biomarker verification. *Curr. Opin. Chem. Biol.* **13**, 518–525
431. Wang, Q., Chaerkady, R., Wu, J., Hwang, H. J., Papadopoulos, N., Kopelovich, L., Maitra, A., Matthaei, H., Eshleman, J. R., Hruban, R. H., Kinzler, K. W., Pandey, A., and Vogelstein, B. (2011) Mutant proteins as cancer-specific biomarkers. *Proc. Natl. Acad. Sci. U. S. A.* **108**, 2444–2449
432. Picotti, P., and Aebersold, R. (2012) Selected reaction monitoring-based proteomics: workflows, potential, pitfalls and future directions. *Nat. Methods*. **9**, 555–566
433. Kondrat, R. W., McClusky, G. A., and Cooks, R. G. (1978) Multiple reaction monitoring in mass spectrometry/mass spectrometry for direct analysis of complex mixtures. *Anal. Chem.* **50**, 2017–2021
434. Chambers, A. G., Percy, A. J., Simon, R., and Borchers, C. H. (2014) MRM for the verification of cancer biomarker proteins: recent applications to human plasma and serum. *Expert Rev. Proteomics*. **11**, 137–148
435. Fahlman, R. P., Chen, W., and Overall, C. M. (2014) Absolute proteomic quantification of the activity state of proteases and proteolytic cleavages using proteolytic signature peptides and isobaric tags. *J. Proteomics*. **100**, 79–91
436. Wiita, A. P., Hsu, G. W., Lu, C. M., Esensten, J. H., and Wells, J. A. (2014) Circulating proteolytic signatures of chemotherapy-induced cell death in humans discovered by N-

terminal labeling. *Proc. Natl. Acad. Sci. U. S. A.* **111**, 7594–7599
437. Patil, P. A., Blakely, A. M., Lombardo, K. A., Machan, J. T., Miner, T. J., Wang, L.-J., Marwaha, A. S., and Matoso, A. (2018) Expression of PD-L1, indoleamine 2,3-dioxygenase and the immune microenvironment in gastric adenocarcinoma. *Histopathology*. **73**, 124–136
438. Tzima, E., and Schimmel, P. (2006) Inhibition of tumor angiogenesis by a natural fragment of a tRNA synthetase. *Trends Biochem. Sci.* **31**, 7–10
439. Ghanipour, A., Jirstrom, K., Ponten, F., Glimelius, B., Pahlman, L., and Birgisson, H. (2009) The prognostic significance of tryptophanyl-tRNA synthetase in colorectal cancer. *Cancer Epidemiol. Biomarkers Prev.* **18**, 2949–2956
440. Cheong, J.-H., Yang, H.-K., Kim, H., Kim, W. H., Kim, Y.-W., Kook, M.-C., Park, Y.-K., Kim, H.-H., Lee, H. S., Lee, K. H., Gu, M. J., Kim, H. Y., Lee, J., Choi, S. H., Hong, S., Kim, J. W., Choi, Y. Y., Hyung, W. J., Jang, E., Kim, H., Huh, Y.-M., and Noh, S. H. (2018) Predictive test for chemotherapy response in resectable gastric cancer: a multi-cohort, retrospective analysis. *Lancet. Oncol.* **19**, 629–638
441. Lee, C.-W., Chang, K.-P., Chen, Y.-Y., Liang, Y., Hsueh, C., Yu, J.-S., Chang, Y.-S., and Yu, C.-J. (2015) Overexpressed tryptophanyl-tRNA synthetase, an angiostatic protein, enhances oral cancer cell invasiveness. *Oncotarget*. **6**, 21979–21992
442. Ling, Z., Yanling, Z., Zhe, F., Kui, C., Xiushi, Z., Min, Y., and Wei, M. (2014) Recombinant human tyrosyl-tRNA synthetase, a novel thrombopoietic agent. *Eur. J. Pharmacol.* **738**, 293–300
443. Gernsheimer, T. B. (2008) The pathophysiology of ITP revisited: ineffective thrombopoiesis and the emerging role of thrombopoietin receptor agonists in the management of chronic immune thrombocytopenic purpura. *Hematol. Am. Soc. Hematol. Educ. Progr.* **2008**, 219–226
444. Oshima, Y., Yuji, K., Tanimoto, T., Hinomura, Y., and Tojo, A. (2013) Association between Acute Myelogenous Leukemia and Thrombopoietin Receptor Agonists in Patients with Immune Thrombocytopenia. *Intern. Med.* **52**, 2193–2201
445. McCormick, M. E., Rojas, M., Moser-Katz, T., Tzima, E., and Reader, J. S. (2014) Natural aminoacyl tRNA synthetase fragment enhances cardiac function after myocardial infarction. *PLoS One*. **9**, e109325
446. Zeng, R., Wang, M., You, G., Yue, R., Chen, Y., Zeng, Z., Liu, R., Qiang, O., and Zhang, L. (2016) Effect of Mini-Tyrosyl-tRNA Synthetase/Mini-Tryptophanyl-tRNA Synthetase on Angiogenesis in Rhesus Monkeys after Acute Myocardial Infarction. *Cardiovasc. Ther.* **34**, 4–12
447. Banin, E., Dorrell, M. I., Aguilar, E., Ritter, M. R., Aderman, C. M., Smith, A. C. H., Friedlander, J., and Friedlander, M. (2006) T2-TrpRS inhibits preretinal neovascularization and enhances physiological vascular regrowth in OIR as assessed by a new method of quantification. *Invest. Ophthalmol. Vis. Sci.* **47**, 2125–2134
448. Oprescu, S. N., Griffin, L. B., Beg, A. A., and Antonellis, A. (2017) Predicting the pathogenicity of aminoacyl-tRNA synthetase mutations. *Methods*. **113**, 139–151
449. Meyer-Schuman, R., and Antonellis, A. (2017) Emerging mechanisms of aminoacyl-tRNA synthetase mutations in recessive and dominant human disease. *Hum. Mol. Genet.* **26**, R114–R127
450. Tsai, P.-C., Soong, B.-W., Mademan, I., Huang, Y.-H., Liu, C.-R., Hsiao, C.-T., Wu, H.-T., Liu, T.-T., Liu, Y.-T., Tseng, Y.-T., Lin, K.-P., Yang, U.-C., Chung, K. W., Choi, B.-O., Nicholson, G. A., Kennerson, M. L., Chan, C.-C., De Jonghe, P., Cheng, T.-H., Liao, Y.-C., Zuchner, S., Baets, J., and Lee, Y.-C. (2017) A recurrent WARS mutation is a novel cause of autosomal dominant distal hereditary motor neuropathy. *Brain*. **140**, 1252–1266

451. Jordanova, A., Irobi, J., Thomas, F. P., Van Dijck, P., Meerschaert, K., Dewil, M., Dierick, I., Jacobs, A., De Vriendt, E., Guergueltcheva, V., Rao, C. V, Tournev, I., Gondim, F. A. A., D'Hooghe, M., Van Gerwen, V., Callaerts, P., Van Den Bosch, L., Timmermans, J.-P., Robberecht, W., Gettemans, J., Thevelein, J. M., De Jonghe, P., Kremensky, I., and Timmerman, V. (2006) Disrupted function and axonal distribution of mutant tyrosyl-tRNA synthetase in dominant intermediate Charcot-Marie-Tooth neuropathy. *Nat. Genet.* **38**, 197–202
452. Hyun, Y. S., Park, H. J., Heo, S.-H., Yoon, B. R., Nam, S. H., Kim, S.-B., Park, C. I., Choi, B.-O., and Chung, K. W. (2014) Rare variants in methionyl- and tyrosyl-tRNA synthetase genes in late-onset autosomal dominant Charcot-Marie-Tooth neuropathy. *Clin. Genet.* **86**, 592–594
453. Nowaczyk, M. J. M., Huang, L., Tarnopolsky, M., Schwartzentruber, J., Majewski, J., Bulman, D. E., Hartley, T., and Boycott, K. M. (2017) A novel multisystem disease associated with recessive mutations in the tyrosyl-tRNA synthetase (YARS) gene. *Am. J. Med. Genet. A*. **173**, 126–134
454. Williams, K. B., Brigatti, K. W., Puffenberger, E. G., Gonzaga-Jauregui, C., Griffin, L. B., Martinez, E. D., Wenger, O. K., Yoder, M., Kandula, V. V. R., Fox, M. D., Demczko, M. M., Poskitt, L., Furuya, K. N., Reid, J. G., Overton, J. D., Baras, A., Miles, L., Radhakrishnan, K., Carson, V. J., Antonellis, A., Jinks, R. N., and Strauss, K. A. (2018) Homozygosity for a mutation affecting the catalytic domain of tyrosyl-tRNA synthetase (YARS) causes multisystem disease. *Hum. Mol. Genet.* 10.1093/hmg/ddy344
455. Tracewska-Siemiatkowska, A., Haer-Wigman, L., Bosch, D. G. M., Nickerson, D., Bamshad, M. J., van de Vorst, M., Rendtorff, N. D., Moller, C., Kjellstrom, U., Andreasson, S., Cremers, F. P. M., and Tranebjaerg, L. (2017) An Expanded Multi-Organ Disease Phenotype Associated with Mutations in YARS. *Genes (Basel).* **8**, E381
456. Kepp, O., Gdoura, A., Martins, I., Panaretakis, T., Schlemmer, F., Tesniere, A., Fimia, G. M., Ciccosanti, F., Burgevin, A., Piacentini, M., Eggleton, P., Young, P. J., Zitvogel, L., Van Endert, P., and Kroemer, G. (2010) Lysyl tRNA synthetase is required for the translocation of calreticulin to the cell surface in immunogenic death. *Cell Cycle*. **9**, 3072–3077
457. Kim, D. G., Choi, J. W., Lee, J. Y., Kim, H., Oh, Y. S., Lee, J. W., Tak, Y. K., Song, J. M., Razin, E., Yun, S.-H., and Kim, S. (2012) Interaction of two translational components, lysyl-tRNA synthetase and p40/37LRP, in plasma membrane promotes laminin-dependent cell migration. *FASEB J.* **26**, 4142–4159
458. Kim, D. G., Lee, J. Y., Kwon, N. H., Fang, P., Zhang, Q., Wang, J., Young, N. L., Guo, M., Cho, H. Y., Mushtaq, A. U., Jeon, Y. H., Choi, J. W., Han, J. M., Kang, H. W., Joo, J. E., Hur, Y., Kang, W., Yang, H., Nam, D. H., Lee, M. S., Lee, J. W., Kim, E. S., Moon, A., Kim, K., Kim, D., Kang, E. J., Moon, Y., Rhee, K. H., Han, B. W., Yang, J. S., Han, G., Yang, W. S., Lee, C., Wang, M. W., and Kim, S. (2014) Chemical inhibition of prometastatic lysyl-tRNA synthetase-laminin receptor interaction. *Nat. Chem. Biol.* **10**, 29–34
459. Mirando, A. C., Abdi, K., Wo, P., and Lounsbury, K. M. (2017) Assessing the effects of threonyl-tRNA synthetase on angiogenesis-related responses. *Methods*. **113**, 132–138
460. Sajish, M., Zhou, Q., Kishi, S., Valdez, D. M., Kapoor, M., Guo, M., Lee, S., Kim, S., Yang, X. L., and Schimmel, P. (2012) Trp-tRNA synthetase bridges DNA-PKcs to PARP-1 to link IFN-γ and p53 signaling. *Nat. Chem. Biol.* **8**, 547–554